Endocytosis and Wingless signalling

Maria Gagliardi

This thesis is submitted to University College London
for the degree of Doctor of Philosophy

March 2012

Jean-Paul Vincent's group
Division of Developmental Biology
MRC- National Institute for Medical Research
The Ridgeway, Mill Hill
London, NW7 1AA

Declaration

'I, Maria Gagliardi, confirm that the work presented in this thesis is my own. Where information has been derived from other sources, I confirm that this has been indicated in the thesis.'

Abstract

Wingless (*Drosophila* Wnt-1) is a secreted glycoprotein that triggers an evolutionary conserved signal transduction pathway. The role of endocytosis in Wnt/Wingless signalling is not clearly understood and highly debated. In my thesis I explore the role that endocytosis/endocytic trafficking has on Wingless signalling activation and termination.

In the canonical pathway Wingless binds to a member of the Frizzled family of seven-pass transmembrane receptors (Frizzled1 or Frizzled2) and to Arrow. Formation of this trimeric complex leads to the inactivation of the Armadillo degradation complex and translocation of Armadillo into the nucleus where it contributes to the activation of target genes. I show that internalization of the ligand-receptor complex is not required for signalling activation. I also show that Wingless has different effects on the trafficking route of its receptors: it induces the degradation of Frizzled2 and the recycling of Arrow.

To identify post translational modifications that regulate Arrow trafficking I conducted an RNAi screen in *Drosophila* S2R^{+} cells for de-ubiquitylating enzymes (DUBs) and ubiquitin conjugating enzymes (E2) that modulate signalling. To carry out this screen, improvements on the current TOPFlash Wnt/Wingless signalling reporter were made.

I also directly assessed the role of endocytic trafficking on signalling using a chemical inhibitor of endocytosis, Dynasore. I find that Dynasore inhibits signalling by causing a strong decrease in Armadillo levels. Future experiments will determine whether it is the stability or the rate of production of Armadillo that is affected.

Acknowledgements

I would like to thank Jean–Paul Vincent for his support and guidance over the years, and the members of his lab, past and present, for their help.
I would also like to thank:

Jacky Wilson in the large scale laboratory for all the medium she provided.
Donald Bell for his patience and help with imaging.
Hayley Wood for her illustrator talents.
Eileen McCarthy for taking care of everything with a smile.

A special thanks to Eugenia Piddini who taught me, inspired me and supported me in so many ways. It is thanks to her guidance and advice that I enjoyed my work despite the endless Western blots!
I have always enjoyed coming to work thanks to my friends who fill my days with fun and laughter. I thank Jenny Grant for all her stories and for showing me that we have no limits and can accomplish with great success anything we set our minds to; Rita Sousa-Nunes for her encouragement, her contagious energetic spirit and organizing game nights; Rami Makki for all our chats and for always having the sweet potato; Patricia Serpente for her wisdom, fashion critique and glimpse into my future; Pietro Saiu per tutte le battute and Panayotis Pachnis for standing by me, and giving me a new appreciation of the library which is the only place to avoid his singing.

Most of all I would like thank my family, Carmelo, Norma, Luisa, Gisella and in particular my mother, Gabriela Medeiros. Everything I accomplish is thanks to her and dedicated to her.

Table of Contents

List of Figures

List of Tables

List of Abbreviations

°C	degree Celsius
aa	amino acid
A/P	Antero-Posterior
ADAM	A Disintegrin And Metalloproteinase
Ap	Apterous
AP-2	Adaptor Protein 2
APC	Adenomatous Polyposis Coli
Arm	Armadillo (the Drosophila homolog of β-catenin)
ARM	Armadillo repeats
Arr	Arrow
BSA	Bovine Serum Albumin
Ca^{2+}	Calcium
CaMKII	Calmodulin-dependent Kinase II
CBP	CREB-Binding Protein
CHX	Cycloheximide
CK1γ	Casein Kinase 1 γ
CLS	DNA-binding protein LAG-1
CMV	Cytomegalovirus
CRD	Cysteine Rich Domain
CREB	cAMP Response Element-Binding
crl	courtless
Ct	Cut
Cy5	Cyanine 5
D/V	Dorso-Ventral
Dgo	Diego
Diap1	Drosophila inhibitor of apoptosis 1
DIX	Dishevelled/Axin
Dkk	Dickkopf
Dl	Delta
Dll	Distalless
DMSO	Dimethyl sulfoxide
DN	Dominant Negative
Dsh	Dishevelled
DSHB	Drosophila Studies Hybridoma Bank
DUB	De-ubiquitylating enzymes
Dvl	Dishevelled in vertebrates
Dyna	Dynasore
E1	Ub-activating enzymes
E2	Ub-conjugating enzymes
E3	Ub-ligating enzymes
ECD	Extracellular Domain
EDD	E3 ubiquitin ligase identified by Differential Display
EEA1	Early Endosome Antigen 1
eff	effete
EGFR	Epidermal Growth Factor Receptor
En	Engrailed
ESCRT	Endosomal Sorting Complex Required for Transport
faf	Fat facets
FCS	Fetal calf serum
Fz	Frizzled
FL	Firefly Luciferase
g	G force
$G\alpha_o$	G protein α subunit
GFP	Green fluorescent protein

GPI	Glycosylphosphatidylinisitol
GPCR	G Protein Coupled Receptor
GSK3	Glycogen Synthase Kinase 3
GTP	Guanosine Triphosphate
Hh	Hedgehog
HECT	Homologous to the E6-AP Carboxyl Terminus
HMG	High-Mobility-Group
hr	hours
HRP	Horse Radish Peroxidase
Hrs	Hepatocyte growth factor-regulated tyrosine kinase substrate
HSPG	Heparan Sulfate Proteoglycans
Hyd	Hyperplastic discs
Hyx	Hyrax
ICD	Intracellular domain
IKK	Inhibitor of KappaB Kinase
IP	Immunoprecipitation
JNK	Jun N-terminal Kinase
kb	Kilobase
kDa	kilo Daltons
LacZ	β-galactosidase
LAMP	Lysosomal Associated Membrane Proteins
LBPA	Lysobisphosphatidic Acid
LDL	Low-Density Lipoprotein
LEF	Lymphoid Enhancer factor
Lgs	Legless
LRP	(LDL)-receptor-Related Protein
lwr	lesswright
MCF-2 cells	Human breast adenocarcinoma cell line
min	Minutes
mM	Millimolar
MT	Methallothreoinin
MVB	Multi Vesicular Bodies
MW	Molecular Weight
N	Notch
NEM	N-ethylmaleimide
NEMO	NF-κB Essential Modulator
NF-κB	nuclear factor kappa B
not	non-stop
NRT	Neurotactin
p300	E1A binding protein p300
PAF1	Polymerase associated factor 1
Pan	Pangolin
PBS	phosphate buffer saline
PBST	PBS, 0.1% triton X100
PCP	Planar Cell Polarity
PCR	Polymerase Chain Reaction
PFA	Paraformaldehyde
Pk	Prickle
PKC	Protein Kinase C
PolIII	Polymerase III
PP1	Protein Phosphatase 1
PS	Parasegment
PtdIns(4,5)P2	Phosphatidylinositol 4,5-bisphosphate
PTRF	Protein polymerase 1 Transcript Release Factor
Pygo	Pygopus
Rac1	Ras-related C3 botulinum toxin substrate 1
Rho	Rhomboid
RhoA	Ras Homolog gene family member A
RING	Really Interesting New Gene

RGS	Regulators of G-protein Signalling
RL	Renilla Luciferase
RNA	Ribonucleic acids
ROCK	Rho-associated, coiled-coil containing protein kinase
ROI	Region of Interest
ROR2	Receptor tyrosine kinase-like Orphan Receptor 2
S	Segment
S2 cells	Schneider's cells
$S2R^{+}$	S2 Receptor plus cells
SARA	Smad Anchor for Receptor Activation
Sb	Substrate
Sens	Senseless
Ser	Serrate
SFM	Serum Free Medium
Sgg	Shaggy
Shi	Shibire
Smurf	Smad Ubiquitylation Regulatory Factor 2
Src	Sarcoma
STAM	Signal-Transducing Adaptor Molecule
Stan	Starry Night
Stbm	Strabismus
SUMO	Small Ubiquitin-Related Modifier
Svb	Shavenbaby
TβR	TGFβ Receptor
TCA	Trichloroacetic acid
TCF	T-Cell Factor
TGFβ	Transforming Growth Factor Beta
TK	Thymidine Kinase
TOP	Tcf Optimal Promoter
TNFα	Tumor Necrosis Factor alpha
ts	Temperature sensitive
Tsg-101	Tumor susceptibility gene 101
Tub	Tubulin
UAS	Upstream Activating Sequence
Ub	Ubiquitin
UBPY	Ubiquitin-specific proteases Y
USP	Ubiquitin-specific proteases
µl	Microliter
Vang	VanGogh
VDRC	Vienna Drosophila RNAi Center
Vps	Vacuolar protein sorting-associated protein
Wg	Wingless
Wg CM	Wingless Conditioned Medium
WTX	Wilms tumor gene on the X chromosome

Introduction

Chapter 1

"There are more things in heaven and earth, Horatio,
Than are dreamt of in your philosophy."

William Shakespeare
Hamlet (Act 1. Scene V)

Chapter 1- Introduction

General Introduction

Development is the process by which a single cell proliferates and differentiates to develop into a multi-cellular organism. It is an intricate process regulated by a co-ordinated network of signalling molecules, which orchestrate cell proliferation and gene expression. Wnt proteins, first identified in the 1980s, form a highly conserved family of secreted signalling molecules. They have critical roles both during development, in specifying cell fate, tissue patterning, and during adult tissue homeostasis. Aberrant signalling leads to many developmental defects and diseases such as schizophrenia, epilepsy and cancer.

Wingless (Wg), the *Drosophila* homologue of Wnt-1, acts as a short-range inducer in embryos and both a short range and long range inducer in larval development. In the canonical signalling pathway, upon binding to its receptors, Wingless instigates a signalling cascade to stabilise its signal transducer, Armadillo.

The signal transduction of different signalling molecules often involves and varies with endocytic trafficking. Different studies have investigated and debated the requirement and role of endocytosis and intracellular trafficking in Wingless signalling, yet no concerted model has been established.

During my PhD I contributed to this field of research by analyzing the possible function of endocytosis along different steps in the Wingless signalling pathway. I characterized the trafficking of the Wingless co-receptor Arrow, and began to explore possible post-translational modifications that could direct its trafficking.

1.1 Wnt/Wingless genes

1.1.1 Wingless/Wnt genes

Wnt genes encode secreted glycoproteins and are conserved from flies to humans. The first Wnt gene, *wnt-1*, was identified in mice as a proto-oncogene for mammary tumors (Nusse & Varmus, 1982). It was originally known as Int-1 (integration 1) as it was activated by integration of the Mouse Mammary Tumor Virus (MMTV) but was renamed due to its un-relatedness to *int-2 and int-3* and similarity to the *Drosophila wingless* gene (Nusse et al, 1991). The *Dint-1* gene proved to be identical to the *wingless* gene (Cabrera et al, 1987; Rijsewijk et al, 1987), thus identifying *wingless* as the *Drosophila* homologue of *Wnt-1*.

The *wingless* gene was first identified in 1973 by Sharma, R.P. Loss of function mutants resulted in flies lacking halteres and wings, which were replaced by duplicated notum structures (Sharma & Chopra, 1976). The *wingless* gene was classified as a segment polarity gene when isolated in a genetic screen, performed by Eric Wieschaus and Christiane Nusslein-Volhard, for zygotic mutations that interfere with embryonic patterning (Nusslein-Volhard & Wieschaus, 1980).

In addition to *wingless* there are 6 other DWnt genes in *Drosophila*. Besides *Dwnt8* all have vertebrate orthologs. Dwnt genes have multiple functions in development although not studied to the same extent as *wingless*. *Dwnt2,* is involved in the development of the tracheal system (Llimargas & Lawrence, 2001) and in the development of the testis sheath in the male reproductive tract. *Dwnt2* mutants lack pigment cells which make up the outer layer of the sheath and the inner muscle cell layer is malformed or absent. Expression of *Dwnt2* in females results in the appearance of male-specific pigment cells (Chen & Baker, 1997; Kozopas et al, 1998). The principal role of Dwnt3/5 is in axon guidance in the embryonic CNS (Fradkin et al, 1995; Fradkin et al, 2004). Dwnt4 has been identified as a Wingless antagonist and is required in the anterior compartment of parasegments for denticle formation (Gieseler et al, 1999). It also regulates retinal axon guidance, ovarian cell motility and innervation, and specificity of ventral muscles (Cohen et al, 2002; Sato et al, 2006). *Dwnt8* mutants have a defective immune system due to hyper-activation and over-expression of dorsal target genes (Gordon et al, 2005). The functions of

Dwnt6 and *Dwnt10* have not yet been determined. *Dwnt6* is expressed in a similar pattern as *wingless* in imaginal discs. *Dwnt10* is expressed in the gut, the CNS and in the embryonic mesoderm (Janson et al, 2001).

1.1.2 Function of Wingless in embryonic development

Early in embyrogenesis *wingless*, along with other segment polarity genes such as *hedgehog* (*hh*) and *engrailed* (*en*), is responsible for segmental patterning along the Anterior/Posterior axis (A/P), establishing the blueprint for epidermal cell types and larval segmentation (14 segments) (Nusslein-Volhard & Wieschaus, 1980; Rijsewijk et al, 1987; Sharma & Chopra, 1976).

In the ventral ectoderm 5 hr post egg deposition (stage 9/10) *wg* and *hh* are expressed interdependently in adjacent domains delineating parasegments. *Wingless* is expressed in the most posterior row of cells in each parasegment and Wingless protein is distributed symmetrically, maintaining *en* expression in posterior adjoining cells (DiNardo et al, 1988). These cells, in turn, secrete *hh*, which maintains *wingless* expression (Bejsovec & Wieschaus, 1993; Heemskerk & DiNardo, 1994; Ingham, 1991) (Fig 1.1).

At stage 11 *en/hh* expression becomes independent of Wingless and Wingless protein distribution transits from symmetrical to asymmetrical, present 3-4 cells anterior to the source and 1 cell to the posterior (Bejsovec & Martinez Arias, 1991; Sanson et al, 1999). The restricted posterior distribution is mediated by an increase in lysosomal targeting and degradation. Reduced activity of clathrin, a protein required for endocytosis, or Deep-orange, a protein involved in lysosomal sorting, restore Wingless distribution at the cell membrane and in intracellular vesicles respectively (Dubois et al, 2001; Sevrioukov et al, 1999). Wingless degradation requires expression of *Rhomboid* (*Rho*), which is regulated by Hh and Notch signalling. The latter is activated by the membrane bound ligand Serrate (Ser), expressed 4 rows of cells posterior to the row of En expressing cells (Alexandre et al, 1999; Walters et al, 2005). *Rhomboid* encodes a transmembrane protein necessary for the activation of the EGFR (Epidermal Growth Factor Receptor) ligand *spitz*. Thus implicating EGF signalling in antagonising Wingless signalling and regulating degradation (Golembo et al, 1996; Szuts et al, 1997). EGF and Wingless signalling competitively regulate *shavenbaby* (*svb*) expression. The EGF pathway stimulates *svb* expression leading to

the formation of denticles (Payre et al, 1999; Szuts et al, 1997). Wingless signalling suppresses *svb* expression thus specifying naked cuticle (Payre et al, 1999). Ubiquitous Wingless expression, therefore, results in completely naked cuticle (Noordermeer et al, 1992), whereas in *wg* mutant embryos all naked cuticle is lost and denticles form all along the embryo also known as the "lawn phenotype" (Bejsovec & Martinez Arias, 1991).

In conclusion, at the beginning of embryogenesis Wingless and Hh expression are mutually dependent. At stage 11 their expression is independent and the Wingless protein gradient transits from symmetrical to asymmetrical. The regulation of Wingless distribution and signalling, pivotal in embryonic segmentation, is regulated by endocytosis and intracellular trafficking, processes analysed and discussed throughout this thesis.

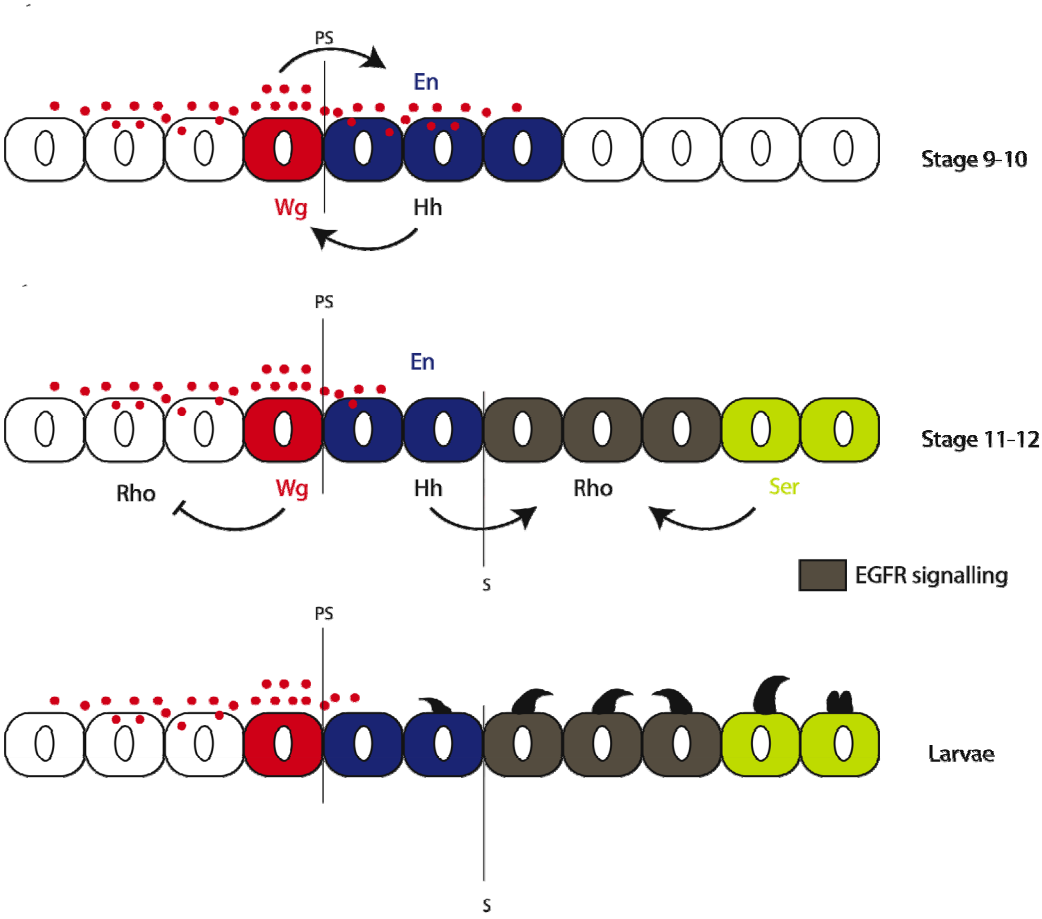

Figure 1.1 Embryonic segmental patterning.

Wingless (wg, red dots) is secreted from the posterior row of cells in each parasegment (PS). At stage 9-10, Wg distribution is symmetrical. *wg* expression and *en/hh* expression are interdependent. At stage 11-12 Wg distribution becomes asymmetric. Reduced Wg levels within En expressing cells is a result of increased degradation mediated by EGFR signalling. EGFR signalling requires Rho expression, whith is regulated by Hh and Ser-Notch signalling. At the end of embryogenesis, denticles form over Rho/Ser expressing cell and the most posterior row of En expressing cells. Wg signalling specifies naked cuticle in 4 cells anterior and 1 cell posterior to its source. S = segment boundary. (Adapted from Dubois et al, 2001).

1.1.3 Function of Wingless in the development of wing imaginal discs

Besides its primary role in embryonic patterning Wg also directs the initial formation of imaginal disc primordia and later in larval development, imaginal disc patterning (Cohen, 1990; Couso et al, 1994). Early loss of Wingless function leads to a 'wing-to-notum transformation', with complete loss of adult wings, whereas loss of function later in larval development, when the wing disc has already been specified, results in loss of wing margin tissue (Couso et al, 1994; Diaz-Benjumea & Cohen, 1995; Neumann & Cohen, 1997; Zecca et al, 1996).

The wing imaginal disc begins as a pouch of ~ 50 cells at the time of embryo hatching. During larval development cells of the wing disc proliferate exponentially reaching a total of 50 000 cells by the end of third instar larvae (Whittle, 1990). *Wg* is expressed in a dynamic pattern throughout disc development. It is first detected in early second instar discs in about 10 cells within each imaginal disc. Expression expands throughout second instar occupying the ventral portion of the disc (Williams et al, 1993). By early third instar, expression is stabilised and restricted to a line along the presumptive wing margin, 3 cells wide. (Couso et al, 1994; Williams et al, 1993). This dynamic sequential expression directs wing disc patterning, providing a blueprint for cell fate and adult structures (Fig 1.2 A).

The wing disc is compartmentalised both anterior/posteriorly and dorso/ventrally (Fig 1.2 C). The A/P compartment boundary is established during embryonic segmentation and is maintained throughout larval development as indicated by the expression of engrailed (Garcia-Bellido et al, 1973; Lawrence & Morata, 1976; Vincent & O'Farrell, 1992) The D/V axis, is established in second instar larvae (Garcia-Bellido et al, 1976). The ventral and dorsal regions are defined by the opposing expression of *wg* and *ap* (*apterous*) respectively (Williams et al, 1993). In *wg* mutant discs *ap* expression expands into the ventral region suggesting that wg sets the limit of *ap* expression (Williams et al, 1993). During development, while *ap* expression remains unaltered, in early-mid third instar discs *wg* expression is confined along the D/V boundary by Notch signalling. Notch activation in D/V boundary cells stimulates *wg* expression (de Celis et al, 1996). Wingless signalling induces expression of *dl* (*delta*) and *ser* (*serrate*), ligands of the Notch receptor, in cells flanking the D/V boundary thus establishing a positive feed back loop which maintains Notch activation and Wingless expression in boundary cells (Diaz-Benjumea & Cohen, 1995; Rulifson et al, 1996). Notch activation is restricted to D/V

boundary cells by cut, a Notch target gene. Cut expression in boundary cells silences *Dl* and *Ser* expression at the boundary thereby inhibiting Notch activation in flanking cells (de Celis et al, 1996; Micchelli et al, 1997). The high levels of *Dl* and *Ser* expression in flanking cells do not activate Notch in flanking cells themselves as high levels act in an autonomous dominant negative manner (Fig 1.2 B)

Despite restricted expression of Wingless at the D/V boundary all cells of the wing pouch are subject to Wingless signalling. Wingless is observed in a steep gradient up to 10-15 cells away from the source and target genes are expressed in a concentration dependent manner. This graded distribution and differential gene expression classifies Wingless as a morphogen in the wing disc (Neumann & Cohen, 1997; Zecca et al, 1996). High levels of Wingless signalling in cells adjacent to the D/V boundary promotes expression of *neuralized* and *senseless*, responsible for formation of specialized bristles that make up the adult wing margin (Couso et al, 1994). Low-level target genes such as *distalless* (*dll*) and *vestigal* (*vg*), responsible for wing growth, are expressed in a graded fashion, decreasing towards the edges of the wing pouch (Neumann & Cohen, 1997; Zhu, 2011). Evidence that different target genes require discrete thresholds of Wingless signalling comes from an experiment using mutant discs in which *wg* expression is temperature sensitive (wg^{ts}). At 22°C, a temperature that reduces Wingless activity, *dll* expression is narrowed relative to that of *vg*, which is unchanged (Neumann & Cohen, 1997).Therefore, although both *dll* and *vg* are low target genes, *dll* expression requires higher levels of Wingless signalling than *vg*. The failure of clones expressing membrane tethered Wingless to activate target gene expression at a distance suggests that Wingless does not trigger a relay system but rather acts directly on receiving cells (Neumann & Cohen, 1997) (Fig 1.2 D).

A classical morphogen is defined by its ability to induce gene expression and act directly at a distance. Although Wingless does act at a distance, *dll* and *vg* expression are not initiated by Wingless signalling, but rather maintained. This suggests that Wingless may refine expression of genes already induced by classical morphogens, thus possibly describing a novel class of morphogen (Martinez Arias, 2003).

Figure 1.2 Wingless expression in wing imaginal discs and wing patterning.

(A) *wingless* (*wg*) is first expressed in the ventral portion of the wing disc at 2nd instar. By 3rd instar *wg* expression occupies the entire wing premordium and then becomes restricted along the dorsoventral boundary by mid-late 3rd instar. (Adapted from Martinez Arias, 2003) (B) At mid-late 3rd instar *wg* expression is regulated by Notch signalling. In boundary cells Notch induces *wg* and *cut* expression. Wingless triggers *Dl/Ser* expression in flanking cells thus creating a postitive feedback loop, further activating Notch signalling. Cut inhibits *Dl/Ser* expression thereby preventing activation of Notch in flanking cells. High levels of *Dl/Ser* in flanking cells induced by Wingless also inhibit Notch activation. (Adapted from Gonzalez et al, 2006). (C) Schematic of the wing imaginal disc (left) that develops into the adult wing (right).The wing disc is compartmentalized into the anterior (white) posterior (lilac), dorsal (striped) and ventral (clear) compartments. The D/V boundary demarked by a row of *wg* expressing cells makes up the wing margin of the adult wing. (D) The Wingless gradient produced from the D/V boundary activates different genes in a concentration dependent manner, *senseless* (*sens*), *dll* (*distalless*), *vestigial* (*vg*). (C and D are adapted from Strigini & Cohen, 1999).

A

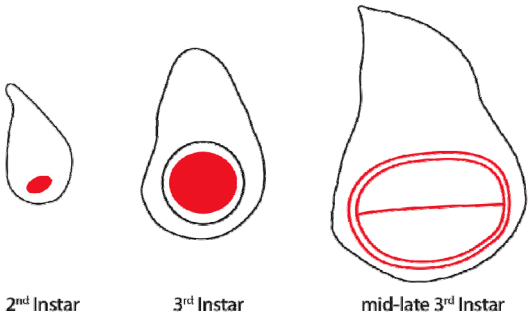
2nd Instar
3rd Instar
mid-late 3rd Instar

B

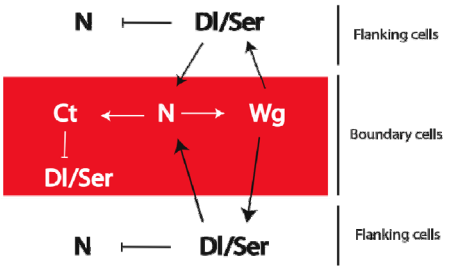
N
Dl/Ser
Flanking cells
Ct
N
Wg
Dl/Ser
Boundary cells
N
Dl/Ser
Flanking cells

C

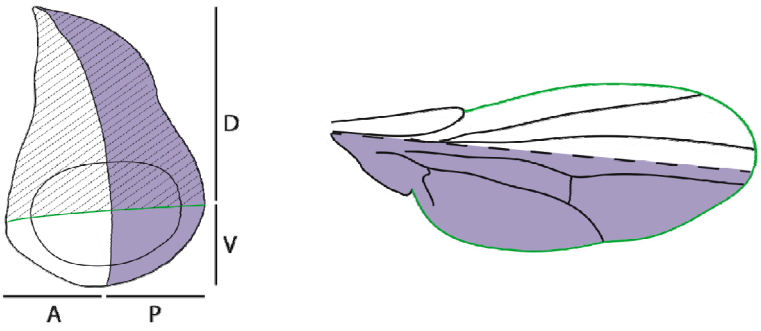
D
V
A
P

D

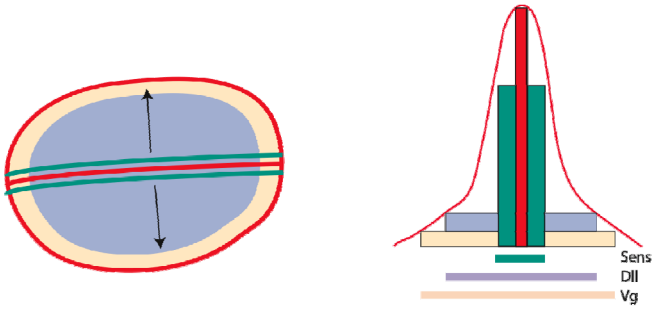
Sens
Dll
Vg

1.2 Wingless/Wnt signalling

1.2.1 Wingless/Wnts signalling pathways

Three different Wnt signalling pathways have been described: the Wnt/beta-catenin (canonical) pathway, the planar cell polarity (PCP) pathway and the Wnt/Ca^{2+} pathway. Common to these three pathways is the Fz receptor. Relatively recently a new Wnt signalling pathway involving a distinct receptor, the orphan tyrosine kinase Ror2, has been described. (Angers & Moon, 2009; Liu et al, 2008; Mikels & Nusse, 2006)

1.2.1.A. The canonical signalling pathway

The key effector of the canonical Wingless pathway is Armadillo (β-catenin in vertebrates), a transcriptional co-activator. In the absence of Wingless, Armadillo is targeted for proteasomal degradation by a complex made up of adenomatous polyposis coli (APC), Axin and Shaggy (Glycogen Synthase Kinase3, GSK3 in vertebrates) (Seto & Bellen, 2004). The latter phosphorylates Armadillo, allowing subsequent ubiquitylation by $SCF^{\beta\text{-}TrCP}$, which acts as a proteasomal degradation signal (Gordon & Nusse, 2006). Wingless signalling is mediated by the seven transmembrane proteins Frizzled and Frizzled 2, which function as redundant Wingless receptors in *Drosophila* (Bhanot et al, 1999), and by Arrow (LRP5/6 in vertebrates). The binding of Wingless to its receptors leads to the activation and recruitment of Dishevelled (Dsh/Dvl in vertebrates) to the plasma membrane and the phosphorylation of Arrow at five conserved PPPS/TP motifs by GSK3 (Tamai et al, 2004; Zeng et al, 2005). These phosphorylation events promote the recruitment of Axin to Arrow, leading to the disruption of the degradation complex and hence stabilization of Armadillo. Accumulated Armadillo translocates to the nucleus and activates target genes by interacting with transcription factors of the high-mobility-group (HMG)-box family, specifically TCF (T-cell factor) (DasGupta et al, 2005). In the absence of Wingless these transcription factors are repressed by co-repressor Groucho and dCBP (CREB-binding protein) (Cavallo et al, 1998; Waltzer & Bienz, 1998). Arrow acts as a co-receptor as it associates with Frizzled/Frizzled2 in a ligand dependent manner (Blitzer & Nusse, 2006; Piddini et al, 2005) (Fig 1.3 A). Both

receptors harbour internalization signals, which become active upon ligand binding. Frizzled/Frizzled2 is primarily involved in ligand capture at the cell surface via its cysteine rich domain (CRD), while Arrow contributes to formation of the signalling complex and subsequently to Wingless degradation (Piddini et al, 2005).

1.2.1.B. The PCP pathway

The PCP pathway, first identified in *Drosophila* (Gubb & Garcia-Bellido, 1982; Struhl et al, 1997) directs the orientation of a cell and co-ordinates it with that of the tissue. This is evidenced in *Drosophila* by the orientation of hair on the wing and ommatidia in the eye (Mitchell et al, 2009; Mlodzik, 2002). Similar to the canonical pathway, activation of the pathway involves the recruitment and binding of Dsh to the Fz receptor at the plasma membrane (Axelrod, 2001). After this initial step the PCP pathway diverges from the canonical pathway, with the recruitment of polarity proteins: transmembrane proteins VanGogh (Vang)/Strabismus (Stbm) and Flamingo (Fmi)/Starry Night (Stan), and cytosolic proteins Diego (Dgo) and Prickle (Pk). Although the recruitment and localization mechanisms are not clear, once at the plasma membrane these polarity proteins form a multiprotein complex with Fz/Dsh that spans cell-cell junctions (Axelrod, 2001; Strutt, 2003). This complex, through RhoA and Rac1 GTPases activates JNK and ROCK (Rho Kinase) signalling cascades (Boutros et al, 1998), resulting in cytoskeletal remodelling, correct hair number and direction, and ommatidium rotation (Choi & Benzer, 1994; Verheyen et al, 2001; Winter et al, 2001) (Fig 1.3 B). Although the Wnt ligand for the PCP pathway in *Drosophila* has not been identified, Wnt ligands activate an analogous pathway in vertebrates (Strutt, 2003).

1.2.1.C. The Wnt/Ca^{2+} pathway

Like the PCP pathway the Wnt/Ca^{2+} pathway has also been implicated in cytoskeleton organization and cell adhesion (Kuhl et al, 2000a; Slusarski et al, 1997). Wnt binding to the Fz receptor activates G proteins and leads to release of Ca^{2+} from intracellular stores (Slusarski et al, 1997). Increased Ca^{2+} concentration then activates Ca^{2+} dependent protein kinase C (PKC) and calmodulin-dependent kinase II (CaMKII) (Kuhl et al, 2000b). These kinases regulate transcription factors and

inhibit canonical signalling (Kuhl et al, 2001) (Fig 1.3 C). This pathway, however, has not been shown in *Drosophila*.

1.2.1.D. Ror2 mediumted signalling

The single pass transmembrane protein Ror2 has recently been shown to act as a Wnt receptor. Binding of Wnt5 induces receptor dimerization and activation of JNK signalling, affecting cell migration and inhibiting Wnt canonical signalling. Wnt5 binding to Fz4 has the opposite effect, potentiating Wnt canonical signalling (Angers & Moon, 2009; Liu et al, 2008; Mikels & Nusse, 2006). A similar dual effect is seen for Wnt3a: canonical signalling is inhibited with Ror2 as the sole receptor and activated in the presence of Fz2 (Li 2008, reviewed in Akira Kikuchi 2009). This illustrates an interesting part of Wnt signalling: that a single Wnt can initiate discrete pathways depending on the receptors employed (Fig 1.3D).

Figure 1.3 Wingless signalling pathways.

(A) Canonical Wnt/Wingless signalling: In the absence of Wnt/Wg β-catenin /Armadillo is bound to and phorphorylated by the degradation complex, composed of GSK3, CK1, APC and Axin. Phosphorylated Armadillo is then recognised and ubiquitylated by βTrcB, leading to proteosomal degradation. Wnt/Wg target gene expression is suppressed in the absence of Wnt/Wg by the repressor protein Groucho, and CBP. In the presence of Wnt/Wg, formation of a ligand-receptor complex (Arrow-Wnt/Wg-Fz2) leads to the dismantling of the degradation complex. The recruitment of Dishevelled (Dsh) to the Fz2 receptors mediates the phosphorylation and recruitment of Axin, GSK3 and CK1 to the Arrow receptor. β-catenin /Armadillo, is stabilized and translocates to the nucleus to activate target gene transcription with TCF, Legless (Lgs)/Bcl9, Pygopus (Pygo) and Hyrax (Hyx).
(B) Planar cell polarity: ligand binding to the Fz receptor recruits Dsh to the membrane. The formation of a multiprotein complex with transmembrane proteins VanGogh (Vang)/ Strabimus (Stbm) and Flamingo (Fmi)/ Starry Night (Stan), and cytosolic proteins Diego (Dgo) and Prickle (Pk) results in activation of GTPases RhoA and Rac1 leading to JNK and ROCK signalling. In *Drosophila* a Wnt ligand has not been identified to activate the pathway.
(C) The Wnt/Ca^{2+} pathway: Activation of G proteins upon Wnt binding to Frizzled leads to accumulation of Ca^{2+} which activates Protein Kinase C (PKC) and Calmodulin-dependent kinase II (CaMKII).
(D) Ror2 signalling: Dimerization of the Ror2 receptor upon ligand binding leads to receptor phosphorylation by GSK3 and JNK signalling.
(Adapted from Buechling & Boutros, 2011).

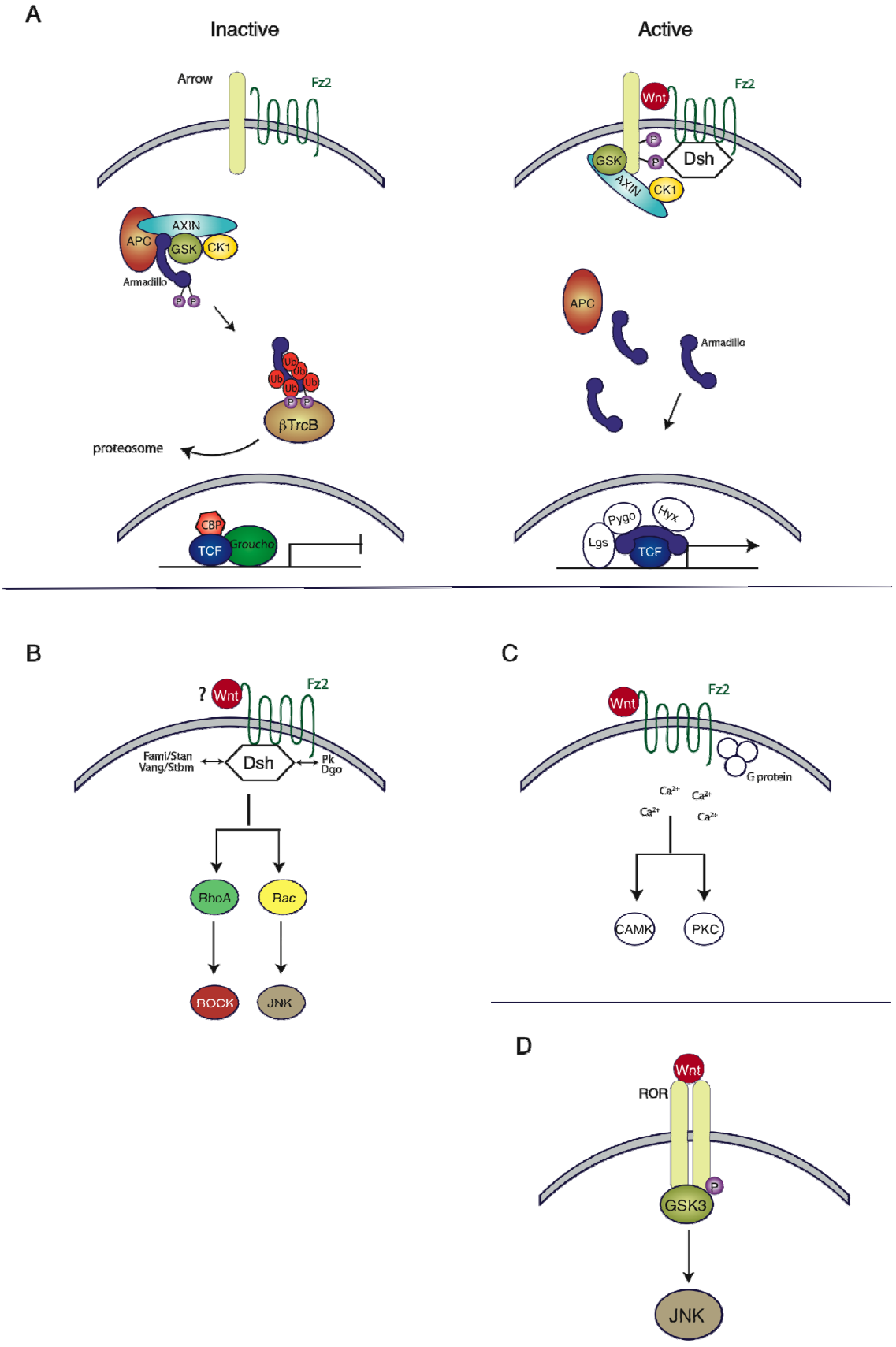
A
Inactive
Active
Arrow
Fz2
AXIN
APC
GSK
CK1
Armadillo
P
Ub
βTrcB
proteosome
CBP
TCF
Groucho
Wnt
Dsh
Pygo
Hyx
Lgs
B
?
Fami/Stan
Vang/Stbm
Pk
Dgo
RhoA
Rac
ROCK
JNK
C
G protein
Ca2+
CAMK
PKC
D
ROR
GSK3

1.2.2 Frizzled and Arrow receptors

1.2.2.A Frizzled receptor

Frizzled (Fz) receptors constitute a family of G-protein coupled, seven-pass-transmembrane proteins that are key to Wnt signalling. Frizzled's serpentine structure is composed of a conserved cysteine rich domain (CRD), containing 10 cysteine residues, a flexible hydrophilic region of 40-100 amino acids, seven transmembrane domains, and a conserved S/T-X-V sequence at the C terminus (Bhanot 1996). Wnt proteins interact with Frizzled receptors at the CRD domain, comprised of 120-125 amino acids. Mutational analysis revealed that Dsh interacts with 3 intracellular residues, Arg340 in the first loop and Leu524, Leu527 in the third (Cong et al, 2004) (Fig. 1. 4).

There are four Frizzled receptors in *Drosophila*; the first, DFz, was identified from its role in the *Drosophila* PCP pathway (Vinson & Adler, 1987). Loss of DFz results in loss of hair, bristle and ommatidia polarity (Gubb & Garcia-Bellido, 1982). In addition to DFz, DFz2 is a Wingless receptor and has a higher affinity for Wingless than DFz (Bhanot et al, 1999; Kennerdell & Carthew, 1998; Lecourtois et al, 2001; Sato et al, 1999; Tomlinson et al, 1997; Wu et al, 2002). DFz3 binds to Wingless and is transcriptionally up regulated upon signalling (Sato et al, 1999). DFz3 does not transduce Wingless signally, but rather acts as an attenuator. The mutant wg^{1} phenotype, which transforms the wing into a duplicated notum, is partially rescued by the elimination of DFz3 (Baker, 1988; Sato et al, 1999). Unlike the others, DFz4 does not interact with Wingless (Wu et al, 2002), it is expressed in the central nervous system, gut, mesoderm and at low levels in the wing disc (Janson et al, 2001). Mutated forms of *Dfz4* are not available thus its function is unknown.

DFz takes part in both PCP and canonical signalling. Indeed *Dfz2* homozygous null mutant flies are viable and do not appear deficient in Wingless signalling. Wingless signalling is abolished only when both *Dfz* and *Dfz2* are deleted. Knockdown of both *Dfz2* and *Dfz* in the embryo results in loss of embryonic patterning, and excess naked cuticle (Chen & Struhl, 1999). In wing discs, cells lacking *Dfz* and *Dfz2* fail to express Wingless target genes (Chen and Struhl, 1999). The redundancy of the DFz/DFz2 receptors is evidenced by the ability of *Drosophila* S2 cells to transduce Wingless signalling, shown by the accumulation of Armadillo, when transfected with either *Dfz* or *Dfz2* (Bhanot et al, 1999; Chen & Struhl, 1999). Despite their

redundancy in Wnt/beta-catenin signalling, DFz and DFz2 do display signalling pathway specificity. Over-expression of *Dfz* results in severe PCP phenotypes and mild/low canonical signalling phentotypes. The opposite is true with regards to *Dfz2* (Boutros et al, 2000).

The distribution in the wing disc of Wingless and DFz2 are interdependent. Wingless stimulates DFz2 internalization, degradation and also represses its expression (Cadigan et al, 1998; Piddini et al, 2005). Therefore, close to the D/V boundary, where there is a high level of Wingless, there are low levels of DFz2. Wingless spreads from its source and as its concentration decreases the level of DFz2 increases. Therefore, the high levels of DFz2 far from the source are able to capture the small amounts of Wingless that reach it and activate low target gene expression. DFz2 also mediates Wingless internalization. Expression of DFz2 bound to cell surface membranes by means of a GPI (Glycosylphosphatidylinisitol) anchor in imaginal discs greatly reduces Wingless internalization (Cadigan et al, 1998; Piddini et al, 2005). In addition, $S2R^{+}$ cells exposed to Wingless at temperatures that inhibit endocytosis accumulate Wingless at the cell surface. Upon shifts to temperatures permissive of endocytosis Wingless is internalized and localized in DFz2-positive vesicles (Piddini et al, 2005). Therefore, as Wingless stimulates DFz2 internalization, DFz2 in turn mediumtes Wingless internalization.

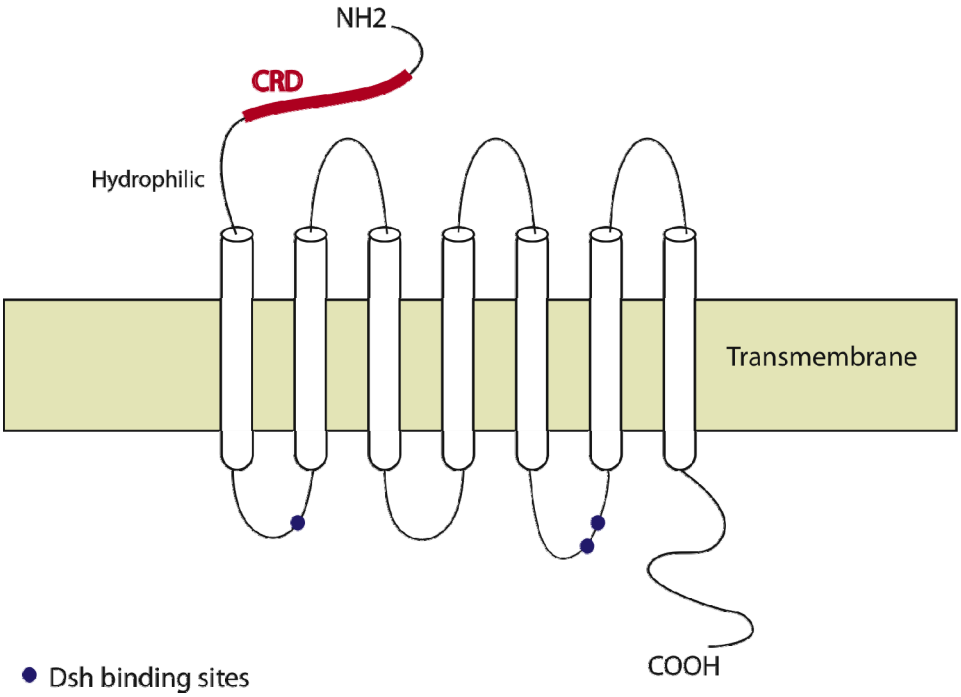

Figure 1.4 The Frizzled receptors.

Frizzled (Fz) receptors are composed of a cystein rich domain (CRD) at the N terminus to which Wg binds, a hydrophilic domain region of 40-100 amino acids, 7 transmembrane domains and conserved sequences at the C terminus. Dishevelled (Dsh) binds to Fz at Arg 340 in the first intracellular loop and Lys 524/Lys 527 in the third intracellular loop.

1.2.2.B Arrow receptor

The Arrow receptor is a low-density lipoprotein (LDL)-receptor-related protein (LRP), homologous to mammalian LRP5/6. It acts as a Wingless co-receptor and is an essential component of the Wingless canonical pathway. Embryos lacking both maternal and zygotic *arrow* function are identical to *wg* mutant embryos, being devoid of smooth cuticle and lacking *en* expression. In the wing pouch *arrow* mutant clones mimic *Dfz/Dfz2* clones, with loss of *dll* expression and wing margin defects. Over-expression, on the other hand, results in ectopic bristles in wing margin, a signature of excess Wingless signalling (Wehrli et al, 2000). The dual requirement of Arrow and Frizzled 2 is illustrated by the inability of over-expressed *Dfz2* to restore Wingless signalling in *arrow* mutant clones and by the impairment of signalling in S2 cells with double stranded RNA against either receptor (Schweizer & Varmus, 2003; Wehrli et al, 2000).

Arrow is a single pass transmembrane protein comprising, on the extracellular side, of 4 epidermal growth factor (EGF)-like repeats, each preceded by 6 YWTD spacer domains, and 3 LDL type A repeats. Both types of repeats are implicated in ligand binding. The cytoplasmic tail, composed of 209 amino acids residues, contains 5 conserved PPPS/TP domains required for Arrow/LRP6 activation (Tamai et al, 2004; Wehrli et al, 2000) (Fig 1.5 A).

Studies exploring the activation of LRP6 have shown that the PPPS/TP domains are phosphorylated and act in a combinatorial fashion to activate signalling via the recruitment of Axin (MacDonald et al, 2008; Wolf et al, 2008; Zeng et al, 2008). Phosphorylation is mediumted by membrane associated GSK3. GSK3 over-expression promotes LRP6 phosphorylation whereas inhibition of GSK3 or genetic deletion of *gsk3α* and *gsk3β* abolishes it (Zeng et al, 2005). Adjacent to the PPPS/TP motif is a second phosphorylation site (PPPS/TPxS/T), targeted by CK1γ, a membrane associated kinase. GSK3 phosphorylation precedes CK1γ and has a fundamental role, as mutant PPPS/TP motifs abrogate Axin binding whereas mutation of the CK1γ motifs only diminish it (Davidson et al, 2005; Zeng et al, 2005).

There are two models that describe the manner in which LRP6 phosphorylation is regulated: the signalosome model and the recruitment/amplification model. In the signalosome model, Wnt binding to a Fz receptor leads to polymerization of Dvl at

the plasma membrane. Upon this Dvl scaffold LRP6 co-clusters with other signalling components (Axin, Fz, GSK3) thus forming a 'signalosome'. High receptor concentration in the signalosome triggers phosphorylation of LRP6 by CK1γ and Axin recruitment (Bilic et al, 2007; Metcalfe et al, 2010) (Fig 1.5 C). In the recruitment/amplification model LRP6 is initially phosphorylated by the Axin-GSK3 complex recruited by Dvl to the receptor complex. This initial phosphorylation generates additional docking sites thereby recruiting additional Axin-GSK3 to amplify signalling (Zeng et al, 2008). (Fig 1. 5 B)

While Fz2 is primarily responsible for Wingless capture and internalization, Arrow directs the degradation of the Fz2/Wingless complex. This accounts for the initially confounding observation that upon Fz2 over-expression instead of increased internalization and degradation, Wingless is stabilized within the cell. Such stabilization is only abolished with Arrow over-expression. Arrow also has an internalization signal thus driving both Wingless internalization and degradation (Piddini et al, 2005). Arrow's degradation signal lies between residues 1477 and 1612, as expression of a truncated form of Arrow does not remedy Fz2 induced Wingless stabilization, but rather potentiates it (Piddini et al, 2005).

Figure 1.5 The Arrow receptor.

(A) Arrow is a single pass transmembrane receptor. Its extracellular domain consists of four epidermal growth factor (EGF) like repeats and three LDL type A repeats. Intracellularly Arrow has five conserved PPPS/TP domains. (B) There are two models for Arrow activation. In the recruitment/amplification model initial recruitment of Dsh and Axin-GSK3-CKI to the receptor leads to partial receptor phosphorylation which is amplified by additional recruitment of Axin-GSK3. (C) In the signalosome model Dsh polymerization at the ligand-receptor complex leads to complex aggregation, resulting in recruitment of Axin-GSK3-CKI and Arrow phosphorylation. (B and C are adapted from MacDonald et al, 2009).

A

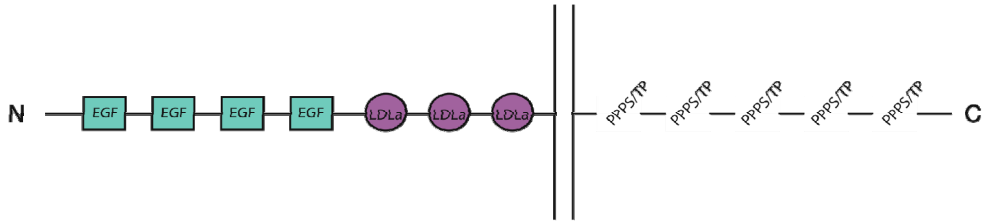
N
EGF
EGF
EGF
EGF
LDLa
LDLa
LDLa
PPPS/TP
PPPS/TP
PPPS/TP
PPPS/TP
PPPS/TP
C

B

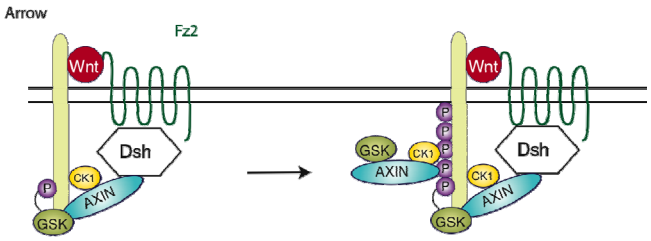
Arrow
Fz2
Wnt
Dsh
CK1
AXIN
GSK
P

C

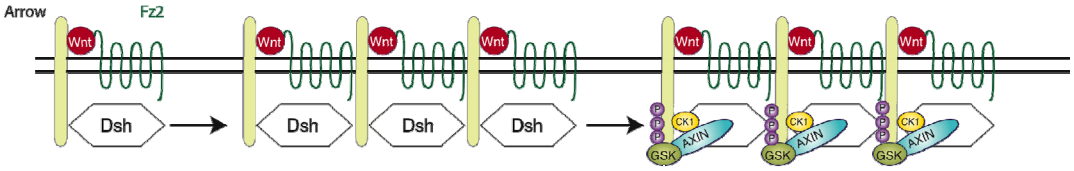
Arrow
Fz2
Wnt
Dsh
CK1
AXIN
GSK
P

1.2.3 The degradation complex

As the name implies, the degradation complex regulates Wnt signalling by inducing Armadillo ubiquitylation and subsequent proteasomal degradation. It is composed of GSK3, APC, Axin and CK1γ. Armadillo/β-catenin enters the complex through interaction with APC and Axin, which act as a scaffold. Once captured Armadillo/β-catenin is phosphorylated by CK1γ at Ser-45 and GSK3 at Thr-41, Ser-37 and Ser33. Phosphorylation promotes ubiquitylation by β-TrCP on Lys-19 and ultimately degradation. Recently, WTX (Wilms Tumor gene on the X chromosome) has been identified as a novel member of the complex, it interacts with β-catenin, Axin, APC and β-TrCP potentiating the affinity of β-TrCP for β-catenin and thus ubiquitylation (Major et al, 2007) (Fig 1.6).

1.2.3.A. GSK3

GSK3, identified in 1980 (Embi et al, 1980) is a highly conserved kinase with numerous substrates and roles in multiple signalling pathways. It has dual function in the Wnt pathway, both inhibiting signalling as part of the degradation complex and promoting signalling by activating Arrow/LRP6 (as described in 1.2.2.B). GSK3 interacts with its substrates at two sites: a priming phosphate site and an active site. Pre-phosphorylated substrates bind to the priming phosphate site. This interaction aligns the substrate with the active site to be phosphorylated. GSK3 activity is inhibited by growth factors/insulin via the phosphorylation of a Serine in GSK3's N terminal domain. This phosphorylation induces the N-terminal domain to fold back on itself and acts as a pseudo-substrate, occupying the priming phosphate site and inhibiting the interaction between GSK3 and possible substrates (Fig 1.7 A) (Ding et al, 2000; Frame et al, 2001). The manner in which Wnt negatively regulates GSK3 function differs from that described above, as Wnt does not induce GSK3 phosphorylation. There are currently two contrasting models for Wnt-induced GSK3 inhibition. The first is a biochemical model, which depicts pre-phophorylated LRP6 occupying GSK3's priming site thus inhibiting its interaction with other substrates (Bilic et al, 2007; Davidson et al, 2005; Wu et al, 2009).

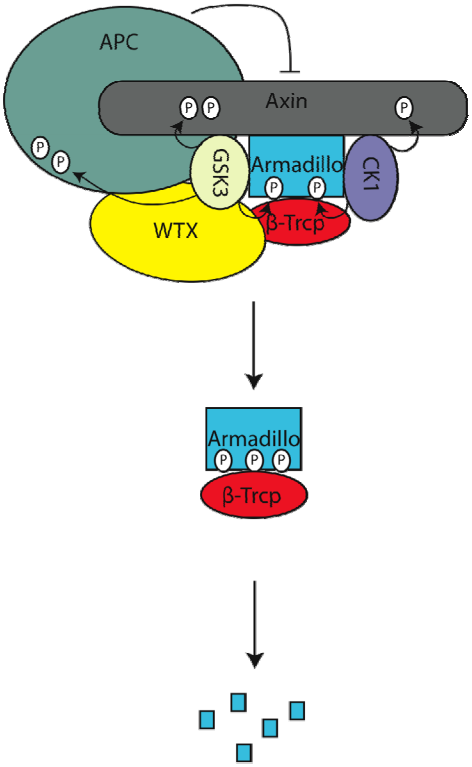

Figure 1.6 The Degradation complex

In the absence of Wg, Armadillo is phosphorylated and ubiquitylated in the degradation complex for subsequent proteosomal degradation. Axin is the scaffold for the degradation and binds to APC, Armadillo, WTX, GSK3 and CK1. APC in conjunction with Axin mediates the assembly of the degradation complex and capture of Armadillo. GSK3 and CK1 phosphorylate Armadillo priming it for ubiquitylation by E3 β-Trcp. The affinity of β-Trcp for Armadillo is potentiated by WTX. Wingless signalling disassembles the degradation complex thus stabilising Armadillo. (Adapted from Huang & He, 2008).

The second model is a cell biological model inferring the sequestration of GSK3 into multi vesicular bodies (MVB) as the mechanism of GSK3 inhibition. It has been suggested that Wnt induced GSK3 inhibition affects the half-life of multiple proteins as numerous proteins have been identified as being potential GSK3 targets (Taelman et al, 2010), thereby involving Wnt signalling in the modulation of other signalling pathways. Both models are reviewed in (Metcalfe & Bienz, 2011)

GSK3 has also been found to have a role in enhancing Wnt signalling. Ubiquitin ligase EDD promotes GSK3 nuclear localization, here β-Catenin is ubiquitylated by EDD and stabilised in a GSK3 dependent manner (Hay-Koren et al, 2011). This will be further described in section 1.4.3 A

1.2.3 B. Axin

Axin is the scaffold of the degradation complex and orchestrates the phosphorylation of Armadillo/β-Catenin for degradation. Axin contains two conserved domains. An N terminal domain, homologous to members of the regulators of G-protein signalling family (RGS), is required for APC binding. A C terminal DIX domain mediates polymerization of Axin, required for its function. A rescue assay in *Drosophila axin* null mutant embryos, which possess entirely naked cuticle, shows restoration of denticle belts with the expression of wild type *axin* but not with DIX domain mutated *axin*, proving that polymerization is required for inhibition of Wingless signalling (Fiedler et al, 2011). Axin DIX domains are also a key target for Dsh mediated Axin regulation. Upon Wingless signalling Dsh DIX domains acquire high affinity for Axin DIX domains thus destabilizing Axin assemblies and recruiting Axin to the plasma membrane for signalosome formation (Fiedler et al, 2011; Schwarz-Romond et al, 2007). Evidence for this comes from the altered distribution of Axin mutant proteins. Polymerization defective Axin mutant proteins appear as diffuse cytosolic puncta in Wingless expressing zones in the embryo as opposed to wild type plasma membrane associated puncta (Fiedler et al, 2011). Therefore through its DIX domain, Axin exerts its function both in the degradation complex and in the signalosome.

Axin function is also regulated by phophorylation. Through an RNAi screen of protein phosphatases, PP1, a serine-threonine phosphatase was identified as a positive regulator of Wnt signalling. Over-expression of PP1 alone activates

signalling by dephosphorylating Axin at a CK1γ site thus decreasing its interaction with GSK3 and destabilizing the degradation complex (Luo et al, 2007) (Fig 1.7 B). Another post translation modification that regulates Axin stability and affects signalling is ubiquitylation, and will be described in section 1.4.3.A.

1.2.3.C. APC

Adenomatous polyposis coli (APC), which is mutated in most cases of colorectal adenomas and carcinomas (Kinzler et al, 1991), affects Wingless signalling both positively and negatively. There are two APC homologues in *Drosophila* (APC1/2) that are ubiquitously expressed and have redundant roles.

In the degradation complex APC binds to Axin, via SAMP (Ser-Ala-Met-Pro) repeats, and β-catenin via seven 20-amino acid repeats and three 15-amino acid repeats (Fig 1.7 C). The latest model of degradation complex function bestows APC two roles in β-catenin regulation.

1) A functional degradation complex cycles between assembly and disassembly. Interaction of APC and Axin via SAMP mediates assembly and capture of β-catenin. After phosphorylation of β-catenin, specific APC sequences mediate the separation of APC from Axin allowing disassembly of the complex and transfer of β-catenin to E3. This cycling allows continuous β-catenin degradation (Kimelman & Xu, 2006; Roberts et al, 2011).
2) The 15 and 20 amino acid repeats retain residual, non-degraded, cytoplasmic β-catenin. Thus preventing translocation of β-catenin to the nucleus (Roberts et al, 2011).

APC also inhibits signalling by translocating into the nucleus and favouring the replacement of co-activator by co-repressor complexes at Wnt target genes (Henderson, 2000; Sierra et al, 2006). Phosphorylated APC interacts with co-repressor CtBP and recruits it to the Wnt co-activator complex (Bcl-9/Lgs, Pygo). Complex exchange results in the detachment of β-catenin from TCF/LEF, and its binding, with higher affinity, to phosphorylated APC (Sierra et al, 2006). Nuclear export signals in the C terminus of APC mediate transport of β-catenin from the nucleus (Rosin-Arbesfeld et al, 2000). Therefore APC inhibits signalling both cytoplasmically as part of the β-catenin degradation complex and inside the nucleus as an export chaperone.

In addition to preventing Wingless signalling, it has been suggested that APC also

promotes it. While extensive reduction of *APC1/APC2* levels results in hyper-activation of the Wingless pathway, smaller reduction lead to inhibition of signalling, presented by loss of sternites in the ventral abdomen and the wing blade (Takacs et al, 2008). APC's promotion of signalling is attributed to its negative regulation of Axin levels. With mild reductions of *APC1/APC2* both Armadillo and Axin levels rise and increased Axin levels mediate Armadillo degradation thus preventing signalling (Takacs et al, 2008).

In conclusion, APC function alternates from inhibiting signalling in the absence of Wingless by regulating β-catenin levels, to promoting it in the presence of Wingless by regulating Axin levels.

Figure 1.7 Components of the degradation complex, GSK3, Axin, APC.

(A) GSK3 is a conserved kinase involved in multiple signalling pathways. In the degradation complex it phosphorylates APC, Axin and Armadillo/β-catenin. In the active state, pre-phophorylated substates bind to GSK3's priming site and are phosphorylated at the active site. GSK3 is inactivated by the folding back of the phosphorylated N terminus which occupies the priming site thus inhibiting substrate binding. (Adapted from Cohen & Frame, 2001). (B) Axin is the scaffold of the degradation complex. APC binds to Axin via a conserved RGS domain. Their interaction mediates the capture of Armadillo/β-catenin and formation of a ternary complex. GSK3 and CK1 phosphorylate Axin, APC and Armadillo/β-catenin. Phosphorylation of APC regulates its affinity for Armadillo/β-catenin while phosphorylation of the latter primes it for degradation. At the C terminus Axin has a conserved DIX domain, which permits Axin polymerization required for its function and dimerization with Dsh, which destabilizes the degradation complex. De-phosphorylation of Axin by PP1 also destabilizes the complex by impairing Axin's interaction with GSK3. (Adapted from Fagotto et al, 1999; Kikuchi, 1999). (C) APC-interacting proteins bind to APC at an armadillo repeat domain at the N terminus. APC binds to Axin via 3 Ser-Ala-Met-Pro repeats and to Armadillo/β-catenin via seven 20 aa (amino acid) repeats and three 15 aa repeats. (Adapted from Cabrera & Lopez-Nevot, 2005).

A

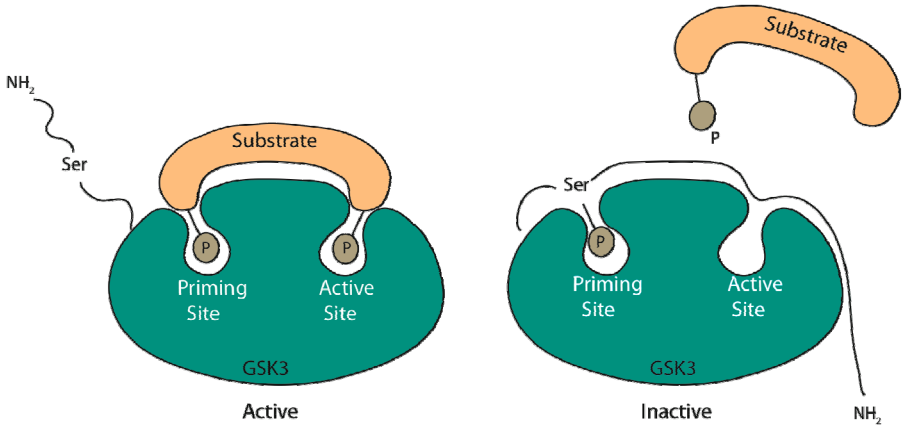
NH2
Ser
Substrate
P
Priming Site
Active Site
GSK3
Active
Substrate
P
Ser
Priming Site
Active Site
GSK3
Inactive
NH2

B

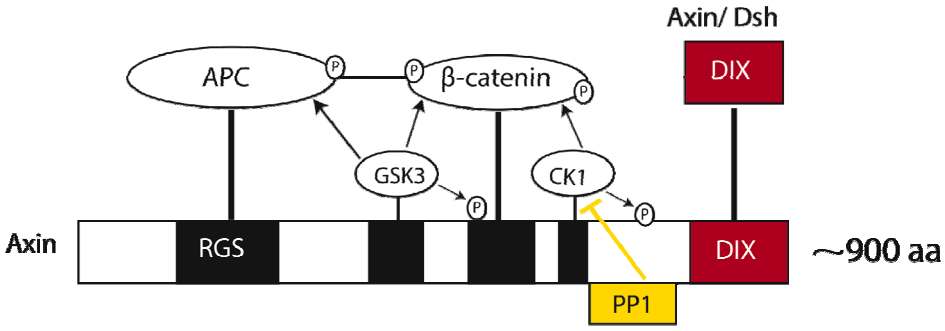
Axin/ Dsh
DIX
APC
β-catenin
GSK3
CK1
Axin
RGS
DIX
~900 aa
PP1

C

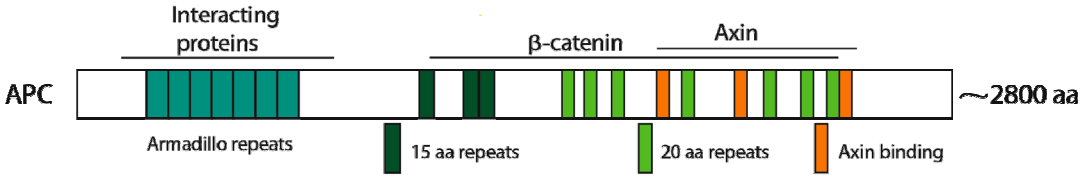
Interacting proteins
β-catenin
Axin
APC
~2800 aa
Armadillo repeats
15 aa repeats
20 aa repeats
Axin binding

1.2.4 Armadillo

Armadillo is a large, 843 amino acid protein with multiple conformations, functions and binding partners (Fig 1.8 A). The degradation complex, promoting its ubiquitylation and degradation, regulates cytoplasmic levels of Armadillo. Upon Wnt signalling the degradation complex is inactivated and active Armadillo/β-catenin accumulates in the nucleus to trigger transcription of target genes together with TCF transcription factors. In addition to requiring standard proteins such as histone acetyltransferases (CBP) and histone remodelling factors such as Brg-1 (Brahma-related gene-1) (Barker et al, 2001; Hecht et al, 1999; Takemaru & Moon, 2000), Wnt target gene transcription also requires Legless (Lgs), Pygopus (Pygo) and Hyrax (Hyx) (Fig 1.8 B). Lgs (mammalian BCL9) binds to the amino terminus of Armadillo and escorts it into the nucleus. In the nucleus it plays an essential role in transcription. The "naked" phenotype of embryos expressing constitutively active Armadillo (Arm^{S10}) is suppressed in the absence of *lgs*, leading to the "lawn of denticles" phenotype, indicative of no Wingless signalling (Kramps et al, 2002). The main task of Lgs is the recruitment and tethering of Pygo to Armadillo. *Pygo* is another segment polarity gene with a constitutively nuclear localization and acts as a transcriptional activator, enhancing Pangolin (TCF) target genes (Kramps et al, 2002). Hyx (mammalian Parafibromin) binds to Armadillo's C-terminus and is also a positive regulator of signalling as mutant clones in wing discs display loss of *Dll* expression (Mosimann et al, 2006). Hyx over-expression enhances Wingless signalling and prevents the formation of wing notches induced by dominant negative lgs^{17E}, suggesting it to act downstream of Lgs (Mosimann et al, 2006). A model of Wingless target gene activation proposed by Mosimann et al entails the binding of Hyx to Armadillo to mediate the recruitment of the PAF1-like complex (Polymerase associated factor 1), which is required for RNA polymerase II transactivation. Pygopus is thought to orchestrate the action of PAF1 and Hyx/ Parafibromin, indeed Pygo is found to co-immunoprecipitate with the Parafibromin-PAF1 complex and down regulation of hPygo by RNAi inhibits the increase in signalling attained with increased Parafibromin levels (Mosimann et al, 2006).

In addition to its role in signalling Armadillo is also required at cell junctions connecting DE-cadherin to α-catenin and the cytoskeleton (Cox et al, 1996; Orsulic & Peifer, 1996; Takeichi, 1995) (Fig 1.8 C). The weakening of cell junctions during Wingless signalling, required for cell proliferation, delamination and motility reflects

the crosstalk between cell adhesion and canonical Wingless signalling. Increased DE-cadherin levels attenuate signalling by promoting N-terminal phosphorylation of transcriptionally active Armadillo and by enhancing the activity of junction localized degradation complexes (Maher et al, 2009). Proteolytic cleavage of E-cadherin, on the other hand, leads to reduced cell adhesion, and translocation of β-catenin to the nucleus for gene transcription (Huber & Weis, 2001).

The relative distribution of Armadillo between junctions and the nucleus may be regulated interdependently or independently. Overlapping regions of Armadillo are required for both cell adhesion and signalling, thus the choice of binding partners, Lgs vs α-catenin, may direct its function (Brembeck et al, 2004). Gottardi et al (Gottardi & Gumbiner, 2004), suggest that Wnt induces a conformational change of β-catenin, rendering it signalling competent. Depending on the number of arm repeat domains obstructed by the folding back of β-catenin's C terminus determines preferential binding of TCF vs E-cadherin. TCF binding requires the 8 central motifs (3 to 10) whereas E-cadherin binding involves all 12 repeats (Gottardi & Gumbiner, 2004; Huber & Weis, 2001). Furthermore, having 14 phosphorylation sites β-catenin has multiple conformations some of which may be specialized for transcription or cell-cell adhesion. Phophorylation at Ser-45 Thr-41, Ser-37 Ser33, for example, promotes β-catenin degradation, phosphorylation at Thr-41, Ser-37 promotes transcription, while Armadillo phosphorylated at Ser-45 Thr-41 co-immunoprecipitates with E-cadherin (Maher et al, 2010). In summary distribution of β-catenin/Arm is directed by its binding partners, its conformation and phosphorylation sites.

It was initially thought that the increased cytoplasmic pool of Armadillo upon Wingless induced stabilization instigated signalling. It is now clear, however, that cytoplasmic Armadillo levels do not necessarily correlate with signalling. The majority of transcriptionally active Armadillo resides at the cell membrane (Hendriksen et al, 2008; Maher et al, 2009). One model proposes the membrane recruitment of β-catenin to a Wnt receptor complex is the initial and activating step of β-catenin upon Wnt stimulation. Indeed, cells expressing active ΔN-LRP6 (N terminally cleaved LRP6) display predominant membrane localization of endogenous β-catenin and signal equally strongly as cells over-expressing β-catenin. Thus a minor pool of β-catenin at the membrane is as active as an elevated cytosolic pool. It may be that the conformational changes required for activation, described

above, occur at the cell surface (Hendriksen et al, 2008). Receptor dependent activation also provides a more refined control of signalling, as receptor inactivation is more effective than degradation complex regulation. Although an additional study describes membrane localization as a requirement for β-catenin activation, it is suggested to depend on specific interactions with E-cadherin. β-catenin Y654E mutations that inhibit membrane localization of β-catenin decrease transcriptional read out, as does depletion of E-cadherin (Howard et al, 2011). This model partly contradicts the aforementioned function of E-cadherin in competitively binding β-catenin and inhibiting signalling. Howard et al., suggest that either over-expression or depletion of E-cadherin down-regulates signalling. Over-expression leads to high affinity binding to β-catenin thus limiting dissociation, whereas depletion leads to decreased activation. Therefore, optimal signalling is dependent on β-catenin/E-cadherin interactions. The effect of E-cadherin internalization and turnover is also thought to promote signaling, possibly due to the release of β-catenin from E-cadherin intracellularly. This will be discussed in more detail in Chapter 6.

Figure 1.8 Armadillo structure and function

(A) At the N terminus of Armadillo/β-catenin are the sites of GSK3/CKI phosphorylation, needed for its degradation. The central region consists of twelve armadillo repeats that bind proteins involved in Wnt signalling and cell adhesion. E-cadherin, involved in cell adhesion, binds to all twelve Armadillo repeats. In the degradation complex APC also occupies the twelve armadillo repeats. For signalling, TCF binds to eight central Armadillo repeats, while lgs and Hyx bind to the first four and the last two respectively. (Adapted from Bienz, 2005). (B) In the nucleus, transcription activator Pygo is recruited to TCF bound Armadillo/β-catenin by lgs/BCL9 and binds N terminally. Hyx binds to the C terminus to enable RNA polymerase II activation. (C) Armadillo has a role at adherens junctions bridging E-cadherin to α-catenin and actin filaments. Unbound Armadillo is either degraded or signals.

A

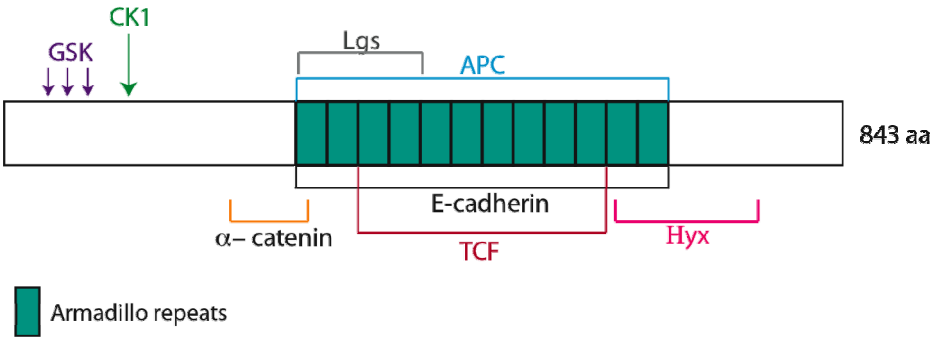
CK1
GSK
Lgs
APC
843 aa
E-cadherin
α– catenin
TCF
Hyx
Armadillo repeats

B

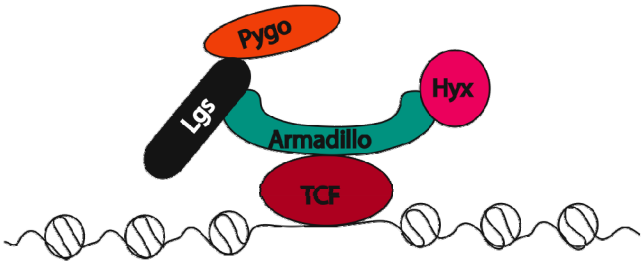
Pygo
Lgs
Armadillo
Hyx
TCF

C

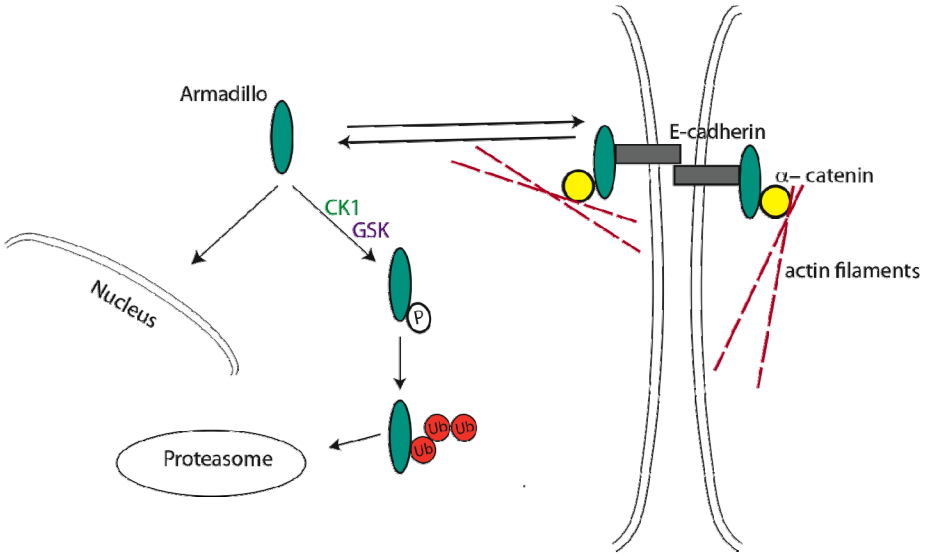
Armadillo
E-cadherin
α– catenin
CK1
GSK
actin filaments
Nucleus
P
Ub
Ub
Ub
Proteasome

1.3 Endocytosis and Signalling

Endocytosis is a highly dynamic and co-ordinate cellular process that allows cells to take up nutrients, regulate plasma membrane homeostasis, interpret extra-cellular cues and regulate signalling. With regards to signalling, endocytosis was originally considered a mere attenuator, targeting receptor/ligand complexes to lysosomes. It is now clear that endocytosis plays a prominent role in both the generation and propagation of signals.

1.3.1 Endocytic pathway

1.3.1.A. Clathrin/Caveolin mediumted endocytosis

There are various endocytic processes. Phagocytosis and macropinocytosis, which involve bulk internalization of cargo or fluids and require extensive membrane and cytoskeleton re-modelling. Clathrin and caveolin mediumted endocytosis, which is what I will describe, are of a smaller scale and require specific molecules for vesicle formation and detachment from the cell membrane.

Clathrin mediated endocytosis is the best understood process to date. It consists of the formation of clathrin coated vesicles of 100-200nm in diameter. Clathrin is a triskelion composed of three heavy and three light chains. With adaptor protein AP-2, clathrin forms a clathrin lattice along the plasma membrane. Various other accessory proteins function in target recognition, membrane curvature and vesicle budding (Fig 1.9 A). Epsin, in addition to stabilizing the clathrin assembly, induces membrane curvature via interaction with PtdIns(4,5)P2 on the inner layer of the plasma membrane. Endophilin and amphysin also facilitate membrane bending and in conjunction with dynamin mediate vesicle severance from the plasma membrane. The function of dynamin (called *shibire* in *Drosophila*) was initially determined via the analysis of vesicle formation using *shibire*^{ts} mutants. High temperatures led to an increase in pit-like structures but a decrease in vesicle formation (Kosaka & Ikeda, 1983), thus attributing to dynamin the role of vesicle scission. GTP hydrolysis mediates this event by driving dynamin oligomerization, hence the formation of a

ring around the collar of the budding vesicle. Constriction and twisting of this ring mediates the 'pinching off' of vesicles from the cell surface (Bashkirov et al, 2008; Danino et al, 2004; Roux et al, 2006) (Fig 1.9 A). In addition to endocytic vesicle formation, dynamin also plays a role in intracellular trafficking, which will be addressed in this thesis.

Caveolae are described as flask-shaped membrane invaginations. In vertebrates their principal component is caveolin, an integral membrane protein that directly binds to and is dependent on membrane cholesterol. Protein polymerase 1 transcript release factor (PTRF), also known as cavin, is also a caveolar component, whose interaction with the cytoskeleton mediates caveolae formation and stability (Briand et al, 2011; Liu & Pilch, 2008). Caveolae can also be formed in the absence of caveolin with flotillin, another integral membrane protein and structural component of caveolae membranes (Bickel et al, 1997). The lack of a caveolin gene in *Drosophila* suggests that caveolae formation relies primarily on flotillin. There are two flotillin-related genes expressed in *Drosophila* (Galbiati et al, 1998). As with clathrin mediated endocytosis, caveolae mediated internalization also requires dynamin and additional Src-family kinases for membrane budding (Frick et al, 2007; Sverdlov et al, 2007).

1.3.1.B. Endosomes

Once internalized, vesicles interact with early endosomes in a Rab5 dependent manner. Rabs are GTPases located on different membrane compartments involved in vesicle formation and membrane fusion. Early endosomes are the sorting centre of endocytic pathway directing proteins to recycling or degradation. They are located in proximity to the plasma membrane and have a complex structure with vacuolar and tubular domains. The tubular domains give rise to recycling endosomes, which are marked by Rab4/Rab11. These structures recycle proteins back to the plasma membrane and also to the trans-golgi-network, thereby supplying the secretory pathway. Proteins to be degraded are localized in vacuolar domains of early endosomes, which develop into late endosomes (Fig 1.9 B). This process involves multiple steps: 1) Late endosomes accumulate Rab7. It has been suggested that Rab5 recruits Rab7 to early endosomes creating a Rab5/7 endosome from which Rab7 domains arise to generate late endosomes (Gruenberg & Stenmark, 2004). 2) Luminal acidification, mediated by V-ATPases proton pumps, is required for

hydrolytic reactions (Mesaki et al). 3) Generation of multi vesicular bodies (MVB). This process sorts proteins for degradation and also silences signalling by removing the intracellular domains of receptors from the cytosol. MVB formation involves inward budding of vesicles from the late endosomal membrane by the sequential activity of ESCRT (Endosomal Sorting Complex Required for Transport) complex -0, -I, -II, III. Two proteins form the ESCRT-0 complex: Hrs (Hepatocyte growth factor-Regulated tyrosine kinase Substrate) and STAM (Signal-Transducing Adaptor Molecule). Hrs binds to endosomal phosphatidylinositol 3-phosphate thus recruiting ESCRT-0 to endosomal membranes, where Hrs and STAM both recognize ubiquitylated proteins and direct them onto the surface of maturing MVB. Hrs also recruits ESCRT-I to endosomes via interaction with one of its subunits, Tsg101 (other subunits: Vps28, Vps37, Mvb12). ESCRT-I Vps28 binds to ESCRT-II Vps36 (other subunits: Vps22, Vps25), which mediates membrane invagination and recruitment of ESCRT-III. The ESCRT-III subunits, Vps20, Vps32, Vps24 and Vps2 sequentially activate each other and form spiral shaped filaments around the neck of the forming vesicle. Recruitment of Vps4 results in constriction of the filaments and membrane abscission. Prior to abscission ESCRT-III recruits deubiquitylating enzymes that deubiquitylate endosomal cargo so that ubiquitin is recycled (Fig 1.9 C) (Rusten et al, 2012).

1.3.1.C. Lysosomes

Upon completion of MVB formation, late endosomes interact with lysosomes, characterized by lysobisphosphatidic acid (LBPA) and Lysosomal associated membrane proteins (LAMPs), in which degradation occurs. Transfer of MVB contents to lysosomes is mediated by direct fusion as well as transient fusion named "kiss-and-run". Direct fusion occurs via tubules derived from the lysosome that bind to the late endosome, thus forming a hybrid compartment in which degradation occurs (Bright et al, 2005; Luzio et al, 2003). Lysosomes then reform from the hybrid compartment and export digested products. Thus entitling direct fusion as the "fusion-fission" model. Lysosomes and late endosomes can also interact transiently, maintaining separate compartment identity (kiss and run). This allows transient cargo exchange, which is described as kissing events and at times precedes complete fusion (Bright et al, 2005).

Figure 1.9 The endocytic pathway

(A) Diverse internalization routes: clathrin mediated, caveolin mediated and flotillin mediated, all of which require dynamin for membrane scission (Adapted from Kumari et al, 2010). (B) Regardless of the above mentioned internalization routes, vesicles converge in early endosomes in a Rab5 dependent manner. From early endosomes, proteins can recycle back to the cell surface or remain in early endosomes, which mature into late endosomes with accumulation of Rab7, luminal acidification and MVB formation. Late endosomes interact both transiently and by direct fusion with lysosomes, in which degradation occurs. (Adapted from Huotari & Helenius, 2011). (C) MVB formation in late endosomes is mediated by ESCRT complexes. ESCRT 0 recognizes ubiquitylated cargo to be degraded and recruits ESCRTI and ESCRTII, which mediate membrane invagination. ESCRT III forms a spiral around the budding vesicle and recruits DUBs to deubiquitylate cargo. Vps4 mediates membrane scission by promoting constriction and disassembly of ESCRTIII. (Adapted from Rusten et al, 2012).

A

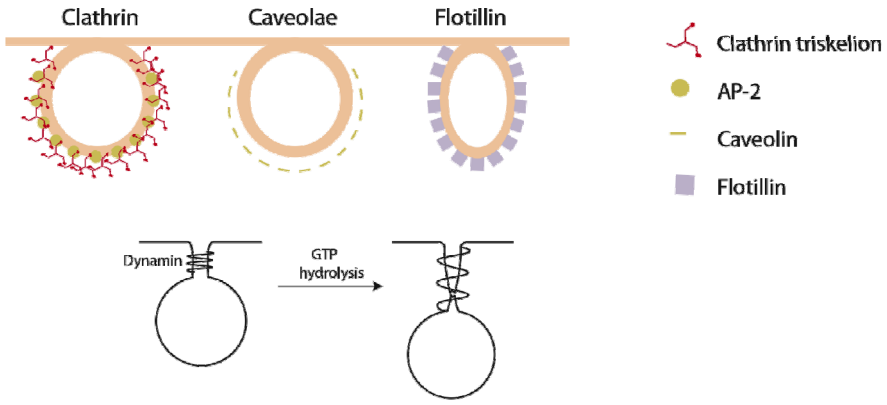
Clathrin
Caveolae
Flotillin
Clathrin triskelion
AP-2
Caveolin
Flotillin
Dynamin
GTP
hydrolysis

B

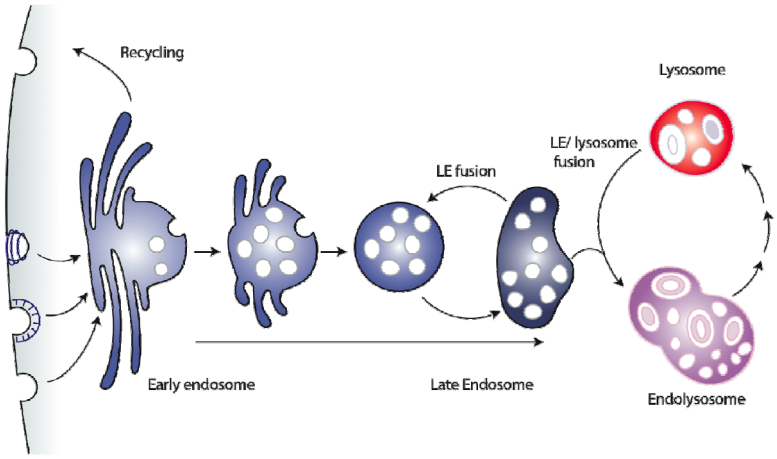
Recycling
Lysosome
LE/ lysosome
fusion
LE fusion
Early endosome
Late Endosome
Endolysosome

C

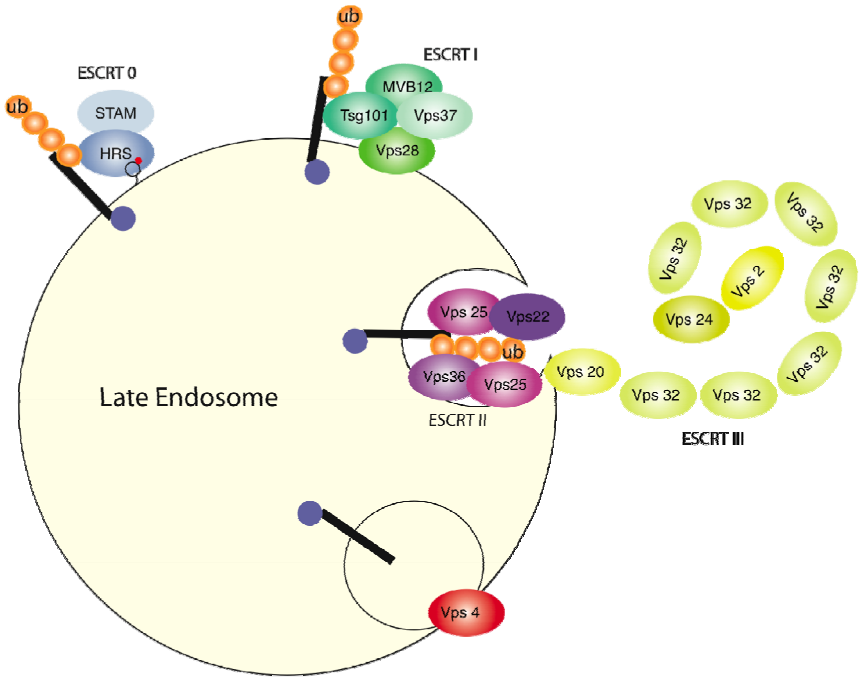
ub
ESCRT I
MVB12
Tsg101
Vps37
Vps28
ESCRT 0
ub
STAM
HRS
Late Endosome
Vps 25
Vps22
ub
Vps36
Vps25
ESCRT II
Vps 20
Vps 32
Vps 32
Vps 32
Vps 2
Vps 32
Vps 24
Vps 32
Vps 32
Vps 32
ESCRT III
Vps 4

1.3.2 Signalling pathways involving endocytosis

1.3.2.A. Notch signalling pathway

Activation of the Notch signalling pathway and endocytic sorting of Notch and its ligands exemplifies the function of endocytosis in signal activation and regulation. The Notch pathway is conserved throughout the animal kingdom and functions in cell specification, lateral inhibition and boundary formation in development (Bray, 1998; Bray, 2006; Ehebauer et al, 2006). Notch is a single-pass transmembrane receptor whose activation is juxtacrine as its ligands, Delta and Serrate (in *Drosophila)* are also transmembrane proteins. The interaction between Notch and its ligands leads to two cleavage events. The first (S2), which is a pre-requisite for the second, occurs in the Notch extracellular domain (ECD) and is catalyzed by ADAM (A Disintegrin And *M*etalloproteinase)-family metalloproteinase (Bray, 2006). The second cleavage (S3), mediated by γ-secretase, releases the Notch intracellular domain (ICD), which translocates to the nucleus and activates transcription in a complex with DNA binding protein CLS and its co-activator Mastermind (Fig 1.10 A).

Notch signalling requires the internalization of both the ligands and the receptor (Hansson et al, 2010). Dynamin inhibition in both signal sending and receiving cells inhibits Notch activity (Parks et al, 2000; Seugnet et al, 1997). There are currently two, non-mutually exclusive, models that explain the role of ligand endocytosis in signal activation: the ligand activation model and the pull force model. In the first model the ligand remains inactive until endocytosed and recycled back to the plasma membrane. The mechanism of activation is not yet known however recycling inhibition with dominant negative Rab11 compromises Notch signalling (Emery et al, 2005; Rajan et al, 2009). In the pulling force model, ligand-receptor interaction generates a pulling force resulting in the transcytosis of the Notch ECD as a complex with its ligand into the signal sending cell. The “pulled” Notch receptor is then a substrate for ADAM-family metalloproteinase cleavage (Nichols et al, 2007; Parks et al, 2000).

With regards to Notch itself, the principal debate concerns the requirement of endocytosis for S3 cleavage. It has been suggested that Notch intracellular trafficking is required so that Notch is brought into contact with presenilin, a component of γ-

secretase complex, which is located on endocytic compartments. *Drosophila Rab5* mutants showed less γ-secretase activity and thus reduced Notch S3 cleavage, while receptor accumulation on MVB due to Tgs101 or Vps25 loss of function lead to increased γ-secretase activity, revealing more efficient Notch activation intra-cellularly (Gupta-Rossi et al, 2004; Vaccari et al, 2008; Vaccari et al, 2009). Other studies claim that endocytosis negatively regulates Notch signalling (Sorensen & Conner, 2010; Tagami et al, 2008). Different forms of Notch ICD are generated by different S3 cleavages at distinct subcellular localizations. S3 cleavages at the plasma membrane give rise to a more stable and active form of Notch ICD, while a weaker form is produced in endosomes. Thus the intensity of Notch signalling may be regulated by the rate of endocytosis, with increased transactivation in cells with reduced endocytosis (Tagami et al, 2008).

1.3.2.B. TGFβ signalling pathway

The current discussions regarding endocytic regulation of TGFβ signalling are reviewed in (Chen, 2009). They not only address the involvement of endocytosis in signal induction but also the concept of 'two routes-two outcomes'.

TGFβ is a 25kDa cytokine, part of the TGFβ superfamily that regulates multiple cellular processes such as proliferation, differentiation and apoptosis. TGFβ binds to a heteromeric receptor complex made of type I and II serine/threonine protein kinases. Upon binding, constitutively active type II kinase phosphorylates type I, which in turn phosphorylates receptor regulated Smads, Smad 3 and Smad 2. Recruitment of Smads to the receptors is facilitated by SARA (Smad Anchor for Receptor Activation), which possesses not only a Smad-binding domain but also a FYVE domain, allowing it to interact with EEA1 (Early Endosome Antigen1)-positive and Rab5 containing endosomes (Massague, 1998; Tsukazaki et al, 1998; Wu et al, 2000). Translocation of Smads2 to the nucleus to regulate gene transcription is mediated by Smad 4, which binds to phosphorylated Smad 2 in the heteromeric complex (Fig 1.10 B).

To assess the effects of endocytosis on TGFβ signalling, internalization was inhibited in different ways: a decrease in temperature, dynamin mutation or potassium depletion, which specifically inhibits clathrin mediated endocytosis (Carpentier et al, 1989; Yumoto et al, 2006). TGFβ receptor (TGFβ-R) activation and TGFβ-

R/Smad/SARA complex formation is unaffected by endocytosis inhibition. This is shown by co-immunoprecipitation of TGFβ-R with both Smad and SARA. Smad2/Smad3 activation, on the other hand, is compromised as shown by a marked decrease in phosphorylation and impaired nuclear translocation, suggesting that activation occurs in an endocytic compartment (Penheiter et al, 2002). While Runyan et al (Lu et al, 2002; Runyan et al, 2005) confirmed that TGFβ-R/Smad/SARA complex formation does not depend on endocytosis, the requirement of endocytosis for Smad2 phosphorylation was not detected (Lu et al, 2002; Runyan et al, 2005). Reduction of signalling in response to the inhibition of endocytosis was attributed to impaired dissociation of Smad2 from SARA thus preventing Smad2 translocation to the nucleus and transcription activity (Runyan et al, 2005; Xu et al, 2002). It has therefore been shown, although not conclusively, that clathrin mediated endocytosis has a positive role in signalling.

As endocytosis consists of multiple internalization routes, a signalling pathway can be affected by endocytosis in different ways depending on the route taken. As mentioned above clathrin mediated endocytosis of the TGFβ receptor promotes signalling, caveolae mediated endocytosis, on the other hand, was shown to have the opposite effect. Receptors in lipid rafts recruit the inhibitory Smad7 and the ubiquitin ligase Smurf2 (Smad ubiquitylation regulatory factor 2), leading the receptors to proteasomal degradation (Di Guglielmo et al, 2003). Interference with caveolae internalization with Nystatin, which titrates cholesterol, increases signalling and receptor half-life from 1.5hr to 4.5hr (Di Guglielmo et al, 2003). Therefore whether the receptors traffic through clathrin coated pits or lipid rafts determines the outcome of the TGFβ pathway. Clathrin inhibition blocks ligand endocytosis and signalling but does not affect receptor internalization, which displays increased localization to membrane lipid rafts. Caveolae inhibition interferes with receptor degradation, thus potentiating signalling. (Di Guglielmo et al, 2003). Protein Kinase C (PKC) regulates such trafficking decisions, as inhibition increases the proportion of TGFβ in endosomes and phosphorylated Smad2 levels, while over expression results in increased receptor degradation presumably via a caveolar route (Gunaratne et al, 2012). In conclusion, endocytosis has dual function in the TGFβ pathway, affecting signalling both positively and negatively depending on the internalization route taken (Fig 1.10 B).

Figure 1.10 Endocytosis in Notch and TGFβ signalling.

(A) In the Notch signalling pathway, signal sending cells present the transmembrane ligands Dl/Ser to signal receiving cells. Two cleavage events (S2, S3) are then needed to release the ICD of the Notch receptor for signalling. There are two models for the role of endocytosis in initiating signalling (1). In the first model, recycling of the ligands is required to activate them. In the second, the ligand "pulls" the ECD of Notch and both are endocytosed into signal sending cells. Only after removal of the ECD is the Notch receptor susceptible to S2 cleavage. Whether S3 also requires endocytosis is not clear (2). γ-secretase cleavage of the receptor may take place at the plasma membrane or in endosomes. (B) The outcome of TGFβ signalling depends on the internalization route taken. Clathrin mediated endocytosis has a positive role in signalling. Upon ligand binding, receptors are phosphorylated and in turn phosphorylate receptor Smads (Smad2/3) that are recruited to the receptors by SARA. After activation and internalization, Smad4 escorts Smad2 to the nucleus for transcription. Caveolae mediated endocytosis of receptors in lipid rafts has a negative role in signalling with the recruitment of Smad 7 and ubiquitin ligase Smurf2 to the receptors leading to receptor degradation.

A

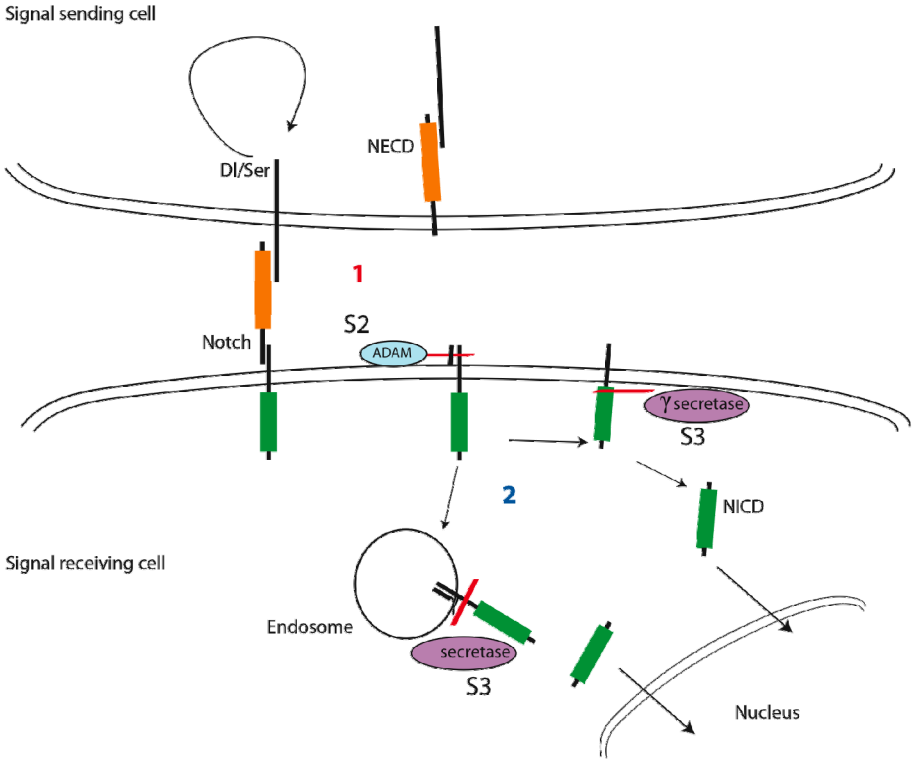
Signal sending cell
Dl/Ser
NECD
1
S2
Notch
ADAM
γ secretase
S3
2
NICD
Signal receiving cell
Endosome
secretase
S3
Nucleus

B

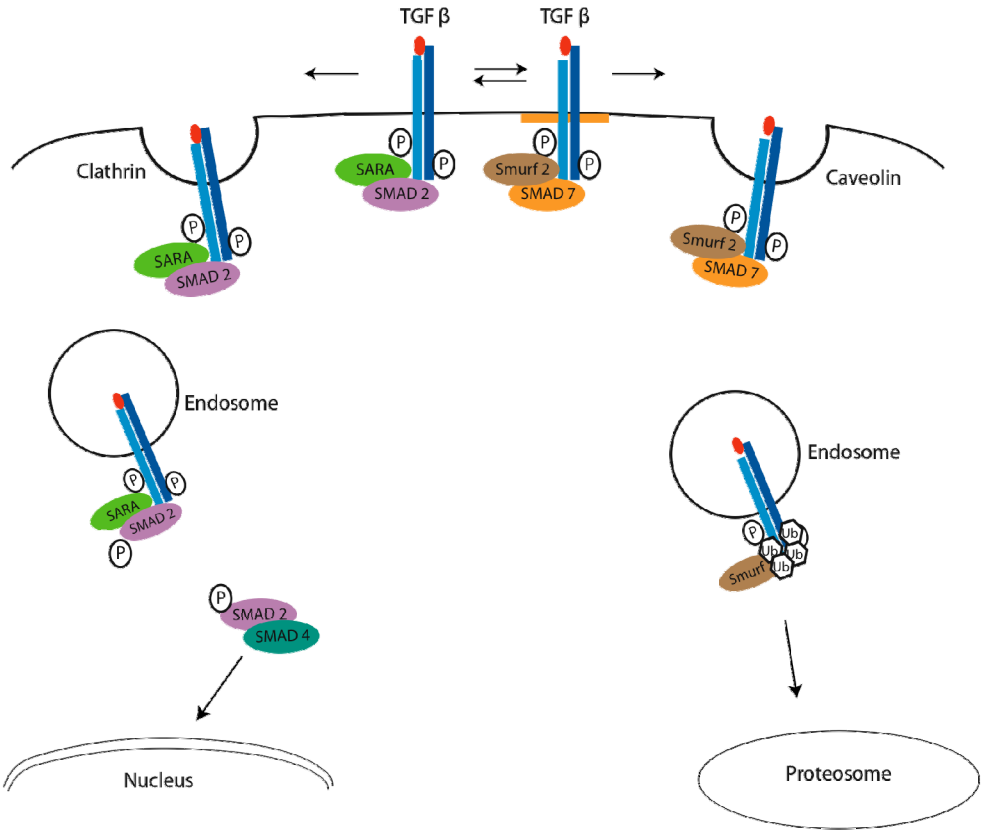
TGF β
TGF β
Clathrin
SARA
SMAD 2
Smurf 2
SMAD 7
Caveolin
Endosome
SMAD 2
SMAD 4
Nucleus
Endosome
Ub
Proteosome

1.3.3 Endocytosis in Wingless/Wnt signalling

The question of whether endocytosis inhibits or promotes Wingless/Wnt signalling is yet unanswered and controversial. The most convincing evidence for its requirement was obtained by assessing signalling in cultured mammalian L cells in which internalization was inhibited. A Wnt luciferase reporter showed a decrease in signalling and a Western blot showed no rise in β-catenin levels, thereby demonstrating that endocytosis is required for signalling (Blitzer & Nusse, 2006). Further evidence comes from experiments involving dynamin loss of function. In cells, dsRNA against dynamin or expression of K44E mutated dynamin prevents signalling (Blitzer & Nusse, 2006; Seto & Bellen, 2006). Likewise in wing discs shi^{DN} expression shows a significant decrease in signalling (Seto & Bellen, 2006). Having determined that internalization is required for Wingless/Wnt signalling, it then became necessary to identify the endocytic compartments involved in signalling.

Early endosome function was assessed by knockdown of *rab5* in $S2R^{+}$ cells. This resulted in a 93% decrease in signalling (Seto & Bellen, 2006). An earlier study gave opposite results, with an increase in signalling (Rives et al, 2006). The discrepancy was attributed to the use of different normalizing constructs in the signalling reporter. The role of endosomal trafficking in Wingless signalling was assessed in vivo by expressing dominant-negative *rab5* in wing imaginal discs. This led to a reduction in signalling, shown by the decreased expression of *senseless* and *distalless*. Conversely, over-expression of dominant active *rab5* caused signalling enhancement, thus suggesting that endosomal transport positively regulates signalling. (Seto & Bellen, 2006). Rives et al. also observed a decrease in signalling when expressing dominant negative *rab5*, however they were unable to draw the same conclusions as inhibition of *rab5* caused disruption of *engrailed* expression, which is not controlled by Wingless signalling in imaginal discs. Reduced *engrailed* expression suggests that reduced signaling may be due to the poor health of the cells. Indeed many cells over-expressing $rab5^{DN}$ were caspase immunoreactive (Rives et al, 2006). Accordingly, decreased *senseless* and *distalless* expression could be due to a non-specific toxic effect of early endosomal inhibition. Seto and Bellen reported no increase in apoptosis, thus the effect of Rab5 removal on signalling remains ambiguous. Interestingly it has recently been suggested that Rab5 recruitment via $G\alpha_o$ to Fz receptors regulates Fz endocytosis and activation of both canonical and

PCP signalling. Inhibition of Rab5 independently decreases both canonical and PCP signalling while over expression enhances both. This increase in canonical signalling, however, is inhibited by co-expression of both Rab5 and recycling Rabs (Rab4/11), which favours only the PCP pathway. Therefore downstream trafficking post Rab5-mediated internalization determines which pathway is activated. A model has arisen where activation of Rab5 recruited to Fz receptors leads to accumulation of Fz in endosomes and canonical signalling, whereas recruitment of Rab5 in conjunction with Rab4 induces Fz recycling, supporting PCP signalling (Purvanov et al, 2010). Thus Rab5 dependent endocytosis regulates both canonical and PCP signalling.

The signalling role of Hrs, which is involved in the formation of MVBs, was also tested. *Hrs* mutant clones in wing discs again gave conflicting results. It has been suggested that Hrs terminates signalling as *senseless* and *distalless* expression are increased in mutant clones and decreased following Hrs over-expression (Seto & Bellen, 2006). This suggests that early endosomes would be the compartment where Wingless signalling takes place. This is disputed by Rives et al and Piddini et al, who observed no change in Wingless target gene expression following *hrs* loss of function (Piddini et al, 2005; Rives et al, 2006). Unaltered signalling levels despite endosomal accumulation of Fz2, Wingless and Arrow suggest that signalling is attenuated prior to lysosomal targeting.

In contrast to Seto's observation, Taelman et al, observed that RNAi against Hrs and other ESCRT components, led to a decrease in signalling (Taelman et al, 2010). This has led them to suggest a novel model for the role of trafficking in Wnt signalling, in which Hrs is required to sequester GSK3 into MVBs. This would constitute a novel mechanism of GSK3 regulation (Taelman et al, 2010). Although an attractive model, an earlier experiment calls it into question. The activation of signalling induced by the inhibition of GSK3 was still prevented with the inhibition of endocytosis. Therefore it appears that endocytosis affects Wingless signalling at a step of the pathway that lies downstream of GSK3 (Blitzer & Nusse, 2006). The role of Hrs is addressed in my work in Chapter 6.

1.4 Ubiquitylation

1.4.1 Ubiquitylation machinery

Ubiquitylation is a highly conserved post-translational modification that modulates both protein stability and trafficking behaviour. The fact that ubiquitin is highly conserved from yeast to humans is testimony of its functional importance (Haglund & Dikic, 2005; Mosesson & Yarden, 2006). Ubiquitin (Ub) is an 8 kDa protein that is covalently attached to specific lysine residues of target proteins. Ubiquitylation involves a three step ATP-dependent process involving Ub-activating enzymes (E1), Ub-conjugating enzymes (E2) and Ub-ligating enzymes (E3). There are two types of E3s, characterized by the presence of either a HECT domain or RING finger domain. HECT domain (Homologous to the E6-AP Carboxyl Terminus) E3s form a bond with ubiquitin and then transfer it onto substrates, whereas RING finger E3s mediate the direct transfer of ubiquitin from E2s to the substrate. E3s are responsible for substrate specificity (Hershko & Ciechanover, 1998) (Fig 1.11). Ub itself has 7 lysine residues (K6, K11, K27, K29, K33, K49, K63) allowing the formation of chains of various configurations and therefore diverse protein modifications and fates. K48-linked polyubiquitin chains, for example, target proteins to proteosomal degradation whereas K63-linked polyubiquitin chains regulate membrane trafficking and protein kinase activation (Adhikari & Chen, 2009; Johnson, 2002). Ubiquitylation is reversed by de-ubiquitylating (DUBs) enzymes. De-ubiquitylation can be complete or partial. Partial removal can lead to the formation of different ubiquitin conjugates that trigger different cellular process (Hershko & Ciechanover, 1998).

The most classically described role of ubiquitylation is that it provides a signal for protein degradation by the 26S proteosome. In this case target, proteins are polyubiquitylated by a series of Ub molecules chained together via Lysine-48. Recently, however, the non-proteolytic functions of ubiquitin have been attracting attention, particularly with regards to signalling and trafficking. Related to ubiquitin is SUMO (small ubiquitin-related modifier). SUMO has a similar structure to ubiquitin and is attached to proteins in the same manner. Unlike ubiquitylation, SUMOylation does not target proteins for degradation. Rather, it regulates protein-

protein interactions, cellular localization and protein stability (reviewed in Gareai, JR 2010).

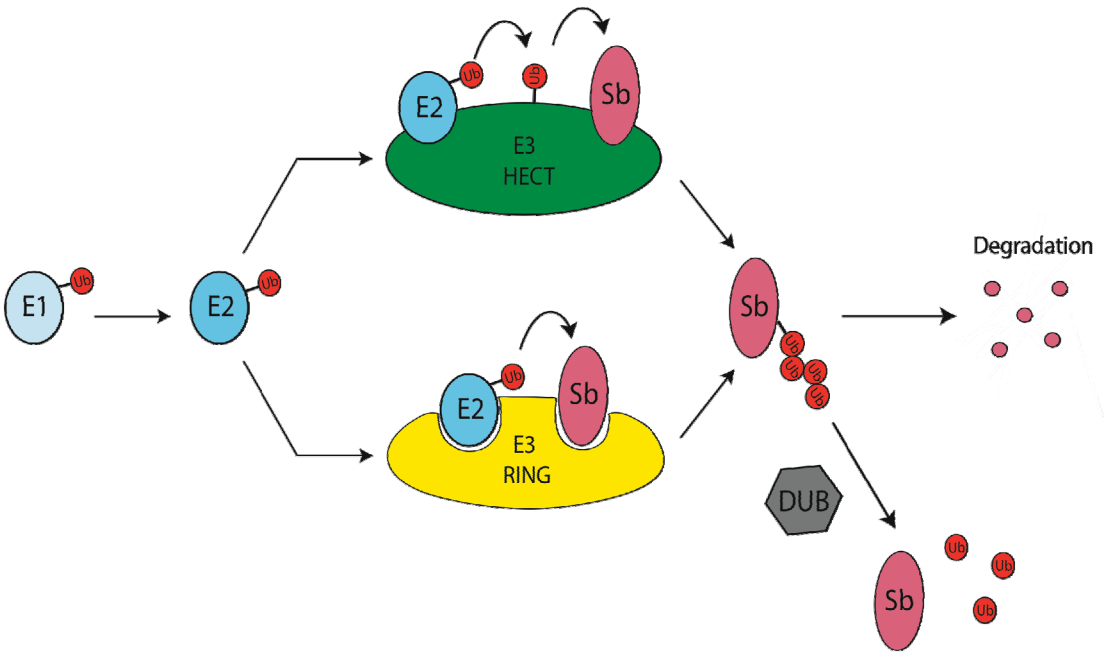

Figure 1.11 The ubiquitylation machinery.

The covalent attachment of ubiquitin to target proteins involves three consecutive enzymatic reaction. Initially the E1 activating enzyme forms a high energy thioester bond with ubiquitin. The bound ubiquitin is then transfered to the E2 conjugating enzyme. The E3 ligases recognize protein substrates (Sb) and catalyze the transfer of ubiquitin from E2 onto the substrate. There are two classes of E3 ligases. One class has a HECT domain, which forms a thioester bond with the ubiquitin from E2s and then transfers the ubiquitin onto the substrate. A second class has a RING finger domain and is capable of interacting with both E2 and the substrate. Ubiquitin is directly passed from the E2 onto the substrate. Substrates that are polyubiquitylated undergo proteosomal degradation. Ubiquitylation is reversible, by deubiquitylating (DUB) enzymes, which cleave poly-ubiquitin chains or ubiquitin conjugated protein. (Adapted from Ou et al, 2003).

1.4.2 Ubiquitylation in signal transduction

Ubiquitylation has dual functions in the TGFβ signalling pathway, depending on which signalling component is ubiquitylated. Signalling is negatively regulated by the ubiquitylation and degradation of Smads 2/3 and the receptors. As previously mentioned the receptors are modified by E3 ligase Smurf2. Smurf2 is nuclear, however binding to Smad7 induces its nuclear export and recruitment to the receptors, which are then ubiquitylated and degraded (Kavsak et al, 2000). Ubiquitylation of Smad7 has the opposite effect and enhances signalling. The E3 ligase Arkadia has been shown to interact with Smad7 and induce its degradation both in the cytoplasm and nucleus, thus amplifying signalling by inhibiting receptor degradation (Liu et al, 2007). This shows that different E3 ligases have different roles in signalling regulation (reviewed in (Inoue & Imamura, 2008).

Signalling can also be regulated by the modification of proteins with different types of ubiquitin chains. NF-κB (*Drosophila* Relish) is part of a conserved family of 5 transcription factors, which are activated by different cytokines involved in innate immunity, differentiation and apoptosis. Signalling depends on the activation of the IKK complex composed of IKKα, IKKβ and NEMO. This complex promotes the phosphorylation and degradation of NF-κB inhibitors. Upon activation of the TNFα receptor, NEMO is modified by two different ubiquitin chains: a Lys63 and a linear chain, in which ubiquitins are linked in a head to tail manner: C terminal Gly to N terminal Met residues (Hadian et al, 2011; Tokunaga et al, 2009). It has been suggested that Lys63 chains recruit NEMO to the receptors where there is a greater concentration of linear ubiquitin complexes. Linear ubiquitylation fully activates NEMO (Hadian et al, 2011; Tokunaga et al, 2009). Thus sequential binding of different ubiquitin chains optimises signalling.

Like ubiquitylation, SUMOylation also plays multiple roles in signalling regulation. It has recently been shown that SUMOylation contributes to G-protein coupled receptor (GPCR) internalization via arrestin modifications. SUMOylation of the adaptor protein β-arrestin by E2 Ubc9 is required to mediate interactions with endocytic components such as AP2 and clathrin. Therefore knockdown of Ubc9 specifically inhibits GPCR internalization (Wyatt et al, 2011).

Ubc9 is also involved in TGFβ signalling. SUMOylation of TβR I, facilitated by TβR II phosphorylation, enhances SMAD2/3 recruitment to the receptor and activation. In

addition to activating SMAD, SUMOylation affects TGFβ signalling by increasing SMAD4 stability, which is counteracted by ubiquitylation (Lee et al, 2003; Wan et al, 2004; Wang et al, 2008). Therefore, SUMOylation and ubiquitylation may have opposing effects on protein function providing a mechanism for the fine tuning of signalling regulation.

1.4.3 Ubiquitylation in the Wingless signalling pathway

The ubiquitylation and degradation of β-catenin/Armadillo is the hallmark of ubiquitylation's role in regulating Wnt/Wingless signalling. However, novel regulatory functions of ubiquitylation are now known.

1.4.3.A. Ubiquitylation

EDD (E3 ligase identified by differential display) (*Drosophila hyperplastic disc* (*hyd*)) has been identified as an E3 involved in ubiquitylation of β-catenin (Hay-Koren et al, 2011). EDD/Hyd is a nuclear protein with a key role in the DNA damage response, cell proliferation and spermatogenesis (Bartek et al, 2001; Henderson et al, 2002; Mansfield et al, 1994; Pertceva et al). Whether EDD suppresses or potentiates Wingless signalling is not yet clear. When complexed with GSK3, EDD ubiquitylates β-catenin, increasing its stability, nuclear localization and activity. In the absence of GSK3 ubiquitylation does not take place, perhaps because GSK3 dependent phosphorylation is required to prime β-catenin for ubiquitylation. In HEK293T cells, over-expression of EDD and GSK3 results in a three-fold increase in nuclear GSK3 (Hay-Koren et al, 2011). This nuclear translocation of GSK3 could deprive it from its negative role in signalling and direct it to positively regulate β-catenin. Indeed, over-expression of EDD abolishes the decrease in β-catenin levels caused by GSK3 over-expression. Thus EDD bestows GSK3 a dual role in Wnt signalling, as an inhibitor in the degradation complex and activator in the EDD ubiquitylation complex (Hay-Koren et al, 2011).

Previous studies have described EDD/Hyd as a suppressor of Wnt signalling. Knockdown of EDD in MCF-2 cells (Human breast adenocarcinoma cell line) enhances β-catenin levels (Ohshima et al, 2007) and hyd loss of function causes overgrowth of *Drosophila* imaginal discs (Mansfield et al, 1994). These conflicting results may be attributed to the use of different cell lines and experimental conditions, leaving the effect of EDD on β-catenin stability unresolved.

EDD may be indirectly affecting β-catenin levels, by ubiquitylating and stabilizing APC. EDD over-expression increases cytoplasmic APC levels, while knockdown dramatically reduces it (Ohshima et al, 2007). The cytosolic co-localization of APC and EDD is unexpected in light of the predominant nuclear localization of EDD,

however it is possible that APC translocated to the nucleus upon Wnt signalling sequesters EDD and escorts it to the cytoplasm. In consequence β-catenin stability is compromised and the increase in APC stability negatively regulates signalling. Therefore EDD targeting and function may be context dependent, aiding in both signal activation and suppression.

Axin is both ubiquitylated and SUMOylated. The "C6 motif", a 6 amino acid sequence (KVEKVD) at the C terminus, is the site of SUMOylation, which counteracts ubiquitylation thereby increasing Axin stability. Mutant Axin-ΔC6 displays greater poly-ubiquitylation and increased proteosomal degradation. It is not yet clear how Axin ubiquitylation/SUMOylation affects or regulates Wnt signalling. In addition the E3 ligase involved is not known (Kim et al, 2008).

Dishevelled is negatively regulated by ubiquitylation. The key proteins in this process are the Cullin-3 E3 ligase and KLHL12, a substrate specific adaptor. Wnt stimulation triggers KLHL12 mediated recruitment of Dsh to Cullin-3. KLHL12 over-expression inhibits Wnt signalling by increasing Dsh degradation whereas KLHL12 siRNA leads to signalling activation (as shown by a luciferase assay). This activation is prevented by dominant negative Cullin-3 thus showing that a KLHL12-Cullin-3 ubiquitylation complex is required to effectuate ubiquitylation/degradation, and antagonise signalling (Angers et al, 2006). It has recently been reported that an additional E3 ligase, Malin, ubiquitylates Dvl and antagonises Wnt signalling. Malin mutations cause a severe form of progressive epilepsy, implicating aberrant Wnt signalling in this disease (Sharma et al, 2012).

1.4.3.B. DUBs

Specific proteins have been implicated in the de-ubiquitylation of Axin and APC. Surprisingly this does not seem to counteract their proteosomal degradation instigated by ubiquitylation. The de-ubiquitylating enzyme (DUB) Trabid preferentially cleaves K-63 linked ubiquitin chains from APC. Trabid siRNA in the presence of Wnt decreases expression of target genes (*c-MYC*, *AXIN2*) without an apparent decrease in β-catenin levels. This suggests a role of APC de-ubiquitylation that bypasses β-catenin, although the underlying mechanism is not known. Since Trabid depletion also leads to enhanced APC nuclear localization, it has been suggested that Trabid could stimulate the nuclear export of APC. It has also been

suggested to play a part in exchanging co-activator for co-repressors in the regulatory region of TCF target genes. Moreover, Trabid may also regulate the formation and/or maintenance of the TCF-β-catenin complex (Tran et al, 2008).

Axin is de-ubiquitylated by USP34. This de-ubiquitylation increases its stability and similar to Trabid siRNA, USP34 depletion decreases signalling even in the presence of constitutively active β-catenin, suggesting it has a positive role in signalling downstream of the degradation complex. Like APC, Axin undergoes nucleo/cytoplasmic shuttling to ensure that it is removed from the nucleus in the absence of Wnt signalling (Wiechens et al, 2004). This observed together with the reduction of nuclear levels of Axin observed following USP36 knockdown suggests that Axin has a role in the nucleus that requires de-ubiquitylation. The precise function of nuclear Axin is yet not understood (Lui et al, 2011).

Ubiquitylation and de-ubiquitylation are also implicated in the regulation of Fz2. The E3 ligase responsible for ubiquitylation has not been identified, but UBPY (*Drosophila* dUBPY, CG5798) has been found to de-ubiquitylate Fz2. UBPY over-expression leads to maintenance of Fz2 at the cell surface and increased luciferase reporter activity while UBPY knockdown leads to a reduction in *senseless* expression and loss of sensory bristles in *Drosophila* wings. (Mukai et al, 2010). Mukai *et al* propose a model in which ubiquitylation of cell surface Fz2 leads to its internalization. Subsequent de-ubiquitylation would allow recycling back to the cell surface. Otherwise, ubiquitylated Fz2 would proceed to degradation. Recycling of Fz2 is suggested by the observation that it accumulates intracellularly following expression of dominant negative Rab11. Conversely, accumulation into Rab7 intracellular compartments upon knockdown of UBPY indicates degradation of ubiquitylated Fz2. The rate ubiquitylation/de-ubiquitylation appears to be unaffected by Wnt/Wingless stimulation and thus serves only to maintain appropriate cell surface Fz2 levels in receiving cells (Mukai et al, 2010).

1.5 Aims of the Thesis

The work presented in this thesis aims to contribute to the understanding of endocytosis and receptor trafficking in Wingless signalling.

Chapter 3 describes the optimization of the TOPFlash signalling reporter. This was required to achieve a more reliable readout of Wingless signalling. This tool eliminated variability that plagued previous studies.

Chapter 4 addresses the effect of Wingless on Arrow internalization and intracellular trafficking. Previous work had shown Arrow to be responsible for directing internalized Wingless bound Fz2 to degradation. My results suggest that whilst doing so Arrow is recycled back to the cell surface and is not degraded in response to Wingless signalling.

Chapter 5 assesses the role of ubiquitylation and de-ubiquitylation in Wingless signalling. It also asks whether this post-translational modification could affect Arrow trafficking. A small scale RNAi screen of E2s and DUBs was performed in $S2R^{+}$ cells using the optimized TOPFlash reporter. The roles of these enzymes were also assessed in vivo, using *dll* expression as a measure of Wingless signalling.

The role of endocytosis in Wingless signalling is explored in Chapter 6. Receptor internalization is found to be un-necessary. The key endocytic event appears to be downstream of the degradation complex. Levels of Armadillo expression are strongly reduced following treatment with Dynasore, a drug that inhibits dynamin function. Whether this is a result of increased degradation or compromised synthesis is assessed but not yet determined.

Materials and Methods

Chapter 2

"Cooking requires confident guesswork and improvisation--
experimentation and substitution, dealing with failure and uncertainty in
a creative way"

Paul Theroux
Sir Vidia's Shadow: A Friendship Across Five Continents (2001)

Chapter 2 - Materials and Methods

2.1 *Drosophila* Genetics

2.1.1 *Drosophila* Stocks

Table 2.1 Fly stocks used

Genotype	Stock information
General	
yw	Lab stock
Glbc / Cyo ; hhGal4 UASflp / TM6	Lab stock
arm lacZ M(2) / CyO	Lab stock
hrs^{D28}FRT40 / CTG	H.Chanut
enGal4 UASflp / CyO ; FRT2 ubiGFP / TM6	Lab stock
sgg^{D127} FRT101 / FM6	P Heitzler
ubiGFP FRT101	Lab stock
yw ; Pin/CyO ; UAS CD8GFP / TM3	Lab stock
Drivers	
w ; enGal4 / CyO	Lab stock
w ; apGal4 / GlBc ; UAS dicer/TM6	Lab stock
w ; enGal4 / GlBc ; UAS dicer/TM6	Lab stock
UAS lines	
UAS NRT wg/CyO	K. Basler
UAS HA wg	Lab stock
UAS arrow HA / TM6	Lab stock
UAS fz3 (I)	T. Kojima
Heat shock lines	
hs Gal4	Lab stock
hsFLP; Act > stop > Gal4 UASGFP	Lab stock
RNAi lines	
CG15437 Transformant ID: v11090	VDRC
CG7425 Transformant ID: v26011	VDRC
CG7425 Transformant ID: v26012	VDRC
CG2574 Transformant ID: v40173	VDRC
CG4443 Transformant ID: v34109	VDRC
CG4443 Transformant ID: v34111	VDRC
CG7220 Transformant ID: v34198	VDRC
CG7220 Transformant ID: v34199	VDRC
CG3018 Transformant ID: v33684	VDRC
CG3018 Transformant ID: v33685	VDRC
CG5794 Transformant ID: v27517	VDRC
CG1945 Transformant ID: v2955	VDRC
CG1945 Transformant ID: v2956	VDRC
CG1945 Transformant ID: v30679	VDRC
CG1945 Transformant ID: v30680	VDRC
CG3016 Transformant ID: v7090	VDRC
CG3016 Transformant ID: v110616	VDRC
CG4166 Transformant ID: v45775	VDRC
CG4166 Transformant ID: v45776	VDRC
CG14619 Transformant ID: v37929	VDRC
CG14619 Transformant ID: v37930	VDRC

2.1.2. Stocks

Stocks were maintained at 18°C and 25°C. Crosses were performed at 25°C in vials.

2.1.3 FRT/FLP Clones

The FRT/FLP technique was used to make clones in wing imaginal discs (Golic & Lindquist, 1989). Expression of FLP recombinase induces recombination between FRT sequences in a 'flip out' cassette. FRTs flank a transcriptional stop signal, which is placed between the upstream activating sequence (UAS) and gene of interest. Upon FLP expression the transcriptional stop signal is removed and desired gene expression is activated in clones of cells.

UAS NRT-HA-Wg / CyO ; UAS CD8GFP/ TM6b or *UAS HA-Wg / Cyo; UAS CD8GFP/ TM6b* were crossed with *hsFLP; Act > stop > Gal4 UAS GFP* females to produce *NRT-HA-Wg* and *HA-Wg* clones. 48 hours after egg laying larvae were heat shocked at 37°C for 8 min and then kept at the standard 25°C until late 3rd instar.

To generate *hrs* mutant posterior compartments, *hrs^{D28} FRT40/ CTG (*CyO-Twist-GFP) flies were crossed with flies of the genotype *armlacZ M(2)FRT40/GlBc; hhGal4 UASFlp/+*. All cells in the posterior compartment of the wing disc undergo mitotic recombination event giving rise to daughter cells that are either *hrs^{D28}-/-* or *Minute -/-*. *Minute* loss of function clones undergo apoptosis, therefore the whole posterior compartment becomes *hrs^{D28}-/-* marked and is marked by the absence of *lacZ.*

shaggy null clones were made using *sgg^{D127} FRT101;; engGal4 UASFlp* flies crossed with *ubiGFP FRT 101*. Again *sgg^{D127}* clones are solely induced in the posterior compartment and are marked by the absence of GFP.

2.1.4 Heat Shock induction

To produce wing discs over-expressing Arrow-HA uniformly, *hsGal4* flies were crossed with *UAS Arrow-HA/TM6.* 3rd instar larvae were heat shocked at 37°C for 35 min. Larvae were then allowed 1hr to recover at 25°C, before wing discs were dissected.

To assess protein ubiquitylation, S2R^{+} cells were transfected with Hs-Ub-HA. After 2 days they were treated with protesome inhibitor, MG132 (30μM), and a de-ubiquitylation enzyme inhibitor, N-ethylmaleimide (NEM, 1mM) and then heat shocked at 37°C for 35min. 2 hours post heat shock and 1 hour of Wingless

treatment, cells were lyzed and HA was immunoprecipitated using ProFound™ HA Tag IP/Co-IP Kit (Pierce)

2.1.5 Wing mounting

Flies of the desired genotype were collected and stored in isopropanol. Wings were dissected in isopropanol and mounted in Euparal (Agar Scientific) followed by incubation overnight at 65°C. Wings were analyzed and photographed with Zeiss Axiophot 2.

2.2 Immunofluorescense

2.2.1 Wing disc dissection and fixation

3rd instar larvae were dissected in PBS and extracted wing discs were transferred to PBS (Phosphate buffered saline) on ice. Discs were fixed in 4% PFA (paraformaldehyde) in PBS at room temperature for 20min and were then washed in PBS.

2.2.2 Wing disc Immunostaining

Fixed wing discs were permeabilised in 0.1% PBT (PBS-BSA-Triton: 0.2% bovine serum albumin (BSA) and 0.1% Triton-X in PBS) and then blocked for 1h at room temperature in 4% FCS (fetal calf serum) in PBT. After blocking they were incubated in primary antibodies, diluted in blocking buffer, overnight at 4°C. The following day the discs were washed in PBT and then incubated for 2 hr at room temperature in secondary antibody coupled to Alexa fluorophores (488, 555, 647) diluted in PBT. After incubation discs were again washed in PBT and mounted on slides in Vectashield. Slides were stored at 4°C.

2.2.3 Cell Immunostaining

Cells plated on coverslips were washed in PBS and fixed in 4% PFA for 10min. They were then washed in PBS, quenched with 50mM NH_4Cl/PBS for 10min, permeabilized for 10min with 0.1% Triton X-100, blocked for 30min with blocking solution (2%FCS-2%BSA in PBS) and subsequently incubated in the appropriate primary antibody diluted in 50% blocking solution in PBS for 1hour. After several washes in PBS, cells were incubated in Alexa conjugated secondary antibody, also diluted in 50% blocking solution in PBS for 30 min. Cell preparations were mounted onto slides using MOWIOL 4-88 reagent (Calbiochem) reconstituted following the protocol provided. Images were acquired using a Leica SP5 confocal microscope.

2.2.4 Dextran labeling

Cells were plated on coverslips and incubated in blocking solution (S2 cell serum free medium (Gibco) containing 1g/L glucose and 2%BSA) at 25°C for 1hr. Different concentrations of Dynasore were added to the solution for an additional

30min. The blocking solution was then replaced with fresh blocking solution containing 2mg/ml of dextran (Alexa 488 dextran. Invitrogen) and appropriate amounts of Dynasore. Cells were incubated for at least 2hr at 25°C, then washed in blocking solution and fixed in in 4% PFA. Coverslips were then mounted onto slides using MOWIOL 4-88 reagent (Calbiochem).

2.2.5 Image analysis

Images of stained wing discs and cells were obtained using a laser Leica SP5 scanning confocal microscope and analysed using Fiji software.

2.2.6 Live cell imaging

Chambered coverglass slides (Thermo Scientific 177445) were coated in a 0.001% Poly-L-Lysine solution (Sigma-P4707), in sterile water. After an overnight incubation in the hood, the poly-L-Lysine solution was aspirated and slides were washed 3 times with large amounts of sterile water of Poly-L-Lysine. 70% EtOH was used for a final wash and coated slides were allowed to dry. Cells were then plated as usual.

Cells were transfected with 0.5µg of pArm-GFP-Armadillo and 0.5µg of ptub-myristoyl-Cherry. 2 days after transfection, cells were plated in the chambers and were treated with Dynasore (200µM) or DMSO (200µM) as a control. Imaging was carried out on a DeltaVision RT fluorescence microscope Imaging System (Applied Precision Inc) at 2min time points for 1.5 hrs. Images were analysed using Fiji software.

2.3 Antibodies

Table 2.2 Antibodies used

Antibody	Dilution for Western blots	Dilution for Immunofluorescence	Origin / Reference
Mouse anti-Wingless	1/5000	1/500	DSHB, 4D9
Rabbit anti-GFP	1/1000	1/1000	Abcam, 6556
Chicken anti-GFP	-	1/500	Abcam, 13970-100
Mouse anti Armadillo	1/5000	1/500	DSHB N2 7A1
Guinea-Pig anti Arrow	1/8000	1/500	Suzanne Eaton
Mouse anti Actin	1/5000	-	DSHB JL20
Mouse anti Distalless	-	1/800	Dian Duncan
Chicken anti beta galactosidase	-	1/1000	Abcam 13970
Mouse anti lamin	1/10 000	-	DSHB ADL84.12
Mouse anti syntaxin	1/1000	-	DSHB 8C3
Rabbit anti GSK3	-	1/300	Abcam 18893
Rabbit anti LAMP	-	1/300	Abcam 24170
Mouse anti HA	-	1/500	Babco 101R
Rabbit anti Fz2	-	1/100	Raised against peptide 232-251
Guinea-Pig anti Senseless	-	1/500	Hugo Bellen
Guinea-Pig anti Hrs	1/20 000	-	Invitrogen 46-0705
Mouse anti-V5	1/5000	-	Invitrogen R960CUS
Rabbit anti-Caspase	-	1/50	Cell signalling 9662

Secondary antibodies were anti-mouse, anti-rat, anti-Guinea-pig and anti-rabbit Alexa-555, Alexa-488 or Alexa-633 (Molecular Probes). DAPI was used at 1/20000.

2.4 Cell culture

2.4.1. Cells

Table 2.3 cell lines

Cell Line	Obtained from	Function
S2 cells	Drosophila Genomic Research center (DGRC)	Schneider's cells, from a primary culture of late stage embryos.
S2 R^+ cells	DGRC	An early isolate of S2 cells that express Dfz2 and Dfz1.
S2 ptub-Wg cells	R.Nusse. Stanford University.	Used to provide a reliable source of Wg conditioned medium.
S2 GFP-Wg cells	Designed and made by Dr. Eugenia Piddini.	Designed to provide a source of GFP-Wg conditioned medium

All cells were cultured in T75cm^2 flasks in Schneider's medium containing 10% (v/v) FCS, 1% Penicilin/Streptomycin (P/S) and 1% L-glutamine. The medium was stored at 4˚C and warmed to 25˚C when needed for seeding or sub-culturing of cells. The cells were passaged every four days to prevent confluency.
DNA transfection was carried out using Effectene Transfection Reagent (Qiagen) following the procedure provided in the user manual.

2.4.2. Wingless conditioned medium

Due to the fact that S2 GFP-Wg cells produced conditioned medium with low and unstable activity, alternative sources were sought. S2 ptub-Wg cells, kindly provided by Roel Nusse, not only produced medium that, even un-concentrated, activated the TCF reporter strongly but also remained stable for over a month in the presence of serum. The large scale laboratory facility at the NIMR cultured the cells and provided medium that had been conditioned by ptub-Wg cells for two days. Cells were spun down at 200 g after two days and re-suspended in fresh medium. The medium collected from the spin was spun down again at 4700 g to remove debris and was then ready for use.

2.4.3. Cell Lysis

Following treatments, cells were washed in PBS and lysed using Triton Extraction Buffer (TEB) (50mM Tris pH7.5, 150mM NaCl, 1mM EDTA, 1% Triton X100, protease inhibitor cocktail (Pierce), phosphatase inhibitor cocktail 2 (Sigma)). Cells were incubated in TEB for 20min at 4˚C, harvested, and spun at 5000g for 5 min at 4˚C. Pellets were discarded and the supernatants were stored at -20˚C.

Wing discs were lysed in 1% SDS in PBS with protease inhibitors (Pierce), phosphatase inhibitors (Sigma) at room temperature and spun down at 5000 g.

2.4.4. Drug Treatments

Table 2.4 Drugs used

Drug	Provider	Use
Dynasore	Sigma-Aldrich D7693	GTPase inhibitor that targets dynamin, thus blocking endocytosis. Used at a concentration of 200μM. Cells were pre-treated with Dynasore for 20min before use.
MG 132	Sigma-Aldrich C2211	Cell permeable proteosome inhibitor used at 30μM
Cycloheximide	Sigma-Aldrich C4859	Inhibits protein synthesis. Used at 350μM
SB-216763	Sigma-Aldrich S3442	Cell permeable glycogen synthase kinase-3 (GSK-3) inhibitor. Used at 20μM

2.4.5 Reporter assay

$S2R^{+}$ cells were plated in a 6 well dish, and transfected with WISIR vector (0.4μg), pUAST (0.6μg) and the dsRNA of choice (0.2μg). After two days, cells were counted (Casy TT cell counter) and seeded into a 48 well plate with 500 000 cells per well. Cells were treated with either 300μl of Wingless conditioned medium or S2 cell medium as a control. One day later, cells were lysed in 1X Passive Lysis Buffer and both Firefly and Renilla luciferase levels were assessed (Dual-Luciferase Reporter Assay-Promega).

2.4.6 Endocytosis inhibition

2.4.6 a Wingless endocytosis assay

$S2R^+$ cells and S2 cells were plated in 6 well plates. The $S2R^+$ cells were transfected with the WISIR vector (0.4µg) and pUAST (0.6µg). The S2 cells were transfected with either pMT-NRT-HA (0.5µg), pMT-NRT-HA-Wingless (0.5µg) or pMT-HA-Wingless (0.5µg/ul). Expression of genes under the MT (Metallothionein) promoter was induced the next day by addition of $CuSO_4$ (0.7mM) and the $S2R^+$ cells were replated in a 24 well plate. The $S2R^+$ cells were then mixed with an equal number of S2 cells transfected with the different constructs or S2 tub-Wingless cells for 24hrs. S2 cells were washed off the $S2R^+$ cells with PBS. $S2R^+$ cells were lysed with 1X Passive Lysis Buffer and signalling was assessed using the TOPFlash assay. S2 pTub-Wg cells, were also used as an alternative to HA-Wg transfection. Staining the S2R+ cells for Wingless monitored endocytosis of NRT-HA-Wg. For this, $S2R^+$ cells were plated onto coverslips in a 6 well plate and exposed to S2 cells expressing NRT-HA-Wingless /NRT-HA/S2 ptub-Wingless cells for 2 hr. After washing off the S2 cells, the $S2R^+$ cells were then fixed and stained for Wingless as described above.

2.4.6 b Dynasore treatments.

Endocytosis was inhibited with Dynasore at 200 µM. Controls were treated with DMSO. To test the effect of Dynasore on Wingless signalling, $S2R^+$ cells were plated and treated with Dynasore for 20 min before exposure to Wingless. After different times, cells were lysed for Western blotting or TOPFlash assay.

To test the effect of endocytosis inhibition in the presence of a GSK3 inhibitor, $S2R^+$ cells were treated with Dynasore (200µM) for 20 min followed by treatment with SB-216763 (20µM) for up to 6 hr. To test the effect of endocytosis inhibition in cells over-expressiong Armadillo, $S2R^+$ cells were transfected with pMT Armadillo (0.2 µg) and expression was induced 24hr later with CuSO4 (0.7mM). In different experiments Dynasore was added either prior to activation for 30min or 30min before cell lysis.

Cells in the above treatments were lysed for either western blots with TEB or in 1X Passive Lysis Buffer for the TOPFLash assay, in which case the cells were transfected with WISIR (0.4µg).

To assess the effect of Dynasore treatment on Armadillo expression in vivo, third instar wing discs were dissected and placed in complete medium with 200μM Dynasore for desired time and then lysed with 1%SDS in PBS.

2.4.7 Armadillo stability assay

$S2R^+$ cells were either left un-transfected to monitor endogenous Armadillo levels or transfected with pMT Armadillo-V5 or pMT S10-Armadillo-V5 to over-express wild type Armadillo or a stable form Armadillo. 24hr post transfection, Armadillo expression was activated with the addition of CuSO4 (0.7mM) and cells were replated into a 24 well plate for 2/3 hours. To monitor Armadillo degradation rates cells were treated with protein synthesis inhibitor cycloheximide (100μg/ml) +/- Dynasore (200 μM) for different time points (10min, 20min, 40min 1hr, 2hr). To assess changes in Armadillo synthesis cells were treated with proteosome inhibitor MG132 (30μM) for 3hr, either prior to, following or in conjunction with Dynasore (200μM).

Cells were lyzed with TEB and a bicinchoninic acid (BCA) protein assay was performed to determine total protein concentration (Sigma). Equal protein concentrations were analysed by Western blot.

2.5 Biochemistry

2.5.1 Western blot

Proteins were separated by SDS-PAGE using 4-12% NuPAGE® Novex Bis-Tris gels (Invitrogen) with NuPAGE® MOPS SDS Running Buffer (Invitrogen) and SeeBlue® Plus2 Pre-Stained Standard as a molecular weight marker (Invitrogen), or NuPAGE® Novex 3-8% Tris-Acetate gels (Invitrogen) with NuPAGE® Tris-Acetate SDS Running Buffer (Invitrogen) and HiMark™ Pre-stained Standard (Invitrogen) for high molecular weight protein. Proteins were transferred to a PVDF membranes (0.45µM pore size) with a semi-dry transfer (14V for 30min). Membranes were blocked with 5% (w/v) Marvel milk dissolved in TBST (Tris buffer saline + 0.1% Tween) for one hour at room temperature and then incubated with the appropriate primary antibody in 5% milk for 2 hrs at room temperature or alternatively overnight at 4°C. The membrane was then washed 3x10min in TBST and incubated with secondary antibody (HRP conjugated) for 1 hr at room temperature in 5% milk. Further washes were performed. Enhanced chemiluminescence (ECL) (GE Healthcare) was used to detect the signals form the HRP conjugated antibody and membranes were exposed to Amersham Hyperfilm ECL (GE Healthcare).

2.5.2 Arrow IP

For each experimental condition $3x10^8$ cells were seeded onto two 15cm plates. The cells were treated with either Wingless conditioned medium or complete medium for 1hr, after which they were lysed in 6ml of Triton Extraction Buffer (50mM Tris pH7.5, 150mM NaCl, 1mM EDTA, 1% Triton X100, 1mM NEM (Sigma), protease inhibitor cocktail (Pierce), phosphatase inhibitor cocktail (Sigma), and 0.1% SDS for one of the IPs) by incubating at 4°C for 20min. Lysates were then spun down at 5000g at 4° C for 5min. Prior to addition of primary antibody the supernatant was pre-cleared by incubation with protein A-sepharose beads for 3 hours at 4° C. Beads were removed via centrifugation (4500 g) and the supernatant was incubated overnight with anti-Arrow antibody (3ul) at 4° C. The samples were then again incubated with fresh protein A-sepharose beads for 3-4 hours 4°C and then centrifuged. The supernatant was discarded, while the beads were washed 3X in TBS

(50mM Tris pH7.5, 100mM NaCl). Protein was eluted from the beads by the addition of TBS+2%SDS, heating at 90°C for 5min and centrifugation. Eluted proteins were precipitated using TCA precipitation and resuspended in PBS+ Tris pH9.5 + 0.1M DTT and 0.8% β-mercaptoethanol (30ul). Samples were then separated on 4-12% pre-cast were NuPAGE® Novex Bis-Tris gels (Invitrogen) and protein bands visualized by staining for 1hours with SimplyBlue SafeStain (Invitrogen) and photographed with Kodak ID3.5.

2.5.3 Biotin Pull Down

To label cell surface Arrow and monitor its stability in response to Wingless, $2x10^8$ cells were counted and plated in 15cm dishes. Before each experiment a 10mM solution of Sulfo-NHS-SS-Biotin (Thermo Scientific) was prepared in ultrapure water (0.6mg Sulfo-NHS-SS-Biotin per 100ul ultrapure water). Plated cells were washed three times in ice cold PBS and then incubated at 4˚C in 20ml (reaction volume) of PBS containing Sulfo-NHS-SS-Biotin for 30min. The concentration of Sulfo-NHS-SS-Biotin to be added was calculated using the standard provided in the Thermo Scientific protocol. Following incubation cells were once again washed in cold PBS, to remove non-reactive biotinylation reagent. Cells were then detached from the dishes and dispensed in tubes containing Wingless conditioned medium or complete medium. After 1hr, 2.5hr and 4hr incubation times cells were spun down at 200 g, the supernatant was removed and cells were lyzed in TEB (50mM Tris pH7.5, 150mM NaCl, 1mM EDTA, 1% Triton X 100, protease inhibitors (Pierce), phosphatase inhibitors (Sigma). Cell lysates were incubated overnight at 4˚C with avidin beads at a concentration of 1mL of avidin beads per 8mg of Sulfo-NHS-SS-Biotin. The following day the avidin beads were spun down at 5000 g for 3 min, and washed 3 times in PBS. Proteins were eluted from the beads by the addition of 50mM of DTT in TEB for 30 min at room temperature and centrifugation. Protein concentration was determined with a bicinchoninic acid (BCA) protein assay (Sigma). Equal protein amounts were then run on NuPAGE® Novex 3-8% Tris-Acetate gels (Invitrogen) and analyzed on Western blots.

2.5.4 Double IP

A few modifications were made to optimize the biotin/Arrow double IP aimed at isolating cell surface Arrow for Mass Spec. First, the number of cells was doubled to $3x10^8$. The biotin pull down protocol was itself modified from that described above by having a single Wingless treatment of 15 min, the addition of NEM (1mM) to the TEB used to lyze the cells and incubation of the lysate with avidin beads for 2 hr (as opposed to overnight).

During the biotin IP, the Arrow antibody was covalently crosslinked onto protein A/G agarose resin (Pierce: Crosslink Immunoprecipitation kit), adopting the protocol provided by the manufacturer. Samples eluted from the biotin pull down were pre-cleared by incubation with A/G agarose resin for 1 hr and then incubated with A/G agarose resin crossliked to the Arrow antibody, overnight at 4˚C. Proteins were eluted using the Elution buffer provided and protocol described in the kit.

2.5.5 HA IP

To assess protein ubiquitylation $S2R^+$ cells were transfected with hs-Ub-HA. After 2 days they were treated with proteasome inhibitor, MG132 (30μM), and a de-ubiquitylation enzyme inhibitor, N-ethylmaleimide (NEM, 1mM), and then heat shocked at 37°C for 35min. 2 hours post heat shock and 1 hour of Wingless treatment, cells were lyzed and HA was immunoprecipitated using ProFound™ HA Tag IP/Co-IP Kit (Pierce)

2.5.6 Biotin label stripping

$S2R^+$ cell surface Arrow proteins were biotin labelled as described above (2.5.3). After treatment with Wingless medium for desired time points, cells were re-suspended in 2ml of ice cold glutathione stripping solution (50mM glutathione, 75mM NaCl, 1mM EDTA and prior to use 75mM NaOH and 10%FBS was added). This was followed by a 15 min rotation in stripping solution at 4°C. Cells were then centrifuged for 5 min at 200 g and re-suspended in fresh stripping solution and rotated for another 30min at 4°C. Several PBS washes were then done to remove stripping solution, after which cells were lyzed in TEB. A biotin pull down was carried out to pull down endocytosed Arrow.

An additional stripping reagent (50mM DTT) was also tested due to the inefficiency of glutathione stripping. As described above, this was performed at 4°C with multiple PBS washes.

2.5.7 Mass Spec

Protein bands of interest from the IP were excised from the NuPAGE® Novex Bis-Tris gels (Invitrogen) following coomassie staining. Cysteines were reduced with 10mM DTT and alkylated with 50mM iodoacetamide. Proteins were then trypsinized overnight in 25mM ammonium bicarbonate (12.5 ng/ul Trypsin Gold; Promega). Phosphopeptides from Arrow bands were enriched by TiO_2 affinity chromatography. Peptides were loaded onto TiO_2 micro-columns in 2% trifluoroacetic acid (TFA) and up to 80% MeCN. Columns were washed with 20ul of 100mg/ml 2,5-dihydroxybenzoic acid (DBH), 80% MeCN, 2%TFA and then twice more with 80% MeCN, 2%TFA. Peptides were eluted with 50mM Na_2HPO_4 and diluted in NH_4OH. Eluates were desalted using C18 ZipTips (Millipore). Samples were analysed by liquid chromatography tandem mass spec (LC-MS/MS) in a 7 Tesla LTQ FT mass spectrometer (Thermo Electron), by Dr. Steve Sweet at Birmingham University.

2.6 Molecular Biology

2.6.1 WISIR

The WISIR vector (WIngless SIgnalling Reporter) was designed and made by Dr. Cyrille Alexandre. It contains: Firefly Luciferase under the control of 8 consensus binding sites for TCF, a HisYFP cassette consisting of a Histone2A promoter driving His2A cDNA fused to YFP (His2AYFP), and a copia promoter driving Renilla isolated from pCopia-Renilla. See Fig. 3.3.

2.6.2 Renilla-HA-Armadillo

The pUbiquitin-luciferase expression construct was made by isolating luciferase cDNA from pGL3 (Promega) and inserting it into the BglII/Xba site of lit28, which contains the ubiquitin promoter (pUbi pro28).

To generate the pUbiquitin-Renilla-HA-Armadillo expression construct, Renilla cDNA was amplified using NOTA and SPEB oligonucleotides resulting in Renilla-HA cDNA with a NotA/BamH1 site at the 5' terminus and an Spe site at the 3' terminus. Both Not1 and Spe1 restriction sites are also present in the E9 vector upstream from the Armadillo cDNA, which contains a BamH1 site at its 3' end. Thus, these sites (Not1 and Spe1) were used in order to generate E9 Renilla-HA-Armadillo fusion, which was subsequently isolated using BamH1 and cloned into pUbi pro28.

NOTA:
gatgacGCGGCCGCGGATCCACCAAGATGACttcgaaAGTTTATGATCCAGAACAAAGG

SPEB:
GATCACTAGTcgcatagtcagggacgtcgtatgggtaTTGTTCATTTTTGAGAACTCGCTCAACG

2.6.3 RNAi generation

Norbert Perrimon (Harvard) kindly provided over 100 amplicons for genes involved in signalling and trafficking including E2 ligases. Amplicons for de-ubiquitinating enzymes (DUBs) were kindly provided by Marie Odile Fauvarque (Institut de Recherches en Technologies et Sciences pour le Vivant). These amplicons, all

containing the T7 promotor, were amplified via PCR and in vitro transcription was performed using Ambion T7Megascript kit. The RNA was then purified using the (Quiagen) RNeasy mini kit and samples were quantified by optical density (OD) measurements at 260nm using the NanoDrop spectrophotometer.

Results

Chapter 3, 4, 5, 6

"No amount of experimentation can ever prove me right; a single experiment can prove me wrong."

Albert Einstein
Science News-Letter, Volume 14, 1928 page 52

Chapter 3 – Results - Wingless signalling reporter

3.1 Introduction

With the discovery that TCF is a transcriction factor that interacts with β-catenin (Korinek et al, 1997; Korinek et al, 1998; Nusse, 1997; van de Wetering et al, 1991), the TOPFlash (TCF optimal promoter) construct was designed and used as a reporter for Wnt/Wingless signalling. This construct contains multiple copies of TCF binding motifs (CCTTTGATC) upstream of a minimal c-Fos promoter driving the expression of Firefly luciferase (FL). Therefore, when monomeric Armadillo becomes available upon Wnt/Wingless signalling its interaction with TCF leads to transcription of FL. As a control for signalling specificity FOPFlash, which has mutant TCF binding sites, (CCTTTGGCC), is often used (Korinek et al, 1997). An alternative control is the concomitant transfection of a control reporter expressing Renilla luciferase (RL) under a ubiquitously expressed promoter that is unaffected by signalling. The TOPFlash/RL ratio quantifies Wnt/Wingless signalling. The efficiency of this tool for signalling assays is exemplified by its use in a genome wide RNAi screen to identify novel components of the Wingless signalling pathway (DasGupta et al, 2005). This screen identified 238 candidate proteins. One of the most interesting genes found to have an effect was Rab5. This finding contributed to the debate over the involvement of endocytosis in signalling, which I will discuss in detail further on. A flaw of the TOPFlash assay described above is illustrated by a discrepancy in results evaluating the role of Rab 5 in Wingless signalling (Rives et al, 2006; Seto & Bellen, 2006). In one case upon transfection of dsRNA against Rab5 there was a 2 fold decrease in signalling (Seto & Bellen, 2006) in the other a 1.6 to 2.3 fold increase (Rives et al, 2006; Seto & Bellen, 2006). This discrepancy can be explained by the use of different constitutive promoters for RL expression. Indeed, reporters driving RL expression using pCMV (Cytomegalovirus) or TK (Thymidine Kinase) promoters showed a decrease in signalling with Rab5 dsRNA while an increase was seen using PolIII (Polymerase III) (Seto & Bellen, 2006). The observation that different control reporters can produce such different RL levels, thus affecting the results, compromises their use as controls. The use of different RL vectors would be required to verify results.

In this chapter I will discuss the improvements made to the TOPFlash construct to produce reliable RL levels and subsequent optimization of assays. I will also describe my attempt to generate a new reporter with a faster signalling readout to allow the immediate effects of drug treatments to be assessed.

3.2 Generation of a novel Wingless signalling reporter assay

Although the widespread use of the conventional TOPFlash reporter is testimony to its power, it is not without limitations. These arise mainly due to the fact that the readout depends on the transcription and translation of the reporter (FL). It takes at least 2-3 hours to accumulate a sufficient amount of Luciferase activity (Faria et al, 2000). This slow readout eliminates the possibility of looking at genes which, when chronically disrupted, compromise cell viability. With the hope of overcoming this limitation I designed an alternative reporter system. In my system, both FL and RL are under the control of the ubiquitin promoter, which is constitutively expressed (Fig 3.1 A). The RL is fused to the N terminus of Armadillo, and is predicted to be degraded in the absence of Wingless signalling. Therefore, in this new assay, FL acts as a control for cell number and viability and the increase in the RL/FL ratio acts as measure of Wingless signalling. The fact that Armadillo, and hence RL, stabilization is the immediate response to signalling (Muller et al, 1999), would permit me to assess signalling minutes after induction and thus allow the use of drugs that would compromise viability over a longer period (Fig 3.1 B)

Cell lines stably transfected with pUbiquitin-Firefly-luciferase and pUbiqutin-Renilla-HA-Armadillo constructs were generated. Three promising clones were selected displaying both FL and RL activity. However, in all three lines (Aiii9, Aii9, Aiii23) Wingless induced no significant increase in the RL/FL ratio. Moreover, when cells were treated with SB-216763 (GlaxoSmithKline), a drug that inhibits GSK3 and is expected to dramatically increase the reporter response, only a mild effect was observed (Fig 3.2 A). In light of these puzzling results, Western blots were performed against Armadillo to determine whether the Armadillo-Renilla fusion behaves as the endogenous protein in response to Wingless signalling (Fig 3.2 B). All three clones showed an accumulation of Armadillo, both endogenous Armadillo and the fusion with Renilla, in response to treatment of cells with Wingless or SB-216763. However, Armadillo-Renilla bands were also evident in the absence of signal induction, suggesting that the fusion protein is degraded less efficiently than Armadillo alone. Multiple bands were also detected below the Armadillo band regardless of Wingless treatment. These bands could represent breakdown products of the fusion protein. It is possible that this breakdown product could be compromising Renilla luciferase readings by establishing a high basal level of

Renilla luciferase, thus making any increase in the presence of Wingless negligible. It would have been necessary to confirm the presence of a breakdown product by staining the Western blot with an anti-Renilla antibody. To overcome the interference of breakdown products, an alternative construct, with Renilla fused to the C terminus of Armadillo, was attempted but not achieved.

In conclusion the instability of the Armadillo-Renilla construct prevented the creation of an immediate reporter system. As I was attempting to create the new reporter I concomitantly improved the standard TOPFlash assay in a variety of ways, described below.

Figure 3.1 Novel reporter constructs and model.

(A) pUbiquitin-Firefly-luciferase and pUbiquitin-Renilla-HA-Armadillo constructs. (B) Reporter model: In the absence of Wingless, cells transfected with pUbiquitin-Firefly-luciferase and pUbiquitin-Renilla-HA-Armadillo would constitutively express Firefly luciferase as an indicator of cell health. Low levels of Renilla luciferase, would be expected due to degradation in conjunction with Armadillo. This would result in a low RL/FL ratio. Upon Wingless treatment Armadillo stabilization would lead to increased expression of Renilla luciferase. The increase of RL/FL ratio would directly reflect signalling levels.

A

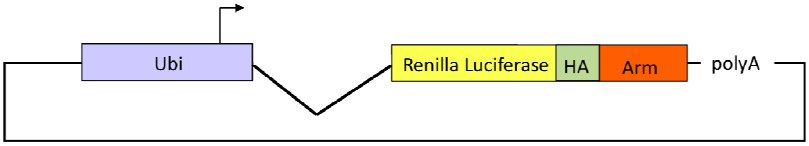

Lit 28 Chi vector

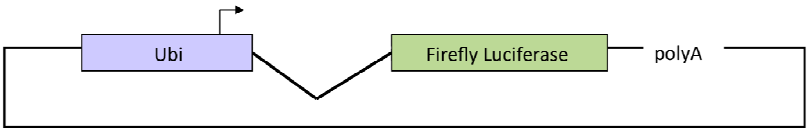

Lit 28 Chi vector

B

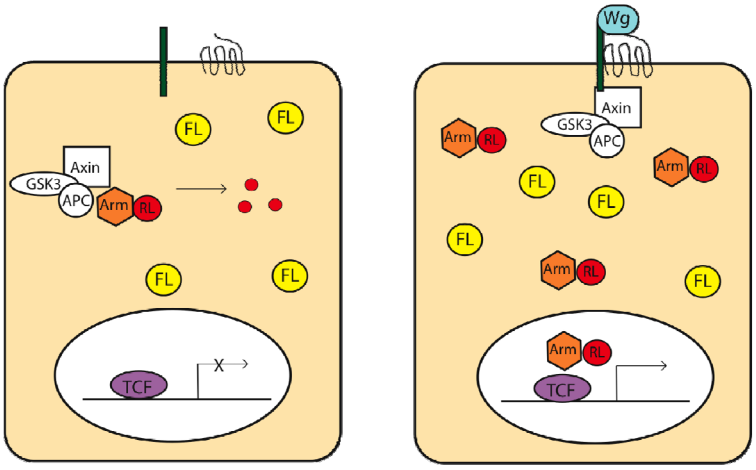

No signalling
RL/FL Low

Signalling
RL/FL High

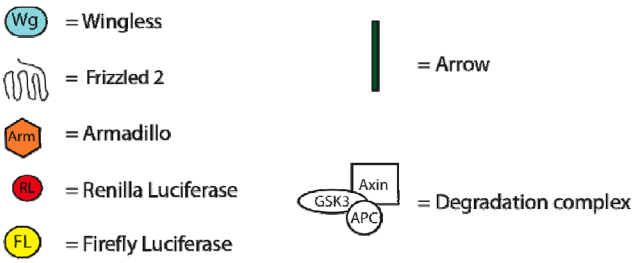

Figure 3.2 Analysis of pUbiquitin-Luciferase and pUbiquitin-Renilla-HA-Armadillo.

Stably transfected cell lines (Aii9, Aiii9, Aiii23) expressing pUbiquitin-Firefly-Luciferase and pUbiquitin-Renilla-HA-Armadillo constructs were generated and treated either with S2 medium, Wingless conditioned medium or complete medium containing SB-216763 (SB-2), an inhibitor of GSK3, for 6 hours. (A) In all cell lines the increase in Renilla luciferase activity in response to Wingless signalling or GSK3 inhibition was not significant. (B) Comparison of Renilla-HA-Armadillo levels to endogenous Armadillo levels in stable cell lines. Endogenous Armadillo is stabilized in the presence of Wingless and even more so when the pathway is constitutively activated by SB-216763. Renilla-HA-Armadillo mimics this pattern of stabilization however high basal levels are already expressed in the absence of Wingless/SB-216763 treatments. Multiple bands, which could be breakdown products of the construct, were also detected and may contribute to high background levels of Renilla luciferase activity.

A

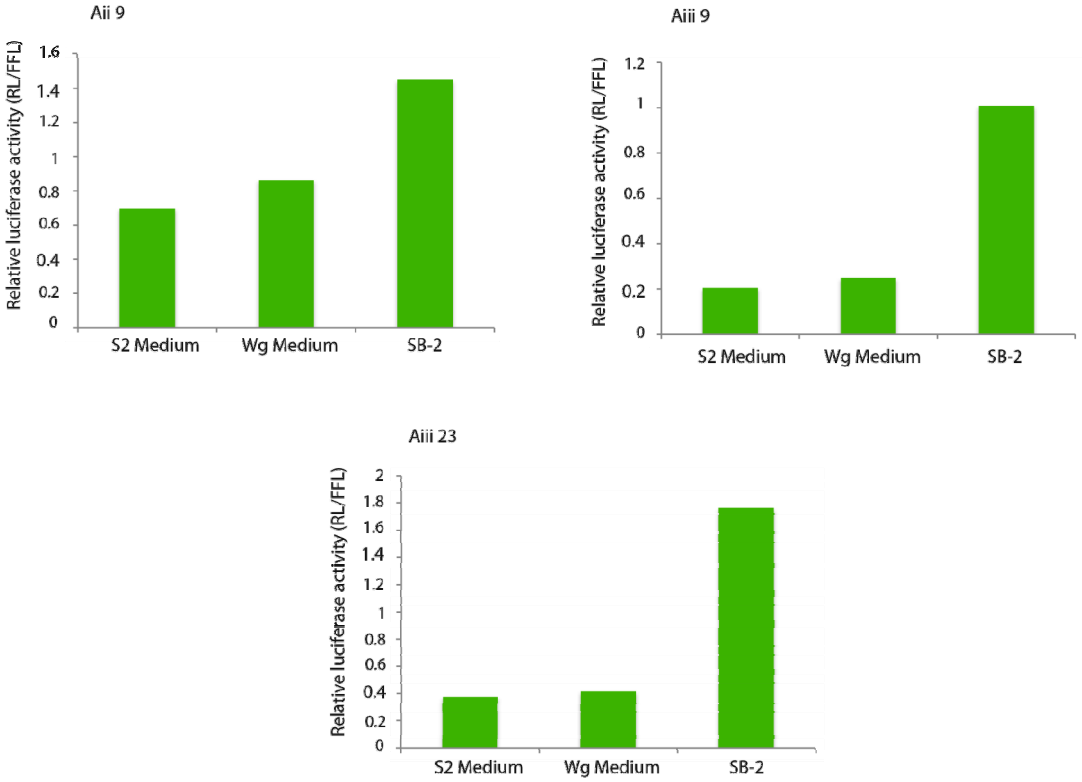
Aii 9
Relative luciferase activity (RL/FFL)
1.6
1.4
1.2
1
0.8
0.6
0.4
0.2
0
S2 Medium
Wg Medium
SB-2
Aiii 9
Relative luciferase activity (RL/FFL)
1.2
1
0.8
0.6
0.4
0.2
0
S2 Medium
Wg Medium
SB-2
Aiii 23
Relative luciferase activity (RL/FFL)
2
1.8
1.6
1.4
1.2
1
0.8
0.6
0.4
0.2
0
S2 Medium
Wg Medium
SB-2

B

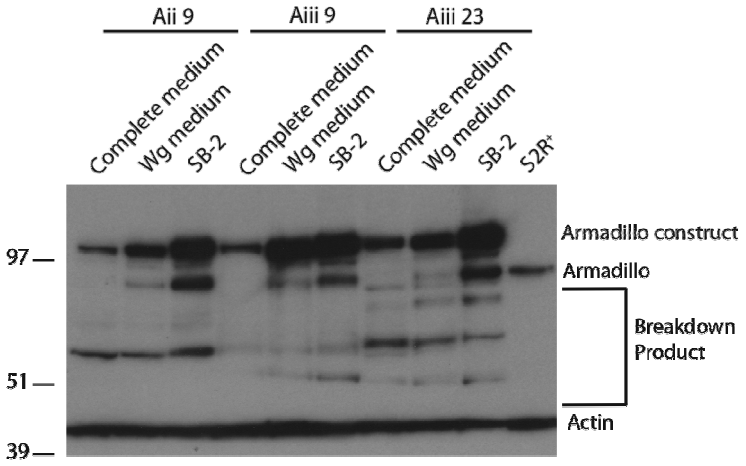
Aii 9
Aiii 9
Aiii 23
Complete medium
Wg medium
SB-2
Complete medium
Wg medium
SB-2
Complete medium
Wg medium
SB-2
S2R+
97
51
39
Armadillo construct
Armadillo
Breakdown Product
Actin

3.3 Optimization of conventional TOPFlash Assay

Unable to overcome the temporal response limitation of the TOPFlash reporter I focused on optimising the response efficiency. This was accomplished with a new reporter vector and by optimising several assay parameters such as cell type used, timing of assay, source of Wingless and number of GFP-Wingless cells used.

As discussed above, the use of different RL control vectors impacts the quantification of Wingless signalling. To overcome this Dr. Cyrille Alexandre created the WISIR vector (WIngless SIgnalling Reporter). This vector harbours Firefly luciferase under the control of 8 consensus binding sites for TCF upstream of the TCF/TATA box promoter and is therefore only expressed in the presence of Wingless signalling. Renilla luciferase, on the other hand is constitutively expressed under the copia promoter, acting as the transfection control and a control for cell viability. A HisYFP cassette consisting of a Histone2A promoter driving His2A cDNA fused to YFP (His2AYFP) is also included and may also be used to determine transfection efficiency (Fig 3.3).

To optimise conditions for the signalling assay I first determined which cell line was best to use. I tested $S2R^+$ cells and FA8 cells, which express both Fz2 and Arrow. $S2R^+$ proved more sensitive (Fig 3.4 A). I attempted to further boost their sensitivity to Wingless by transfecting them with Fz2 along with WISIR vector. This had little effect on signalling levels. This is surprising, as one would expect more receptor to lead to more signalling. However, it may be that the increased level of Fz2 titrate out Wingless, preventing it from interacting with the co-receptor Arrow, thereby decreasing signalling instead of enhancing it (Fig 3.4 A).

After establishing the best cell type to measure Wingless signalling, I determined the optimal number of pMT-GFP-Wg cells needed to interact with $S2R^+$ cells in order to give the highest induction. These cells express GFP-Wg under the control of the methallothionein (MT) promoter, which is activated upon the addition of copper sulfate. Approximately 500,000 R^+ cells were exposed to differing amounts of induced and non-induced pMT-GFP-Wg cells, ranging from 5 000 to 500 000 cells for 24 hours. 100 000 pMT-GFPWg cells gave the highest fold induction (Fig 3.4 B).

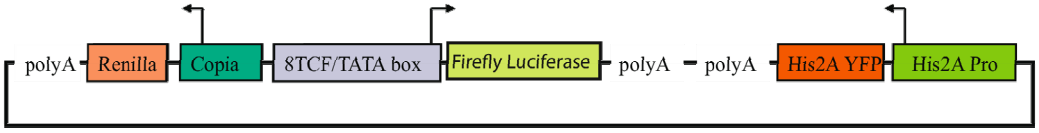

Figure 3.3 WISIR reporter.

This reporter was designed and made by Dr. Cyrille Alexandre. The WISIR (WIngless SIgnalling Reporter) vector harbours Firefly luciferase under the control of the TCF/TATA box promoter that will only be expressed in the presence of Wingless signalling. Renilla luciferase is constitutively expressed under the copia promoter acting as a control for cell viability. YFP expression from a HisYFP cassette consisting of a Histone2A promoter driving the expression of His2A cDNA fused to YFP (His2AYFP) determines transfection efficiency.

Figure 3.4 Ideal cell type and number for TOPFlash assay

(A) The TOPFlash assay was done using $S2R^+$ cells, FA8 cells which over-express both Arrow and Fz2, and $S2R^+$ cells that over-express Fz2. $S2R^+$ cells proved to be the most effective. (B) The ideal number of $S2R^+$ cells to use in the TOPFLash assay was assessed, 100 000 provided the highest fold induction. Values represent means ± SEM.

A

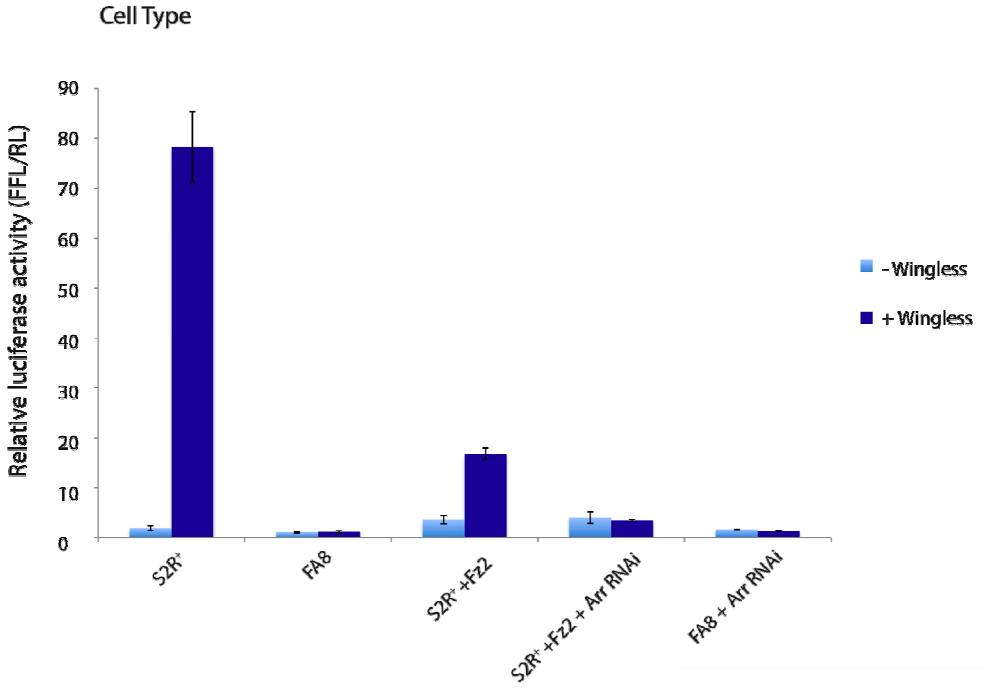
Cell Type
Relative luciferase activity (FFL/RL)
90
80
70
60
50
40
30
20
10
0
S2R+
FA8
S2R+ +Fz2
S2R+ +Fz2 + Arr RNAi
FA8 + Arr RNAi
- Wingless
+ Wingless

B

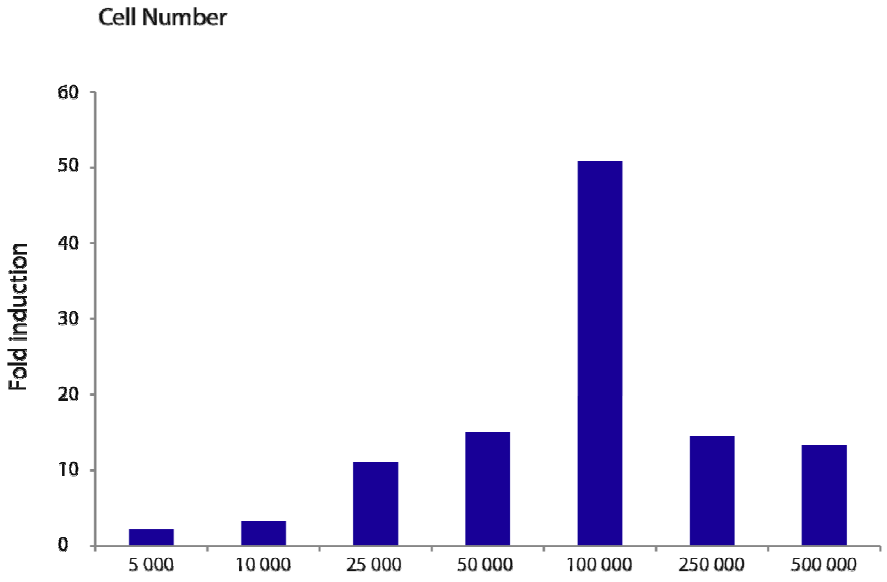
Cell Number
Fold induction
60
50
40
30
20
10
0
5 000
10 000
25 000
50 000
100 000
250 000
500 000

A lower fold induction was observed when using a greater number of cells. This could be due to a leaky pMT promoter yielding an increased basal level of FL expression in $S2R^{+}$ cells that are exposed to non-induced pMT-GFPWg S2 cells.

Despite the mentioned improvements, I was still unsatisfied with the increase of FL levels upon exposure to Wingless. High basal levels of FL expression could be the cause of this reduced effect. To remedy this I tried reducing the number of days between transfection of the WISIR vector and Wingless treatment from three to two days. This significantly increased the Wingless induction, not by increasing signalling per se, but by decreasing noise, which was most probably due to leakiness of the TCF/TATA box promoter (Data not shown).

The final and most efficacious improvement came from testing different sources of Wingless. As mentioned above, initially, stably transfected pMT-GFP-Wg cells provided a source of Wingless. Later I used these pMT-GFP-Wg cells as a source of Wingless conditioned medium (GFP-Wg CM). The use of conditioned medium not only reduced variability as one no longer had to worry about cell number but also simplified the assay protocol. This medium however was stable for only an average of three days, therefore a new preparation was needed with each assay. This was not only time consuming but also reintroduced variability.

Since the GFP-Wg CM proved unreliable, variable and unstable, we decided to test the conditioned medium from S2 pTub-Wg cells (Wg CM). Contrary to the pMT-GFP-Wg cells the pTub-Wg cells not only constitutively express Wingless but are also devoid of the GFP tag, which may interfere with Wg function. Dr. Gregor Zimmermann compared the induction of signalling by medium obtained from pMT-GFPWg and pTub-Wg cells, as well as by co-culturing with pMT-GFPWg cells directly (Fig 3.5.A.). He found that concentrated conditioned medium from pTub-Wg cells induced the strongest response and that its activity was longer lasting (up to a month) (Fig 3.5. B). This may be due to the presence of serum, which is thought to contain compounds that aid the stability and solubility of Wingless. Serum contains both heparan sulfate proteoglycans (HSPGs) which stabilize Wnt activity by preventing aggregation, and lipoproteins which interact with HSPGs and mediate Wingless distribution in extracellular environments (Fuerer et al, 2010; Panakova et al, 2005). Fig 3.6.C shows that in the presence of serum, Wg CM medium activity is longer lasting even in the un-concentrated form. Thanks to these studies it is now possible for me to mass-produce Wingless conditioned medium (Wg CM) and use it

over a longer period long time (up to one month) without the need for concentration, thus reducing the workload and eliminating variation between medium used in each assay.

In conclusion, productive signalling assay involves transfection of the WISIR vector into $S2R^{+}$ without additional Fz2 expression and treatment of cells with Wingless conditioned medium, containing serum, from pTub-Wg cells two days post transfection. Reporter activity is then measured 24 hrs later with a luminometer.

Figure 3.5 Conditioned medium from S2 ptub-Wingless cells is stable and induces the strongest response.

$S2R^+$ cells transfected with the WISIR vector were exposed to conditioned medium from S2 cells, pTub-Wingless cells (Wg CM), pMT-GFP Wingless medium (GFP-Wg CM) or to pMT-GFP Wingless cells (conditioned medium either 1 or 21 days old). After a 24 hr treatment cells were lyzed and their relative Firefly luciferase and Renilla luciferase activity measured (FL/RL). (A) One day old pTub-Wingless medium induces the strongest response. (B) After 21 days of storage pTub-Wingless medium still provides the strongest response thus showing longer lasting activity. Values represent means ± SEM.

A

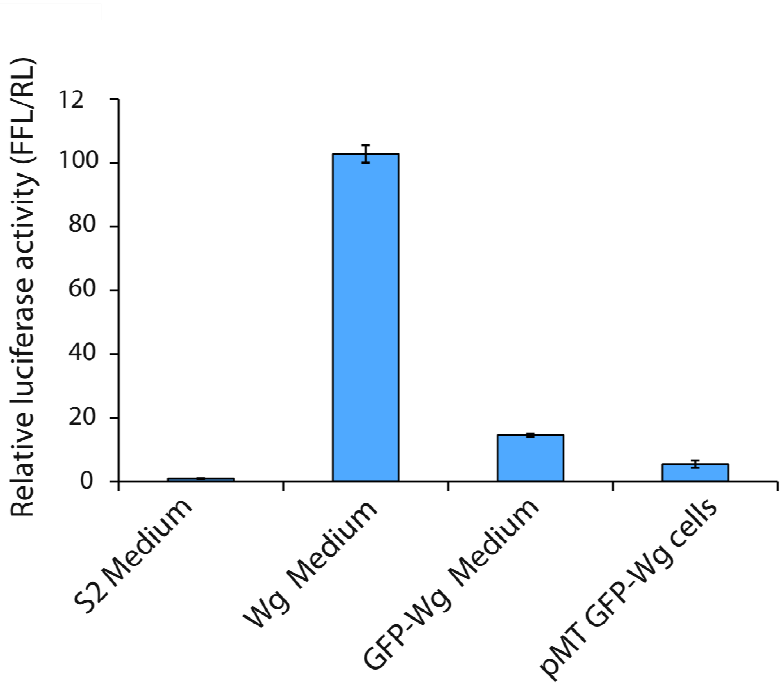
Relative luciferase activity (FFL/RL)
12
100
80
60
40
20
0
S2 Medium
Wg Medium
GFP-Wg Medium
pMT GFP-Wg cells

B

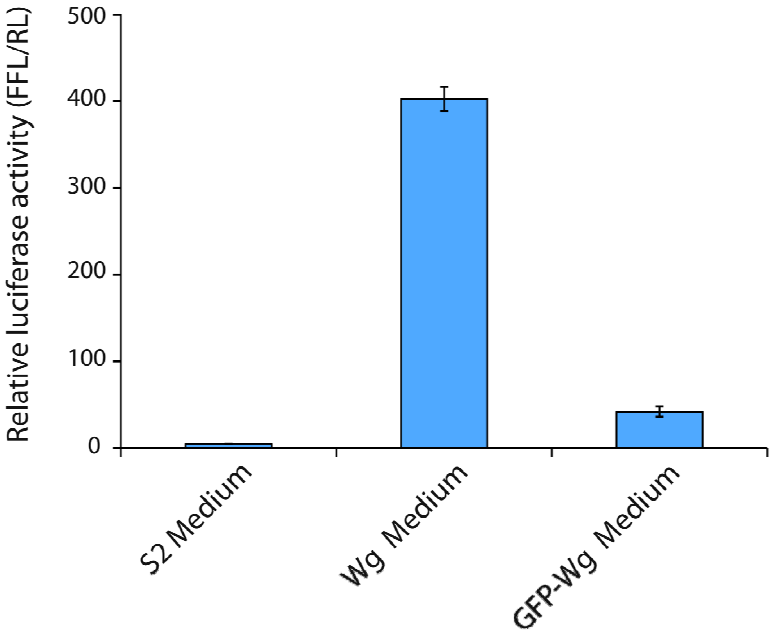
Relative luciferase activity (FFL/RL)
500
400
300
200
100
0
S2 Medium
Wg Medium
GFP-Wg Medium

Figure 3.6 Serum increases pTub-Wingless medium activity

$S2R^{+}$ cells transfected with the WISIR vector were treated with S2 complete medium (S2 CM) or Wingless conditioned medium (Wg CM) in the concentrated and unconcentrated form, both in the presence and absence of serum. The medium used ranged from one day old to 14 days old. Firefly luciferase activity was measured after 24 hr of treatment. Activity of Wg CM is increased in the presence of serum and is high even in the unconcentrated form. Values represent means ± SEM

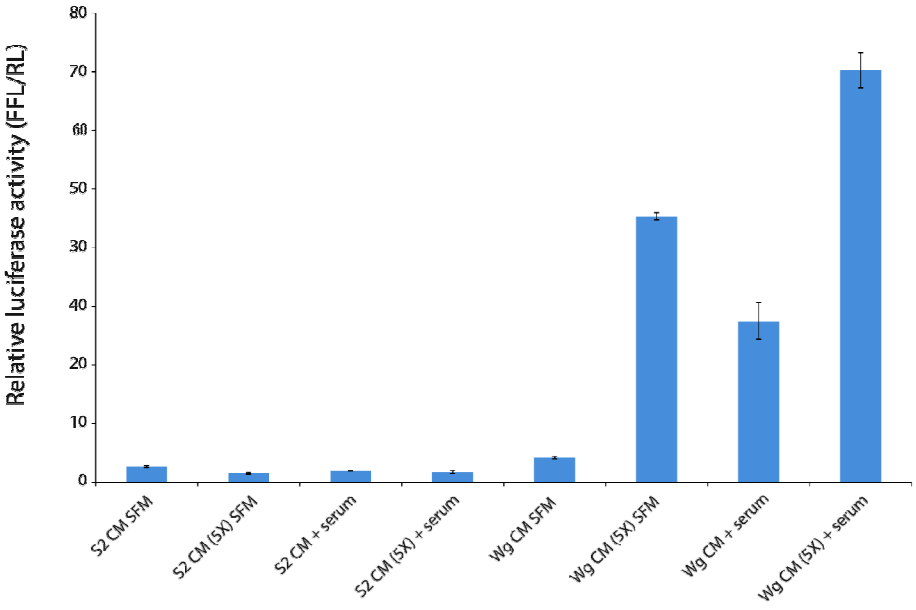

Day 1

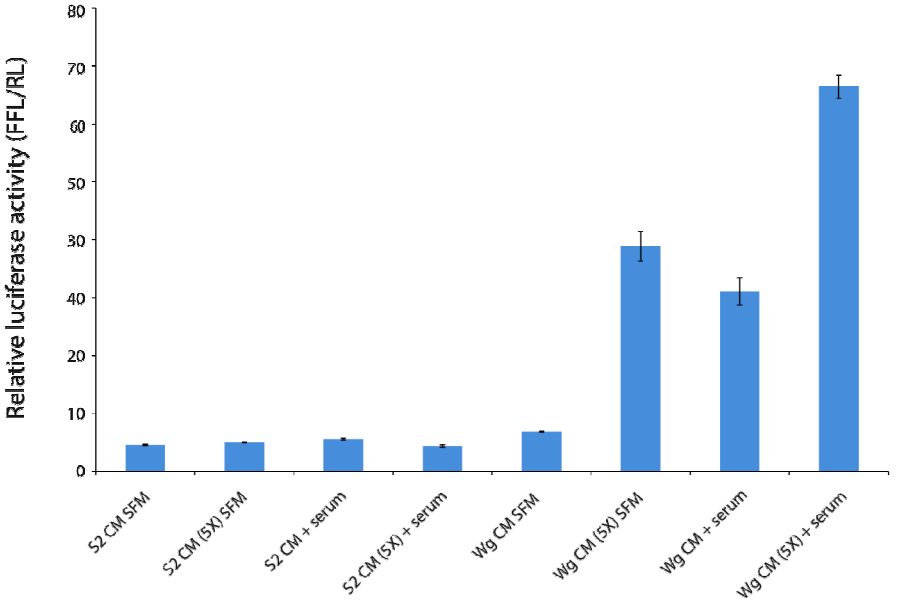

Day 5

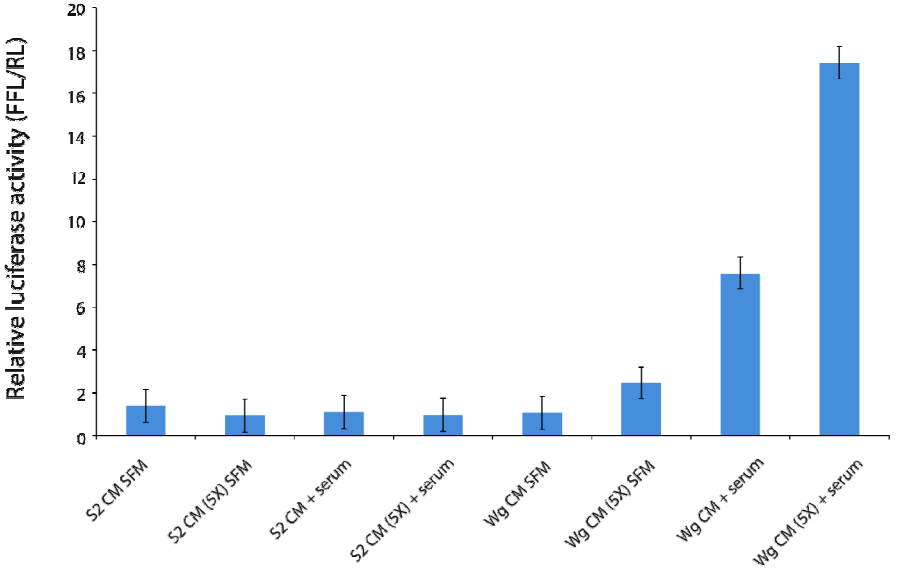

Day 14

3.4 Summary

In this brief chapter I have shown the design of a new signalling promoter, which constitutively expresses Firefly Luciferase as a control for transfection and cell viability and Renilla Luciferase fused to Armadillo. Upon Wingless signalling the latter would be immediately stabilised even in the absence of transcription and translation, to report signalling. It would therefore be possible to monitor immediate effects of chemicals/RNAi that compromise cell viability upon long-term exposure. Initial results showed inefficient degradation of RL-Armadillo in the absence of Wingless signalling and inefficient stabilization of RL-Armadillo upon signalling. Unable to produce a reliable and temporally efficient signalling reporter, I focused on optimising the TOPFlash reporter.

The original TOPFlash signalling reporter was improved in a variety of ways. Importantly, Dr. Cyrille Alexandre designed a vector co-expressing Firefly luciferase and Renilla luciferase, thus creating the WIngless SIgnalling Reporter (WISIR) and abolishing the differences in signalling relative to the RL control vector used.

I improved the use of the TOPFlash assay by determining that S2R+ cells are the best cell line to use, that treatment of the cells with Wingless can occur as early as 2 days post transfection and that the best source of Wingless is from the medium of S2 pTub-Wg cells.

The improvements I made strengthen the ability to reliably analyse RNAi effects on Wingless signalling. This protocol was used as a readout of Wingless signalling throughout this thesis.

Chapter 4 – Results - Arrow stability and recycling

4.1 Introduction

Trafficking of receptors/ligands determines signalling initiation, amplification and termination. Notch is an excellent example, as not only ligand internalization in signal sending cells is required but also internalization of the receptor (reviewed in Le Borgne et al, 2005). Regarding the receptor, Vaccari *et al* showed that the expression of dominant negative Rab5 (DNRab5), which is needed for the formation of early endosomes, resulted in Notch accumulation below the cell surface and a reduction in signalling. The opposite, a strong increase in signalling, was observed with over-expression of Rab5 (Vaccari et al, 2008). Mutation of *hrs*, a gene involved in transport to MVB, showed no significant change in signalling. Therefore it was concluded that trafficking of the Notch receptor into early endosomes promotes signalling (Vaccari et al, 2008). It was proposed that the low pH within the early endosomes triggers signalling by activating γ-secretase, which is required to cleave the Notch receptor liberating the intracellular domain for signalling (Vaccari et al, 2010). With regards to the Wingless pathway the internalization of the ligand/receptor complex is well known, as is the degradation of Frizzed upon Wingless binding (Bilic et al, 2007; Blitzer & Nusse, 2006; Piddini et al, 2005). Arrow takes a different trafficking route to Frizzled post internalization, and it is yet unclear whether it is degraded or recycled.

Post translational modification (PTM) are often responsible for directing receptor trafficking and signalling. One of the most common modifications is ubiquitylation. For example; K63-linked poly ubiquitylation of prolactin (a polypeptide hormone) receptor, is required for multiple trafficking steps. Interaction with AP2 and thus internalization via clathrin coated pits, trafficking to lysosomes and degradation all require ubiquitylation mediated mainly by β-transducin-repeat-containing protein (β-TrCP) E3 ubiquitin ligase (Varghese et al, 2008). In the Wnt/Wingless pathway ubiquitylation has several roles. It is responsible for targeting β-catenin to proteosomal degradation, regulating Fz2 cell surface levels and regulating APC and Axin levels. It may also play a role in Arrow trafficking. In this chapter I explore the trafficking route of Arrow in response to Wingless and the possible PTM involved.

4.2 Wingless does not induce Arrow degradation

Fz2 is considered the predominant receptor for Wingless signalling because of its high affinity for Wingless. Indeed, it is the sole receptor in non-canonical signalling pathways (Cadigan et al, 1998; Wehrli et al, 2000; Wu et al, 2002). Arrow has low affinity for Wingless and acts as a co-receptor in canonical signalling (Piddini et al, 2005; Wehrli et al, 2000; Wu et al, 2002). Upon Wingless binding both receptors are internalized in a heterodimeric complex. Fz2 is targeted to degradation in a Wingless dependent manner (Piddini et al, 2005). Considering the diversity of these receptors in terms of structure and function it is not clear whether Arrow has the same fate as Fz2 or separates from it to take a different trafficking route.

To determine the effect of Wingless on Arrow stability, cell surface Arrow of $S2R^{+}$cells was labelled with biotin and its fate was determined in the presence of Wingless. Labelling of Arrow was carried out at 4°C so that endocytosis is inhibited. Cells were treated with complete medium or Wingless conditioned medium at 25°C for up to 4hr. At different time points (1hr, 2.5 hr and 4hr) cells were lysed and biotin pulled down with avidin beads. The immunoprecipitated material was analysed for Arrow by Western blot. Fig 4.1 A, B shows that the amount of cell surface Arrow gradually decreases in 4 hours but the rate is not affected by the presence of Wingless. It is known that LRP6 has half life of 4.7hr (Semenov et al, 2008).

To confirm that the lack of change in cell surface Arrow degradation is not due to the biotinylation process inhibiting Wingless signalling, cells were biotinylated, treated with Wingless, and signalling was determined by probing western blot of cell lysates for Armadillo (Fig 4.1 C). An increase in Armadillo upon Wingless treatment of biotinylated cells was observed, confirming that biotinylation does not inhibit Wingless signalling. Upon internalization Wingless is targeted to degradative compartments (Dubois et al, 2001; Piddini et al, 2005). I showed this by performing co-localization of Wingless with Hrs, a protein involved in MVB formation, and LAMP (lysosomal Associated Membrane Protein) (Fig 4.2). I assessed Arrow trafficking upon Wingless signalling in the same way. As shown in Fig 4.2, Arrow does not co-localise with LAMP and thus is not trafficked to lysosomes upon signalling.

Figure 4.1 Arrow stability in the presence of Wingless signalling.

(A) Cell surface proteins of $S2R^+$ cells were labelled with Sulfo-NHS-SS-Biotin. Cells were then treated with Wg conditioned medium or complete medium for 1hr, 2.5hr and 4hr. Cells were lyzed and biotinylated proteins were pulled down with avidin beads. Western blots were probed with anti-Arrow antibody. (B) Western blot of the 4hr time point and reloading of the 2.5 hr time point to allow comparability to previous time points. (C) Western blot of Armadillo accumulation as a result of Wingless signalling in biotinylated $S2R^+$ cells to verify that signalling is not impeded by biotinylation.

A

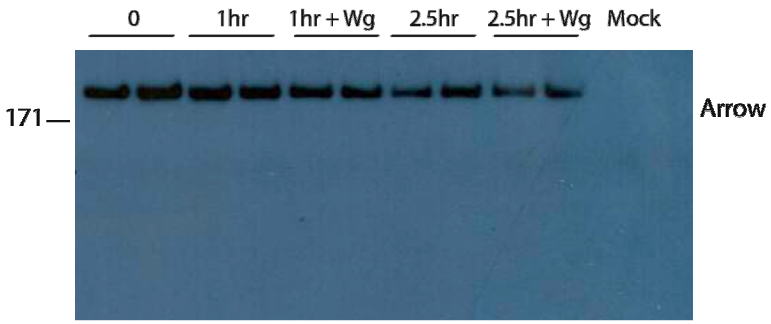
0
1hr
1hr + Wg
2.5hr
2.5hr + Wg
Mock
171
Arrow

B

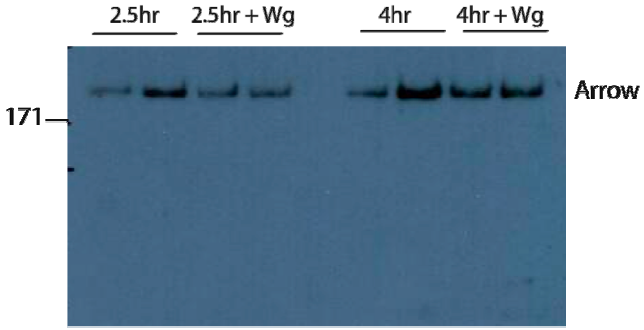
2.5hr
2.5hr + Wg
4hr
4hr + Wg
171
Arrow

C

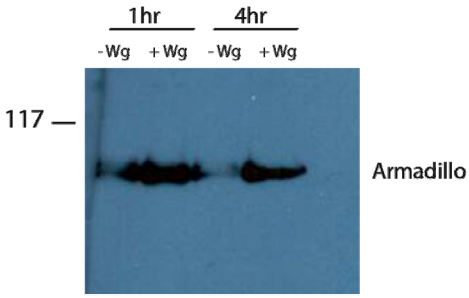
1hr
4hr
-Wg
+Wg
-Wg
+Wg
117
Armadillo

This suggests that Wingless and Arrow take different trafficking paths upon internalization and that Arrow is not degraded. It was not possible to determine co-localization of Arrow with HRS as both antibodies available to us are made in Guinea Pig. Co-localization of Arrow with Vps28, another MVB marker, was tested but the staining was inconclusive.

To further assess receptor trafficking in response to Wingless, I assayed Arrow degradation in response to Wingless signalling in the wing imaginal disc using a similar technique to that described by Piddini et al 2005. In this paper the effect of Wingless on the stability of Fz2 was assessed in 3rd instar larvae. FLAG-tagged Frizzled2 was expressed uniformly under the control of a heat-shock promoter. Levels of FLAG-tagged Frizzed were then monitored at defined time points. After 3 hours, preferential degradation of Frizzed2 near the source of Wingless was observed, suggesting that Wingless triggers Frizzled 2 degradation. To induce uniform Arrow expression, transgenic flies expressing UAS Arrow-HA, and the heat shock (hs) Gal4 driver were used. Stainings were done using anti-Arrow antibody as anti-HA gave poor results. The latter would have been preferable, as it would allow endogenous Arrow to be ignored. 2 hour post heat shock, uniform expression of Arrow-HA was seen in the wing disc of third instar larvae (Fig 4.3). 3 hour later Arrow-HA staining was present at various levels in cells across the disc, which can be interpreted as random degradation of Arrow-HA in cells irrespective of their position relative to the Wingless source. Although these results are in accordance with those obtained in cell culture, described above, they are inconclusive. An internal control would have been needed to verify that Arrow is being degraded, not simply continuously expressed randomly, and that degradation is specific to Arrow. This could be achieved by simultaneously inducing expression of tagged Delta under hs-Gal4 control. Uniform expression of Delta in the 3rd instar wing disc would be expected and, as is the case of Fz2, preferential degradation along the dorsal/ventral interface due to Notch signalling (Lai et al, 2001)**.** This would indicate that Arrow expression due to hs-Gal4 is uniform and that the random degradation observed is specific to Arrow. Non-uniform expression of Delta or random degradation of Delta would suggest that the results are an artefact of the hs-Gal4 expression system used. It would have also been advantageous to make a new construct, hs-Arrow-HA, thus avoiding hs-Gal4. Despite the need for these controls to properly validate this

experiment, it can be concluded from the $S2R^{+}$ cells based experiment alone that Wingless signalling does not induce degradation of Arrow.

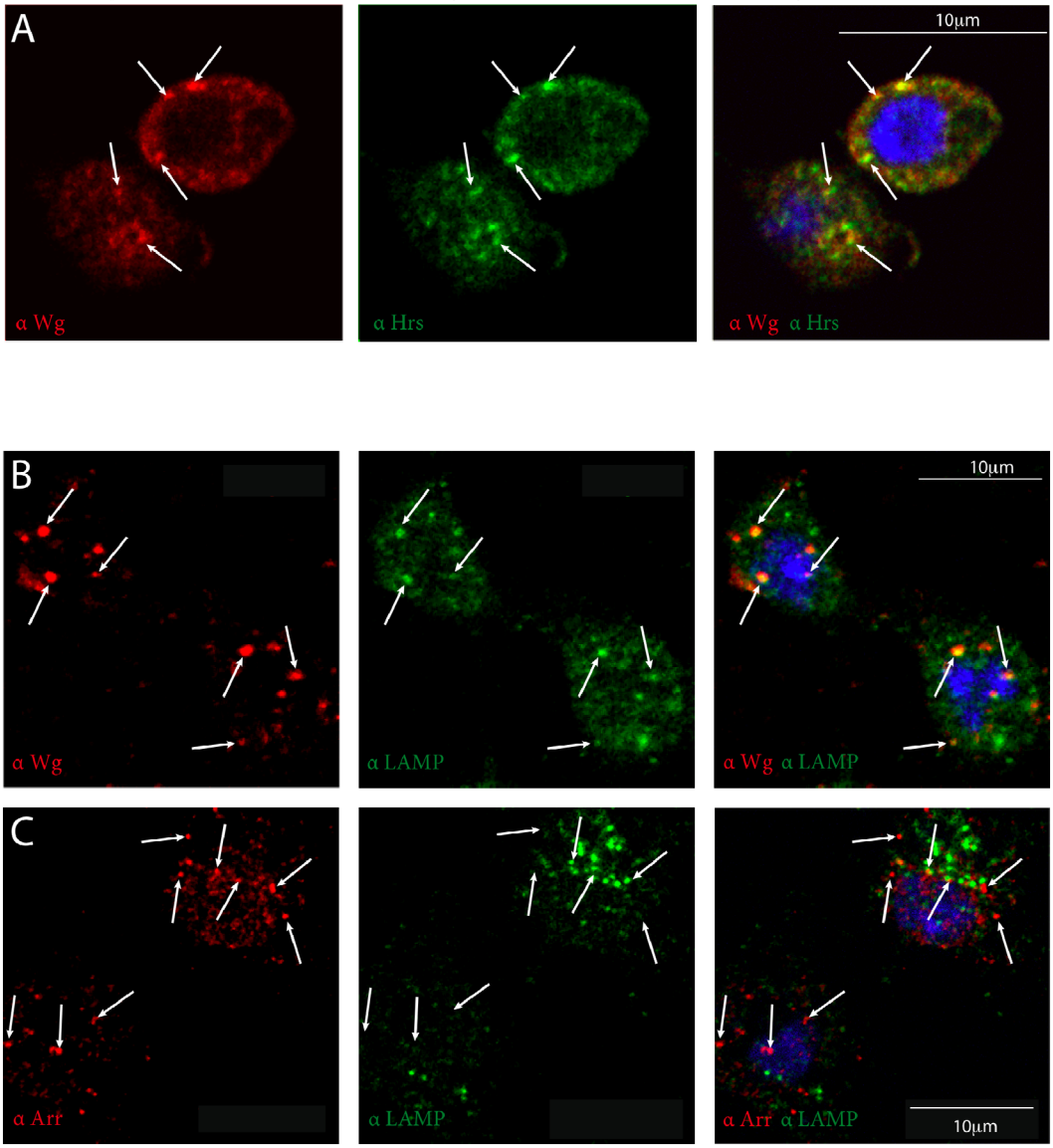

Figure 4.2 Arrow is not present in lysosomes upon Wingless signalling.

(A) Wingless traffics to MVBs as S2R^{+} cells exposed to Wingless display Hrs/ Wingless co-localization (B,C) S2R^{+} cells exposed to Wingless were stained for Wingless (B) Arrow (C) and LAMP. Wingless and LAMP co-localize indicating Wingless degradation. Arrow and LAMP co-localization is not detected suggesting that Arrow is not trafficked along the degradation route in response to Wingless signalling.

Figure 4.3.Wingless does not stimulate Arrow degradation.

Wing discs of the *Hs Gal4 ; UAS Arr FL- HA* genotype were heat shocked at 37 °C for 35 min. Larvae were dissected and stained for Arrow prior to hs (A), 2hr after hs, showing a significant increase in Arrow expression (B) and 3hr after hs, showing that Arrow is not preferentially reduced in proximity to Wingless expressing cells (C). These results suggest that Arrow stability is not affected by Wingless signalling. Dotted line indicates the source of Wingless.

Hs Gal4; UAS Arr FL-HA

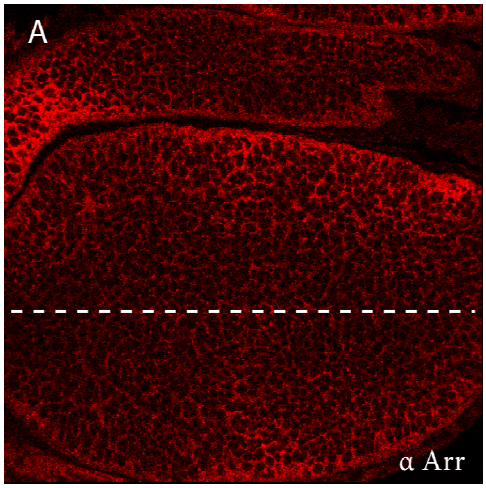

No hs

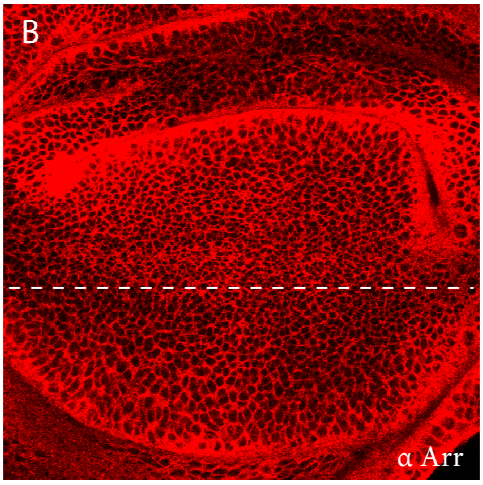

2hr post hs

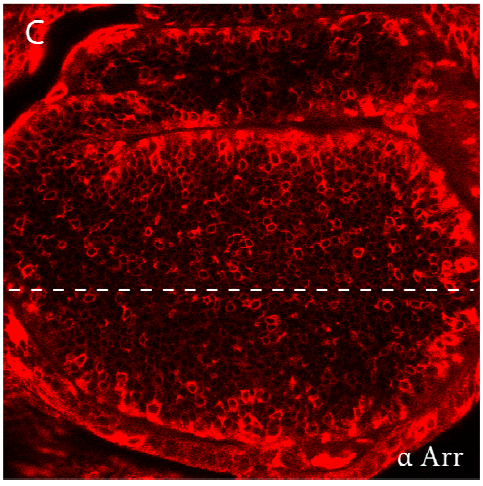

3hr post hs

4.3 Arrow is recycled

If Arrow is internalised but not degraded in response to Wingless, the most likely trafficking route is recycling. A relatively recent study (Khan et al, 2007) shows that Wnt3a induces LRP6 internalization and recycling back to the cell surface. This was shown by treating cells with Wnt3a for different times and subsequent biotinylation of cell surface LRP6 and immunoprecipitation of the lysates with streptavidin beads. Within 10min of Wnt3a treatment a decrease in cell surface LRP6 levels was observed, which continued at the 30min and 1hr time points. Cell surface levels returned back to that observed in untreated cells after 3hr. Although it is possible that Wnt3a could induce LRP6 recycling, this is not necessarily proven by this experiment. Seeing a decrease in cell surface LRP6 post Wnt treatment is expected as it has been shown that internalization occurs (Marois et al, 2006; Piddini et al, 2005; Piddini & Vincent, 2009; Seto & Bellen, 2006; Wehrli et al, 2000). However, since cell surface LRP6 was biotinylated post Wnt treatment, the restoration of LRP6 cell surface levels may be due to protein synthesis rather than recycling. The same experiment was repeated in the presence of a protein synthesis inhibitor, cycloheximide. The results, not shown, were said to be the same. This use of cycloheximide, however, does not provide reliable results as cycloheximide could not only be inhibiting LRP6 synthesis but also the production/function of proteases involved in degradation. To address these issues I hoped to take advantage of cleavable EZ-Link Sulfo-NHS-SS-Biotin. $S2R^{+}$ cells were biotinylated at 4°C then treated +/- Wingless at 25°C allowing internalization of labeled cell surface Arrow. At different time points cell surface biotin was stripped off. Therefore, only internalized biotin labeled Arrow, which was protected from stripping, would be precipitated with avidin beads. If Arrow were recycled, a progressive decrease of biotin-Arrow pulled down would be seen. (Fig 4.4 A). This procedure was previously used to demonstrate that Dkk1 internalizes LRP6, which is then recycled back to the cell surface (Sakane et al, 2010). I was unable to obtain results as efficient stripping was not achieved. Both DTT and Glutatione were tested but neither was consistently cleaving the biotin disulfide (-S-S-) bond adequately. The following experimental protocol could overcome this problem. Although simple in principle it would require some time to develop. As previously, cell would be biotinylated at 4°C and endocytosis would then be allowed for various time at 25°C.

At different time points, instead of being stripped cells would be returned to 4°C and labeled with avidin, which would only bind to biotinylated cell surface proteins. Thus only recycled Arrow would be double labeled. Cells would then be lyzed and avidin labeled proteins would be precipitated using biotin columns. Results could be analyzed by immunoblotting for Arrow (Fig 4.4 B).

Figure 4.4 Protocols to assess Arrow recycling.

(A) The protocol used to assess Arrow recycling involved the biotinylation of cell surface Arrow with Sulfo-NHS-SS-Biotin and treatment with Wingless medium. At different times post treatment, cell surface biotin was stripped with glutatione or DTT and internalised tagged Arrow was pulled down with avidin beads. As stripping proved to be inefficient a novel protocol was designed. (B) To avoid biotin stripping from the cell surface, at different time points during Wingless treatment, biotinylated cell surface proteins would be labelled with avidin. Double labelled proteins would be pulled down in biotin columns and Western blots probed with anti Arrow would determine if the receptor is recycled.

A

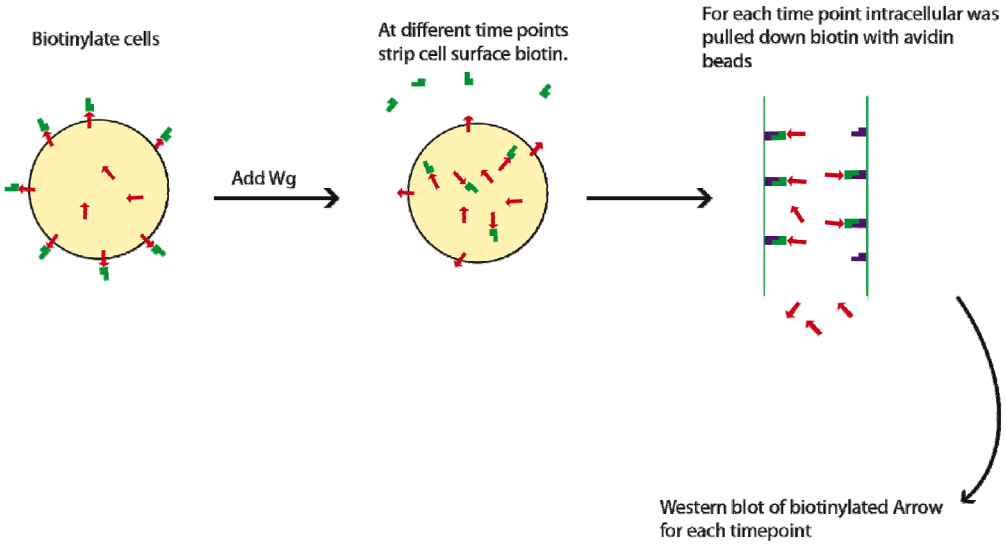

B

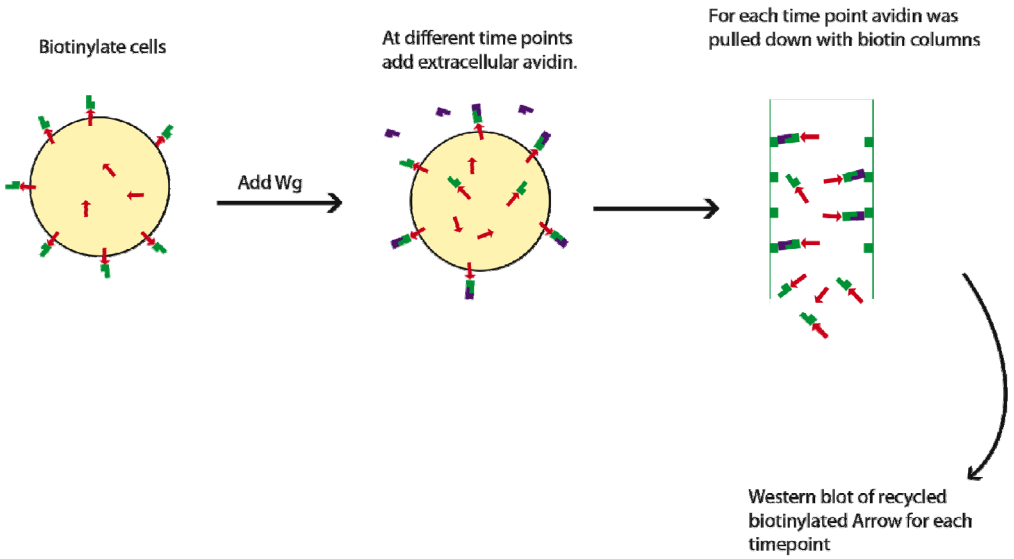

= Biotin
= Avidin
= Arrow

4.4 Immunoprecipitation and Mass spec of Arrow

In light of the fact that Arrow takes a different trafficking route to Fz2/Wingless I became interested in exploring possible post translational modifications (PTM), in addition to phosphorylation, that could divert Arrow into a recycling trafficking route. Many post translation modifications such as ubiquitylation, methylation, acetylation, glycosylation and sumoylation have already been shown to initiate or modify signalling (reviewed in: Deribe et al, 2010). To identify novel trafficking signals required for Arrow recycling/trafficking I decided to use mass spectrometry (mass spec). This technique has several benefits and would not only allow me to accurately map the site of any modification but would also allow me to identify Arrow interacting proteins.

Arrow was immunoprecipitated (IP) from cells both in the presence and absence of Wingless. The IP protocol was considered suitable for mass spec only after certain criteria were met. Firstly, Arrow was purified only from samples to which the antibody was added demonstrating that Arrow is specifically being immunoprecipitated. Secondly, only a minimum amount of Arrow was present in the insoluble pellet post lysis of the cells, illustrating efficient solubilisation of this receptor from the membrane upon cell lysis. Thirdly, the ratio of antibody to beads was such that no Arrow was in the lysate post incubation with the antibody (Fig 4.5 A). Finally, it was established that 2 elutions were needed to thoroughly elute Arrow off the beads (Fig 4.5 B). After the IP was optimised, it was scaled up for mass spectrometry. Fig. 4.5 C shows gels obtained from two different immunoprecipitations. The important difference between these two is that in the second IP SDS was added in the lysis buffer. In the gel obtained from the first IP the Arrow band was denser, which initially led me to believe that it would be well suited for mass spec, as high protein content is needed. This however, was not the case. Although a weaker band was obtained with the second IP, it proved to contain more Arrow. The second IP also provided non Arrow bands that appeared only in the presence of the anti-Arrow antibody. Determining the identity of these bands via mass spec could reveal novel Arrow interacting proteins that may take part in signalling. The desired bands, highlighted in Fig 4.5C, were excised and analysed by standard LC-MS/MS either directly or after phosphopeptide enrichment by Dr. Steve Sweet at the University of Birmingham.

The Arrow protein itself was identified with 15% sequence coverage. Of the five phosphorylated PPPSP motifs only one was recovered (IVPESSCPPsPSSR). Identification of all the phosphorylation sites already documented in the literature was required to ensure that both the IP and the mass spec were functioning optimally. Proteins that were co-immunoprecipitated with Arrow are listed in Table. 4.1. Of these, α-Adaptin and Clathrin are interesting, suggesting that Arrow endocytosis could be mediated by clathrin. Expected interactors such as Boca and Axin were not identified. The presence of heat shock proteins and elongation factors indicates the presence of contaminants, while the abundance of proteins involved in ER to Golgi transport and secretion likely indicates that intracellular, secretory Arrow is being pulled down in addition to the active membrane bound Arrow. If most of the Arrow precipitated is intracellular this would explain why expected phosphorylations and cell surface interacting proteins were not identified. To specifically pull down cell surface Arrow, a double IP was adopted. In the first precipitation all cell surface proteins were pulled down. To accomplish this cells were biotinylated at 4°C and biotin labelled cell surface proteins were subsequently precipitated with avidin beads. From this initial pull down Arrow was immunoprecipitated. The initial results of the double IP are shown in Fig 4.6 A. Clear Arrow bands are seen with the initial pull down of biotinylated proteins and with the immunoprecipitation of Arrow. Unfortunately these samples also contain large bands of the size expected from antibody heavy chain (50kDa), light chain (25kDa) or a combination of both. To remove these bands and avoid potential interference with the identification of co-immunoprecipitated proteins, I crosslinked the Arrow antibody to the beads, thereby reducing the amount of antibody that is eluted. Before proceeding with the double IP, I determined the optimal pH of the Arrow elution buffer. As shown in Fig 4.6 B a low pH buffer is more effective at releasing Arrow from its antibody without denaturing the latter. Overall, combining the antibody crosslinking step rendered my double IP efficient and clean (Fig 4.6 C).

My initial IP, in which I precipitated all Arrow in the cell, achieved only 15% sequence coverage. With the double IP only cell surface Arrow was pulled down and would therefore need to be scaled up a great amount, at least 50 times. A minimum of 1.8×10^{10} semi adherent $S2R^{+}$ cells would need to be biotinylate. The use of multi-layered plates would be cumbersome and inefficient for labelling. Biotinylation in suspension would also be problematic as cells clump together thus

decreasing the surface area available for biotinylation. Alternative ways to scale up the double IP include: 1) Double the antibody to determine if a commensurate amount of Arrow is pulled down. 2) Biotinylate cells at a slightly higher temperature in order to label Arrow that continues to be brought up to the cell surface. 3) Pool together eluted samples from multiple IPs. Time would be needed to add these modifications to the protocol.

Despite technical and time limitations, I have established an efficient double immunoprecipitation of cell surface Arrow that will hopefully allow us to determine any post translational modifications that can take place upon ligand binding or have a role in receptor trafficking and to identify interacting proteins.

Figure 4.5 Arrow immunoprecipitation and co-immunoprecipitated proteins.

(A) Western blot of Arrow IP. $S2R^{+}$ cells were treated with either Wingless conditioned medium or complete medium for 1hr. After treatment, cells were lyzed and spun down. The supernatant (input) was pre-cleared by incubation with protein A-sepharose beads after which it was incubated overnight +/- anti-Arrow antibody. The samples were then incubated with fresh protein A-sepharose beads for 3-4 hours. (B) Proteins were eluted from the beads twice and precipitated using TCA precipitation. (C) Gels were run to assess co-immunoprecipitated proteins. Two immunoprecipitations were tested, in the second (right hand gel) 1% SDS was added to the lysis buffer. Gels were coomassie stained and bands indicated by arrows were excised and processed for mass spec. Arrow was recovered from the second gel with a 15% sequence coverage. Other proteins detected are listed in Table 4.1.

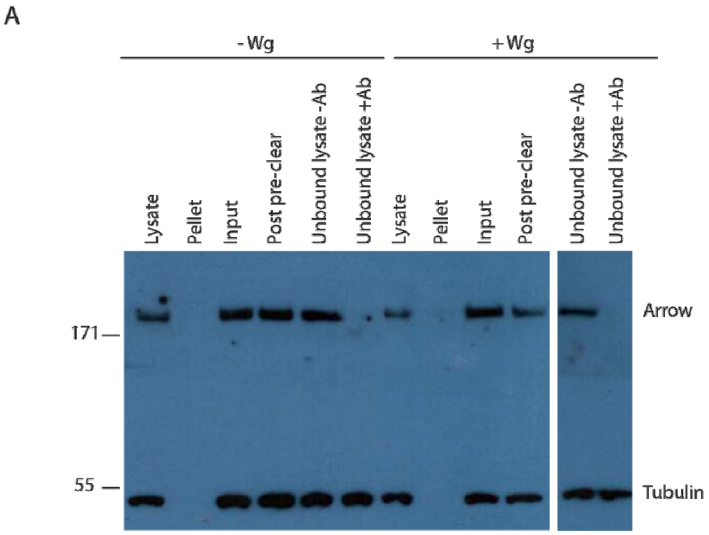
A
-Wg
+Wg
Lysate
Pellet
Input
Post pre-clear
Unbound lysate -Ab
Unbound lysate +Ab
Lysate
Pellet
Input
Post pre-clear
Unbound lysate -Ab
Unbound lysate +Ab
171
55
Arrow
Tubulin

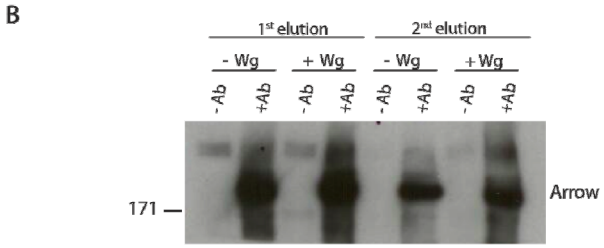
B
1st elution
2nd elution
- Wg
+ Wg
- Wg
+ Wg
- Ab
+Ab
- Ab
+Ab
- Ab
+Ab
- Ab
+Ab
171
Arrow

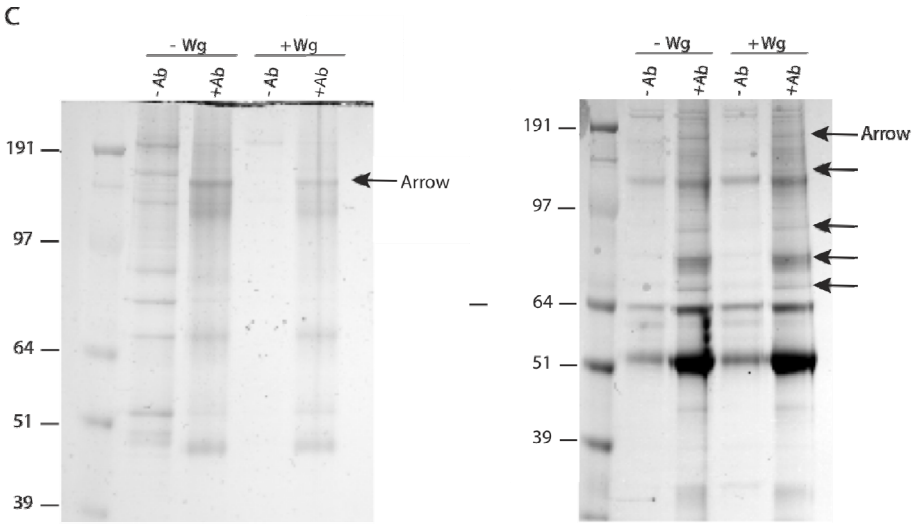
C
- Wg
+Wg
- Ab
+Ab
- Ab
+Ab
191
97
64
51
39
Arrow
- Wg
+Wg
- Ab
+Ab
- Ab
+Ab
191
97
64
51
39
Arrow

Table. 4.1 Proteins co-immunoprecipitated with Arrow

Protein	Function
Sec31	Exocytosis, intracellular (IC) protein transport
Nup 154	IC and nucleo-cytoplasmic transport
eIF3-S10	Translation initiation factor
CG32138	Actin cytoskeleton organization
Gp150	Cell adhesion, metabolism
CG1371	Carbohydrate binding
Coatamer alpha subunit	ER to golgi transport
Isolencyl tRNA synthase	ER to golgi transport, GPCR signalling
CG2025	proteolysis
CG2238	Elongation factor 2B
TER94	Golgi and ER organization
Alpha adaptin	Endocytosis
Hsc70Cb	Heat shock protein
Calcium ATPase	Calcium ion transport, metabolism
Gamma coatamer protein	ER to Golgi transport
Fs(2) Ket	Nuclear transport
Rpn1	Cell cycle regulation, proteolysis
MCM3	DNA replication initiation
CG6718	Lipid metabolism
Ef1-alpha like adaptor	Translation
Trap1	Protein folding
CG5105	Phospholipase A2 activator protein
CG4389	Fatty acid Beta-oxidation
Clathrin heavy chain	Endocytosis
CG8222	VEGF/PDGF related protein

Figure 4.6 Immunoprecipitation of cell surface Arrow.

(A) Cell surface proteins of $S2R^{+}$ cells treated with Wingless/complete medium were biotinylated, lysed and pulled down with avidin beads. Equal levels of cell surface Arrow are detected in lysates for each treatment. Cell surface Arrow was then immunoprecipitated from biotin lysates with anti-Arrow antibody. Western blot shows Arrow bands in the double IP and bands of antibody heavy and light chains. (B) To diminish antibody elution and thus eliminate antibody bands from gels in order to assess co-immunoprecipitated proteins, the anti Arrow antibody was cross-linked to protein A/G agarose resin. Appropriate pH of Arrow elution buffer was assessed. Elution was most efficient at a low pH. (C) Western blot of optimized Arrow double IP.

A

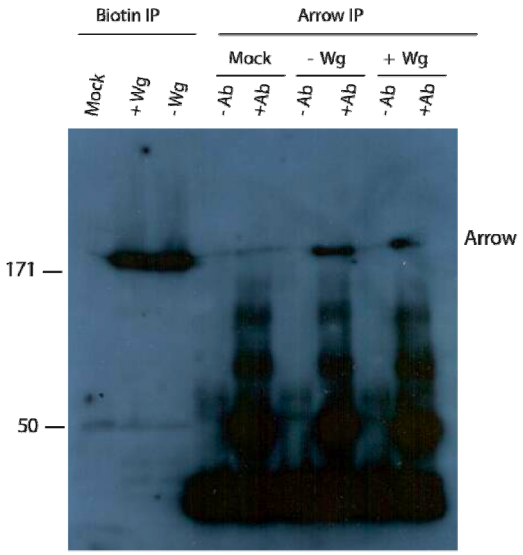
Biotin IP
Arrow IP
Mock
- Wg
+ Wg
Mock
+ Wg
- Wg
- Ab
+Ab
- Ab
+Ab
- Ab
+Ab
171
50
Arrow

B

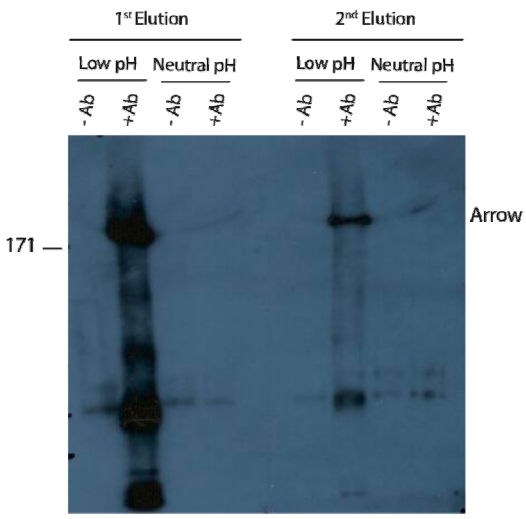
1st Elution
2nd Elution
Low pH
Neutral pH
Low pH
Neutral pH
- Ab
+Ab
- Ab
+Ab
- Ab
+Ab
- Ab
+Ab
171
Arrow

C

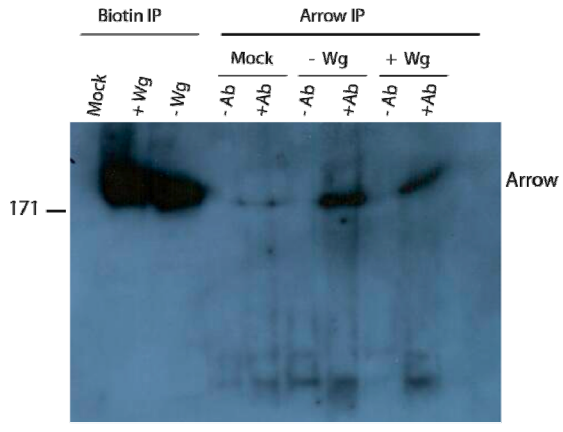
Biotin IP
Arrow IP
Mock
- Wg
+ Wg
Mock
+ Wg
- Wg
- Ab
+Ab
- Ab
+Ab
- Ab
+Ab
171
Arrow

4.5 Possible Ubiquitylation of Arrow

Ubiquitylation has been shown to act as an endocytosis signal, but also has roles in DNA repair and signal transduction. It plays a part in many signalling pathways such as NF-κB, EGF and TGF signalling, regulating receptor degradation and recycling. In regards to Wingless signalling, ubiquitylation not only instigates Armadillo degradation but has also been implicated in the maintenance of cell surface levels of Fz2, which I will discuss in Chapter 7. In many cases, phosphorylation precedes ubiquitylation, the two modifications are tightly linked. As Arrow is both phosphorylated and has a distinct trafficking route it is rational to investigate its ubiquitylation.

Previous work in the lab by Dr. Francis Marshal began to explore the role of Arrow ubiquitylation in Wingless degradation. He created a form of Arrow in which all the lysines in the intracellular domain are mutated to alanines and investigated its ability to be endocytosed, to target Wingless to degradation and to cause ectopic signalling. Although his mutated Arrow prevents Wingless degradation, its ability to be endocytosed and ectopically signal when over-expressed are also inhibited. Thus, Arrow function is compromised and the inhibition of Wingless degradation could be an indirect effect. To approach this hypothesis in a different manner, I wanted to identify ubiquitylation and then determine possible sites. I started by simply probing a western blot of immunoprecipitated Arrow with anti-ubiquitin (Fig 4.7 A). A band is detected at the level of Arrow in the absence of Wingless. This is an interesting result, as one would expect Arrow to be ubiquitylated upon signalling not deubiquitylated. Of course this band is not proven to be Arrow. It could be any other protein of a similar molecular weight that is pulled down with Arrow. To carry on from this preliminary result with a more stringent experiment, cells were transfected with Hs-Ub-HA, treated with both a proteosome inhibitor (MG132) and a de-ubiquitylation enzyme inhibitor (NEM) and then heat shocked. 2 hours post heat shock and 1 hour of Wingless treatment cells were lysed and HA was immunoprecipitated. A Western blot was run and probed for both Arrow and Armadillo. Armadillo is known to be ubiquitynated and therefore serves as a control. It is evident that the IP carried out is not optimal as there is an abundance of Arrow and Armadillo in the flow through (Fig 4.7 B). Perhaps the heat shock time would have to be increased to increase expression of Hs-Ub-HA. A greater length of time

between the heat shock and the IP could also allow a greater accumulation of ubiquitylated Armadillo/Arrow. Furthermore not much material is precipitated, even for Armadillo, which we know is continuously ubiquitylated. The use of NEM and MG132 should lead to an accumulation of ubiquitylated Armadillo. The low pull down could be due to inefficient binding of HA to the beads or elution.

Despite these imperfections an Arrow band can be seen both in the presence and absence of Wingless. This indicates that just as its degradation is not affected by Wingless, neither is its ubiquitylation. An Armadillo band, of equal intensity, can also be seen in both the presence and absence of Wingless. Although this was unexpected as Wingless prevents the ubiquitylation and degradation of Armadillo we must keep in mind that Armadillo plays different functions within a cell and can be modified in different ways. Different forms could continue to be ubiquitylated regardless of the presence of Wingless. Optimization of the IP and repeating it would be needed to confirm these results. Nonetheless it seems plausible that Arrow is ubiquitylated. Whether this ubiquitylation directly affects signalling is another question to be addressed.

Figure 4.7 Assessment of Arrow ubiquitylation.

(A) Small samples of eluents from Arrow immunoprecipitation were used for western blots and probed with anti-ubiquitin antibody. Bands of the same molecular size as Arrow are detected in the absence of Wingless treatment. (B) To assess Arrow ubiquitylation, $S2R^{+}$ cells transfected with Hs-Ub-HA, treated with proteosome inhibitor MG132 and de-ubiquitylation enzyme inhibitor (NEM) were heat shocked at 37°C for 35 min. 3 hr after the heat shock with 1 hr of Wingless treatment, cells were lysed and HA was immunoprecipitated. Western blot analysis shows faint Armadillo and Arrow bands both in the presence and absence of Wingless suggesting that Arrow may be ubiquitylated and that this is unaffected by Wingless signalling.

A

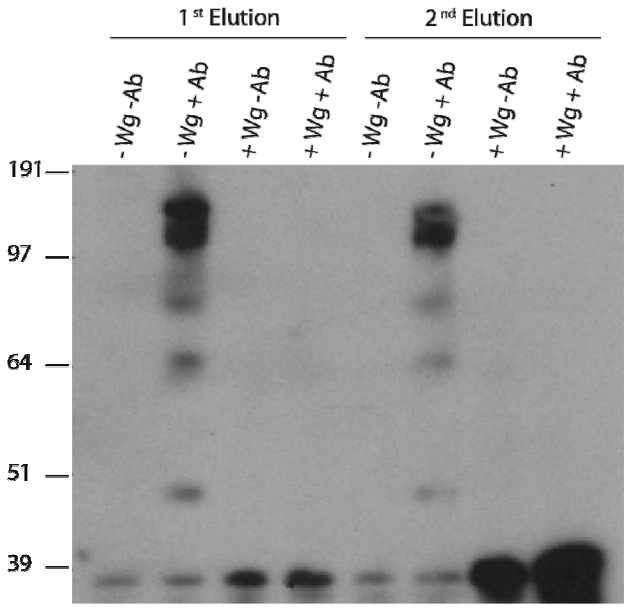
1st Elution
2nd Elution
- Wg -Ab
- Wg + Ab
+ Wg -Ab
+ Wg + Ab
- Wg -Ab
- Wg + Ab
+ Wg -Ab
+ Wg + Ab
191
97
64
51
39

B

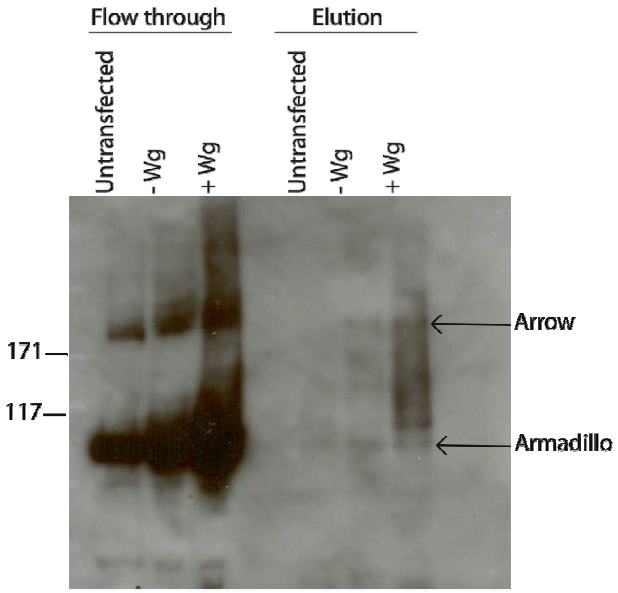
Flow through
Elution
Untransfected
- Wg
+ Wg
Untransfected
- Wg
+ Wg
171
117
Arrow
Armadillo

4.6 Summary

The work in this Chapter shows that Arrow and Fz2 follow different trafficking routes. Instead of inducing degradation, as it does for Fz2, Wingless does not affect Arrow stability (Fig 4.1 A). Thus Arrow may be recycled back to the cell surface post internalization. Although I do not have enough data to confirm this, my initial results do support this hypothesis. I have designed an improved protocol involving the labelling of cell surface Arrow and monitoring its internalization and return to the cell surface post Wingless treatment.

In order to explore Wingless dependent PTM of Arrow, that could direct it to recycling, Arrow was immunoprecipitated and sent for mass spec. Initial results were inconclusive as sequence coverage was low, not all known modifications were detected and the majority of proteins co-IP'd were involved in secretion, indicating that most of the Arrow IP'd was intracellular. Time was invested in developing a stringent double IP of cell surface Arrow. This is a useful tool, which will allow me to learn more about modifications dependent on Wingless and other proteins that play a role in the pathway. Challenged by the need to scale up the IP in order to provide sufficient amounts of Arrow for mass spec, different techniques were considered but would require time to test and optimise.

Finally I continued on from Dr. Marshall's work with the concept of Arrow ubiquitylation. Cells were transfected with Hs-Ub-HA, heat shocked, and following Wingless treatment, ubiquitylated proteins were pulled down with an HA IP. I have shown that ubiquitylation does occur. Although the experiments require optimization, it seems that ubiquitylation may be unaffected by Wingless signalling (Fig 4.7 B). In order to explore the possible role of ubiquitylation, an RNAi screen of E2 ligases and DUBs was completed to determine their involvement in the pathway. I will discuss this in the next chapter.

Chapter 5 – Results - RNAi Screen for DUBs and E2 conjugating enzymes required for Wingless signalling

5.1 Introduction

Following internalization, signalling receptors are either trafficked to lysosomes for degradation or recycled back to the cell surface. Post translational modifications regulate such trafficking, of which mono or poly- ubiquitylation has a prominent role. Ubiquitylation-conjugating enzymes (E2) are key to the ubiquitylation process. They receive ubiquitin from ubiquitin-activating enzymes (E1) and subsequently transfer the ubiquitin moiety to ubiquitin-ligating enzymes (E3). Different combinations of these proteins confer substrate specificity and specify the type (mono/poly) of protein modification. Deubiquitylases (DUBS) counteract ubiquitylation by cleaving ubiquitin moieties.

In the previous chapter it was shown that Arrow embarks on a different trafficking route to Fz2. Ubiquitylation could conceivably confer this specificity. The *Drosophila* genome encodes only one E1 (Uba1), 36 E2s and 130 E3s and 46 DUBs. Although E3s confer substrate specificity, due to their large number, I confined myself to screening DUBs and E2s for a role in Winlgess signalling.

Transgenic expression of double stranded RNA is a relatively efficient and rapid means of knocking down gene expression and is widely used in the study of different signalling cascades. By knocking down gene expression, both in cell culture and in vivo, of various DUBs and E2s, I assessed the potential role of ubiquitylation in Wingless signalling.

5.2 Cell culture RNAi screen

Ubiquitylation is already known to play an important part in the Wingless signalling pathway by regulating degradation of the transcriptional regulator β-catenin, and components of the degradation complex, Axin and APC (Choi et al, 2004; Huang et al, 2009). To identify other possible roles of ubiquitylation, in particular with regards to Arrow trafficking, I performed a small scale RNAi screen, knocking down deubiquitylating enzymes (DUBs) and ubiquitin-conjugating enzymes (E2s) in cell culture. The improved TOPFlash assay, detailed in Chapter 3, was used as a signalling reporter. Before conducting the screen, the optimal method of RNAi treatment was determined using Arrow dsRNA. Two protocols were compared. In one, cells were co-transfeced with the WISIR vector and the dsRNA for 4 days. In another, cells were bathed with the dsRNA for 2 days and then transfected with the WISIR vector, and cultured for a further two days. The former not only displayed higher signalling levels making small differences in signalling easier to detect but also showed more efficient knockdown of Arrow. A further benefit of RNAi transfection is that it requires less dsRNA (0,4 μg vs the 15μg for the bathing method). It was therefore adopted as the method of treatment (Fig 5.1 A/B). Thus my RNAi assay consisted of transfection of $S2R^{+}$ cells with the WISIR vector and individual dsRNA against DUBs or E2s. After 2 days Wingless signalling was induced using Wingless conditioned medium from S2 pTub-Wingless cells. After at least 20 hours of Wingless treatment Firefly and Renilla luciferase activity was measured to calculate signalling levels in the presence and absence of Wingless.

Interfering with ubiquitylation may only influence signalling moderately. Furthermore, the function of targeted DUBs and E2s may be partially compensated by others. For these reasons I considered even slight increases/decreases in signalling as significant, as long as they were reproducible, conducting the assays in quadruplicate/quintuplicate. Nevertheless, it is important to keep in mind that false negatives could result from inefficient knockdown, protein stability or protein function redundancy.

If ubiquitylation were required for Wingless signalling I would expect a decrease in signalling with the knockdown of certain E2s and an increase in signalling with

Figure 5.1 Method of RNAi treatments.

(A) The efficiency of Arrow dsRNA transfection vs bathing of cells in dsRNA was compared. $S2R^{+}$ cells were either transfected with the WISIR vector and dsRNA concomitantly for four days or cells were bathed in dsRNA for two days and then transfected with the WISIR vector, signally was measured after an additional two days. Cells were exposed to Wingless conditioned medium for at least 20 hours before being lyzed. dsRNA transfection proved more efficient and transfection of cells with the WISIR vector for four days provided greater sensitivity to Wingless signalling. (B) Postitive controls for dsRNA. The effect of Axin and CKI knockdown on sigalling was tested. Error bars represent SEM.

A

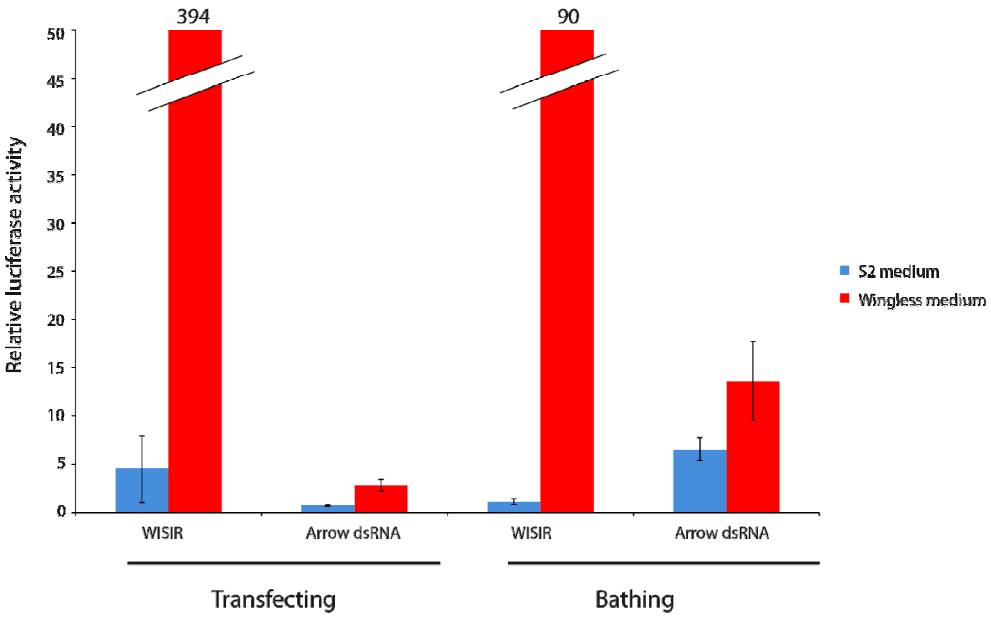
394
90
Relative luciferase activity
50
45
40
35
30
25
20
15
10
5
0
WISIR
Arrow dsRNA
WISIR
Arrow dsRNA
Transfecting
Bathing
S2 medium
Wingless medium

B

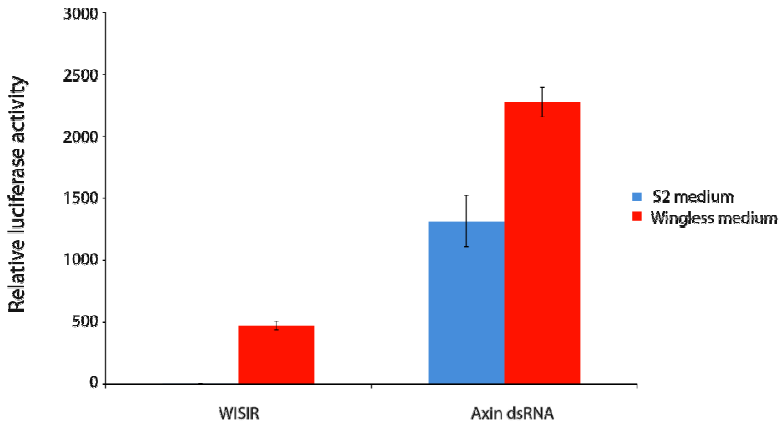
Relative luciferase activity
3000
2500
2000
1500
1000
500
0
WISIR
Axin dsRNA
S2 medium
Wingless medium

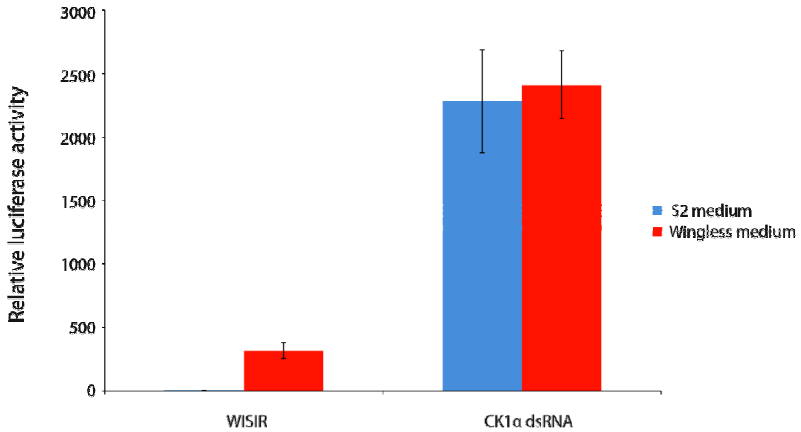
Relative luciferase activity
3000
2500
2000
1500
1000
500
0
WISIR
CK1α dsRNA
S2 medium
Wingless medium

knockdown of DUBs. Conversely, if ubiquitylation had a negative effect on signalling I would expect an increase with E2 and a decrease with DUB knockdown.

Of the 24 DUBs screened (Table 5.1), five hits were obtained (CG5794, CG1945 (*fat facets, faf*), CG3016, CG14619 and CG4166 (*non stop, not*)) (Fig 5.2 A). The knockdown of these genes potentiated Wingless, with no effect observed in the absence of Wingless. A gene which has a role in the degradation complex, such as Axin or CK1α, when knocked down activates signalling regardless of Wingless activity (Fig 5.1 C,D). Thus the genes identified function upstream of the degradation complex and play no direct role in the stabilization of Armadillo itself.

Little is known about most of hits obtained. CG14619 CG5794 and CG7288 are simply known for their ubiquitin thiolesterase activity. They are all expressed in the central nervous system as well as in various other larval and adult organs/tissues. CG3016, is the homologue of mammalian USP30 which has an exclusively mitochondrial function (Nakamura & Hirose, 2008). CG4166, also known as *non-stop*, has multiple biological functions: It has a role in axon guidance and glial migration (Poeck et al, 2001) and also regulates gene transcription as a component of the SAGA (Spt-Ada-Gcn5-acetyltransferase) complex, which catalyzes the deubiquitination of histone H2B (Samara et al; Weake et al, 2008). A lot of information is available about CG1945, also known as *fat facets (faf)*. Faf participates in numerous biological functions such as cellularization, eye development and proteolysis (Flybase, (Wu et al, 1999)); most interesting is its possible role in endocytosis. It has been shown that it modulates the function of Liquid facets (lqf), the homologue of the vertebrate endocytic protein Epsin responsible for membrane curvature (Chen et al, 2002).

In the E2 conjugating enzyme RNAi screen, six candidates were identified (Table 5.1): RNAi against CG4443 (*courtless*, *crl*), CG3018 (*lesswright, lwr*) and CG7220 increases signalling, while RNAi against CG15437 (*Morgue*), CG7425 (*effete*, *eff*), and CG2574 decreases it (Fig 5.2 B). The biological functions of CG7220 and CG2574 are not known whereas there is some information regarding the other hits. *Crl* is the Drosophila UBC7 homologue and is principally involved in male courtship and spermatogenesis. During embryonic development it is expressed primarily in the central nervous system (Orgad et al, 2000). CG3018, also known as *Lesswright* (*Lwr),* is a Small Ubiquitin-like Modifier (SUMO) protein involved in a variety of cellular processes including larval hemocyte production (Huang et al, 2005).

CG7425 (*Eff*) is essential in germline stem cell maintenance (Chen et al, 2009). Interestingly both CG15437 ((*Morgue*), modifier of Reaper and Grim) and CG7425 (*Eff*) have been implicated in apoptosis and reported to act in concert to promote degradation of Diap1 an inhibitor of apoptosis (Bergmann et al, 2003). The lack of a decrease in Renilla luciferase shows that the decrease in signalling is not due to cell death and that these genes are likely to have apoptosis-independent functions.

In conclusion, having optimised the TOPFlash assay as well as the RNAi treatment method, I identified 5 DUBs and 6 E2 that modulate Wingless signalling in cultured cells. Of these hits, CG5794 was previously identified in a genome wide RNAi screen for novel regulators of Wingless signalling and displayed the same effect of increased signalling (DasGupta et al, 2005).

Figure 5.2 RNAi screen of DUBs and E2s.

RNAi screen of 24 DUBs (A) and 33 E2s (B) was assessed using the optimised TOPFlash assay. $S2R^{+}$ were transfected with 0.4μg of the WISIR vector and 0.2μg of the dsRNA of choice. Two days after transfection cells were treated with Wingless conditioned medium or complete medium for one day. Firefly and Renilla luciferase levels were then assessed. Values are the mean of triplicates from one experiment. Errow bars represent the SEM. (A) Five DUBs were identified, that when knocked down increase Wingless signalling: CG5794, CG1945, CG3016, CG4166, CG14619. (B) Knockdown of six E2s affected Wingless signalling. CG15437, CG7425 and CG2574 knockdown increases signalling. CG4443, CG3018 and CG7220 knockdown increases signalling.

A

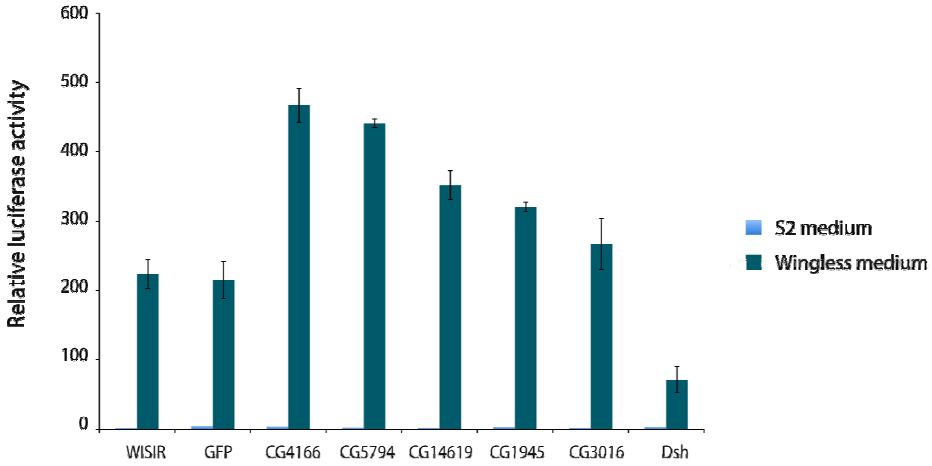
Relative luciferase activity
600
500
400
300
200
100
0
WISIR
GFP
CG4166
CG5794
CG14619
CG1945
CG3016
Dsh
S2 medium
Wingless medium

B

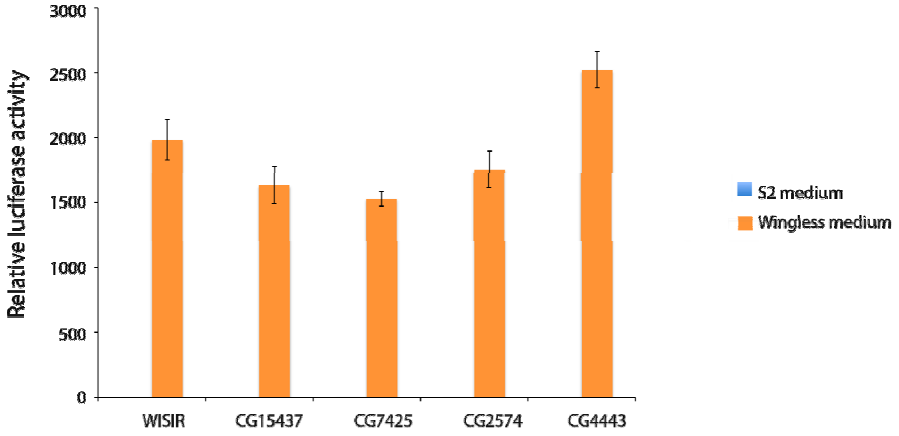
Relative luciferase activity
3000
2500
2000
1500
1000
500
0
WISIR
CG15437
CG7425
CG2574
CG4443
S2 medium
Wingless medium

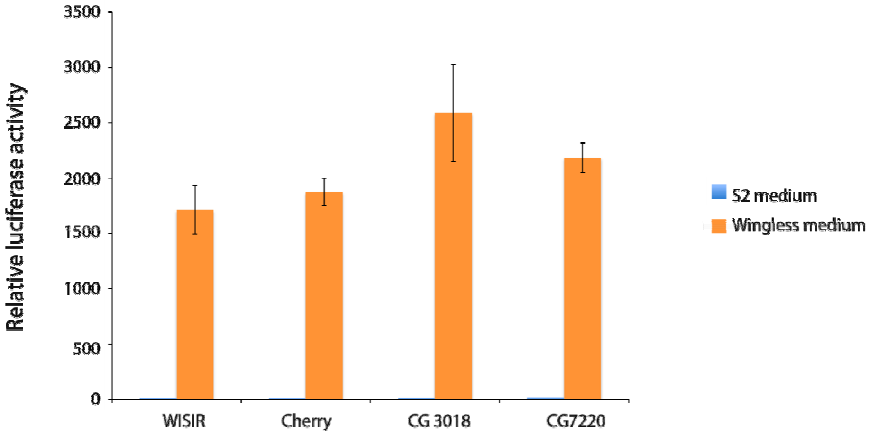
Relative luciferase activity
3500
3000
2500
2000
1500
1000
500
0
WISIR
Cherry
CG 3018
CG7220
S2 medium
Wingless medium

Table 5.1. Hits obtained with TOPFlash assay.

A) DUB hits

Gene	Effect on Signalling	Function in:	Vertebrate homologue
CG5794	Increases	Proteolysis	ubiquitin specific protease 34 (Homo sapiens)
CG1945 (fat facets)	Increases	Endocytosis, cellularization, eye development	Ubiquitin specific protease 9 (homo sapiens)
CG3016	Increases	Proteolysis	ubiquitin specific peptidase 30 (Homo sapiens)
CG14619	Increases	Proteolysis	ubiquitin specific protease 39 (Homo sapiens)
CG4166 (non stop)	Increases	glial cell development and migration, axon target recognition	ubiquitin specific protease 22 (Homo sapiens)

B) E2 hits

Gene	Effect on Signalling	Function in:	Vertebrate homologue
CG15437 (Morgue)	Decreases	Ubiquitylation, apoptosis	ubiquitin-conjugating enzyme E2D 4 (homo sapiens)
CG7425 (Eff)	Decreases	Ubiquitylation, mitosis, compound eye morphogenesis, oogenesis	Ubiquitin-Conjugating Enzyme Ubch5b (homo sapiens)
CG2574	Decreases	Ubiquitylation, protein metabolic process	ubiquitin-conjugating enzyme E2E 2 (UBC4/5 homolog, yeast) (Homo sapiens)
CG4443 (Crl)	Increases	Ubiquitylation, spermatogenesis, courtship behaviour	ubiquitin conjugating enzyme G2 (Homo sapiens)
CG7220	Increases	Ubiquitylation,	ubiquitin conjugating enzyme E2 W (Homosapiens)
CG3018 (Lwr)	Increases	Sumoylation	SUMO conjugating enzyme UBC9 (Homo Sapiens)

5.3 In vivo RNAi assay

The candidate genes identified in the cell based RNAi screen for a potential role in Wingless signalling were further assessed in vivo. UAS RNAi hairpins for each gene were expressed in the posterior or dorsal compartment of wing discs using *engrailed-Gal4* and *apterous-Gal4* respectively. In the experiments involving *engrailed-Gal4* Wingless, Distalless and Fz3 expression was assessed (Table 5.2 A/B) whereas Arrow and Senseless expression was assessed with RNAi driven by *apterous-Gal4* (Table 5.3A/B). A complete screen was only done using *engrailed-Gal4* as I focused on Distalless and Fz3 expression to analyze Wingless signalling.

5.3.1 Genes not pursued:

DUBs: CG4166 (*not*)

E2s: CG7425 (*Eff*), CG3018 (*lwr*)

Unfortunately, the in vivo effects of knockdown of CG4166 (*not*), CG7425 (*Eff*) and CG3018 (*lwr*) could not be assessed. RNAi against CG4166 (*not*) (DUB) was lethal. With regards to CG7425 (*Eff*) (E2), the larvae that did develop were filled with tumors and did not contain identifiable wing imaginal discs (Fig 5.3). Knockdown of CG3018 (*lwr*) in the posterior compartment resulted in a wing disc more distorted than those mutant for Wingless (Fig 5.4, Fig 5.5 A). There was a large reduction of *engrailed* expressing cells and the anterior compartment dominated the pouch. To monitor apoptosis a Caspase staining was preformed revealing no overlap between Capase and engrailed expression (Fig 5.3 C). It could be that cells of the posterior compartment that are dying no longer express engrailed. Although it would be interesting to pursue the role of these genes as they seem to play important parts in development, their involvement in various developmental processes makes it difficult to assess their potential effects specifically on Wingless signalling.

Table 5.2. A Dll / Wg / Fz3 expression in E2 loss of function wing discs

(NA = Not Available)

A) E2s

Gene	Transformant ID	Dll expression in the P compartment	Wg expression in the P compartment	Fz3 expression in the P compartment
CG15437 (Morgue)	11090	Unchanged	Unchanged	-
CG7425 (Eff)	26011	NA	NA	NA
	26012	NA	NA	NA
CG2574	40173	Increase	Unchanged	Unchanged
CG4443 (Crl)	34109	Unchanged	Unchanged	-
	34111	Unchanged	Unchanged	-
CG7220	34198	Unchanged	Unchanged	-
	34199	Unchanged	Unchanged	-
CG3018 (Lwr)	33684	NA	NA	NA
	33685	NA	NA	NA

Table 5.2 B. Dll / Wg / Fz3 expression in DUB loss of function wing discs

B) DUBs

Gene	Transformant ID	Dll expression in the P compartment	Wg expression in the P compartment	Fz3 expression in the P compartment
CG5794	27517	Unchanged	Unchanged	-
CG1945 (fat facets)	2955	Increase	Unchanged	Unchanged
	2956	Increase	Unchanged	-
	30679	Increase	Unchanged	-
	30680	Increase	Unchanged	Unchanged
CG3016	7090	Increase	Unchanged	Unchanged
	110616	Increase	Unchanged	Unchanged
CG4166 (non stop)	45775	NA	NA	NA
	45776	NA	NA	NA
CG14619	37929	Increase	Unchanged	Unchanged
	37930	Increase	Unchanged	Unchanged

Table 5.3.A Senseless/Arrow expression in E2 loss of function wing discs

(A) E2s

Gene	Transformant ID	Dll expression in the P compartment	Wg expression in the P compartment
CG15437 (Morgue)	11090	Unchanged	Unchanged
CG7425 (Eff)	26011	NA	NA
	26012	NA	NA
CG2574	40173	Unchanged	Unchanged
CG4443 (Crl)	34109	-	-
	34111	-	-
CG7220	34198	-	-
	34199	-	-
CG3018 (Lwr)	33684	NA	NA
	33685	NA	NA

Table 5.3 B Senseless/Arrow expression in DUB/loss of function wing discs

(B) DUBs

Gene	Transformant ID	Dll expression in the P compartment	Wg expression in the P compartment
CG5794	27517	Unchanged	Unchanged
CG1945 (fat facets)	2955	-	-
	2956	-	-
	30679	-	-
	30680	-	-
CG3016	7090	-	-
	Nigfly	-	-
CG4166 (non stop)	45775	NA	NA
	45776	NA	NA
CG14619	37929	Unchanged	Unchanged
	37930	Unchanged	Unchanged

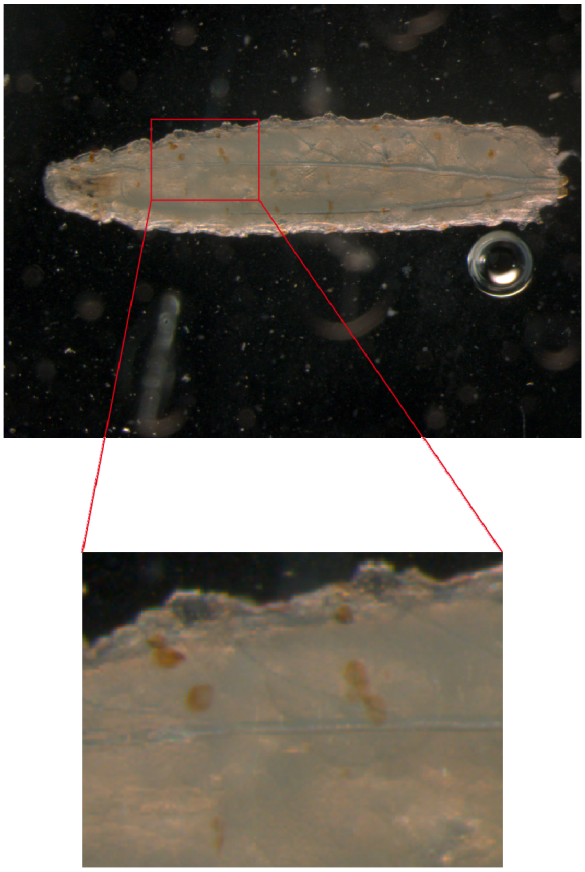

Figure 5.3 CG7425 (*Eff*) knockdown compromises larval development.

RNAi of CG7425 (*enGal4 ; UAS CG7425 RNAi)* results in melanotic tumors in third instar larvae. Wing discs were not identifiable.

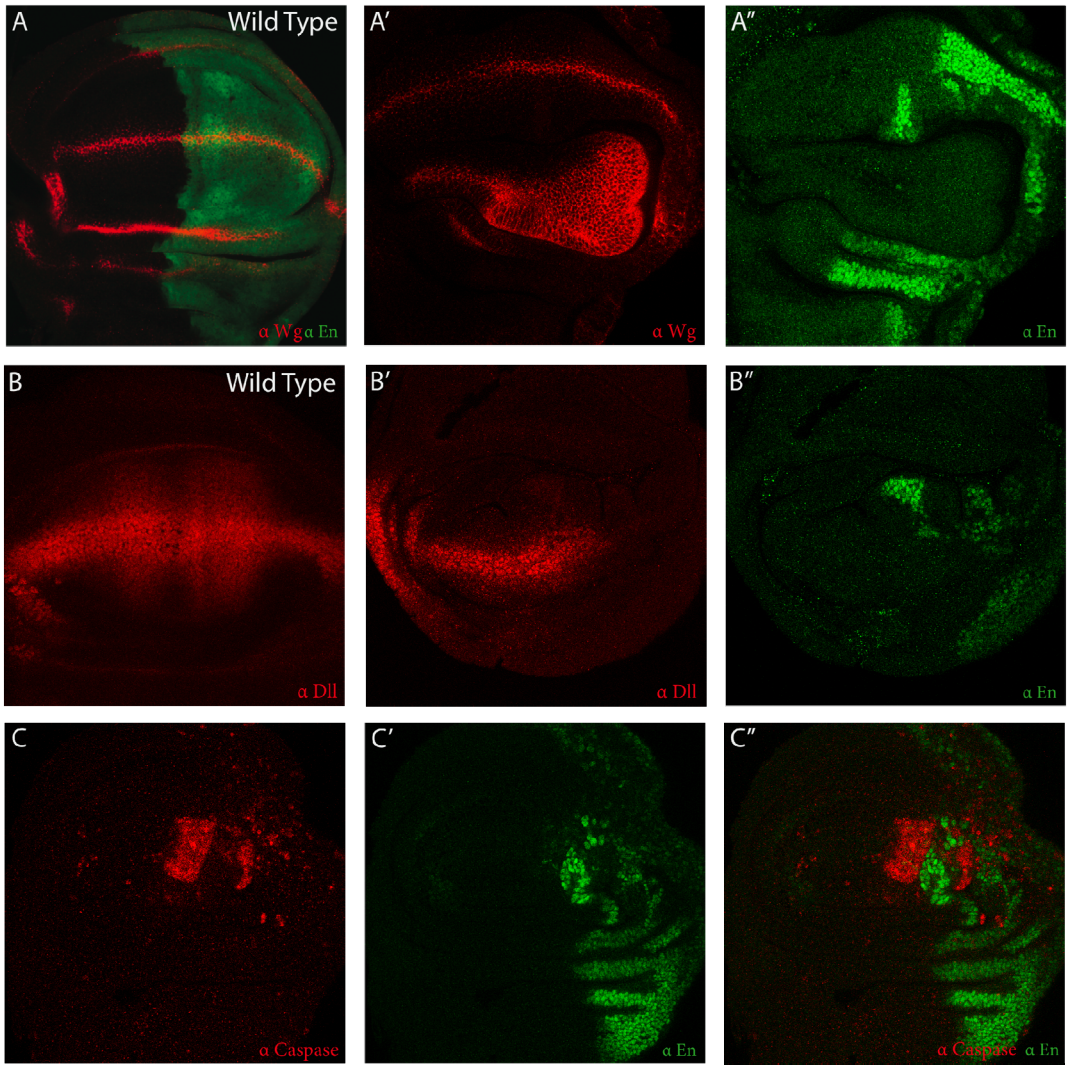

Figure 5.4 Distorted wing discs with CG3018 knockdown.

(A) RNAi of CG3018 (*enGal4 ; UAS CG3018 RNAi)* results in distorted third instar wing discs with overgrowth of the anterior compartment and reduced Engrailed expression. (B) Dll expression is also reduced. (C) No overlap between Caspase 3 and Engrailed stainings detected.

5.3.2 Genes pursued

DUBs: CG3016, CG1945 *(faf)*, CG14619, CG5794

E2s: CG15437 (*Morgue*), CG2574, CG7220, CG4443 (crl)

5.3.3 Effect on Wingless expression

No difference in wingless expression was observed between the anterior and posterior compartments of third instar wing discs with RNAi of any of the DUB or E2 RNAs. Therefore, these DUBs and E2s have no effect on Wingless secretion or gradient formation. (Fig 5.5)

5.3.4 Effect on Distalless expression

The effect of DUB and E2 loss of function in the posterior compartment on gene expression was determined by comparing *dll* expression in the anterior and posterior compartment of the wing disc. To quantify expression levels, outlined in Fig 5.6, equivalent regions of interest (ROI) were delineated in each compartment. The ROI were divided into horizontal lines. The intensity of a horizontal line in the anterior compartment added to the intensity of the corresponding horizontal line in the posterior compartment was normalised to 100% intensity/expression. It was then possible to calculate the % intensity each line contributed to total intensity. Knockdown of CG5794, CG15437 (Morgue), CG7220 and CG4443 had no effect on *dll* expression. Knockdown CG3016, CG1945 *(faf)*, CG14619 and CG2574 on the other hand increased *dll* expression in the wing disc posterior compartment, as illustrated in stacked bar graphs (Fig 5.7). The result obtained with CG2574 RNAi in discs contradicts that of the TOPFlash assay, where a decrease in signalling was observed. This could be due to the fact that *dll* expression is also affected by Decapentaplegic (DPP) and Hedgehog (HH). Thus the increase in expression may reflect the RNAi affecting other signalling pathways.

Figure 5.5 Effect of DUB and E2 knockdown on *wingless* expression.

(A) Winlgess expression with wingless dsRNA in the posterior comparment.
(B,C, D, E,) Wingless expression in third instar wing discs with RNAi of E2 hits.
(F, G, H, I) Wingless expression in third instar wing with RNAi of DUB hits.
All RNAi hairpins are expressed in the posterior compartment (*en Gal4 ; UAS RNAi*).

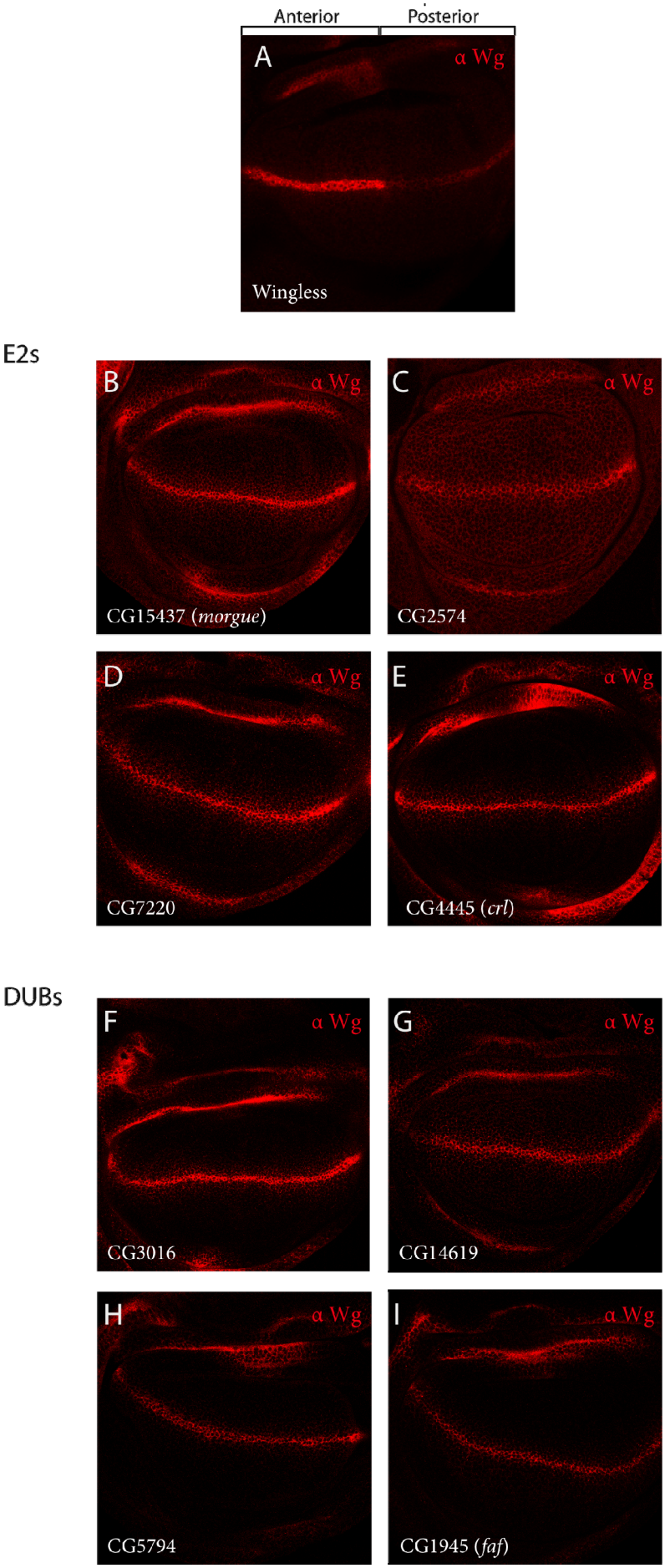
Anterior
Posterior
A
α Wg
Wingless
E2s
B
α Wg
CG15437 (morgue)
C
α Wg
CG2574
D
α Wg
CG7220
E
α Wg
CG4445 (crl)
DUBs
F
α Wg
CG3016
G
α Wg
CG14619
H
α Wg
CG5794
I
α Wg
CG1945 (faf)

Figure 5.6 Quantification of gene expression.

(A) *dll* expression in wild type wing discs. Equivalent ROI were delineated in anterior and posterior comartments. ROI were divided into rows one pixel thick. The sum of the intensity of a row in the anterior comparmtent with the corresponding row in the posterior compartment was normalized to 100%. (B) Calculations of % intensity contributed to final intensity by each row in the ROI.

A

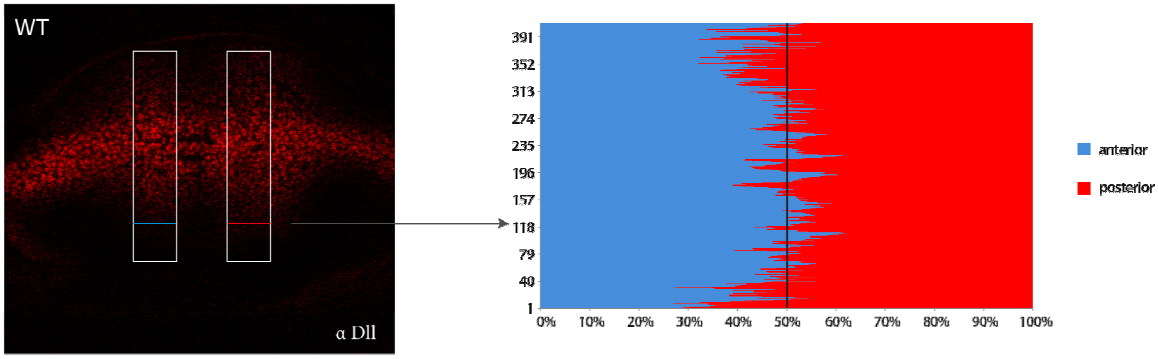

B

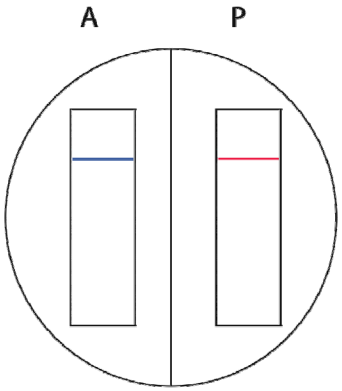

X = intensity of

Y = intensity of

X + Y = 100 %

X % = (X) (100)/ (X+Y)

Y % = (Y)(100)/(X+Y)

X % : Y %

Figure 5.7 Effect of DUB and E2 knockdown on *dll* expression.

An increase in *dll* expression in the posterior compartment of wing discs expressing UAS RNAi hairpins, for E2, CG2574 (A) and DUBS: CG3016, CG1945, CG14619 (B, C,D), driven *engrailed-Gal4*.

A

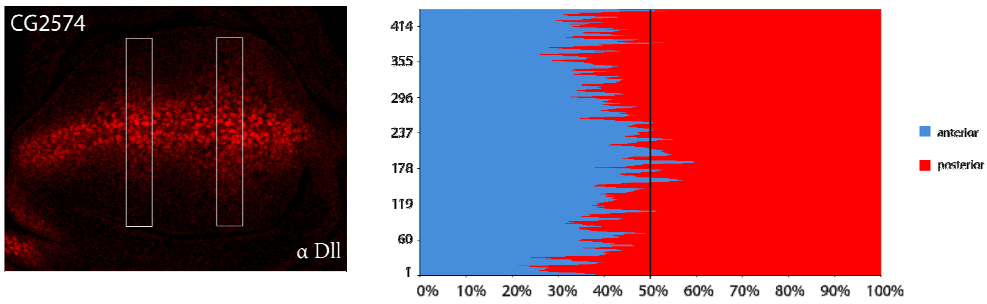
CG2574
α Dll
414
355
296
237
178
119
60
1
0%
10%
20%
30%
40%
50%
60%
70%
80%
90%
100%
anterior
posterior

B

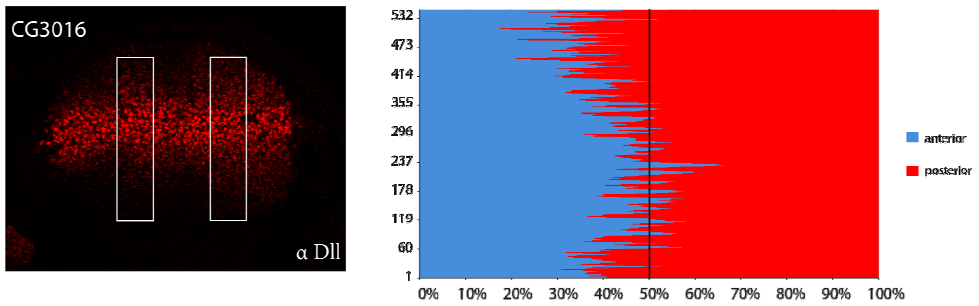
CG3016
α Dll
532
473
414
355
296
237
178
119
60
1
0%
10%
20%
30%
40%
50%
60%
70%
80%
90%
100%
anterior
posterior

C

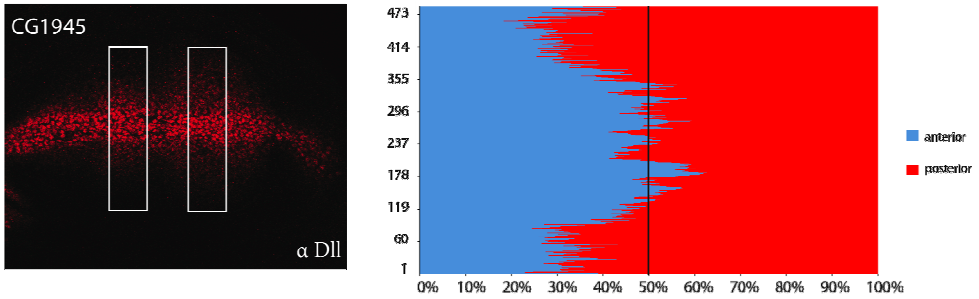
CG1945
α Dll
473
414
355
296
237
178
119
60
1
0%
10%
20%
30%
40%
50%
60%
70%
80%
90%
100%
anterior
posterior

D

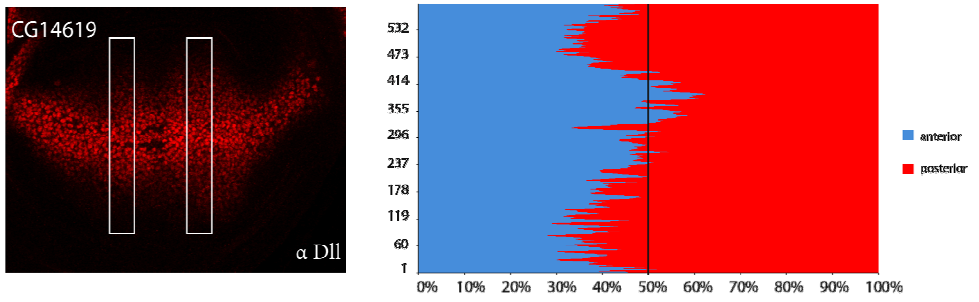
CG14619
α Dll
532
473
414
355
296
237
178
119
60
1
0%
10%
20%
30%
40%
50%
60%
70%
80%
90%
100%
anterior
posterior

5.3.5 Effect on *fz3* expression

To specifically assess Wingless signalling an alternative target gene, *fz3*, was used. (Sivasankaran et al, 2000). As for *dll*, *fz3* expression was quantified and showed no significant difference in the anterior and posterior compartments (Fig 5.8). This shows that Wingless signalling is not affected in a detectable manner.

5.3.6 Effect on *senseless* and *arrow* expression

DUBs: CG14619, CG5794

E2s: CG15437 (*Morgue*), CG2574,

Another Wingless specific target gene that I hoped to assess was *senseless*. *Senseless* is a high level target gene. Thus an effect on expression with DUB/E2 knockdown could show that although ubiquitylation does not have an effect on low level target genes (*dll* / *fz3*) expression it does play a role in high levels of Wingless signalling. RNAi driven by *apterous-Gal4* was only done for genes listed above. No difference between *senseless* expression in the dorsal and ventral compartment was observed (Fig 5.9). *Arrow* expression levels were assessed to determine a possible role of ubiquitylation in receptor stability. No difference in expression levels in the dorsal compartment was observed.

5.3.7 Adult Wing Patterning

Although the DUBs and E2 tested did not show a specific effect on Wingless signalling, adult wing phenotypes were analyzed with the hope of uncovering activities in other signalling pathways. Table 5.3 shows the percentage of adults with DUB/E2 loss of function, thus illustrating weakness/lethality. No wing defects specific to Wingless signalling in the posterior compartment were observed (Fig 5.10, Fig 5.11). A general decrease in wing size shows that multiple pathways are affected. Therefore knockdown of the DUBs and E2 screened either dramatically affected signalling thus inhibiting development and causing lethality or moderately affected signalling allowing wild type phenotypes.

Figure 5.8 Effect of DUB and E2 knockdown on *fz3* expression.

No change in *fz3-LacZ* expression in the posterior compartment of wing discs expressing UAS RNAi hairpins, driven *engrailed-Gal4*, of E2, CG2574 (A) and DUBS: CG14619, CG1945, CG3016 (B, C,D).

A

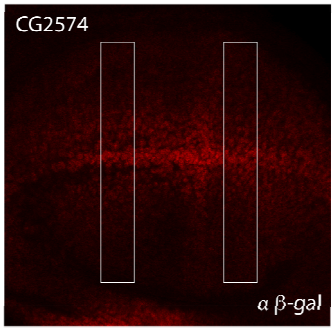
CG2574
α β-gal

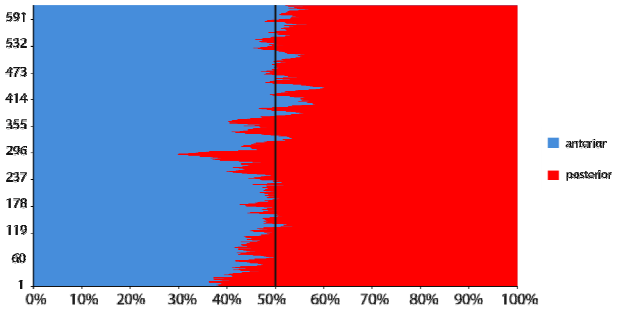
591
532
473
414
355
296
237
178
119
60
1
0%
10%
20%
30%
40%
50%
60%
70%
80%
90%
100%
anterior
posterior

B

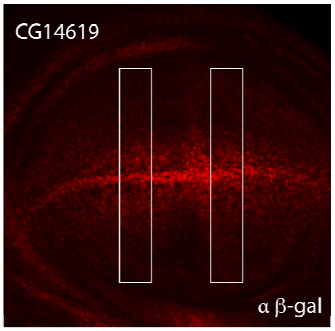
CG14619
α β-gal

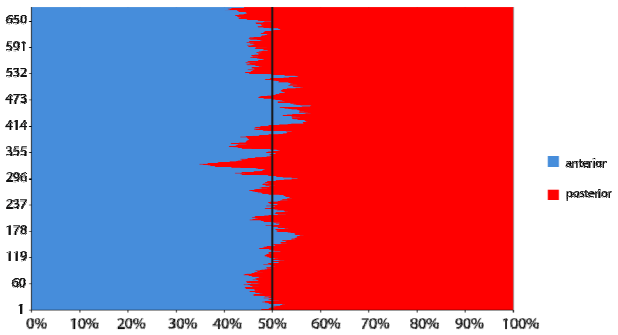
650
591
532
473
414
355
296
237
178
119
60
1
0%
10%
20%
30%
40%
50%
60%
70%
80%
90%
100%
anterior
posterior

C

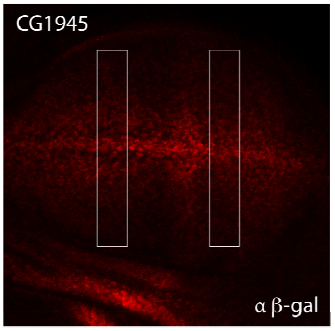
CG1945
α β-gal

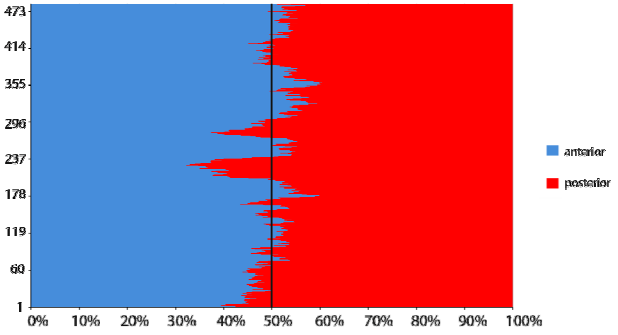
473
414
355
296
237
178
119
60
1
0%
10%
20%
30%
40%
50%
60%
70%
80%
90%
100%
anterior
posterior

D

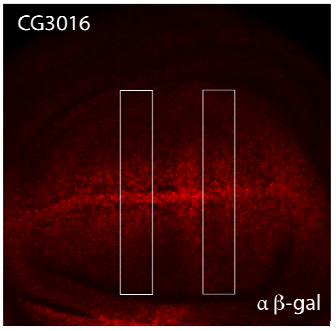
CG3016
α β-gal

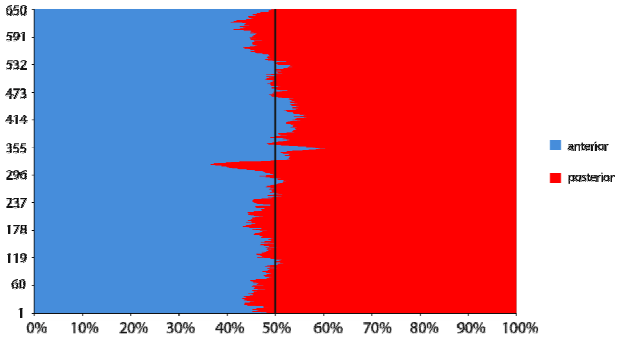
650
591
532
473
414
355
296
237
178
119
60
1
0%
10%
20%
30%
40%
50%
60%
70%
80%
90%
100%
anterior
posterior

Figure 5.9 Effect of DUB and E2 knockdown on *sens and arr* expression.

No change in *sens* or *arr* expression in the dorsal compartment of wing discs expressing UAS RNAi hairpins of E2: CG15437 (A), CG2574 (B) and DUBS: CG14619 (C), CG5794 (D). RNAi hairpin expression is driven by *apterous-Gal4*

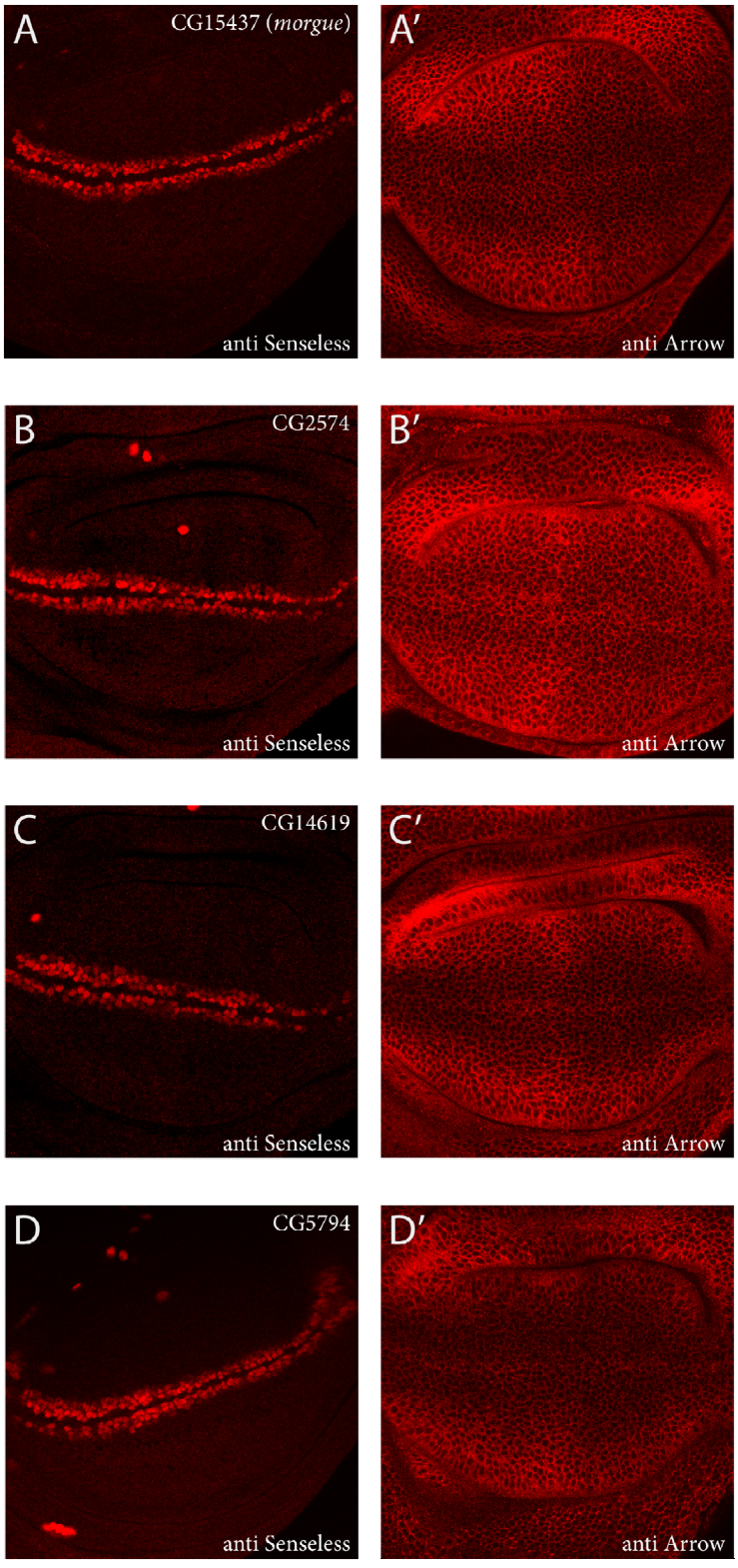
A
CG15437 (*morgue*)
anti Senseless
A′
anti Arrow
B
CG2574
anti Senseless
B′
anti Arrow
C
CG14619
anti Senseless
C′
anti Arrow
D
CG5794
anti Senseless
D′
anti Arrow

Table. 5.4. % Adult Mutants.

A) E2s

Gene	Transformant ID	% Adult Mutants
CG15437 (Morgue)	11090	51%
CG7425 (Eff)	26011	0%
	26012	0%
CG2574	40173	52%
CG4443 (Crl)	34109	47%
	34111	
CG7220	34198	39%
	34199	
CG3018 (Lwr)	33684	0%
	33685	0%

B) DUBs

Gene	Transformant ID	% Adult Mutants
CG5794	27517	20%
CG1945 (fat facets)	2955	38%
	2956	
	30679	
	30680	
CG3016	7090	
	110616	
CG4166 (non stop)	45775	0%
	45776	0%
CG14619	37929	50%

Figure 5.10 Adult wing patterning with DUB knockdown.

Adult wing margins are unaffected by the knockdown of DUBs in wing discs posterior compartments (*en-Gal4: UAS RNAi*). (A) Wild type wing, (B) CG3016, (C) CG14619, (D) CG5794, (E) CG1945.

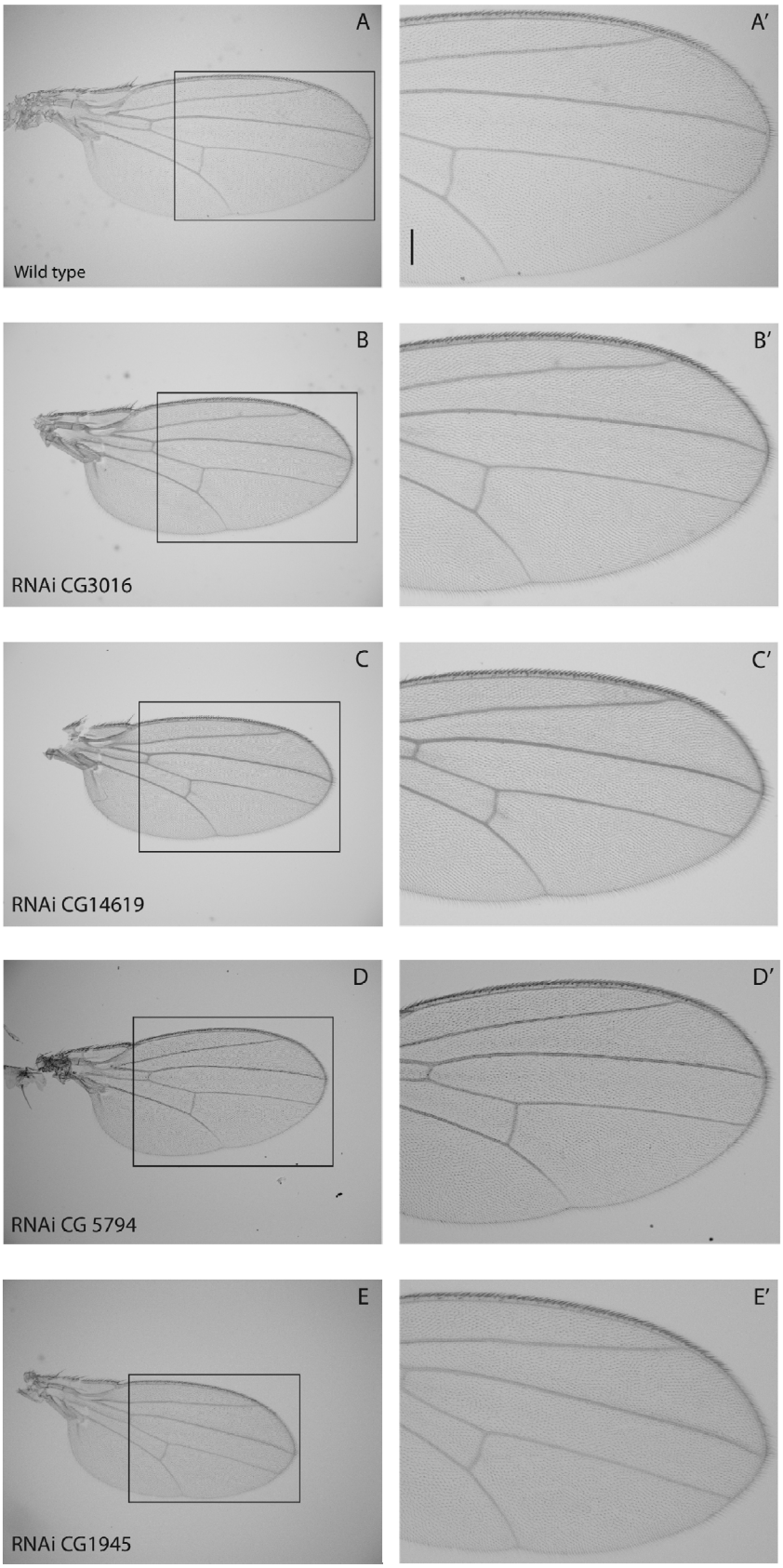
A
A′
Wild type
B
B′
RNAi CG3016
C
C′
RNAi CG14619
D
D′
RNAi CG 5794
E
E′
RNAi CG1945

Figure 5.11 Adult wing patterning with E2 knockdown.

Adult wing margins are unaffected by the knockdown of E2s in wing discs posterior compartments (*en-Gal4: UAS RNAi*). (A) Wild type wing, (B) CG7220, (C) CG15437, (D) CG4443, (E) CG1945.

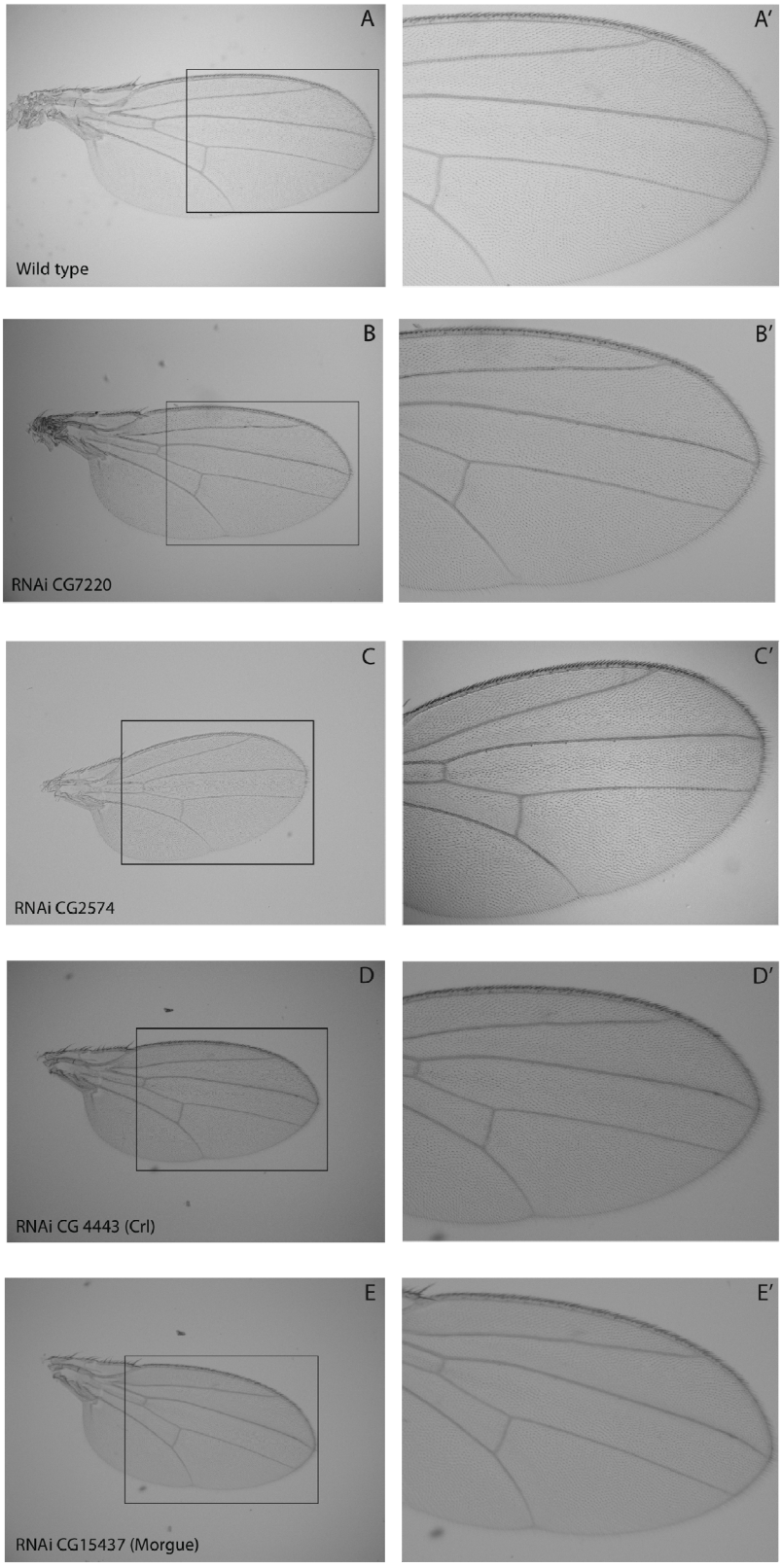
A
A′
Wild type
B
B′
RNAi CG7220
C
C′
RNAi CG2574
D
D′
RNAi CG 4443 (Crl)
E
E′
RNAi CG15437 (Morgue)

5.4 Summary

Ubiquitylation plays a role in numerous cellular processes and is known to be involved in Wingless signalling. I screened 24 DUBs and 33 E2 genes to identify Ubiquitin enzymes that could modulate Wingless signalling. The assay was done both in S2R^{+}cells using the TOPFlash reporter and in vivo, by inducing expression of RNA hairpins in the wing disc. The TOPFlash assay revealed increased Wingless signalling with RNAi against 5 DUBS (CG3016, CG1945, CG4116, CG5794, CG41619) and 3 E2s (CG 4443 (Crl), CG3018, CG7220), and a decrease in signalling with RNAi against 3 E2s (CG15437 (Morgue), CG7425 (Eff), CG2574). In vivo assessment showed that none of the RNAi lines tested interfered with Wingless production, secretion or gradient formation. Effects on signalling were determined by comparing *distalless* expression in wing disc anterior and posterior compartments. CG14619, CG30160, CG1945 (DUBs) and CG2574 RNAi (E2) showed an increase in *distalless* expression. To ask if this was specifically due to an effect on Wingless signalling I assessed *fz3* and *senseless* expression. No difference in *fz3* levels was observed between anterior and posterior compartments or *senseless* expression levels between dorsal and ventral compartments. Therefore none of the DUBs or E2s identified in the cell culture screen showed a potential role for Wingless signalling in wing imaginal discs. Despite these results one cannot conclude that the DUBs and E2s screened do not play a role. It is important to keep in mind the limits of an RNAi approach, which I will discuss in Chapter 7, and the possibility that an effect may be masked by the function of other DUBs/E2s or the involvement of other signalling pathways.

Chapter 6 – Results - Endocytosis and Signalling

6.1 Introduction

Endocytosis has been implicated in the initiation, maintenance and termination of various signalling cascades. Endocytosis has a critical role in Wingless signalling, yet which step along the endocytic pathway is involved is not clear. It has been suggested that internalization of the receptor complex is required for signalling and that signalling may be initiated by the aggregation of signalling components on special signalling endosome (signalosome) (Bilic et al, 2007). It has also been suggested that further down in the endocytic pathway formation of multi vesicular bodies (MVBs) may have the role of confiscating components of the degradation complex thus allowing accumulation of Armadillo and transport to the nucleus (Taelman et al, 2010). In this chapter the effects of modulating various steps along the endocytic pathway on Wingless signalling are investigated.

6.2 Endocytosis of Wingless is not needed for signalling

The role of endocytosis and endocytic trafficking in Wingless signalling has long been debated. I assessed the requirement of endocytosis from the beginning of the signalling pathway by determining the requirement of internalization of the Wingless ligand itself for signalling. To do this I used NRT-HA-Wingless, in which Wingless is fused to a type-II transmembrane protein: Neurotactin (Nrt), which prevents the release of Wingless from expressing cells. $S2R^+$ cells, transfected with the WISIR vector, were mixed with S2 cells transfected with, NRT-HA-Wingless, or with a stable S2 cell line expressing *wg* under the control of the tubulin promoter (pTub-Wg) as a positive control. After 20 hours of treatment the TOPFlash assay revealed signalling in $S2R^+$ cells co-cultured with pTub-Wingless cells, as expected. NRT-HA-Wingless cells also triggered signalling. This result suggests that endocytosis of Wingless in receiving cells is not necessary for signalling (Fig 6.1 A). The level of signalling in the cells exposed to NRT-HA-Wingless however, was less than in cells exposed to pTub-Wingless cells. This may be due to the different levels of Wingless expression in NRT-HA-Wingless transfected cells compared to the S2 pTub-Wingless stable cell line. To achieve comparable levels of expression I replaced S2 pTub-Wingless cells with S2 cells transfected with HA-Wingless. More comparable levels of signalling were expected but there was still less signalling in cells exposed to NRT-HA-Wingless compared to HA-Wingless (Fig 6.1 B). To confirm that the signalling occurring is not due to endocytosis of NRT-Wingless, the $S2R^+$ cells were stained for Wingless. In contrast to cells exposed to pTub-Wingless cells, no Wingless was observed in cells exposed to NRT-HA-Wingless (Fig 6.1.C, D, E). This strongly suggests that NRT-HA-Wingless is not cleaved and any signalling that occurs is due to cell-cell contact.

To confirm these results in vivo I generated clones in 3^{rd} instar wing discs expressing either NRT-HA-Wingless or HA-Wingless. As shown in Fig 6.2 Wingless is present in cells around HA-Wingless producing clones. This is not the case for clones expressing NRT-HA-Wingless, thus proving that NRT-HA-Wingless is not released from expressing cells or endocytosed by neighbouring cells.

It has previously been shown that clones expressing UAS > Nrt-HA-Wingless activate the expression of Wingless target genes such as *Vestigial (Vg), Distalless (Dll-lacZ)* and Neuralized (Neur-lacZ) in neighbouring cells (Zecca et al, 1996). The boundary of expression is sharp in contrast to a graded boundary of target gene

activation observed surrounding HA-Wingless clones. This difference is expected since HA-Wingless signals at a distance from its source, whereas NRT-HA-Wingless is not released and signals via cell-cell contact.

It can be concluded that NRT-HA-Wingless, while not being released from expressing cells and endocytosed by neighbouring cells, is still able to induce signalling. However NRT-HA-Wingless and HA-Wingless could trigger different levels of signalling. This could be due to the requirement of endocytosis to potentiate signalling, as discussed further in Chapter 7.

Figure 6.1 Membrane bound Wingless signals.

$S2R^+$ cells transfected with the WISIR vector were exposed to S2 cells expressing NRT-HA (A, B), NRT-HA-Wingless (A, B), HA-Wg (B) or to tub-Wingless cells (A). After a 20hr treatment, TOPFlash assay reveals that NRT-HA-Wingless is able to signal. Values are the mean of triplicates from one experiment. Error bars represent the SEM.

(C,D,E,) Confocal microscopy of $S2R^+$ cells mixed with S2 cells expressing NRT-HA (C), NRT-HA-Wingless (D) and Wingless expressing S2 cells (E). Internalized Wingless is only detected in cells exposed to tub-Wingless cells. (D) An S2 cell expressing NRT-HA-Wingless seen amongst the $S2R^+$ cells (red arrow). (C', D') HA stainings of transfected S2 cells shows efficient NRT-HA and NRT-HA-Wingless expression.

A

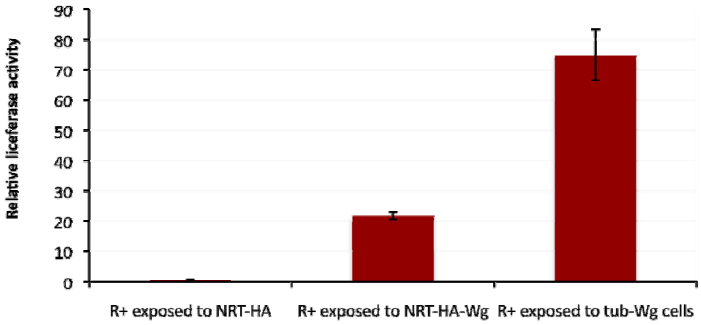
Relative liceferase activity
90
80
70
60
50
40
30
20
10
0
R+ exposed to NRT-HA
R+ exposed to NRT-HA-Wg
R+ exposed to tub-Wg cells

B

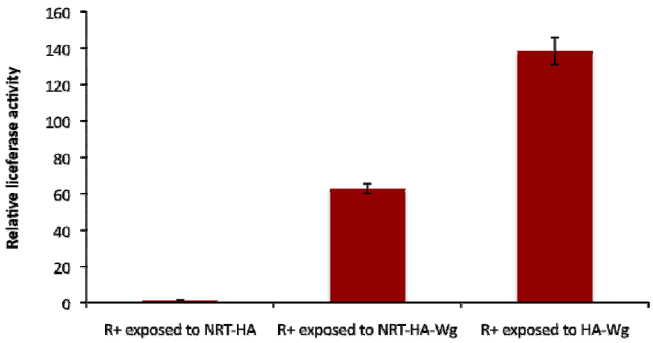
Relative liceferase activity
160
140
120
100
80
60
40
20
0
R+ exposed to NRT-HA
R+ exposed to NRT-HA-Wg
R+ exposed to HA-Wg

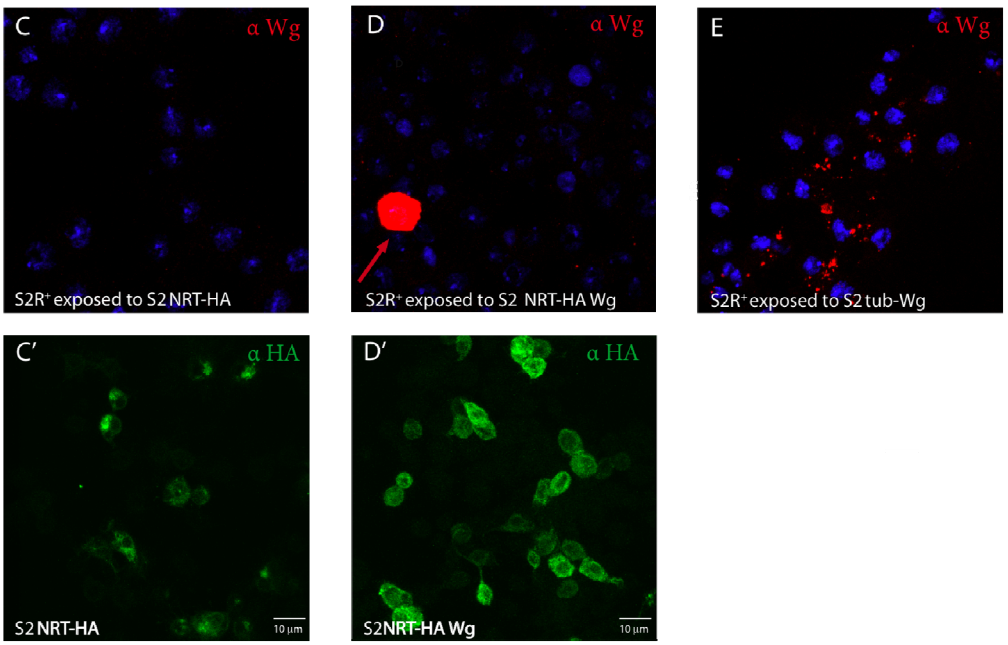
C
α Wg
S2R+ exposed to S2 NRT-HA
D
α Wg
S2R+ exposed to S2 NRT-HA Wg
E
α Wg
S2R+ exposed to S2 tub-Wg
C′
α HA
S2 NRT-HA
10 µm
D′
α HA
S2NRT-HA Wg
10 µm

Figure 6.2 NRT-HA-Wingless remains bound to membranes.

(A, B) Projection of NRT-HA-Wingless and NRT-HA clones, marked by the expression of GFP (blue). (A', A''') HA-Wingless is released from these clones, and Wingless (red) is detected in surrounding cells. (A'') Lack of an effective HA antibody prevented detection of HA (green). (B', B'') Contrarily to HA-Wingless, NRT-HA-Wingless is not in cells surrounding clones proving it to remain tethered to membrane.

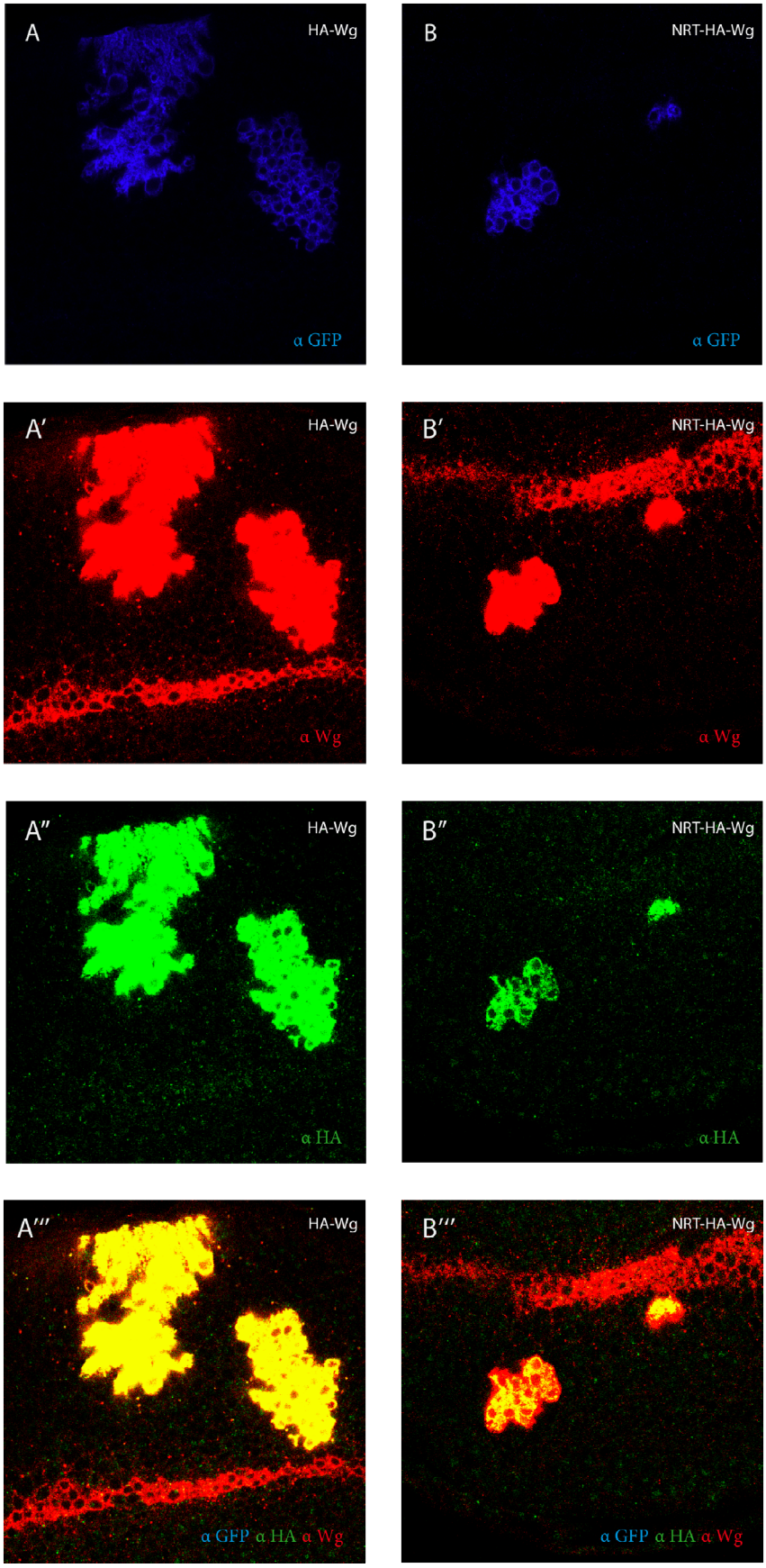
A
HA-Wg
α GFP
B
NRT-HA-Wg
α GFP
A′
HA-Wg
α Wg
B′
NRT-HA-Wg
α Wg
A″
HA-Wg
α HA
B″
NRT-HA-Wg
α HA
A‴
HA-Wg
α GFP α HA α Wg
B‴
NRT-HA-Wg
α GFP α HA α Wg

6.3 Role of MVB formation in Wingless Signalling

A recent paper suggested that sequestration of GSK3 into MVBs (Multi Vesicular Bodies) is a pivotal step in Wingless signalling. According to this model, GSK3 molecules are recruited to the receptor complex upon activation of signalling. Subsequent trafficking of GSK3, along with other components of the receptor complex, leads to sequestration into MVBs, which allows β-catenin to become stabilized and to activate transcription of target genes (Taelman et al, 2010). In this paper one of the results that established the requirement of MVBs for signalling was the finding that signalling is inhibited upon knockdown of *hrs* (hepatocyte growth factor-regulated tyrosine kinase substrate). Hrs mediates MVB formation by recruiting ESCRT-I (Endosomal Sorting Complexed Required for Transport) to endosomes. ESCRT I, II, and III function sequentially to sort endosomal vesicles for degradation. (Bache et al, 2003). To assess the requirement of Hrs in Wingless signalling, I generated hrs^{D28} mutant clones in the posterior compartment of wing discs. As expected, inhibiting MVB formation led to an accumulation of Wingless and Fz2 (Fig 6.3 A, B). However no accumulation of Arrow was observed, but rather a slight decrease, (Fig 6.3 C) supporting the model that Arrow trafficking differs from that of its co-receptor and is not targeted to MVBs for degradation. To determine the effect of Hrs loss on signalling I stained for two Wingless target genes: *distalless*, a low level target gene, and *senseless*, a high level target gene (Fig 6.4 A, B). Blocking Hrs function had no effect on *dll* expression. Yet, *sens* expression was decreased. Two possible interpretations are 1) that MVBs may be required for high levels of signalling or 2) that the loss of *senseless* expression is due to delayed development in the posterior compartment.

A TOPFlash assay was used to assess the function of Hrs in Wingless signalling. $S2R^{+}$ cells were transfected with WISIR and Hrs dsRNA and then exposed to Wingless conditioned medium. With an efficient knockdown of *Hrs* there was an over two fold increase in signalling (Fig 6.4 C) suggesting that Hrs could be needed for signalling termination instead of activation. Western blot proved that Hrs RNAi was effective (Fig 6.4 D). Knockdown of *vps16*, a protein required in trafficking to lysosomes and *tsg101*, a component of ESCRT I was also used to determine MVB involvement in signalling.

Figure 6.3 Impaired MVB formation does not result in Arrow accumulation.

(A', B', C') Projected view of wing discs with hrs^{D28} mutant posterior compartments marked by the absence of β-gal. (A, B) Loss of *hrs* function leads to the accumulation of both Wingless and Fz2, showing their trafficking along the degradation pathway. (C) Arrow levels do not increase upon disruption of MVB formation, suggesting that Arrow follows a different trafficking route from Wingless and Fz2. (D) Arrow expression in wild type discs.

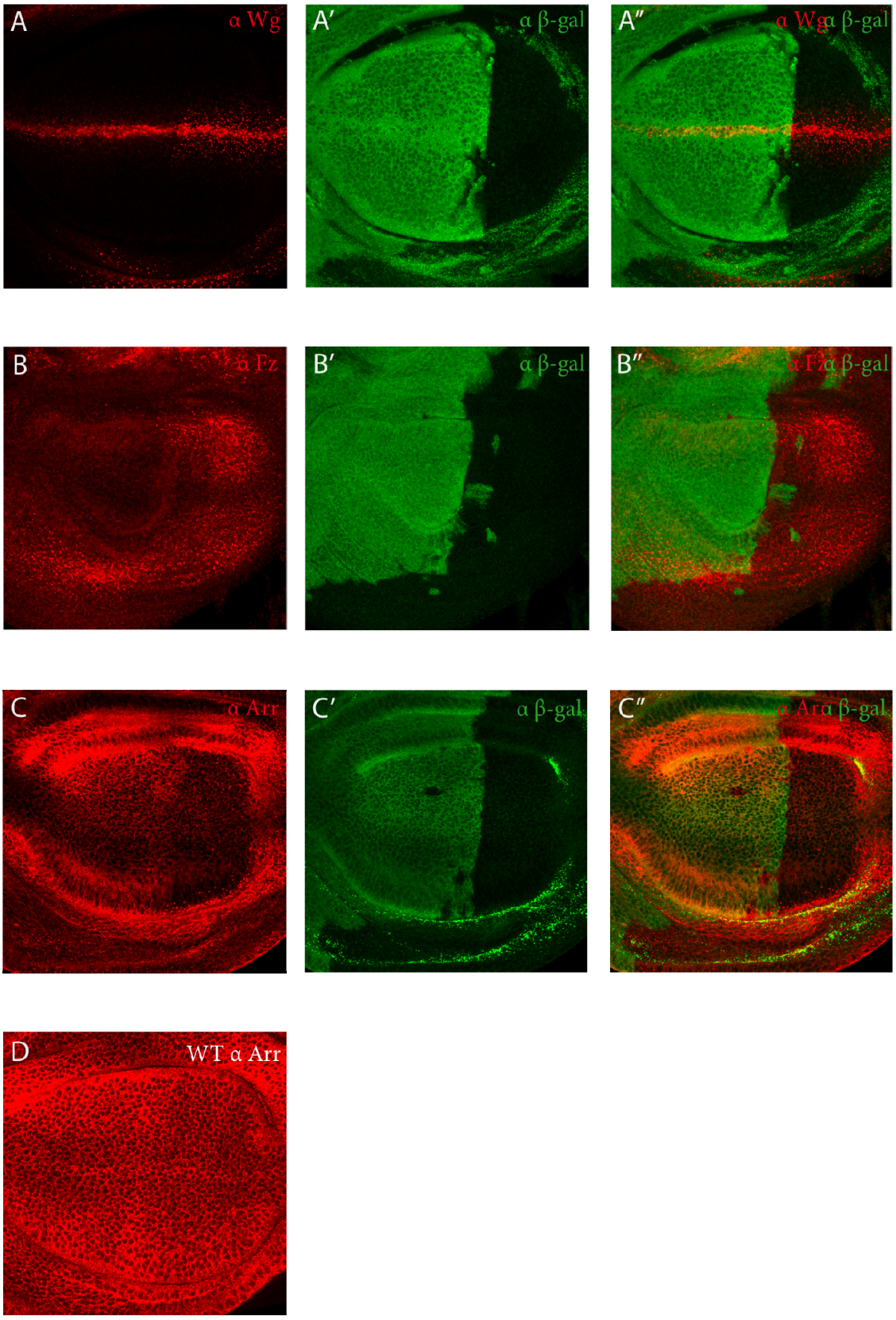
A
α Wg
A′
α β-gal
A″
α Wgα β-gal
B
α Fz
B′
α β-gal
B″
α Fzα β-gal
C
α Arr
C′
α β-gal
C″
α Arα β-gal
D
WT α Arr

Figure 6.4 Wingless signalling with knockdown of *hrs*

hrs^{D28} mutant clones marked by the absence of β-gal were stained for Wingless target genes *distalless* (*dll*), a low target gene, and *senseless* (*sens*), a high target gene. (A) *dll* expression is unaltered. (B) *Senseless* expression is decreased in the clones. (C) Knockdown of *hrs* with dsRNA, in $S2R^+$ cells transfected with the WISIR TOPFlash reporter, showed an increases Wingless signalling. The effective knockdown of *hrs* is shown by western blot. *vsp16* and *tsg101*, addition components of the endosomal sorting complex required for transport (ESCRT), were also knocked down. Similarly to *hrs*, *vps16* knockdown increased signalling while *tsg101* dsRNA had no effect. Due to the lack of antibodies the knockdown of *vps16 tsg101*, could not be verified.

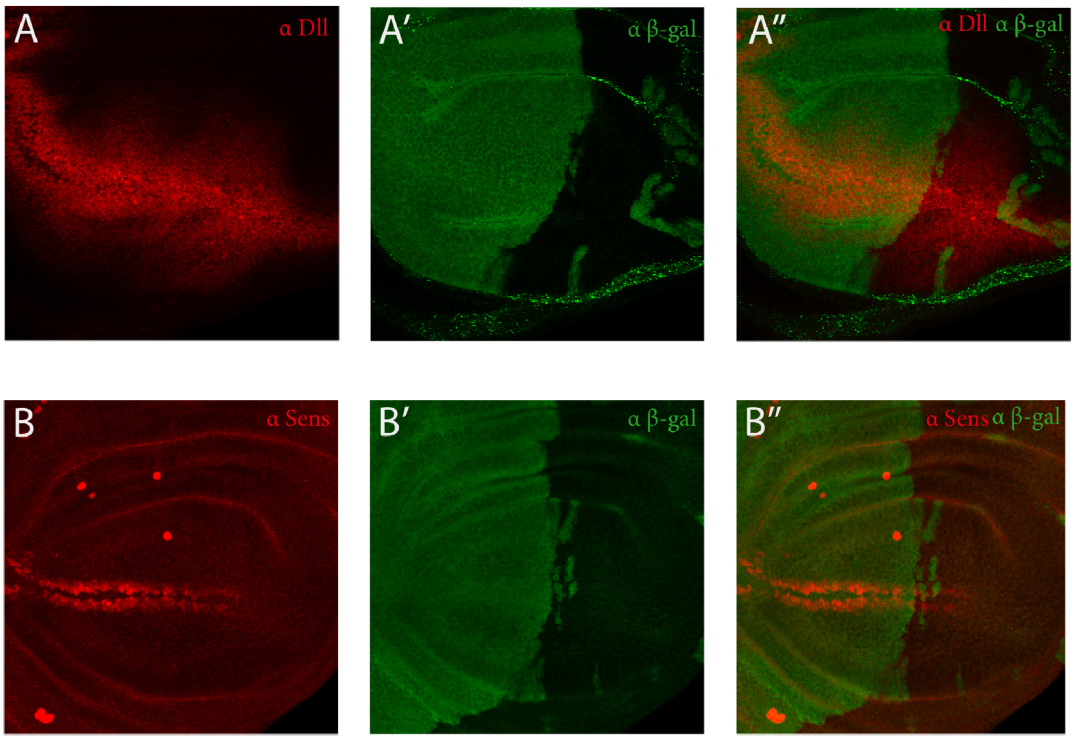
A
α Dll
A′
α β-gal
A″
α Dll α β-gal
B
α Sens
B′
α β-gal
B″
α Sens α β-gal

C

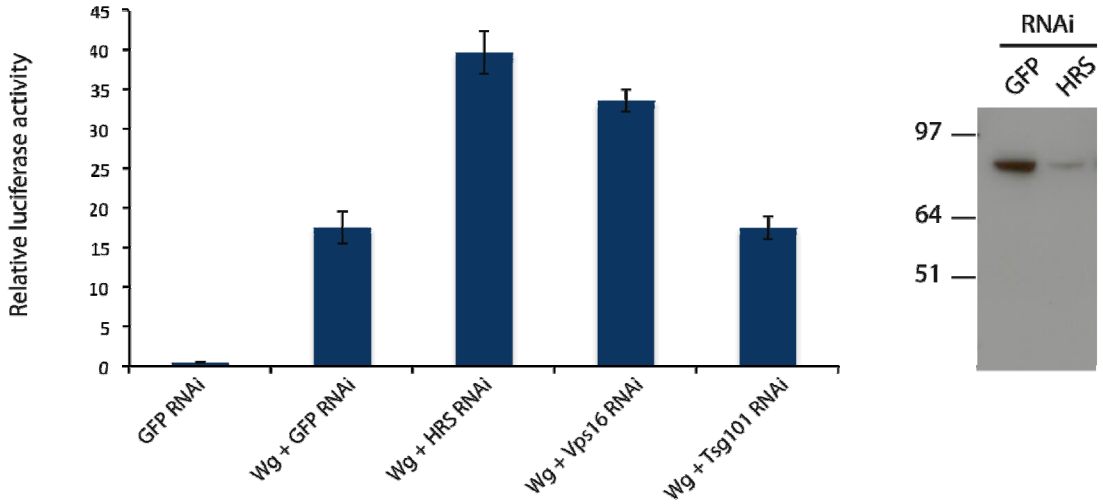
Relative luciferase activity
45
40
35
30
25
20
15
10
5
0
GFP RNAi
Wg + GFP RNAi
Wg + HRS RNAi
Wg + Vps16 RNAi
Wg + Tsg101 RNAi
RNAi
GFP
HRS
97
64
51

Knockdown of VPS16 also led to an increase in signalling whereas Tsg101 dsRNA had no effect although knockdown could not be verified for lack of antibodies. Overall, these cell based results suggest that ESCRT proteins are not needed for expression of low level target genes.

The above results for Senseless suggests that MVBs could contribute positively to signalling, but this is not confirmed by the cell based assay. In light of this contradiction I wished to confirm the effect of MVB inhibition on *senseless* by looking at a terminal phenotype that reflects Senseless activity. I looked at adult wings mutant for *hrs* in the posterior compartment. Few larvae with the mutated genotype made it to adulthood (3%), indicating that the mutation is highly larval lethal. The few adult mutants had wings curved in a ventral direction and the two wing layers were not closely apposed (Fig 6.5.C). Importantly, there was no loss of bristles in the posterior compartment, which would be expected if *senseless* was not expressed. Senseless staining of larvae during pupation would be necessary to confirm a delay in *senseless* expression rather than lack of expression. Slow or compromised growth of the posterior compartment also explains the broader anterior compartment, which may be compensating for the delay (Fig 6.5 B). This complex phenotype, with abnormal vein dilation at the wing margin (impaired Notch signalling) and loosely apposed wing layers (integrin disfunction), exemplifies how modifying trafficking not only affects Wingless signalling but also other pathways, thus highlighting the difficult interpretation of these results. Nevertheless my results so far suggest that inhibiting MVB formation does not prevent high level signalling.

Also supporting Taelman et al's model of GSK3 sequestration for signalling was their observation that, in 293T cells GSK3 co-localized with multiple components of the signalosome known to be degraded; such as Wnt, β-catenin, Axin and LRP6. In contradiction to this, as I described above, endocytosis of Wingless is not needed for signalling and Arrow is not degraded upon signalling. I proceeded to analyse the localization of Wingless and GSK3 in $S2R^+$ cells. I treated $S2R^+$ with Wingless for different times and stained with anti-GSK3 (green) and anti-Wingless (red) (Fig 6.6). No co-localization was seen. Taelman et al's assay of co-localization involved over expressing tagged GSK3. To allow direct comparison I over-expressed un-tagged GSK3 in S2 cells and assessed co-localization with Wingless. Once again no co-localization was seen (data not shown). To validate these results I needed to test the antibody staining was specific as the antibody used was raised against mammalian

GSK3. I tried to knockdown GSK3 expression with dsRNA but was unable to generate one that worked therefore I tested the antibody on wing discs containing *sgg* null mutant clones (*sgg*^{D127} *FRT101 / UbiGFP FRT101;;en Gal4 UAS flp*). No difference in staining between wild type or mutant tissue was observed, therefore the antibody is not specific for Sgg, rendering the results from these experiments invalid (Fig 6.7). To re-evaluate Wingless and GSK3 localization either another suitable antibody would need to be tested and used or cells would need to be transfected with a tagged form of GSK3.

Despite being unable to address localization of Wingless and GSK3, knockdown of *hrs* in S2R^{+} cells and *hrs*^{D28} mutant clones in wing discs both show that MVBs are not essential for Wingless signalling.

Figure 6.5 Knockdown of *hrs* does not affect the Wingless phenotype.

(A) Control (*engGal4; UAS Wg RNAi*) depicting the phenotype of wing discs with loss of Wingless signalling. (B) RNAi of *hrs* (*hrs^{D28} FRT40/armlacZ M(2)FRT40; HhGal4 UASFlp*). Wings display a wild type *wingless* phenotype with no loss of sensory bristles in the posterior compartment. However they do display modifications in other signalling pathways. The dilated veins are indicative of impaired Notch signalling. (C) Few larvae with the mutant phenotype develop into adults. Those that do have wings curved ventrally with two not closely apposed wing layers.

A

eng Gal4; UAS Wg RNAi

B

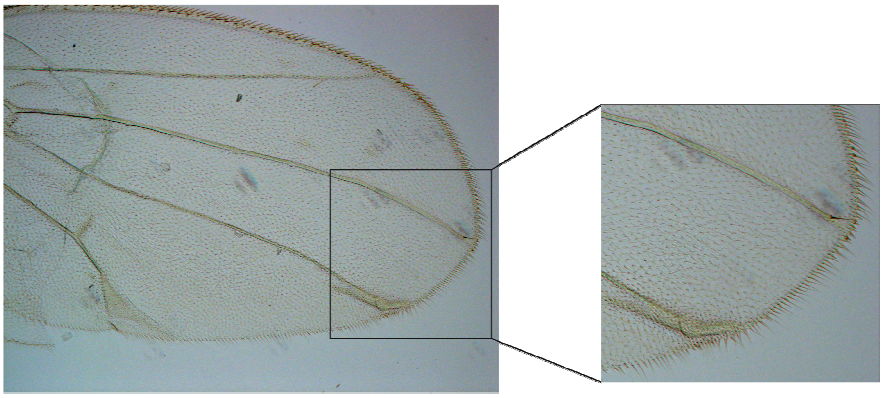

hrs^{D28}FRT40/armlacZ M(2)FRT40 ; Hh Gal4UAS flp

C

hrs^{D28}FRT40/armlacZ M(2)FRT40 ; Hh Gal4UAS flp

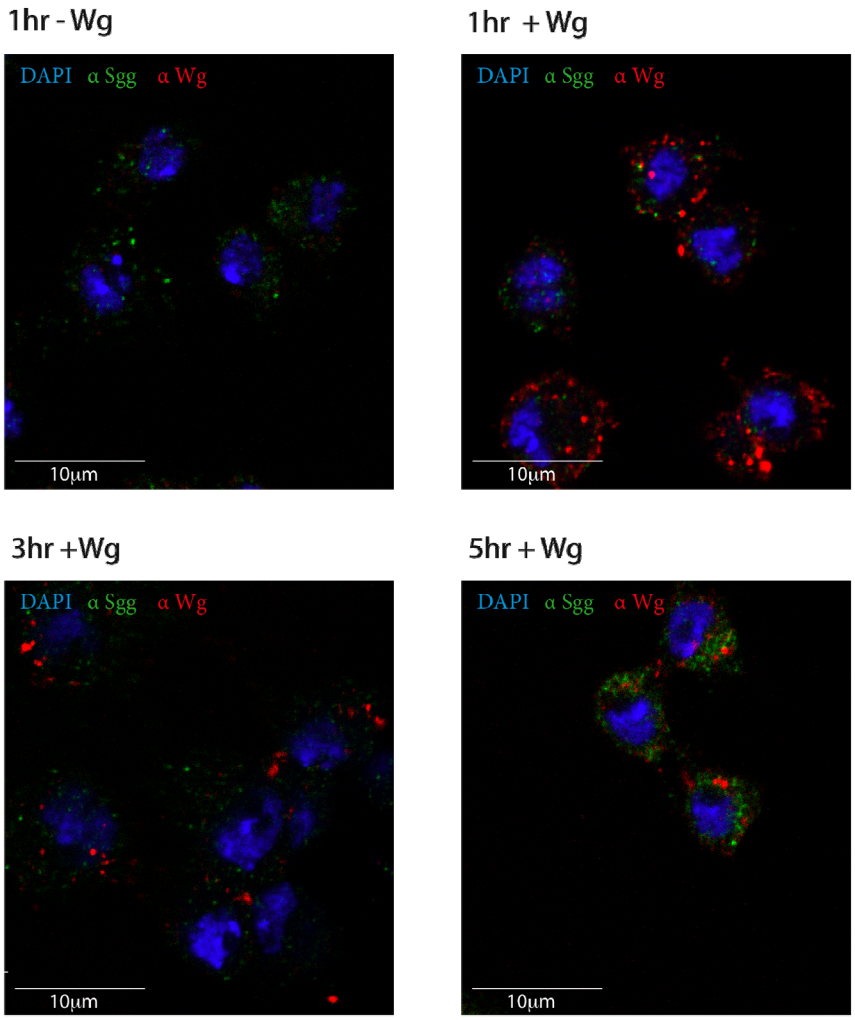

Figure 6.6 Wingless and GSK3 do not co-localize.

$S2R^+$ cells treated with complete medium, as a control, and Wingless conditioned medium for different amounts of time. Cells are stained with anti-Wingless (red) and anti-GSK3 (green). No co-localization is detected, however specificity of anti-GSK3 could not be confirmed (See Fig 6.7).

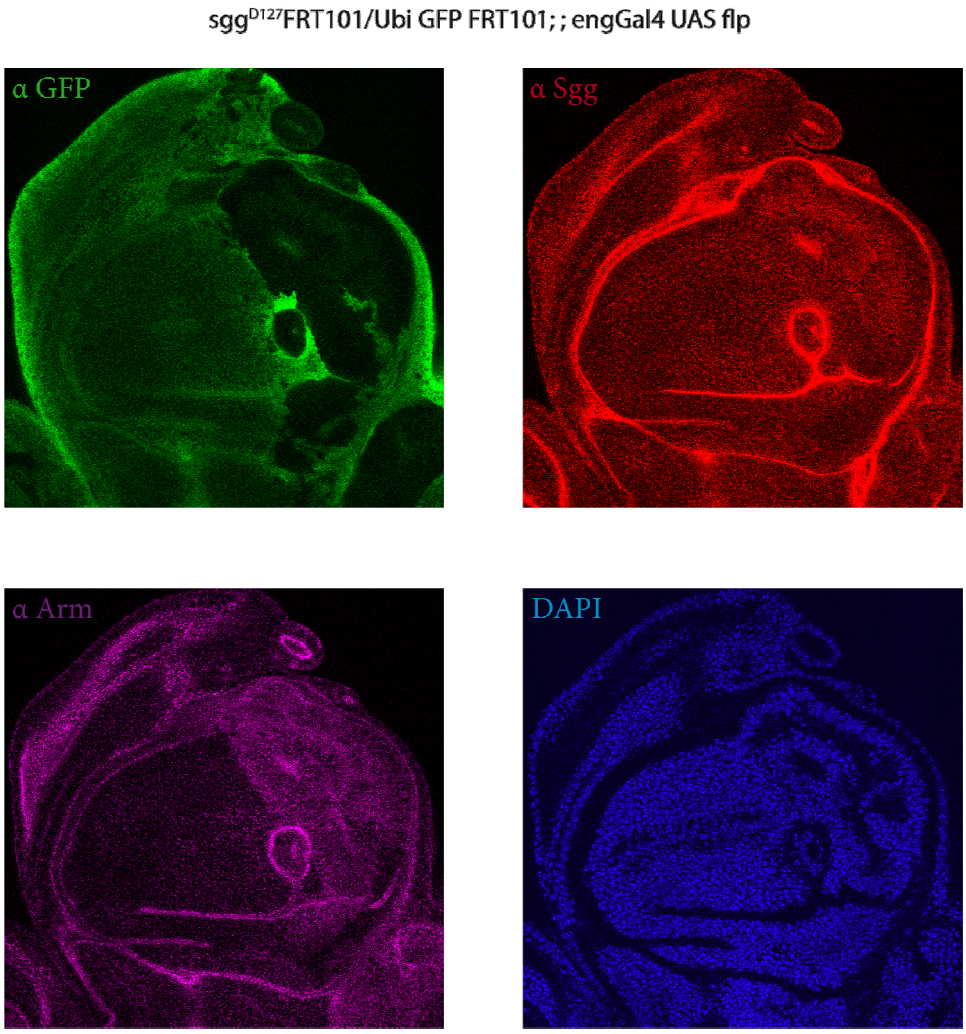

Figure 6.7 Non specific GSK3 antibody

Third instar wing discs with *sgg*^{D127} null mutant clones (lack of GFP). The GSK3 antibody does not detecting Sgg, shown by the uniform staining throughout the wing discs (red) with no decrease in the mutant clone (lack of GFP). Armadillo accumulation within the clone proves increased Wingless signalling due to Sgg disfunction (magenta).

6.4 Role of endocytosis downstream of the degradation complex

It has been established that endocytosis is required for Wnt signalling (Blitzer & Nusse, 2006; Yamamoto et al, 2006). When endocytosis is inhibited there is no signalling and GSK3 accumulates at the plasma membrane (Blitzer & Nusse, 2006). These results are consistent with the Taelman hypothesis. However another experiment published by Blitzer *et. al.* completely contradicts the hypothesis. When activating Wnt signalling in L cells by inhibiting GSK3 with Lithium Cloride (LiCl), β-catenin levels rise, as expected. However, when endocytosis is blocked with 1) monodansycadaverine (MDC), which prevents assembly of clathrin at the cell membrane, 2) chlorpromazine (CPZ), which diverts clathrin accumulation from the cell membrane to endosomal membranes, or 3) hypertonic sucrose, which inhibits formation of clathrin coated pits, the accumulation of β-catenin in response to the inhibition of the degradation complex is abolished. Thus, although endocytosis is required for signalling, its role is not to inhibit GSK3 activity via translocation to MVBs. Instead it appears that endocytosis is required downstream of GSK3 (Blitzer & Nusse, 2006).

I repeated the Blitzer experiment in $S2R^+$ cells with a few modifications. Although LiCl inhibits GSK3 (Stambolic et al, 1996) it lacks specificity and interferes with other protein kinases such as casein kinase-2 (CK2), p38 regulated/activated kinase (PRAK) and MAPK activated protein kinase-2 (MAPKAP-K2) (Davies et al, 2000). To specifically inhibit GSK3 I used SB-216763, which has no known effect on the activity of other protein kinases (Coghlan et al, 2000). SB216763 prevents phosphorylation of GSK3-β at Tyr279/Tyr216, which is required for its activation (Hughes et al, 1993; Sun & Chen, 2008). Another improvement was the use Dynasore (Dyna) to inhibit endocytosis/endocytic trafficking. Dynasore is a cell permeable inhibitor of dynamin. It works by inhibiting dynamin's GTPase activity without affecting the activity of other small GTPases (Macia et al, 2006). Thus Dynasore inhibits both clathrin and caveolae-mediumted endocytosis. Before using Dynasore in my experiments I had to determine the effective concentration needed. I did this by monitoring dextran internalization during a 2 hr period in $S2R^+$ cells treated with three different Dynasore concentrations (Fig 6.8 A). I found that internalization was strongly inhibited using 200μM Dynasore. Having shown that endocytosis from the cell surface is inhibited I also wanted to show that intracellular

trafficking is compromised. To do this I exposed cells to 200μM of Dynasore and then stained for the lysosomal associated membrane protein (LAMP). As its name implies this protein is associated with lysosomes. It is involved both in the fusion of the lysosome with other membranes and in the formation of autophagic vacuoles which are responsible for transportation of proteins/digestive enzymes into lysosomes (Eskelinen et al, 2002). After a one hour treatment with Dynasore the LAMP staining has significantly decreased suggesting that intracellular trafficking is compromised (Fig. 6.8 B). With SB216763 and Dynasore I was able to rapidly inhibit GSK3 and endocytosis. After 2 hr and 6 hr treatment with SB-216763, cells showed an increase in Armadillo levels as they do when treated with Wingless. This accumulation was suppressed when endocytosis was blocked with Dynasore (Fig 6. 9 A). Importantly the health of the cells was not severely compromised in the presence of Dynasore, as shown by the stable levels of actin in Fig 6.9 A and by relatively normal cell morphology in Fig 6.8 A. I also assessed signalling with the TOPFlash assay. High levels of signalling were induced with Wingless and SB-216763 treatment, and were once again inhibited by dynasore (Fig 6.9 B).

Having assessed the requirement of endocytosis for signalling downstream of GSK3 I next tested whether downregulation of another member of the degradation complex was also sensitive to endocytosis inhibition (Fig 6.10). I used Axin dsRNA to activate signalling, as detected by an increase Armadillo levels. Again, Dynasore inhibited the accumulation of Armadillo.

These experiments show that endocytosis is required Wnt/Wingless signalling as suggested previously by Blitzer. My results also suggest that the key endocytic event acts downstream of the degradation complex.

Figure 6.8 Dynasore inhibits endocytosis and endocytic trafficking.

(A) 200μM Dynasore inhibits dextran internalization into $S2R^+$ cells, monitored for 2hr. (B) Intracellular trafficking is also disrupted by Dynasore as shown by the lack of LAMP (lysosomal associated membrane protein) staining in cells subjected to a 1hr Dynasore treatment.

A

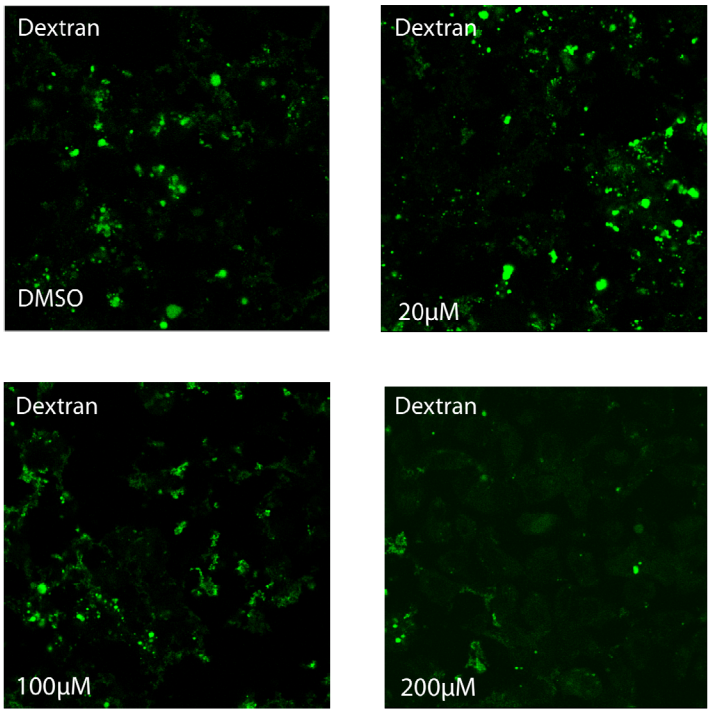
Dextran
DMSO
Dextran
20μM
Dextran
100μM
Dextran
200μM

B

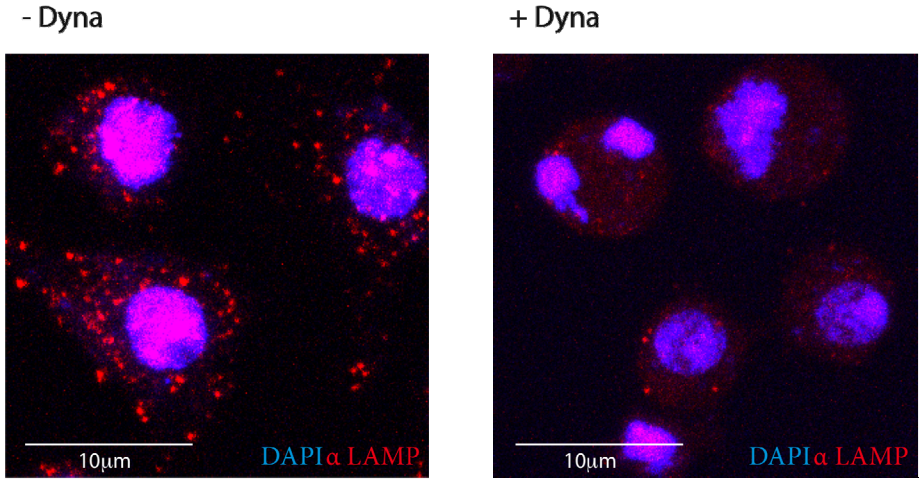
- Dyna
+ Dyna
10μm
DAPI α LAMP
10μm
DAPI α LAMP

Figure 6.9 Blocking endocytosis/endocytic trafficking inhibits Wingless signalling and Armadillo stabilization.

(A) Armadillo stability is assessed by Western blot of Armadillo present in $S2R^+$ cells treated with Wingless conditioned medium or 20μM SB-216763, a GSK3 inhibitor, for 2 hrs and 6 hrs. In each case an increase in Armadillo levels is observed, which is abolished with concomitant Dynasore treatment (200μM). The level of Armadillo in untreated cells is the control. B) Wingless signalling in $S2R^+$ cells, measured with the TOPFlash reporter, increases in response to Wingless medium and SB-216763 treatment. Dynasore inhibits signalling. Relative luciferase activity is shown as the mean of triplicates from a single trial ± SEM.

A

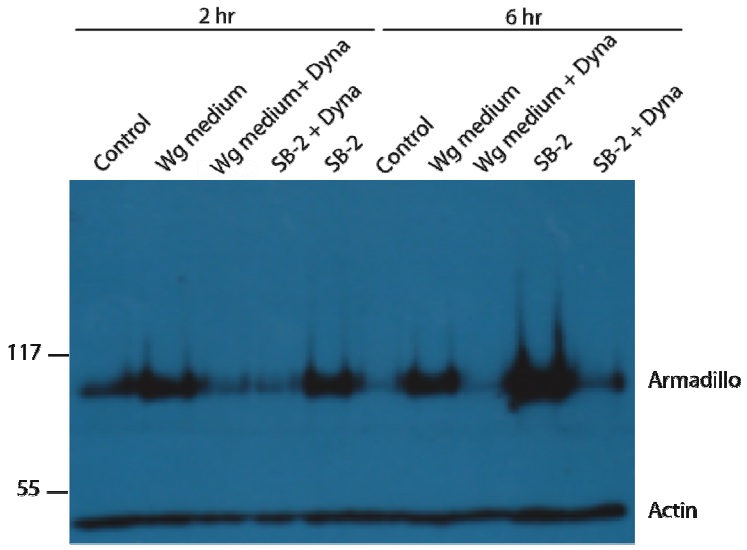
2 hr
6 hr
Control
Wg medium
Wg medium+ Dyna
SB-2 + Dyna
SB-2
Control
Wg medium
Wg medium + Dyna
SB-2
SB-2 + Dyna
117
55
Armadillo
Actin

B

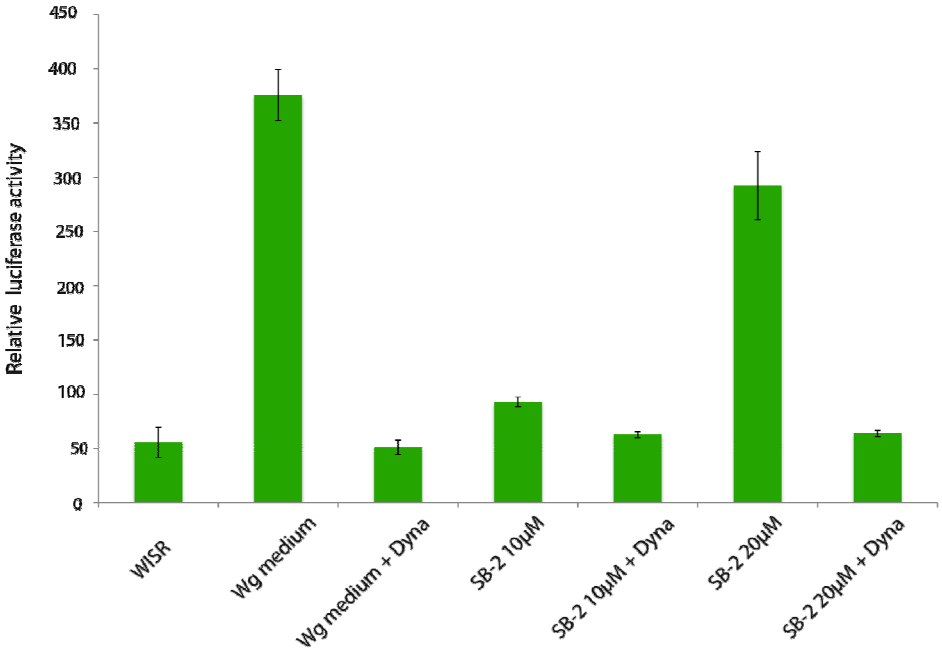
Relative luciferase activity
450
400
350
300
250
200
150
100
50
0
WISR
Wg medium
Wg medium + Dyna
SB-2 10μM
SB-2 10μM + Dyna
SB-2 20μM
SB-2 20μM + Dyna

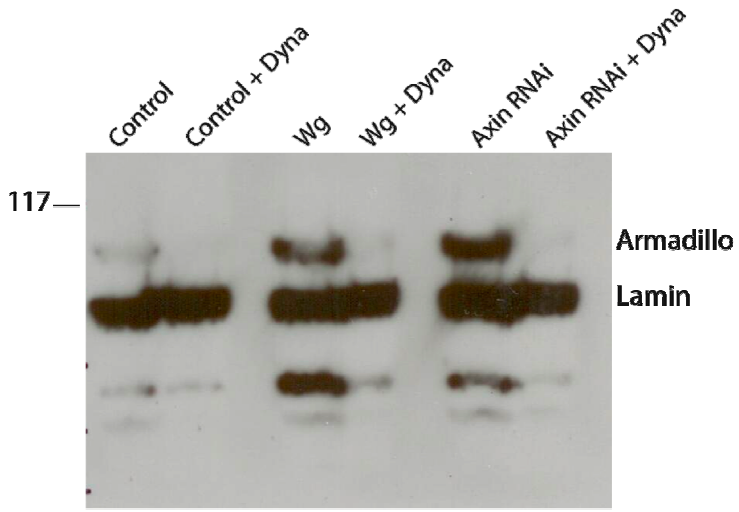

Figure 6.10 Wingless signalling requires endocytic trafficking downstream of the degradation complex.

Knockdown of Axin in $S2R^{+}$ cells leads to an accumulation of Armadillo as does exposure to Wingless conditioned medium. Treatment with Dynasore (200μM) inhibits Armadillo stabilization suggesting that trafficking further down along the endocytic pathway is required for signalling.

6.5 Inhibiting Endocytosis affects Armadillo stability

I have shown that endocytosis plays a role in Wingless signalling downstream of Axin and GSK3. Blitzer *et. al*. showed that blocking endocytosis had no effect on β-catenin levels in SW480 cells, which originate from of a human cancer and lack functional APC (adenomatous polyposis coli). This led them to suggest that endocytosis serves to abrogate APC function. To continue investigating the function of endocytosis further down in the pathway and confirm that endocytosis has a role upstream of Armadillo, the effect of endocytosis inhibition when signalling is activated by Armadillo over-expression was analysed. To over-express Armadillo, $S2R^+$ cells were transfected with a vector expressing Armadillo under the MT promoter. Without addition of copper, which is used to activate the MT promoter, no signalling was detected with the TOPFlash assay (Fig 6.11 A). Upon activation by the addition of copper signalling levels equal those of Wingless treated cells. Surprisingly signalling activated by Armadillo over-expression was inhibited by the addition of dynasore. Therefore endocytosis is required at the level or downstream of Armadillo.

To test the effect of Dynasore on Armadillo levels, cells were transfected with MT-Armadillo. The following day these transfected cells were pre-treated with Dynasore for 30 min and Armadillo expression was then induced by the addition of copper. Likewise, non transfected control cells were pre-treated with Dynasore for 30min followed by activation of Wingless signalling, hence accumulation of Armadillo, using Wingless conditioned medium. Armadillo accumulation induced by Wingless treatment or by MT-Armadillo expression decreased below pre-treatment levels in the presence of Dynasore (Fig 6.11 B). This suggests that Dynasore reduces Armadillo levels independently of signalling activity. To test this possibility I analyzed the effect of Dynasore on endogenous Armadillo levels in the absence of Wingless treatment. Both 2 hours and 1hour treatments with Dynasore led to a decrease in endogenous Armadillo levels (Fig 6.11 C). Levels of other proteins such as Lamin, Actin and Syntaxin were unaffected by Dynasore treatment. The effect of Dynasore on Armadillo levels is reversible; treatment of cells with complete medium post treatment with Dynasore restores Armadillo levels back

Figure 6.11 Dynasore treatment decreases Armadillo levels.

(A) $S2R^+$ cells transfected with pMT-Armadillo, whose expression is activated upon addition of $CuSO_4$ (Cu) display increased TOPFlash reporter activity. Treatment with Dynasore (200μM) suppresses this increase as it does in cells exposed to Wingless. (B) Western blot analysis of Armadillo levels in $S2R^+$ cells exposed to Wingless conditioned medium and in cells over expressing Armadillo with the transfection of pMT-Armadillo (0.2μg and 0.02μg) in the presence and absence of Dynasore. Controls are Armadillo levels in cells exposed to complete medium vs Wingless conditioned medium and cells transfected with, but non-activated pMT-Armadillo. (C) Western blot analysis of Armadillo levels in $S2R^+$ cells treated with Dynasore for 1hr/2hrs displays a decrease in Armadillo expression. Normal levels are restored with the removal of Dynasore and incubation in complete medium for an additional 2hr. Lamin, Actin and Syntaxin levels are unaffected. (D) Western blot analysis of Armadillo levels in third instar wild type wing discs incubated in complete medium +/- Dynasore over a 6hr time course.

A

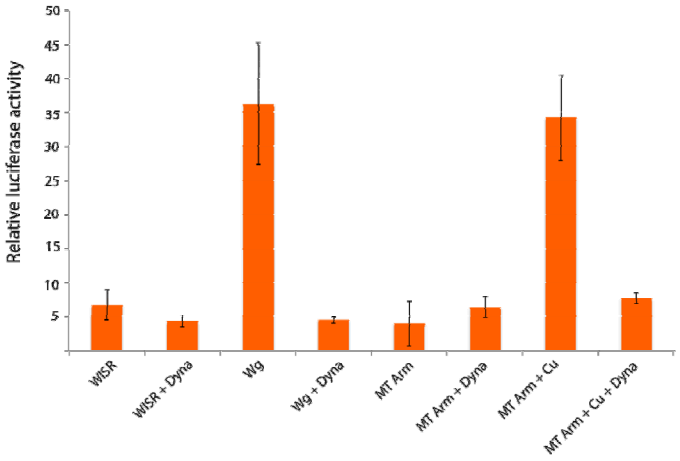
Relative luciferase activity
50
45
40
35
30
25
20
15
10
5
WISR
WISR + Dyna
Wg
Wg + Dyna
MT Arm
MT Arm + Dyna
MT Arm + Cu
MT Arm + Cu + Dyna

B

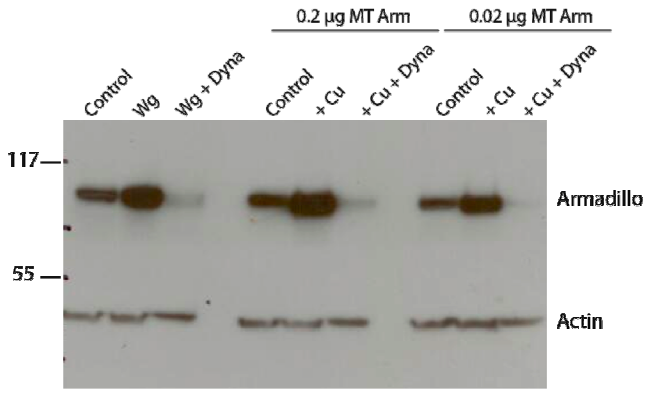
0.2 µg MT Arm
0.02 µg MT Arm
Control
Wg
Wg + Dyna
Control
+ Cu
+ Cu + Dyna
Control
+ Cu
+ Cu + Dyna
117
55
Armadillo
Actin

C

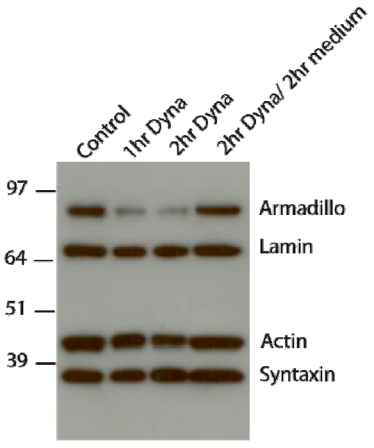
Control
1hr Dyna
2hr Dyna
2hr Dyna/ 2hr medium
97
64
51
39
Armadillo
Lamin
Actin
Syntaxin

D

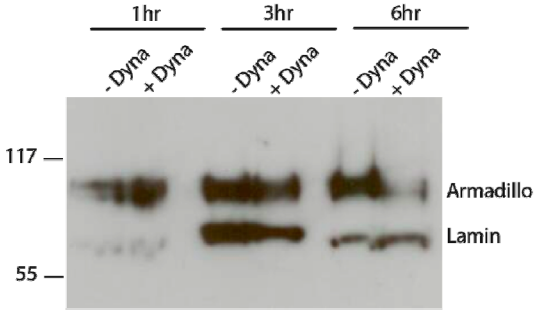
1hr
3hr
6hr
- Dyna
+ Dyna
- Dyna
+ Dyna
- Dyna
+ Dyna
117
55
Armadillo
Lamin

to normal. This result combined with the lack of effect on other proteins suggests that Dynasore does not affect cell viability/function.

To determine if Dynasore also reduced Armadillo levels in vivo, third instar wing discs were dissected and incubated in complete medium in the presence/absence of Dynasore for different times. Unfortunately the results shown in Fig 6.11 D are ambiguous. The 1 hr time point could not be interpreted because the corresponding sample did not transfer onto the western blot membrane efficiently. The 3 hr time point (+/- Dynasore) showed unequal loading probably due to damage or loss of discs during dissections and washes. Keeping these difficulties in mind, there is no suggestion of Dynasore causing a decrease in armadillo levels at these two time points. However, at 6 hr post treatment a decrease in Armadillo was observed in the Dynasore treated samples. Inhibition of endocytosis for 6 hr would affect multiple cell signalling pathways and thus could affect Armadillo levels indirectly. The inefficiency of the Western blot and disruption of unrelated signalling pathways render these results inconclusive.

To assess the effects of Dynasore on a stabilised form of Armadillo, I transfected cells with MT-S10-Armadillo-V5. This form of Armadillo lacks the phosphorylation consensus site for GSK3 and is thus constitutively active and stable. Expression of MT-S10-Armadillo-V5 and MT-Armadillo–V5, was activated in parallel leading to high protein levels after 3 hours. No such increase was seen when a 20 min treatment with Dynasore preceded MT promoter activation. A non-specific band detected by the anti-V5 antibody was also eliminated in the presence of Dynasore (Fig 6.12 A). Identification of the corresponding protein by mass spec may reveal a signature of endocytosis blockade. To make sure that Dynasore did not prevent copper induced activation of the MT promoter, I activated cells for 3 hours and then treated with Dynasore for 30 min. As shown in Fig 6.12 B even when Dynasore is added post activation, Armadillo levels decrease. Thus, the lack of Armadillo upon Dynasore treatment is not due to lack of expression.

The results shown by these western blots suggest that endocytosis may affect signalling indirectly by affecting Armadillo stability. I decided to analyse if endocytosis affects Armadillo degradation or synthesis. I started by investigating the effect of Dynasore on Armadillo degradation by silencing protein synthesis with cycloheximide. As shown in

Figure 6.12 Constitutively active S10-Armadillo levels decrease with dynasore treatment.

$S2R^+$ cells transfected with pMT-Armadillo-V5 and constitutively active pMT-S10-Armadillo-V5. (A) Activation of the MT promoter with the addition of $CuSO_4$ for 3hrs results in high levels of Armadillo, identified by Western blot with an anti-V5 antibody. 30min Dynasore treatment prior to induced expression eliminates the detection of Armadillo bands in conjunction with an identified background band to the V5 antibody. Untransfected $S2R^+$ cells act as a control. (B) The effect of inducing pMT-Armadillo-V5 and pMT-S10-Armadillo-V5 expression (3hrs) prior to a 30min Dynasore treatment was assessed. A decrease in Armadillo levels is also observed although to a lesser extent than with initial Dynasore treatments.

A

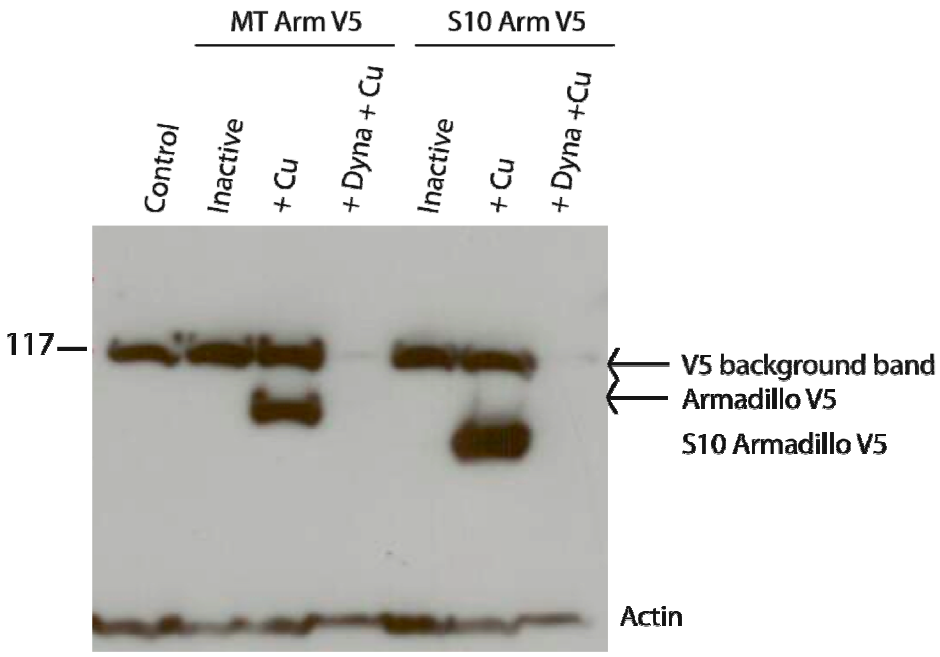
MT Arm V5
S10 Arm V5
Control
Inactive
+ Cu
+ Dyna + Cu
Inactive
+ Cu
+ Dyna +Cu
117
V5 background band
Armadillo V5
S10 Armadillo V5
Actin

B

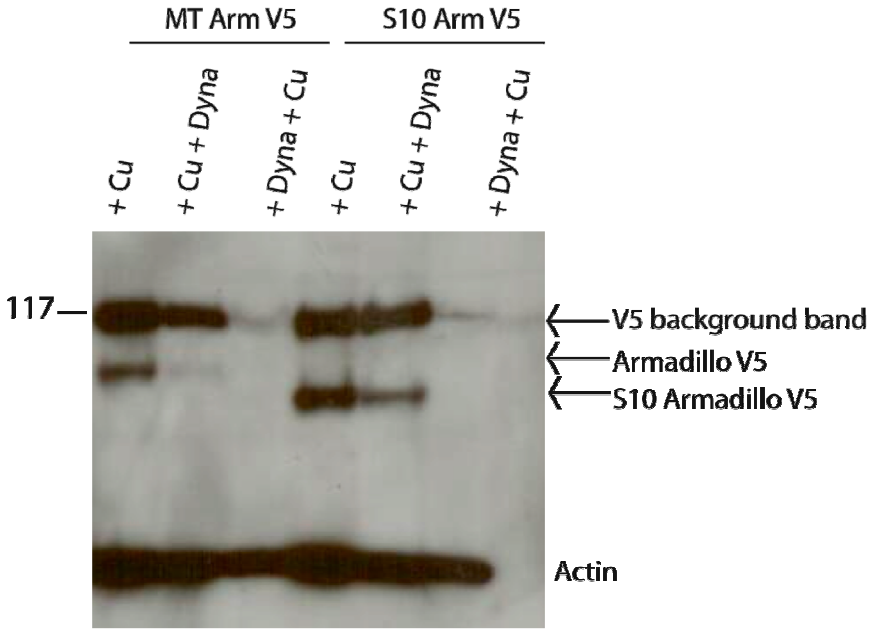
MT Arm V5
S10 Arm V5
+ Cu
+ Cu + Dyna
+ Dyna + Cu
+ Cu
+ Cu + Dyna
+ Dyna + Cu
117
V5 background band
Armadillo V5
S10 Armadillo V5
Actin

Fig 6.13 A cycloheximide efficiently inhibits Armadillo synthesis in response to Wingless signalling. Therefore using cycloheximide the effect of Dynasore on Armadillo degradation can be monitored over time. In the absence of Dynasore, endogenous Armadillo levels remain the same for up to 2 hours of synthesis inhibition. This was quite unexpected as the half-life of Armadillo is around 30min (Pai et al, 1997). This increased stability may be due to cycloheximide inhibiting synthesis of proteins required for degradation. In the presence of Dynasore, Armadillo levels decrease within 40 min of treatment (Fig 6.13 B), suggesting the Dynasore induces Armadillo degradation. The same experiment was done using cells expressing stable S10-Armadillo-V5. Compared to the endogenous Armadillo degradation rate there is a more gradual decrease of S10-Armadillo-V5 in the presence of Dynasore, with no S10-Armadillo-V5 expression after 4 hours (Fig 6.13 C). Quantification of Armadillo levels in S10-Armadillo-V5 expressing cells shows that Dynasore induces an exponential decrease, whereas in the absence of Dynasore levels remain constant (Fig 6.13 D). Therefore, Dynasore affects Armadillo degradation.

I also monitored Armadillo levels in response to Dynasore in live cells by tracking a GFP-Armadillo fusion protein. Cells were transfected with GFP-Armadillo and myristoylated Cherry. Two days post transfection, individual cells were imaged +/- Dynasore every 3 min for 1.5 hr. Preliminary results are quite different from those obtained with the Western blots. Although a decrease in GFP-Armadillo intensity was observed, it was relatively slow, with GFP levels decreasing by only 15% in 1.5hr (Fig 6.14 B). This could be due to the GFP-Armadillo fusion not behaving as wild type Armadillo or the GFP moiety being somehow protected from degradation. A western blot would be needed to determine if Armadillo and GFP-Armadillo degradation levels are in unison. It will also be necessary to use a more appropriate control than membrane tethered Cherry as its degradation could be slowed by association with the membrane. A non-membrane tethered form of Cherry would be more suitable. New developments in photoconvertible fluorescent proteins provide novel means of tracking Armadillo turnover in live cells, as discussed later in the thesis.

The above results suggest that Dynasore induces Armadillo degradation. To determine if synthesis of Armadillo is affected by Dynasore I assessed changes in Armadillo levels in response to Dynasore when degradation is inhibited with

proteasome inhibitor (MG132). When cells were treated with MG132 for 2.5 hr there was an accumulation of Armadillo. Such an accumulation did not occur when cells were treated with Dynasore for 30 min prior to MG132 treatment. This suggests that Armadillo synthesis is impaired by Dynasore. However when the sequence of treatments was reversed and Dynasore was added post 2.5hr of Armadillo accumulation, the level of Armadillo decreased (Fig 6.15 A). This decrease was unexpected, as inhibition of Armadillo synthesis by Dynasore would only stop further accumulation not lead to lower levels. This decrease could be explained by an alternative degradative route independent of the proteasome or reveal inefficient proteasome inhibition by MG132. A similar experiment was also done with cells expressing Armadillo-V5 and S10-Armadillo-V5. Once again an accumulation of Armadillo is seen when Armadillo-V5 expressing cells are treated with MG132. When these cells are concomitantly treated with MG132 and Dynasore no accumulation is observed. It is not clear if reduced expression is due to inhibition of MG132 function or Armadillo synthesis. MG132 treatment does not induce accumulation of S10-Armadillo-V5 expressing cells as Armadillo is stable thus unaffected by the proteasome. However just as in Armadillo-V5 expressing cells Dynasore treatment reduces S10-Armadillo-V5 expression (Fig 6.15 B, C).

In conclusion, inhibition of endocytosis using Dynasore decreases Armadillo levels whether it is affecting synthesis or degradation remains ambiguous.

Figure 6.13 Dynasore induces Armadillo degradation.

(A) Cycloheximide (CHX) inhibits protein synthesis as shown by the lack of increased Armadillo expression in cells exposed to Wingless when pre-treated with 350μM CHX for 30min. (B) Armadillo levels in $S2R^{+}$ cells treated with CHX in the presence and absence of Dynasore monitored over a 2hr time course. Expression levels drop within 40min of Dynasore treatment. (C) Similarly, Dynasore stimulates the degradation of S10-Armadillo-V5, a form that is not sensitive to GSK3. An unidentified background band to the anti-V5 antibody also decreases. (D) Quantification of S10-Armadillo-V5 bands in (C) illustrates an exponential decrease of S10-Armadillo-V5 upon Dynasore treatment. Suggesting that the latter increases degradation of both endogenous and constitutively active Armadillo.

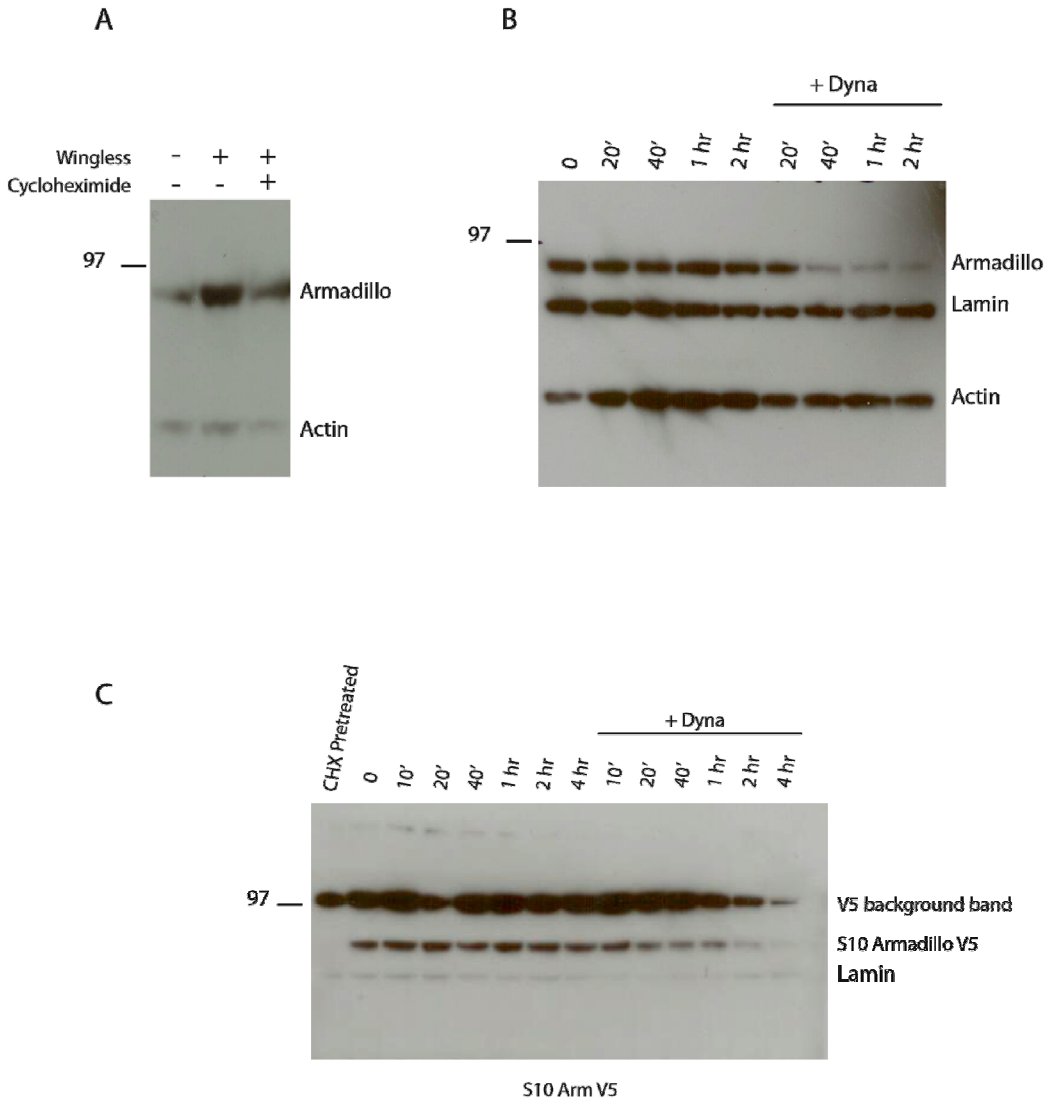
A
Wingless
Cycloheximide
97
Armadillo
Actin
B
+ Dyna
0
20'
40'
1 hr
2 hr
20'
40'
1 hr
2 hr
97
Armadillo
Lamin
Actin
C
CHX Pretreated
+ Dyna
0
10'
20'
40'
1 hr
2 hr
4 hr
10'
20'
40'
1 hr
2 hr
4 hr
97
V5 background band
S10 Armadillo V5
Lamin
S10 Arm V5
Density
180
160
140
120
100
80
60
40
20
0
20'
40'
1 hr
2 hr
4 hr
Time
S10 Arm V5
No Dyna
With Dyna

Figure 6.14 Live cell imaging of Armadillo levels

$S2R^{+}$ cells transfected with GFP-Armadillo and membrane tethered Cherry were treated with Dynasore or DMSO (Dimethyl sulfoxide) as a control. (A) Live cell imaging of cells exposed to DMSO shows that GFP-Armdillo and Cherry levels remain constant. (B) In cells treated with Dynasore Cherry levels are stable but GFP Armadillo decreases by 15%. Images were taken every 3min for 1.5hr.

A

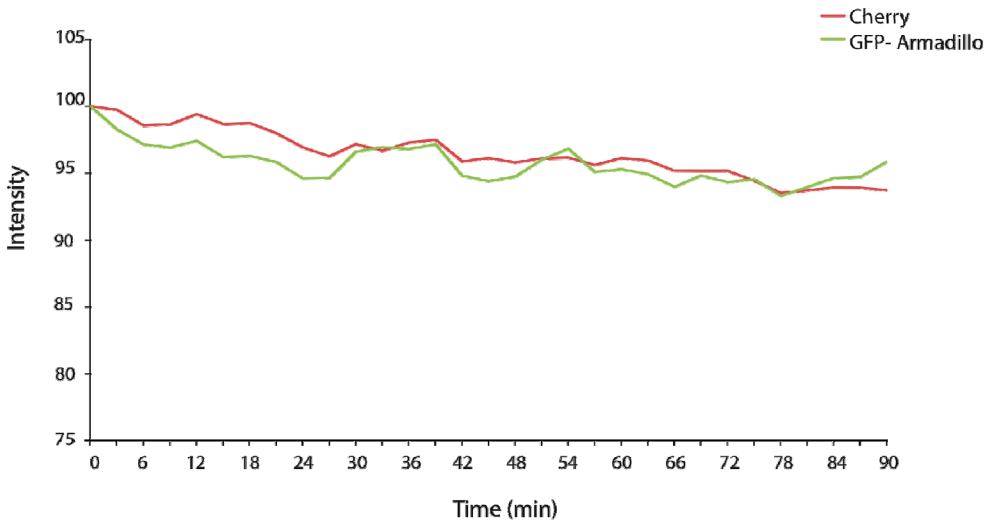
Cherry
GFP- Armadillo
105
100
95
90
85
80
75
Intensity
0
6
12
18
24
30
36
42
48
54
60
66
72
78
84
90
Time (min)

B

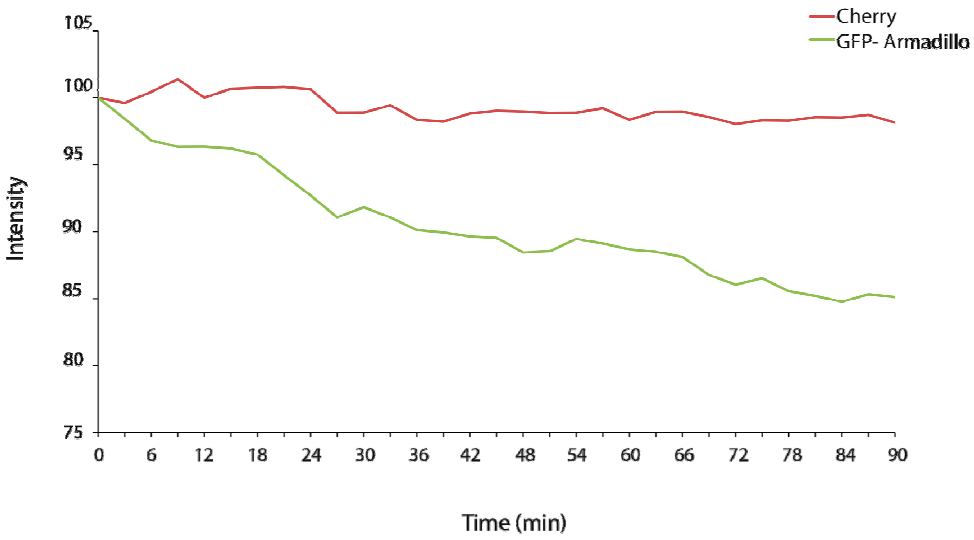
Cherry
GFP- Armadillo
105
100
95
90
85
80
75
Intensity
0
6
12
18
24
30
36
42
48
54
60
66
72
78
84
90
Time (min)

Figure 6.15 Armadillo levels decrease upon Dynasore treatment despite proteosomal inhibition.

(A) Proteosomal inhibition via treatment with MG132 (3hr) leads to Armadillo accumulation. Pre-treatment with Dynasore (20min) inhibits this. Dynasore treatment after MG132 treatment also decreases Armadillo levels although not to the same extent. Western blot probed with anti-Armadillo antibody. (B) In cells over-expressing Armadillo-V5, treatment with MG132 leads to great accumulation of Armadillo. Co-treatment with Dynasore abolishes such an accumulation. (C) The addition of MG132 to cells expressing S10-Armadillo-V5 does not change its levels as S10-Armadillo-V5 is already stable. However, addition of Dynasore and MG132 together still results in a decrease in S10-Armadillo-V5 expression. (B,C) Western blots probed with anti-V5 antibody.

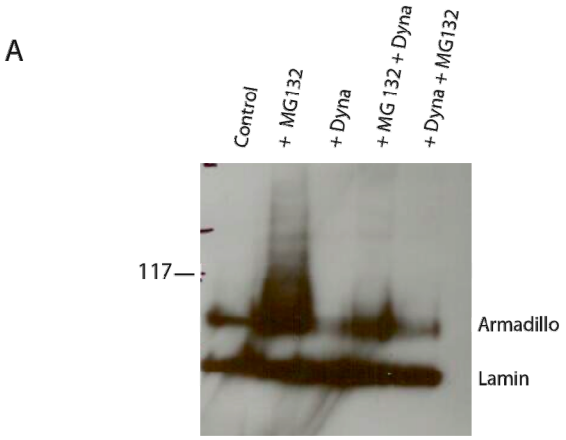
A
Control
+ MG132
+ Dyna
+ MG 132 + Dyna
+ Dyna + MG132
117
Armadillo
Lamin

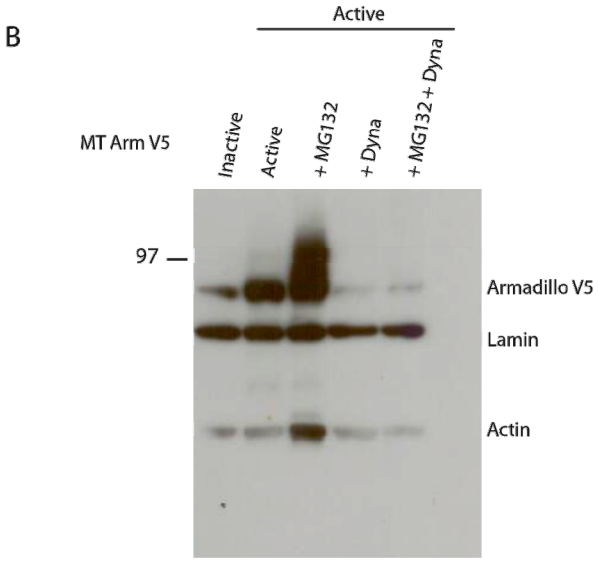
B
Active
MT Arm V5
Inactive
Active
+ MG132
+ Dyna
+ MG132 + Dyna
97
Armadillo V5
Lamin
Actin

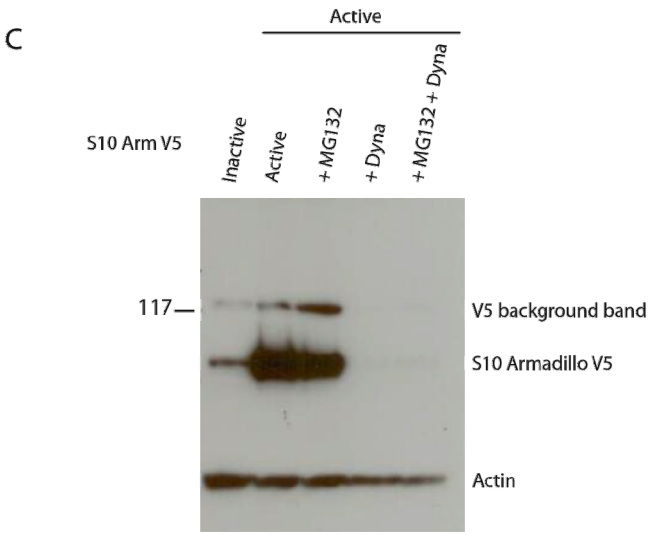
C
Active
S10 Arm V5
Inactive
Active
+ MG132
+ Dyna
+ MG132 + Dyna
117
V5 background band
S10 Armadillo V5
Actin

6.6 Summary

To explore the role of endocytosis in Wingless signalling I started by preventing endocytosis of Wingless itself. Fusion of Wingless to Neurotactin, a transmembrane protein, inhibited its release from expressing cells. $S2R^+$ cells exposed to S2 cells expressing NRT-HA-Wingless cells still signalled, proving that endocytosis of Wingless is not required for signalling initiation. The latest model of the Wingless signalling pathway suggests that receptor bound GSK3 is sequestered in MVB, thereby allowing accumulation of newly transcribed Armadillo. However, I found that inhibition of MVB formation using *hrs* dsRNA resulted in an increase in signalling in cultured cells. *Hrs* mutant clones in the wing disc posterior compartment showed no change in Distalless expression although there was some delay in Senseless expression. Regardless of this delay adult wings displayed a wild type wing margin, suggesting sufficient Wingless signalling. Importantly signalling activity in $S2R^+$ cells triggered by inactivation of GSK3 itself was sensitive to endocytosis inhibition, suggesting that the role of endocytosis is downstream of the degradation complex. To analyse the function of endocytosis further down in the signalling pathway I activated signalling via over-expression of Armadillo and S10-Armadillo (stabilised Armadillo). In both cases inhibition of endocytosis continued to suppress signalling by affecting Armadillo levels. Whether this effect is due to inhibition of Armadillo synthesis of promotion of degradation is not yet clear. Further experiments are needed.

In conclusion, in this chapter I have highlighted flaws in the latest model of Wingless signalling and discovered a potential role of endocytosis in regulating Armadillo expression levels.

Discussion

Chapter 7

"The fundamental cause of the trouble is that in the modern world the stupid are cocksure while the intelligent are full of doubt."

Bertrand Russell
"The Triumph of Stupidity" (1933-05-10) in Mortals and Others: Bertrand Russell's American Essays, 1931-1935

Chapter 7- Discussion

General Introduction

Wnt/Wingless has been a topic of great research for the past 30 years. It has multiple and pivotal functions during development and adulthood tissue homeostasis, which explains its involvement in many developmental defects and diseases.

Although great studies have deciphered the Wnt signalling pathway, identifying and characterizing its components, many questions still remain. For example, how endocytosis and intracellular trafficking contribute to signal initiation and regulation remains unclear.

In this thesis I have shown that receptor/ligand internalization is not required for signalling. However, endocytosis, presumably of another membrane resident protein is required for signalling. I have shown that this endocytic event impinges on the signalling pathway downstream of the degradation complex and may regulate Armadillo expression/stability.

I have also explored the trafficking of Arrow upon signalling and my results suggest that it is recycled, thus taking a different route from Fz2. In an attempt to identify possible post translational modifications of Arrow that may direct its trafficking I developed a double immunoprecipitation of Arrow to allow mass spectrometry analysis of surface and internalized Arrow. A small scale RNAi screen was also conducted to uncover the involvement of ubiquitin conjugating and/or de-ubiquitylating enzymes in Wingless signalling. Some candidates were identified, however their specificity to modulating Wingless signalling could not be determined.

7.1 Arrow stability and recycling

7.1.1 Arrow recycling

In this thesis I assessed the effect of Wingless on Arrow degradation. Previous work has attributed to Arrow the role of directing Wingless degradation upon internalization (Marois et al., 2006; Piddini et al., 2005). I wanted to determine if this involved the degradation of Arrow itself. Cell surface Arrow was biotinylated and cells were exposed to Wingless for various durations (1, 2.5 and 4 hr). There was no decrease in cell surface Arrow levels in the presence of Wingless. This suggests that Arrow is not degraded upon exposure to Wingless. To verify this in vivo, HA-Arrow expression was induced by heat shock in imaginal discs. 3 hr after a pulse of expression, HA-Arrow levels were found to be randomly reduced throughout the wing pouch irrespective of Wingless expression. Although this was the result expected, a further internal control is required to validate it. It is possible that the observed salt and pepper distribution of Arrow reflects persistent expression in various cells. A control could be the co-expression of Delta along with HA-Arrow. Delta is expected to be preferentially degraded at the D/V boundary of the wing pouch (Doherty et al, 1996; Lai et al, 2001). Piddini *et al* show that, unlike Arrow, Fz2 degradation is accelerated in the proximity of the Wingless source. Such degradation can be inhibited by the over-expression of the DUB dUBPY, which suppresses lysosomal trafficking and promotes recycling back to the cell surface (Mukai et al., 2010).

Having provided evidence that Wingless does not stimulate Arrow degradation, I attempted to learn if Arrow traffics to degradative compartments. Co-localization of Arrow and LAMP was not seen. Wingless did co-localise with LAMP, suggesting that although Arrow directs Wingless degradation it does not escort it to lysosomes.

I was unable to assess Arrow co-localization with Hrs as both antibodies available to us were made in guinea pig. To assess Arrow trafficking in vivo, hrs^{D28} mutant clones were generated in the posterior compartment of wing discs. This led to the accumulation of both Wingless and Frizzed, but had no effect on Arrow levels, thus confirming that localization of Arrow is insensitive to a block in MVB biogenesis.

Having shown that Arrow does not follow a degradation route, I attempted to demonstrate Arrow recycling. Cells with biotinylated cell surface Arrow were exposed to Wingless for a 1hr time course. At subsequent times, biotin was stripped

from the cell surface. If Arrow had been internalized and then recycled unlabelled Arrow would reappear at the cell surface. A western blot would show a decrease in biotinylated Arrow levels with time. Alternatively, if recycling did not take place biotinylated Arrow levels would remain constant. Despite various attempts, my stripping was not efficient and I was unable to draw conclusions. To overcome the problem of inefficient stripping a protocol was designed with the aim of labeling recycled biotin-Arrow with avidin. Recycled Arrow would then be pulled down using a biotin column and a western blot would be expected to reveal an increase of recycled Arrow with time.

LRP6 recycling has already been documented. Dickkof (Dkk) is known to bind and induce internalization of LRP6 to prevent its phosphorylation, thus antagonizing Wnt signalling. The DKK-LRP6 complex is internalized and transport to early endosomes in a Rab5 dependent manner. From early endosomes LRP6 is recycled back to cell surface via Rab11 recycling endosomes. DKK1 on the other hand is trafficked to lysosomal degradation (Sakane et al, 2010). Given this precedent for the segregation of complex components onto different trafficking routes, it is possible to imagine that Arrow could also detach from the receptor/ligand complex after targeting Wingless to degradation.

Many signalling pathways are down regulated by ligand induced receptor degradation. This is clearly not the case for LRP6/Arrow. Evidence suggests that both LRP6 and Arrow levels are controlled transcriptionally; Wnt/Wingless signalling represses LRP6/Arrow mRNA production as it does for DFz2 (Cadigan et al, 1998; Khan et al, 2007; Marois et al, 2006). Therefore, repeated rounds of LRP6 internalization and recycling is not a signalling regulatory mechanism and may simply serve to maintain constant cell surface Arrow levels.

Future work to examine the recycling of Arrow would involve assessing co-localization of Arrow with Rabs of recycling endosomes and to determine the effect that inhibition of such Rabs would have on cell surface levels of Arrow.

7.1.1 Arrow Ubiquitylation

Arrow undergoes phosphorylation at 5 different sites upon activation, as shown by point mutation and Western blotting (Tamai et al, 2004). To determine if other post translation modifications, in particular ubiquitylation, are involved in Arrow activation and recycling, Arrow was immunoprecipitated with the aim of identifying post translational modifications by mass spectrometry. In a first attempt Arrow was pulled down with a polyclonal anti-Arrow antibody, which binds the extracellular portion of the protein. Two slightly different protocols were tested, the main difference between the two was the addition of 0.1% SDS in the lysis buffer. It was hoped that the addition of SDS would yield cleaner preparation. Although the amount of Arrow recovered was reduced, the IP was still useful as it isolated interacting proteins. I was interested in determining the identity of these proteins. Unfortunately mass spec revealed that most bands represented proteins involved in secretion, which indicated that not only activated membrane bound Arrow was being pulled down, but also intracellular Arrow. Therefore only a small proportion of activated Arrow could be characterized by mass spec. This explains why only one of the five known phophorylation sites was recovered. To overcome the overwhelming presence of inactive Arrow a double IP protocol was devised. Cell surface proteins were initially biotinylated and after exposure to Wingless were pulled down with avidin beads. From this sample of cell surface proteins Arrow was extracted with the anti-Arrow antibody. Despite having successfully optimized this double IP, mass spec was not carried out as the necessary scaling up, at least 50X, required extended time and expense.

Ubiquitylation, in addition to being a signal for proteasomal degradation (Nobel Prize in Chemistry in 2004), is a modification with multiple roles in signalling and trafficking. To identify possible Arrow ubiquitylation sites I started by probing a Western blot from initial Arrow IPs with anti-ubiquitin. Bands of the same molecular weight as Arrow were detected. To further test whether this ubiquitylated protein could be Arrow, cells expressing HA-Ub were treated with both proteasome and DUB inhibitors (MG132, NEM) and then exposed to Wingless. Ubiquitin was then pulled down and a Western blot was probed for Arrow. Light Arrow bands were detected both in the presence and absence of Wingless. The same was true for Armadillo, which acted as a control. Although the results are inconclusive thus far,

they are also encouraging and further optimization of the ubiquitin IP would be beneficial. The same IP could also be performed with material obtained from embryos expressing hs-HA-Ub +/- Wingless. This could assess Arrow ubiquitylation in vivo and also allow the identification of other proteins that are or could be modified in response to Wingless (armadillo, axin, Fz2).

The possibility that Arrow ubiquitylation is needed for Wingless signalling is supported by the fact that LRP6 ubiquitylation has been shown to have a role in Wnt signalling. Ubiquitylation on Lys1403 was initially identified as a modification used as an ER retention signal for misfolded LRP6. It was later shown to have a crucial role in signalling. Lys1403Arg mutations inhibit signalling despite proper LRP6 localization. (Abrami et al, 2008). In light of the conservation of the amino acids involved in LRP6 function in Arrow and the promising results of ubiquitylation in my preliminary IPs, I am motivated to continue pursuing the investigation of Arrow ubiquitylation not only in the manners described above, but also with the identification of possible enzymes (E2, DUBs) involved, which will de described further down.

In conclusion in this part of my thesis I have shown that Arrow is not degraded in the presence of Wingless. I have developed an efficient double IP to isolate cell surface Arrow, and I have begun examining the possible recycling of Arrow and ubiquitylation with promising preliminary results.

7.2 RNAi screen for DUBs and E2 conjugating enzymes.

7.2.1 TOPFlash reporter

Various groups have used RNAi to knockdown trafficking components and assessed the effect on Wingless signalling using a TOPFash assay (DasGupta et al, 2005; Rives et al, 2006; Seto & Bellen, 2006). Unfortunately many results were inconclusive. Results showed variability and depended on the normalising vector used. It has become apparent that a more stringent signalling assay is required, preferably one with a faster read out, before toxic side effects of RNAi take hold. I aimed to achieve this by designing a reporting vector with Renilla luciferase fused to Armadillo expressed under the control of the ubiquitin promoter. With this reporter, Renilla luciferase would follow the same fate as Armadillo: degraded in the absence of Wingless signalling and stabilised in its presence. This assay is expected to provide a faster and therefore more reliable readout than TOPFlash. Stable cell lines expressing both pUbiquitin-firefly-luciferase and pUbiqutin-Renilla-luciferase-HA-Armadillo were generated. However, no significant increase in Renilla luciferase activity was observed upon exposure to Wingless. Likewise, the GSK3 inhibitor SB-216763 had no effect, indicating either that the constructs were not functional or that there was a high Renilla luciferase baseline. Western blots proved the latter, revealing inefficient degradation of Renilla-luciferase-HA-Armadillo and the presence of a breakdown product, possibly Renilla luciferase, in all cells regardless of Wingless treatment. One way around this dilemma would be to somehow separate the breakdown product from the Renilla-Armadillo fusion protein after cell lysis, perhaps with size exclusion chromatography. Although this is theoretically plausible, this approach has been put on hold because following optimisation, the 'traditional' TOPFlash assay provided me with reliable hits. As mentioned previously this assay was improved in a variety of ways by choosing the right cell type and adjusting cell number and timing. One of the most significant improvements came from the use of un-concentrated Wingless conditioned medium from ptub-Wingless cells containing serum. This medium offers the most stable and long lasting form of Wingless, which yields a higher fold induction. Therefore concentrated conditioned medium is no longer needed, and variability is reduced due to increased stability of the medium.

7.2.2 TOPFlash assay

With this assay, RNAi against DUBs were screened. Of the 24 DUBs screened, five hits were obtained (CG14619, CG5794, CG1945 (*faf*), CG3016 and CG4166 (*not*)) all of which increase signalling following knockdown. The knockdown of these genes leads to increased signalling only in the presence of Wg, with no effect observed in its absence. This tells us that these genes have a role upstream of the degradation complex and play no direct role in the stabilization of Armadillo itself. Knockdown of a gene, that contributes to the degradation complex, such as Axin, activates signalling regardless of Wingless activity. CG5794 was previously identified in a genomewide RNAi screen for regulators of Wnt/Wingless signalling by DasGupta, R and Kaykas, A *et al*, however little is known about its function as is the case for most of the other hits from this study (DasGupta et al, 2005).

CG1945, also known as *fat facets (faf)*, is required for the function of Liquid facets (lqf), the homologue of the vertebrate endocytic protein epsin, which imparts membrane curvature (Chen et al, 2002). Through its ENTH domain, Epsin can interact with both $PI_{45}P_2$ and the transcription factor PLZF. It is thought that monoubiquitination of the ENTH domain determines with what Epsin interacts. When ENTH is ubiquitinated interaction with $PI_{45}P_2$ and consequently endocytosis is inhibited. Faf would therefore restore epsin's endocytic activity by deubiquitinating the ENTH domain. This suggests that *faf* knockdown could increase Wingless signalling by inhibiting endocytosis. This would not be accordance with my other studies where I have shown that a block in Wingless internalization does not increase signalling and that a complete block in endocytosis prevents it. Further experiments would be needed to confirm the effective knockdown of *faf* and that increased FL transcription is due to Wingless signalling and not to a general increase in transcription.

CG14619 has a 47% sequence homology with chick Ubp2. The latter has been shown to take part in the sorting of receptor/ligand complexes into MVB (Lam et al, 2009). The recent model for Wingless signalling which suggests that trafficking of the receptor/degradation complex into MVBs is an essential feature of signalling, could potentially account for the effect of CG14619.

Six hits were obtained from the E2 conjugating enzyme screen: CG15437 (*Morgue*), CG7425 (*Eff*), CG2574, CG7220, CG4443(*crl*), CG3018(*lwr*). Wingless signalling increases with knockdown of CG7220, CG4443(*crl*) and CG3018(*lwr*), also known as dUbc9. The latter is an E2 for SUMOylation, a ubiquitin like modification. SUMOylation has already been shown to increase the stability of Axin, thus counteracting the effect of Axin ubiquitylation. At this point the target of dUbc9 is unknown and further work is needed to confirm and explain its role in Wingless signalling.

Wingless signalling is decreased with knockdown of CG7425 (*Eff*), CG15437 (*Morgue*) and CG2574. The function of CG2574 is not known, but both CG15437 (*Morgue*) and CG7425 (*Eff*), have been implicated in apoptosis. Together, CG15437 (*Morgue*) and CG7425 (*Eff*) ubiquitylate and target for degradation Diap1, an inhibitor of apoptosis (Bergmann et al, 2003). Thus knockdown of these proteins would reduce the degradation of Diap1 leading to a decrease in caspase activity and apoptosis. It has been shown that caspases negatively regulate Wingless signalling by cleaving Sgg to its active state (Kanuka et al, 2005). This would suggest that increased Diap1 levels would lead to decreased caspase and *sgg* activity and thus an increase in signalling. Although my results do not reflect this, it is possible that CG15437 (*Morgue*) and CG7425 (*Eff*), have an apoptosis independent function that somehow aids Wingless signalling.

Even though RNAi screens have been tremendously informative by identifying components of diverse signalling pathways, it is important to keep in mind the weaknesses of RNAi. Hits may represent false positives due to off target effects (OTE) or false negatives because of inefficient knockdown. To minimize possible OTE, more than one dsRNA was used per gene, when available. To decrease the chances of obtaining false negatives the ideal method of delivering the dsRNA to the cells was determined. I compared bathing the cells in dsRNA with transfection. The latter proved most efficient. I replicated my assay 4/5 times to increase the statistical significance of my results. My hits were chosen on the basis of reproducibility rather than the magnitude of the effect.

7.2.3 RNAi in vivo

Having identified hits in vitro it was necessary to characterise them in vivo. UAS RNAi hairpins were expressed in the posterior compartment of wing discs, under the control of *engrailed-Gal4,* and in the dorsal compartment, with *apterous-Gal4*. Phenotypes were assessed by looking at the expression of Wingless, Arrow, Wingless target genes (*senseless, distalless, Fz3*), and wing patterning. Several genes could not be pursued either due to lethality or tissue distortion (CG7425 (*Eff*), CG3018 (*lwr*), CG4166 (*not*)). This suggests that these genes play pivotal roles in development and may affect multiple pathways making their specific effect on Wingless signalling difficult to identify.

Knockdown of DUB and E2 had no effect on Wingless expression or distribution, therefore they do not have a role in exocytosis. Arrow expression was also unaffected, suggesting that if they do modify Arrow, this does not lead to degradation. To examine possible effects on Wingless and Arrow trafficking it would have been ideal to perform extracellular staining and co-localization with components of endocytic compartments.

To determine effects on signalling, target gene expression was assessed. *Dll* expression increased slightly with knockdown of CG3016, CG1945 (*faf*), CG14619 and CG2574. These results match those of the TOPFlash for all except CG2574. This discrepancy could be due to alteration of other signalling pathways that influence Dll. In the hope of overcoming this problem, *fz3* expression, which is positively controlled by Wingless, was assessed. Unlike *dll* expression, *fz3* expression was unchanged by RNAi. *Senseless* expression was also monitored to determine if knocked down genes could affect expression of genes known to require high levels of signalling. No difference was observed. Adult wings had no abnormal patterning.

Even though effects were not seen in vivo I do not think conclusions can be draw regarding their involvement in signalling. Firstly, the function of the E2 and DUBs knocked down may be compensated by others, masking their participation in signalling. Secondly, knockdown may have minor effects on the phenotype that I was unable to detect. Finally I cannot be sure that the dsRNA used was effective.

To further test the function of the hits obtained, I think it would be beneficial to induce dsRNA expression in clones rather than entire compartments and in a

temporally controlled manner. Generation of flies expressing a mutation in the gene of interest would remedy the possible inefficiency of gene knockdown with dsRNA, and would also determine whether any phenotype seen with RNAi is an OTE.

In conclusion, specific trafficking components that unambiguously modulate Wingless signalling remain to be identified. I hope to have contributed to improving the assay of Wingless signalling with my TOPFlash vector and an optimized assay protocol. This has provided me with several hits with regards to DUBs and E2 conjugating enzymes that may play a part in Wingless signalling. Characterization of these hits in vivo did not confirm their involvement in signalling. However, further assessment is required.

7.3 Endocytosis and Signalling

7.3.1 Wingless internalization

The endocytic events required in the Wingless signalling pathway have not yet been mapped. Some claim that endocytosis is essential for the propagation of signal, suggesting that the signalling machinery is assembled on an endocytic compartment (Seto & Bellen, 2006). While others continue to support the conventional idea that endocytosis serves to dampen signalling (Rives et al, 2006). These studies relied on the inhibition of dynamin, Rab5 and MVB components. I began by assessing whether ligand internalization is required. $S2R^{+}$ cells were exposed to cells expressing HA-Wingless or membrane tethered NRT-HA-Wingless. Both forms of Wingless induced signalling but NRT-HA-Wingless induced half as much as secreted Wingless. The different activity could be due to different expression levels, which could be determined via Western blot. Alternatively this result could suggest that endocytosis is required to potentiate the signal. Thus expression of different target genes would depend on trafficking. Low level target genes could be expressed upon Wingless interacting with receptors at the cell surface, while high level target genes would require internalization. This is not an unfounded hypothesis as the role of endocytic events modulating signalling levels has been described for different pathways. For example, the EGFR receptor is internalized via different pathways depending on ligand levels. With high doses of EGF the receptor is internalized via non-clathrin endocytosis (NCE), while at low levels it is internalized via clathrin mediumted endocytosis (CME). The peak signalling phase is independent of the internalization route, but prolonged signalling requires CME (Sigismund et al, 2008). Therefore, if signal duration can depend on the internalization pathway, it is conceivable that Wingless signalling levels may depend on internalization itself.

The analysis of HA-Wingless and NRT-HA-Wingless expressing clones in wing discs showed that NRT-HA-Wingless is not released. It would be interesting to carry out an anti-Senseless staining in these wing discs. If endocytosis is required for high level signalling I would expect to see Senseless expressed around a HA-Wingless clone, but not surrounding a NRT-HA-Wingless clone.

7.3.2 Role of MVBs in signalling

A recent model of Wnt signalling describes it as a two-step process. It begins with the formation of the LRP signalosome, composed of aggregates of Dvl, Arrow, Axin and GSK3, at the plasma membrane. Signalling does not take place in this first step and requires the completion of the second, which consists of the sequestration of GSK3 into MVB. Insulation of GSK3 permits the accumulation of β-catenin, in addition to the extension of other proteins' half-life, and activates signalling (Bilic et al, 2007; Taelman et al, 2010). I evaluated the need for MVBs in Wingless signalling by knocking down *hrs* in $S2R^+$ cells. Knockdown resulted in increased signalling as opposed to the absence of signalling reported by Taelman et al. Taelman also showed that formation of secondary axis in *Xenopus* embryos by constitutively active LRP6 was inhibited by injection of *hrs* antisense morpholino, again reinforcing their claim that MVB trafficking is required for Wnt signalling (Taelman et al, 2010). Like Rives et al., 2006, I looked at Hrs function in vivo by generating *hrs* mutant clones in wing discs and assessing target gene expression. I saw no change in *dll* expression but *senseless* was reduced. The decrease in *senseless* expression may be due to a delay in expression as no loss of margin was seen in the adult wing. Staining of pupal discs could determine if *senseless* expression is restored at a later stage in development. Looking into expression of other Wingless target genes such as Fz3, neuralized or notum would also be informative. Hindsight (hnt) levels have already been assessed and no change was noticed (Rives et al, 2006). Taelman et al., propose that these opposing results regarding Hrs function could be due to redundancy in the *Drosophila* ESCRT machinery compensating for Hrs dysfunction.

In light of this possibility, I decided to bypass the ESCRT machinery and test whether inhibition of endocytosis affects the level of signalling caused by direct chemical inhibition of GSK3. According to Taelman's model, inhibition of endocytosis should not compromise signalling triggered by GSK3 inhbition. Blitzer et al previously performed this experiment in L cells. I carried it out in $S2R^+$ cells. I inactivated GSK3 with SB-216763, which I found to be more effective and specific than LiCL. Dynamin, which is essential for endocytosis was inhibited with Dynasore. With this experimental protocol inhibition of endocytosis still reduced signalling (Blitzer & Nusse, 2006). These results contradict the Wnt signalling model proposed by Taelman. I also found that endocytosis is required for signalling

activated by Axin knockdown. Blitzer et al., found clathrin inhibition did not affect Wnt signalling in SW480 cells, which over-activate signalling because of an APC mutation. This led them to conclude that the required internalization event occurs between GSK3 and APC inactivation. However SW480 cells are highly derived and lack many cellular components, such as cadherin, which has been implicated in Wnt signalling. Therefore I assessed the effect of inhibiting endocytosis on signalling induced by over-expressed Armadillo. Unexpectedly signalling was inhibited by Dynasore. Western blots showed a significant decrease in Armadillo levels. This was reversible as Armadillo levels returned to normal following removal of Dynasore. Surprisingly the level of activated Armadillo (Arm ^{S10}), expressed from an exogenous promoter, was also reduced by Dynasore treatment. Decreased protein levels seem to be specific to Armadillo as Actin, Lamin and Syntaxin levels are unaffected. Other studies have shown Dynasore to increase the level of some proteins, such as PAI-1 (Plasminogen activator inhibitor-1) expression independently of TGFβ treatment (Chung et al, 2009). Therefore Dynasore affects different pathways differently, reflecting the diverse roles that endocytosis plays in signalling.

7.3.3 Endocytosis and Armadillo levels

To determine whether Dynasore affected Armadillo stability or synthesis, I started by inhibiting protein synthesis with cycloheximide. Both endogenous Armadillo and S10-Armadillo levels decreased exponentially in the presence of Dynasore and cycloheximide, suggesting that Dynasore causes increased degradation of Armadillo. Such results are not in accordance with work performed in MDCK cells, where Dynasore treatment did not affect cytosolic β-catenin levels (Howard et al, 2011). The use of different cell types could account for these differences. Alternatively these different results could be due to the fact that in the study of Howard, β-catenin levels were assessed at later time points.

Live imaging of GFP-Armadillo levels in cells treated with Dynasore did not reveal exponential decrease. Rather, fluorescent intensity declined only by 15% over 1.5hr. This experiment was only performed once and various controls would be needed. To determine that persistant GFP levels are not due to detachment of GFP from Armadillo, a Western blot would be need to verify that as Armadillo is degraded, so too is GFP. A Western blot would also reveal if N terminally bound GFP interferes

with Armadillo degradation, in which case C terminally bound GFP would be a better reporter. Finally, a non-membrane bound Cherry would be a more accurate control as its degradation rate would not be influenced by membrane retention.

To address the effects of Dynasore on Armadillo synthesis, degradation was inhibited with the proteasomal inhibitor MG132 and Armadillo levels were monitored in the presence and absence of Dynasore. Surprisingly, Dynasore treatments did not simply inhibit Armadillo accumulation, which would be indicative of compromised synthesis, but led to a decrease in Armadillo levels. This could be explained by Dynasore being more potent than MG132 thus overriding proteasomal inhibition. Alternatively Armadillo may be degraded by a proteasomal independent mechanism that MG132 does not inhibit. Tripeptidyl peptidase II (TPP II), for example, is a serine protease that acts downstream in the ubiquitin-proteasome pathway and has been shown to be up-regulated in the absence of proteasomal function, thus preserving protein turnover (Gavioli et al, 2002; Geier et al, 1999; Rockel et al, 2011). The assessment of Dynasore's effect on protein synthesis could be pursued by labeling and tracking newly synthesized proteins. More informative and advantageous would be the labeling of Armadillo with Dendra2. Dendra2 is a green to red photo-convertible fluorescent protein, which would allow Armadillo synthesis and degradation to be monitored simultaneously live. Given the unreliability and interference of N terminally labeled Armadillo with GFP, Dendra2 would be placed at the C terminus. Newly synthesized Armadillo-Dendra2 would have a green fluorescent state, photo-conversion would yield a stable irreversible red fluorescent state. If Dynasore were affecting synthesis, upon treatment green fluorescent Armadillo would no longer be produced. On the other hand, if degradation were enhanced, red fluorescent Armadillo would rapidly decrease. Therefore Armadillo-Dendra2 would help to simultaneously monitor Dynasore's effect on Armadillo synthesis and degradation.

Although I have not yet understood how Dynasore affects Armadillo levels, I have shown that it has a dramatic effect, namely a strong reduction. To ensure that these changes are not due to indirect effects of Dynasore treatment (Dynasore inhibiting more than just dynamin), it will be important to assess changes in Armadillo levels in response to other drugs that inhibit endocytosis/dynamin such as Dyngo4 which may have more specificity for dynamin and Pitstop1/2 which inhibit clathrin. In conclusion, my results thus far contradict the notion that MVB formation is a key

endocytic step in Wnt signalling. Rather, my results suggest that endocytosis is required to maintain Armadillo levels.

Until now cadherins have been considered negative regulators of signalling as they retain β-catenin from signalling (Orsulic et al, 1999; Sanson et al, 1996). Recent work with MDCK cells describes cadherin expression and turnover as a positive regulator of signalling. It was suggested that β-catenin binds to cadherin at cell junctions and that its dissociation from cadherin upon endocytosis primes it for signalling. Therefore inhibition of cadherin turnover with Dynasore would retain β-catenin/cadherin at the cell membrane thus blocking 'priming' and weakening its transcriptional activity (Howard et al, 2011). Thus, Howard et al., propose a dual function for cadherin. If cadherin is over expressed, Wnt signalling is compromised due to the strong β-catenin/cadherin bond that prevents dissociation. If cadherin is down regulated, β-catenin is no longer activated and unable to signal. Therefore β-catenin transcriptional activity depends both on interaction with cadherin for priming and endocytosis for release. A mutated form of β-catenin, Y654E, that does not bind to cadherin cannot signal (Howard et al, 2001). Although this confirms that cytosolic levels of β-catenin do not necessarily reflect activity, it contradicts previous work in which Y654E has been associated with an increase in signalling activity (Fang et al, 2007). Previous studies also claim that de novo synthesis of β-catenin be required for signalling. This was suggested by the lack of β-catenin accumulation and target gene expression in the presence of cycloheximide (Hendriksen et al, 2008; Willert et al, 2002). Despite inhibition of protein synthesis, MDCK cells treated with HGF (Hepatocyte Growth Factor), which induces epithelial to mesenchymal transition, still accumulate β-catenin and express target genes, supporting activation of β-catenin bound to cadherins in signalling (Howard et al, 2011). These conflicting results along with the fact that endocytosis seems to be required for signalling in L cells that do not express cadherin (Blitzer & Nusse, 2006; Taelman et al, 2010) could be explained by the fact that different cell types were used.

The role of endocytosis and endocytic trafficking in Wnt/Wingless signalling is still unclear. In this thesis I have shown that internalization of the receptor ligand complex is not required and that the critical endocytic step is downstream of the degradation complex, boosting Armadillo stability or expression. I have also begun to explore the trafficking of Arrow that adopts a different route than Fz2 and Wingless, and optimized a protocol to determine post translation modifications.

Further work will be needed to support my results and develop a comprehensive model for Wingless signalling.

References

Abrami L, Kunz B, Iacovache I, van der Goot FG (2008) Palmitoylation and ubiquitination regulate exit of the Wnt signaling protein LRP6 from the endoplasmic reticulum. *Proc Natl Acad Sci U S A* **105**(14)**:** 5384-5389

Adhikari A, Chen ZJ (2009) Diversity of polyubiquitin chains. *Dev Cell* **16**(4)**:** 485-486

Alexandre C, Lecourtois M, Vincent J (1999) Wingless and Hedgehog pattern Drosophila denticle belts by regulating the production of short-range signals. *Development* **126**(24)**:** 5689-5698

Angers S, Moon RT (2009) Proximal events in Wnt signal transduction. *Nat Rev Mol Cell Biol* **10**(7)**:** 468-477

Angers S, Thorpe CJ, Biechele TL, Goldenberg SJ, Zheng N, MacCoss MJ, Moon RT (2006) The KLHL12-Cullin-3 ubiquitin ligase negatively regulates the Wnt-beta-catenin pathway by targeting Dishevelled for degradation. *Nat Cell Biol* **8**(4)**:** 348-357

Axelrod JD (2001) Unipolar membrane association of Dishevelled mediumtes Frizzled planar cell polarity signaling. *Genes Dev* **15**(10)**:** 1182-1187

Bache KG, Brech A, Mehlum A, Stenmark H (2003) Hrs regulates multivesicular body formation via ESCRT recruitment to endosomes. *J Cell Biol* **162**(3)**:** 435-442

Baker NE (1988) Embryonic and imaginal requirements for wingless, a segment-polarity gene in Drosophila. *Dev Biol* **125**(1)**:** 96-108

Barker N, Hurlstone A, Musisi H, Miles A, Bienz M, Clevers H (2001) The chromatin remodelling factor Brg-1 interacts with beta-catenin to promote target gene activation. *EMBO J* **20**(17)**:** 4935-4943

Bartek J, Falck J, Lukas J (2001) CHK2 kinase--a busy messenger. *Nat Rev Mol Cell Biol* **2**(12)**:** 877-886

Bashkirov PV, Akimov SA, Evseev AI, Schmid SL, Zimmerberg J, Frolov VA (2008) GTPase cycle of dynamin is coupled to membrane squeeze and release, leading to spontaneous fission. *Cell* **135**(7)**:** 1276-1286

Bejsovec A, Martinez Arias A (1991) Roles of wingless in patterning the larval epidermis of Drosophila. *Development* **113**(2)**:** 471-485

Bejsovec A, Wieschaus E (1993) Segment polarity gene interactions modulate epidermal patterning in Drosophila embryos. *Development* **119**(2)**:** 501-517

Bergmann A, Yang AY, Srivastava M (2003) Regulators of IAP function: coming to grips with the grim reaper. *Current opinion in cell biology* **15**(6)**:** 717-724

Bhanot P, Fish M, Jemison JA, Nusse R, Nathans J, Cadigan KM (1999) Frizzled and Dfrizzled-2 function as redundant receptors for Wingless during Drosophila embryonic development. *Development* **126**(18)**:** 4175-4186

Bickel PE, Scherer PE, Schnitzer JE, Oh P, Lisanti MP, Lodish HF (1997) Flotillin and epidermal surface antigen define a new family of caveolae-associated integral membrane proteins. *J Biol Chem* **272**(21)**:** 13793-13802

Bienz M (2005) beta-Catenin: a pivot between cell adhesion and Wnt signalling. *Curr Biol* **15**(2)**:** R64-67

Bilic J, Huang YL, Davidson G, Zimmermann T, Cruciat CM, Bienz M, Niehrs C (2007) Wnt induces LRP6 signalosomes and promotes dishevelled-dependent LRP6 phosphorylation. *Science* **316**(5831)**:** 1619-1622

Blitzer JT, Nusse R (2006) A critical role for endocytosis in Wnt signaling. *BMC Cell Biol* **7:** 28

Boutros M, Mihaly J, Bouwmeester T, Mlodzik M (2000) Signaling specificity by Frizzled receptors in Drosophila. *Science* **288**(5472)**:** 1825-1828

Boutros M, Paricio N, Strutt DI, Mlodzik M (1998) Dishevelled activates JNK and discriminates between JNK pathways in planar polarity and wingless signaling. *Cell* **94**(1)**:** 109-118

Bray S (1998) Notch signalling in Drosophila: three ways to use a pathway. *Semin Cell Dev Biol* **9**(6)**:** 591-597

Bray SJ (2006) Notch signalling: a simple pathway becomes complex. *Nat Rev Mol Cell Biol* **7**(9)**:** 678-689

Brembeck FH, Schwarz-Romond T, Bakkers J, Wilhelm S, Hammerschmidt M, Birchmeier W (2004) Essential role of BCL9-2 in the switch between beta-catenin's adhesive and transcriptional functions. *Genes Dev* **18**(18)**:** 2225-2230

Briand N, Dugail I, Le Lay S (2011) Cavin proteins: New players in the caveolae field. *Biochimie* **93**(1)**:** 71-77

Bright NA, Gratian MJ, Luzio JP (2005) Endocytic delivery to lysosomes mediumted by concurrent fusion and kissing events in living cells. *Curr Biol* **15**(4)**:** 360-365

Buechling T, Boutros M (2011) Wnt signaling signaling at and above the receptor level. *Curr Top Dev Biol* **97:** 21-53

Cabrera CM, Lopez-Nevot MA (2005) APC and chromosome instability in colorectal cancer. *Rev Esp Enferm Dig* **97**(10)**:** 738-743

Cabrera CV, Alonso MC, Johnston P, Phillips RG, Lawrence PA (1987) Phenocopies induced with antisense RNA identify the wingless gene. *Cell* **50**(4)**:** 659-663

Cadigan KM, Fish MP, Rulifson EJ, Nusse R (1998) Wingless repression of Drosophila frizzled 2 expression shapes the Wingless morphogen gradient in the wing. *Cell* **93**(5)**:** 767-777

Carpentier JL, Sawano F, Geiger D, Gorden P, Perrelet A, Orci L (1989) Potassium depletion and hypertonic medium reduce "non-coated" and clathrin-coated pit formation, as well as endocytosis through these two gates. *J Cell Physiol* **138**(3)**:** 519-526

Cavallo RA, Cox RT, Moline MM, Roose J, Polevoy GA, Clevers H, Peifer M, Bejsovec A (1998) Drosophila Tcf and Groucho interact to repress Wingless signalling activity. *Nature* **395**(6702)**:** 604-608

Chen CM, Struhl G (1999) Wingless transduction by the Frizzled and Frizzled2 proteins of Drosophila. *Development* **126**(23)**:** 5441-5452

Chen D, Wang Q, Huang H, Xia L, Jiang X, Kan L, Sun Q (2009) Effete-mediumted degradation of Cyclin A is essential for the maintenance of germline stem cells in Drosophila. *Development* **136**(24)**:** 4133-4142

Chen EH, Baker BS (1997) Compartmental organization of the Drosophila genital imaginal discs. *Development* **124**(1)**:** 205-218

Chen X, Zhang B, Fischer JA (2002) A specific protein substrate for a deubiquitinating enzyme: Liquid facets is the substrate of Fat facets. *Genes & development* **16**(3)**:** 289-294

Chen YG (2009) Endocytic regulation of TGF-beta signaling. *Cell Res* **19**(1)**:** 58-70

Choi J, Park SY, Costantini F, Jho EH, Joo CK (2004) Adenomatous polyposis coli is down-regulated by the ubiquitin-proteasome pathway in a process facilitated by Axin. *J Biol Chem* **279**(47)**:** 49188-49198

Choi KW, Benzer S (1994) Rotation of photoreceptor clusters in the developing Drosophila eye requires the nemo gene. *Cell* **78**(1)**:** 125-136

Chung CL, Sheu JR, Liu HE, Chang SC, Chou YC, Chen WL, Chou DS, Hsiao G (2009) Dynasore, a dynamin inhibitor, induces PAI-1 expression in MeT-5A human pleural mesothelial cells. *Am J Respir Cell Mol Biol* **40**(6)**:** 692-700

Coghlan MP, Culbert AA, Cross DA, Corcoran SL, Yates JW, Pearce NJ, Rausch OL, Murphy GJ, Carter PS, Roxbee Cox L, Mills D, Brown MJ, Haigh D, Ward RW, Smith DG, Murray KJ, Reith AD, Holder JC (2000) Selective small molecule inhibitors of glycogen synthase kinase-3 modulate glycogen metabolism and gene transcription. *Chem Biol* **7**(10)**:** 793-803

Cohen ED, Mariol MC, Wallace RM, Weyers J, Kamberov YG, Pradel J, Wilder EL (2002) DWnt4 regulates cell movement and focal adhesion kinase during Drosophila ovarian morphogenesis. *Dev Cell* **2**(4)**:** 437-448

Cohen P, Frame S (2001) The renaissance of GSK3. *Nat Rev Mol Cell Biol* **2**(10)**:** 769-776

Cohen SM (1990) Specification of limb development in the Drosophila embryo by positional cues from segmentation genes. *Nature* **343**(6254)**:** 173-177

Cong F, Schweizer L, Varmus H (2004) Wnt signals across the plasma membrane to activate the beta-catenin pathway by forming oligomers containing its receptors, Frizzled and LRP. *Development* **131**(20)**:** 5103-5115

Couso JP, Bishop SA, Martinez Arias A (1994) The wingless signalling pathway and the patterning of the wing margin in Drosophila. *Development* **120**(3)**:** 621-636

Cox RT, Kirkpatrick C, Peifer M (1996) Armadillo is required for adherens junction assembly, cell polarity, and morphogenesis during Drosophila embryogenesis. *J Cell Biol* **134**(1)**:** 133-148

Danino D, Moon KH, Hinshaw JE (2004) Rapid constriction of lipid bilayers by the mechanochemical enzyme dynamin. *J Struct Biol* **147**(3)**:** 259-267

DasGupta R, Kaykas A, Moon RT, Perrimon N (2005) Functional genomic analysis of the Wnt-wingless signaling pathway. *Science* **308**(5723)**:** 826-833

Davidson G, Wu W, Shen J, Bilic J, Fenger U, Stannek P, Glinka A, Niehrs C (2005) Casein kinase 1 gamma couples Wnt receptor activation to cytoplasmic signal transduction. *Nature* **438**(7069)**:** 867-872

Davies SP, Reddy H, Caivano M, Cohen P (2000) Specificity and mechanism of action of some commonly used protein kinase inhibitors. *Biochem J* **351**(Pt 1)**:** 95-105

de Celis JF, Garcia-Bellido A, Bray SJ (1996) Activation and function of Notch at the dorsal-ventral boundary of the wing imaginal disc. *Development* **122**(1)**:** 359-369

Deribe YL, Pawson T, Dikic I (2010) Post-translational modifications in signal integration. *Nat Struct Mol Biol* **17**(6)**:** 666-672

Di Guglielmo GM, Le Roy C, Goodfellow AF, Wrana JL (2003) Distinct endocytic pathways regulate TGF-beta receptor signalling and turnover. *Nat Cell Biol* **5**(5)**:** 410-421

Diaz-Benjumea FJ, Cohen SM (1995) Serrate signals through Notch to establish a Wingless-dependent organizer at the dorsal/ventral compartment boundary of the Drosophila wing. *Development* **121**(12)**:** 4215-4225

DiNardo S, Sher E, Heemskerk-Jongens J, Kassis JA, O'Farrell PH (1988) Two-tiered regulation of spatially patterned engrailed gene expression during Drosophila embryogenesis. *Nature* **332**(6165)**:** 604-609

Ding VW, Chen RH, McCormick F (2000) Differential regulation of glycogen synthase kinase 3beta by insulin and Wnt signaling. *J Biol Chem* **275**(42)**:** 32475-32481

Doherty D, Feger G, Younger-Shepherd S, Jan LY, Jan YN (1996) Delta is a ventral to dorsal signal complementary to Serrate, another Notch ligand, in Drosophila wing formation. *Genes Dev* **10**(4)**:** 421-434

Dubois L, Lecourtois M, Alexandre C, Hirst E, Vincent JP (2001) Regulated endocytic routing modulates wingless signaling in Drosophila embryos. *Cell* **105**(5)**:** 613-624

Ehebauer M, Hayward P, Arias AM (2006) Notch, a universal arbiter of cell fate decisions. *Science* **314**(5804)**:** 1414-1415

Embi N, Rylatt DB, Cohen P (1980) Glycogen synthase kinase-3 from rabbit skeletal muscle. Separation from cyclic-AMP-dependent protein kinase and phosphorylase kinase. *Eur J Biochem* **107**(2)**:** 519-527

Emery G, Hutterer A, Berdnik D, Mayer B, Wirtz-Peitz F, Gaitan MG, Knoblich JA (2005) Asymmetric Rab 11 endosomes regulate delta recycling and specify cell fate in the Drosophila nervous system. *Cell* **122**(5)**:** 763-773

Eskelinen EL, Illert AL, Tanaka Y, Schwarzmann G, Blanz J, Von Figura K, Saftig P (2002) Role of LAMP-2 in lysosome biogenesis and autophagy. *Mol Biol Cell* **13**(9)**:** 3355-3368

Fagotto F, Jho E, Zeng L, Kurth T, Joos T, Kaufmann C, Costantini F (1999) Domains of axin involved in protein-protein interactions, Wnt pathway inhibition, and intracellular localization. *J Cell Biol* **145**(4)**:** 741-756

Fang D, Hawke D, Zheng Y, Xia Y, Meisenhelder J, Nika H, Mills GB, Kobayashi R, Hunter T, Lu Z (2007) Phosphorylation of beta-catenin by AKT promotes beta-catenin transcriptional activity. *J Biol Chem* **282**(15)**:** 11221-11229

Faria M, Wood CD, Perrouault L, Nelson JS, Winter A, White MR, Helene C, Giovannangeli C (2000) Targeted inhibition of transcription elongation in cells mediumted by triplex-forming oligonucleotides. *Proc Natl Acad Sci U S A* **97**(8)**:** 3862-3867

Fiedler M, Mendoza-Topaz C, Rutherford TJ, Mieszczanek J, Bienz M (2011) Dishevelled interacts with the DIX domain polymerization interface of Axin to interfere with its function in down-regulating beta-catenin. *Proc Natl Acad Sci U S A* **108**(5)**:** 1937-1942

Fradkin LG, Noordermeer JN, Nusse R (1995) The Drosophila Wnt protein DWnt-3 is a secreted glycoprotein localized on the axon tracts of the embryonic CNS. *Dev Biol* **168**(1)**:** 202-213

Fradkin LG, van Schie M, Wouda RR, de Jong A, Kamphorst JT, Radjkoemar-Bansraj M, Noordermeer JN (2004) The Drosophila Wnt5 protein mediumtes selective axon fasciculation in the embryonic central nervous system. *Dev Biol* **272**(2)**:** 362-375

Frame S, Cohen P, Biondi RM (2001) A common phosphate binding site explains the unique substrate specificity of GSK3 and its inactivation by phosphorylation. *Mol Cell* **7**(6)**:** 1321-1327

Frick M, Bright NA, Riento K, Bray A, Merrified C, Nichols BJ (2007) Coassembly of flotillins induces formation of membrane microdomains, membrane curvature, and vesicle budding. *Curr Biol* **17**(13)**:** 1151-1156

Fuerer C, Habib SJ, Nusse R (2010) A study on the interactions between heparan sulfate proteoglycans and Wnt proteins. *Dev Dyn* **239**(1)**:** 184-190

Galbiati F, Volonte D, Goltz JS, Steele Z, Sen J, Jurcsak J, Stein D, Stevens L, Lisanti MP (1998) Identification, sequence and developmental expression of invertebrate flotillins from Drosophila melanogaster. *Gene* **210**(2)**:** 229-237

Garcia-Bellido A, Ripoll P, Morata G (1973) Developmental compartmentalisation of the wing disk of Drosophila. *Nat New Biol* **245**(147)**:** 251-253

Garcia-Bellido A, Ripoll P, Morata G (1976) Developmental compartmentalization in the dorsal mesothoracic disc of Drosophila. *Dev Biol* **48**(1)**:** 132-147

Gavioli R, Vertuani S, Masucci MG (2002) Proteasome inhibitors reconstitute the presentation of cytotoxic T-cell epitopes in Epstein-Barr virus-associated tumors. *Int J Cancer* **101**(6)**:** 532-538

Geier E, Pfeifer G, Wilm M, Lucchiari-Hartz M, Baumeister W, Eichmann K, Niedermann G (1999) A giant protease with potential to substitute for some functions of the proteasome. *Science* **283**(5404)**:** 978-981

Gieseler K, Graba Y, Mariol MC, Wilder EL, Martinez-Arias A, Lemaire P, Pradel J (1999) Antagonist activity of DWnt-4 and wingless in the Drosophila embryonic ventral ectoderm and in heterologous Xenopus assays. *Mech Dev* **85**(1-2)**:** 123-131

Golembo M, Raz E, Shilo BZ (1996) The Drosophila embryonic midline is the site of Spitz processing, and induces activation of the EGF receptor in the ventral ectoderm. *Development* **122**(11)**:** 3363-3370

Golic KG, Lindquist S (1989) The FLP recombinase of yeast catalyzes site-specific recombination in the Drosophila genome. *Cell* **59**(3)**:** 499-509

Gonzalez A, Chaouiya C, Thieffry D (2006) Dynamical analysis of the regulatory network defining the dorsal-ventral boundary of the Drosophila wing imaginal disc. *Genetics* **174**(3)**:** 1625-1634

Gordon MD, Dionne MS, Schneider DS, Nusse R (2005) WntD is a feedback inhibitor of Dorsal/NF-kappaB in Drosophila development and immunity. *Nature* **437**(7059)**:** 746-749

Gordon MD, Nusse R (2006) Wnt signaling: multiple pathways, multiple receptors, and multiple transcription factors. *J Biol Chem* **281**(32)**:** 22429-22433

Gottardi CJ, Gumbiner BM (2004) Distinct molecular forms of beta-catenin are targeted to adhesive or transcriptional complexes. *J Cell Biol* **167**(2)**:** 339-349

Gruenberg J, Stenmark H (2004) The biogenesis of multivesicular endosomes. *Nat Rev Mol Cell Biol* **5**(4)**:** 317-323

Gubb D, Garcia-Bellido A (1982) A genetic analysis of the determination of cuticular polarity during development in Drosophila melanogaster. *J Embryol Exp Morphol* **68:** 37-57

Gunaratne A, Benchabane H, Di Guglielmo GM (2012) Regulation of TGFbeta receptor trafficking and signaling by atypical protein kinase C. *Cell Signal* **24**(1)**:** 119-130

Gupta-Rossi N, Six E, LeBail O, Logeat F, Chastagner P, Olry A, Israel A, Brou C (2004) Monoubiquitination and endocytosis direct gamma-secretase cleavage of activated Notch receptor. *J Cell Biol* **166**(1)**:** 73-83

Hadian K, Griesbach RA, Dornauer S, Wanger TM, Nagel D, Metlitzky M, Beisker W, Schmidt-Supprian M, Krappmann D (2011) NF-kappaB essential modulator (NEMO) interaction with linear and lys-63 ubiquitin chains contributes to NF-kappaB activation. *J Biol Chem* **286**(29)**:** 26107-26117

Haglund K, Dikic I (2005) Ubiquitylation and cell signaling. *The EMBO journal* **24**(19)**:** 3353-3359

Hansson EM, Lanner F, Das D, Mutvei A, Marklund U, Ericson J, Farnebo F, Stumm G, Stenmark H, Andersson ER, Lendahl U (2010) Control of Notch-ligand endocytosis by ligand-receptor interaction. *J Cell Sci* **123**(Pt 17)**:** 2931-2942

Hay-Koren A, Caspi M, Zilberberg A, Rosin-Arbesfeld R (2011) The EDD E3 ubiquitin ligase ubiquitinates and up-regulates beta-catenin. *Mol Biol Cell* **22**(3)**:** 399-411

Hecht A, Litterst CM, Huber O, Kemler R (1999) Functional characterization of multiple transactivating elements in beta-catenin, some of which interact with the TATA-binding protein in vitro. *J Biol Chem* **274**(25)**:** 18017-18025

Heemskerk J, DiNardo S (1994) Drosophila hedgehog acts as a morphogen in cellular patterning. *Cell* **76**(3)**:** 449-460

Henderson BR (2000) Nuclear-cytoplasmic shuttling of APC regulates beta-catenin subcellular localization and turnover. *Nat Cell Biol* **2**(9)**:** 653-660

Henderson MJ, Russell AJ, Hird S, Munoz M, Clancy JL, Lehrbach GM, Calanni ST, Jans DA, Sutherland RL, Watts CK (2002) EDD, the human hyperplastic discs protein, has a role in progesterone receptor coactivation and potential involvement in DNA damage response. *J Biol Chem* **277**(29)**:** 26468-26478

Hendriksen J, Jansen M, Brown CM, van der Velde H, van Ham M, Galjart N, Offerhaus GJ, Fagotto F, Fornerod M (2008) Plasma membrane recruitment of dephosphorylated beta-catenin upon activation of the Wnt pathway. *J Cell Sci* **121**(Pt 11)**:** 1793-1802

Hershko A, Ciechanover A (1998) The ubiquitin system. *Annual review of biochemistry* **67:** 425-479

Howard S, Deroo T, Fujita Y, Itasaki N (2001) A Positive Role of Cadherin in Wnt/beta-Catenin Signalling during Epithelial-Mesenchymal Transition. *PLoS One* **6**(8)**:** e23899

Howard S, Deroo T, Fujita Y, Itasaki N (2011) A positive role of cadherin in Wnt/beta-catenin signalling during epithelial-mesenchymal transition. *PLoS One* **6**(8)**:** e23899

Huang H, He X (2008) Wnt/beta-catenin signaling: new (and old) players and new insights. *Curr Opin Cell Biol* **20**(2)**:** 119-125

Huang L, Ohsako S, Tanda S (2005) The lesswright mutation activates Rel-related proteins, leading to overproduction of larval hemocytes in Drosophila melanogaster. *Dev Biol* **280**(2)**:** 407-420

Huang SM, Mishina YM, Liu S, Cheung A, Stegmeier F, Michaud GA, Charlat O, Wiellette E, Zhang Y, Wiessner S, Hild M, Shi X, Wilson CJ, Mickanin C, Myer V, Fazal A, Tomlinson R, Serluca F, Shao W, Cheng H, Shultz M, Rau C, Schirle M, Schlegl J, Ghidelli S, Fawell S, Lu C, Curtis D, Kirschner MW, Lengauer C, Finan PM, Tallarico JA, Bouwmeester T, Porter JA, Bauer A, Cong F (2009) Tankyrase inhibition stabilizes axin and antagonizes Wnt signalling. *Nature* **461**(7264)**:** 614-620

Huber AH, Weis WI (2001) The structure of the beta-catenin/E-cadherin complex and the molecular basis of diverse ligand recognition by beta-catenin. *Cell* **105**(3)**:** 391-402

Hughes K, Nikolakaki E, Plyte SE, Totty NF, Woodgett JR (1993) Modulation of the glycogen synthase kinase-3 family by tyrosine phosphorylation. *EMBO J* **12**(2)**:** 803-808

Huotari J, Helenius A (2011) Endosome maturation. *EMBO J* **30**(17)**:** 3481-3500

Ingham PW (1991) Segment polarity genes and cell patterning within the Drosophila body segment. *Curr Opin Genet Dev* **1**(2)**:** 261-267

Inoue Y, Imamura T (2008) Regulation of TGF-beta family signaling by E3 ubiquitin ligases. *Cancer Sci* **99**(11)**:** 2107-2112

Janson K, Cohen ED, Wilder EL (2001) Expression of DWnt6, DWnt10, and DFz4 during Drosophila development. *Mech Dev* **103**(1-2)**:** 117-120

Johnson ES (2002) Ubiquitin branches out. *Nat Cell Biol* **4**(12)**:** E295-298

Kanuka H, Kuranaga E, Takemoto K, Hiratou T, Okano H, Miura M (2005) Drosophila caspase transduces Shaggy/GSK-3beta kinase activity in neural precursor development. *EMBO J* **24**(21)**:** 3793-3806

Kavsak P, Rasmussen RK, Causing CG, Bonni S, Zhu H, Thomsen GH, Wrana JL (2000) Smad7 binds to Smurf2 to form an E3 ubiquitin ligase that targets the TGF beta receptor for degradation. *Mol Cell* **6**(6)**:** 1365-1375

Kennerdell JR, Carthew RW (1998) Use of dsRNA-mediumted genetic interference to demonstrate that frizzled and frizzled 2 act in the wingless pathway. *Cell* **95**(7)**:** 1017-1026

Khan Z, Vijayakumar S, de la Torre TV, Rotolo S, Bafico A (2007) Analysis of endogenous LRP6 function reveals a novel feedback mechanism by which Wnt negatively regulates its receptor. *Mol Cell Biol* **27**(20)**:** 7291-7301

Kikuchi A (1999) Roles of Axin in the Wnt signalling pathway. *Cell Signal* **11**(11)**:** 777-788

Kim MJ, Chia IV, Costantini F (2008) SUMOylation target sites at the C terminus protect Axin from ubiquitination and confer protein stability. *FASEB J* **22**(11)**:** 3785-3794

Kimelman D, Xu W (2006) beta-catenin destruction complex: insights and questions from a structural perspective. *Oncogene* **25**(57)**:** 7482-7491

Kinzler KW, Nilbert MC, Vogelstein B, Bryan TM, Levy DB, Smith KJ, Preisinger AC, Hamilton SR, Hedge P, Markham A, et al. (1991) Identification of a gene located at chromosome 5q21 that is mutated in colorectal cancers. *Science* **251**(4999)**:** 1366-1370

Korinek V, Barker N, Morin PJ, van Wichen D, de Weger R, Kinzler KW, Vogelstein B, Clevers H (1997) Constitutive transcriptional activation by a beta-catenin-Tcf complex in APC-/- colon carcinoma. *Science* **275**(5307)**:** 1784-1787

Korinek V, Barker N, Willert K, Molenaar M, Roose J, Wagenaar G, Markman M, Lamers W, Destree O, Clevers H (1998) Two members of the Tcf family implicated in Wnt/beta-catenin signaling during embryogenesis in the mouse. *Mol Cell Biol* **18**(3)**:** 1248-1256

Kosaka T, Ikeda K (1983) Reversible blockage of membrane retrieval and endocytosis in the garland cell of the temperature-sensitive mutant of Drosophila melanogaster, shibirets1. *J Cell Biol* **97**(2)**:** 499-507

Kozopas KM, Samos CH, Nusse R (1998) DWnt-2, a Drosophila Wnt gene required for the development of the male reproductive tract, specifies a sexually dimorphic cell fate. *Genes Dev* **12**(8)**:** 1155-1165

Kramps T, Peter O, Brunner E, Nellen D, Froesch B, Chatterjee S, Murone M, Zullig S, Basler K (2002) Wnt/wingless signaling requires BCL9/legless-mediumted recruitment of pygopus to the nuclear beta-catenin-TCF complex. *Cell* **109**(1)**:** 47-60

Kuhl M, Geis K, Sheldahl LC, Pukrop T, Moon RT, Wedlich D (2001) Antagonistic regulation of convergent extension movements in Xenopus by Wnt/beta-catenin and Wnt/Ca2+ signaling. *Mech Dev* **106**(1-2)**:** 61-76

Kuhl M, Sheldahl LC, Malbon CC, Moon RT (2000a) Ca(2+)/calmodulin-dependent protein kinase II is stimulated by Wnt and Frizzled homologs and promotes ventral cell fates in Xenopus. *J Biol Chem* **275**(17)**:** 12701-12711

Kuhl M, Sheldahl LC, Park M, Miller JR, Moon RT (2000b) The Wnt/Ca2+ pathway: a new vertebrate Wnt signaling pathway takes shape. *Trends Genet* **16**(7)**:** 279-283

Kumari S, Mg S, Mayor S (2010) Endocytosis unplugged: multiple ways to enter the cell. *Cell Res* **20**(3)**:** 256-275

Lai EC, Deblandre GA, Kintner C, Rubin GM (2001) Drosophila neuralized is a ubiquitin ligase that promotes the internalization and degradation of delta. *Dev Cell* **1**(6)**:** 783-794

Lam MH, Urban-Grimal D, Bugnicourt A, Greenblatt JF, Haguenauer-Tsapis R, Emili A (2009) Interaction of the deubiquitinating enzyme Ubp2 and the e3 ligase Rsp5 is required for transporter/receptor sorting in the multivesicular body pathway. *PLoS One* **4**(1)**:** e4259

Lawrence PA, Morata G (1976) Compartments in the wing of Drosophila: a study of the engrailed gene. *Dev Biol* **50**(2)**:** 321-337

Le Borgne R, Bardin A, Schweisguth F (2005) The roles of receptor and ligand endocytosis in regulating Notch signaling. *Development* **132**(8)**:** 1751-1762

Lecourtois M, Alexandre C, Dubois L, Vincent JP (2001) Wingless capture by Frizzled and Frizzled2 in Drosophila embryos. *Dev Biol* **235**(2)**:** 467-475

Lee PS, Chang C, Liu D, Derynck R (2003) Sumoylation of Smad4, the common Smad mediumtor of transforming growth factor-beta family signaling. *J Biol Chem* **278**(30)**:** 27853-27863

Liu FY, Li XZ, Peng YM, Liu H, Liu YH (2007) Arkadia-Smad7-mediumted positive regulation of TGF-beta signaling in a rat model of tubulointerstitial fibrosis. *Am J Nephrol* **27**(2)**:** 176-183

Liu L, Pilch PF (2008) A critical role of cavin (polymerase I and transcript release factor) in caveolae formation and organization. *J Biol Chem* **283**(7)**:** 4314-4322

Liu Y, Rubin B, Bodine PV, Billiard J (2008) Wnt5a induces homodimerization and activation of Ror2 receptor tyrosine kinase. *J Cell Biochem* **105**(2)**:** 497-502

Llimargas M, Lawrence PA (2001) Seven Wnt homologues in Drosophila: a case study of the developing tracheae. *Proc Natl Acad Sci U S A* **98**(25)**:** 14487-14492

Lu Z, Murray JT, Luo W, Li H, Wu X, Xu H, Backer JM, Chen YG (2002) Transforming growth factor beta activates Smad2 in the absence of receptor endocytosis. *J Biol Chem* **277**(33)**:** 29363-29368

Lui TT, Lacroix C, Ahmed SM, Goldenberg SJ, Leach CA, Daulat AM, Angers S (2011) The ubiquitin-specific protease USP34 regulates axin stability and Wnt/beta-catenin signaling. *Mol Cell Biol* **31**(10)**:** 2053-2065

Luo W, Peterson A, Garcia BA, Coombs G, Kofahl B, Heinrich R, Shabanowitz J, Hunt DF, Yost HJ, Virshup DM (2007) Protein phosphatase 1 regulates assembly and function of the beta-catenin degradation complex. *EMBO J* **26**(6)**:** 1511-1521

Luzio JP, Poupon V, Lindsay MR, Mullock BM, Piper RC, Pryor PR (2003) Membrane dynamics and the biogenesis of lysosomes. *Mol Membr Biol* **20**(2)**:** 141-154

MacDonald BT, Tamai K, He X (2009) Wnt/beta-catenin signaling: components, mechanisms, and diseases. *Dev Cell* **17**(1)**:** 9-26

MacDonald BT, Yokota C, Tamai K, Zeng X, He X (2008) Wnt signal amplification via activity, cooperativity, and regulation of multiple intracellular PPPSP motifs in the Wnt co-receptor LRP6. *J Biol Chem* **283**(23)**:** 16115-16123

Macia E, Ehrlich M, Massol R, Boucrot E, Brunner C, Kirchhausen T (2006) Dynasore, a cell-permeable inhibitor of dynamin. *Dev Cell* **10**(6)**:** 839-850

Maher MT, Flozak AS, Stocker AM, Chenn A, Gottardi CJ (2009) Activity of the beta-catenin phosphodestruction complex at cell-cell contacts is enhanced by cadherin-based adhesion. *J Cell Biol* **186**(2)**:** 219-228

Maher MT, Mo R, Flozak AS, Peled ON, Gottardi CJ (2010) Beta-catenin phosphorylated at serine 45 is spatially uncoupled from beta-catenin phosphorylated in the GSK3 domain: implications for signaling. *PLoS One* **5**(4)**:** e10184

Major MB, Camp ND, Berndt JD, Yi X, Goldenberg SJ, Hubbert C, Biechele TL, Gingras AC, Zheng N, Maccoss MJ, Angers S, Moon RT (2007) Wilms tumor suppressor WTX negatively regulates WNT/beta-catenin signaling. *Science* **316**(5827)**:** 1043-1046

Mansfield E, Hersperger E, Biggs J, Shearn A (1994) Genetic and molecular analysis of hyperplastic discs, a gene whose product is required for regulation of cell proliferation in Drosophila melanogaster imaginal discs and germ cells. *Dev Biol* **165**(2)**:** 507-526

Marois E, Mahmoud A, Eaton S (2006) The endocytic pathway and formation of the Wingless morphogen gradient. *Development* **133**(2)**:** 307-317

Martinez Arias A (2003) Wnts as morphogens? The view from the wing of Drosophila. *Nat Rev Mol Cell Biol* **4**(4)**:** 321-325

Massague J (1998) TGF-beta signal transduction. *Annu Rev Biochem* **67:** 753-791

Mesaki K, Tanabe K, Obayashi M, Oe N, Takei K Fission of tubular endosomes triggers endosomal acidification and movement. *PLoS One* **6**(5)**:** e19764

Metcalfe C, Bienz M (2011) Inhibition of GSK3 by Wnt signalling--two contrasting models. *J Cell Sci* **124**(Pt 21)**:** 3537-3544

Metcalfe C, Mendoza-Topaz C, Mieszczanek J, Bienz M (2010) Stability elements in the LRP6 cytoplasmic tail confer efficient signalling upon DIX-dependent polymerization. *J Cell Sci* **123**(Pt 9)**:** 1588-1599

Micchelli CA, Rulifson EJ, Blair SS (1997) The function and regulation of cut expression on the wing margin of Drosophila: Notch, Wingless and a dominant negative role for Delta and Serrate. *Development* **124**(8)**:** 1485-1495

Mikels AJ, Nusse R (2006) Purified Wnt5a protein activates or inhibits beta-catenin-TCF signaling depending on receptor context. *PLoS Biol* **4**(4)**:** e115

Mitchell B, Stubbs JL, Huisman F, Taborek P, Yu C, Kintner C (2009) The PCP pathway instructs the planar orientation of ciliated cells in the Xenopus larval skin. *Curr Biol* **19**(11)**:** 924-929

Mlodzik M (2002) Planar cell polarization: do the same mechanisms regulate Drosophila tissue polarity and vertebrate gastrulation? *Trends Genet* **18**(11)**:** 564-571

Mosesson Y, Yarden Y (2006) Monoubiquitylation: a recurrent theme in membrane protein transport. *Isr Med Assoc J* **8**(4)**:** 233-237

Mosimann C, Hausmann G, Basler K (2006) Parafibromin/Hyrax activates Wnt/Wg target gene transcription by direct association with beta-catenin/Armadillo. *Cell* **125**(2)**:** 327-341

Mukai A, Yamamoto-Hino M, Awano W, Watanabe W, Komada M, Goto S (2010) Balanced ubiquitylation and deubiquitylation of Frizzled regulate cellular responsiveness to Wg/Wnt. *EMBO J* **29**(13)**:** 2114-2125

Muller HA, Samanta R, Wieschaus E (1999) Wingless signaling in the Drosophila embryo: zygotic requirements and the role of the frizzled genes. *Development* **126**(3)**:** 577-586

Nakamura N, Hirose S (2008) Regulation of mitochondrial morphology by USP30, a deubiquitinating enzyme present in the mitochondrial outer membrane. *Mol Biol Cell* **19**(5)**:** 1903-1911

Neumann CJ, Cohen SM (1997) Long-range action of Wingless organizes the dorsal-ventral axis of the Drosophila wing. *Development* **124**(4)**:** 871-880

Nichols JT, Miyamoto A, Olsen SL, D'Souza B, Yao C, Weinmaster G (2007) DSL ligand endocytosis physically dissociates Notch1 heterodimers before activating proteolysis can occur. *J Cell Biol* **176**(4)**:** 445-458

Noordermeer J, Johnston P, Rijsewijk F, Nusse R, Lawrence PA (1992) The consequences of ubiquitous expression of the wingless gene in the Drosophila embryo. *Development* **116**(3)**:** 711-719

Nusse R (1997) A versatile transcriptional effector of Wingless signaling. *Cell* **89**(3)**:** 321-323

Nusse R, Brown A, Papkoff J, Scambler P, Shackleford G, McMahon A, Moon R, Varmus H (1991) A new nomenclature for int-1 and related genes: the Wnt gene family. *Cell* **64**(2)**:** 231

Nusse R, Varmus HE (1982) Many tumors induced by the mouse mammary tumor virus contain a provirus integrated in the same region of the host genome. *Cell* **31**(1)**:** 99-109

Nusslein-Volhard C, Wieschaus E (1980) Mutations affecting segment number and polarity in Drosophila. *Nature* **287**(5785)**:** 795-801

Ohshima R, Ohta T, Wu W, Koike A, Iwatani T, Henderson M, Watts CK, Otsubo T (2007) Putative tumor suppressor EDD interacts with and up-regulates APC. *Genes Cells* **12**(12)**:** 1339-1345

Orgad S, Rosenfeld G, Greenspan RJ, Segal D (2000) courtless, the Drosophila UBC7 homolog, is involved in male courtship behavior and spermatogenesis. *Genetics* **155**(3)**:** 1267-1280

Orsulic S, Huber O, Aberle H, Arnold S, Kemler R (1999) E-cadherin binding prevents beta-catenin nuclear localization and beta-catenin/LEF-1-mediumted transactivation. *J Cell Sci* **112 (Pt 8):** 1237-1245

Orsulic S, Peifer M (1996) An in vivo structure-function study of armadillo, the beta-catenin homologue, reveals both separate and overlapping regions of the protein required for cell adhesion and for wingless signaling. *J Cell Biol* **134**(5)**:** 1283-1300

Ou CY, Pi H, Chien CT (2003) Control of protein degradation by E3 ubiquitin ligases in Drosophila eye development. *Trends Genet* **19**(7)**:** 382-389

Pai LM, Orsulic S, Bejsovec A, Peifer M (1997) Negative regulation of Armadillo, a Wingless effector in Drosophila. *Development* **124**(11)**:** 2255-2266

Panakova D, Sprong H, Marois E, Thiele C, Eaton S (2005) Lipoprotein particles are required for Hedgehog and Wingless signalling. *Nature* **435**(7038)**:** 58-65

Parks AL, Klueg KM, Stout JR, Muskavitch MA (2000) Ligand endocytosis drives receptor dissociation and activation in the Notch pathway. *Development* **127**(7)**:** 1373-1385

Payre F, Vincent A, Carreno S (1999) ovo/svb integrates Wingless and DER pathways to control epidermis differentiation. *Nature* **400**(6741)**:** 271-275

Penheiter SG, Mitchell H, Garamszegi N, Edens M, Dore JJ, Jr., Leof EB (2002) Internalization-dependent and -independent requirements for transforming growth factor beta receptor signaling via the Smad pathway. *Mol Cell Biol* **22**(13)**:** 4750-4759

Pertceva JA, Dorogova NV, Bolobolova EU, Nerusheva OO, Fedorova SA, Omelyanchuk LV The role of Drosophila hyperplastic discs gene in spermatogenesis. *Cell Biol Int* **34**(10)**:** 991-996

Piddini E, Marshall F, Dubois L, Hirst E, Vincent JP (2005) Arrow (LRP6) and Frizzled2 cooperate to degrade Wingless in Drosophila imaginal discs. *Development* **132**(24)**:** 5479-5489

Piddini E, Vincent JP (2009) Interpretation of the wingless gradient requires signaling-induced self-inhibition. *Cell* **136**(2)**:** 296-307

Poeck B, Fischer S, Gunning D, Zipursky SL, Salecker I (2001) Glial cells mediumte target layer selection of retinal axons in the developing visual system of Drosophila. *Neuron* **29**(1)**:** 99-113

Purvanov V, Koval A, Katanaev VL (2010) A direct and functional interaction between Go and Rab5 during G protein-coupled receptor signaling. *Sci Signal* **3**(136)**:** ra65

Rajan A, Tien AC, Haueter CM, Schulze KL, Bellen HJ (2009) The Arp2/3 complex and WASp are required for apical trafficking of Delta into microvilli during cell fate specification of sensory organ precursors. *Nat Cell Biol* **11**(7)**:** 815-824

Rijsewijk F, Schuermann M, Wagenaar E, Parren P, Weigel D, Nusse R (1987) The Drosophila homolog of the mouse mammary oncogene int-1 is identical to the segment polarity gene wingless. *Cell* **50**(4)**:** 649-657

Rives AF, Rochlin KM, Wehrli M, Schwartz SL, DiNardo S (2006) Endocytic trafficking of Wingless and its receptors, Arrow and DFrizzled-2, in the Drosophila wing. *Dev Biol* **293**(1)**:** 268-283

Roberts DM, Pronobis MI, Poulton JS, Waldmann JD, Stephenson EM, Hanna S, Peifer M (2011) Deconstructing the sscatenin destruction complex: mechanistic roles for the tumor suppressor APC in regulating Wnt signaling. *Mol Biol Cell* **22**(11)**:** 1845-1863

Rockel B, Kopec KO, Lupas AN, Baumeister W (2011) Structure and function of tripeptidyl peptidase II, a giant cytosolic protease. *Biochim Biophys Acta* **1824**(1)**:** 237-245

Rosin-Arbesfeld R, Townsley F, Bienz M (2000) The APC tumour suppressor has a nuclear export function. *Nature* **406**(6799)**:** 1009-1012

Roux A, Uyhazi K, Frost A, De Camilli P (2006) GTP-dependent twisting of dynamin implicates constriction and tension in membrane fission. *Nature* **441**(7092)**:** 528-531

Rulifson EJ, Micchelli CA, Axelrod JD, Perrimon N, Blair SS (1996) wingless refines its own expression domain on the Drosophila wing margin. *Nature* **384**(6604)**:** 72-74

Runyan CE, Schnaper HW, Poncelet AC (2005) The role of internalization in transforming growth factor beta1-induced Smad2 association with Smad anchor for receptor activation (SARA) and Smad2-dependent signaling in human mesangial cells. *J Biol Chem* **280**(9)**:** 8300-8308

Rusten TE, Vaccari T, Stenmark H (2012) Shaping development with ESCRTs. *Nat Cell Biol* **14**(1)**:** 38-45

Sakane H, Yamamoto H, Kikuchi A (2010) LRP6 is internalized by Dkk1 to suppress its phosphorylation in the lipid raft and is recycled for reuse. *J Cell Sci* **123**(Pt 3)**:** 360-368

Samara NL, Datta AB, Berndsen CE, Zhang X, Yao T, Cohen RE, Wolberger C Structural insights into the assembly and function of the SAGA deubiquitinating module. *Science* **328**(5981)**:** 1025-1029

Sanson B, Alexandre C, Fascetti N, Vincent JP (1999) Engrailed and hedgehog make the range of Wingless asymmetric in Drosophila embryos. *Cell* **98**(2)**:** 207-216

Sanson B, White P, Vincent JP (1996) Uncoupling cadherin-based adhesion from wingless signalling in Drosophila. *Nature* **383**(6601)**:** 627-630

Sato A, Kojima T, Ui-Tei K, Miyata Y, Saigo K (1999) Dfrizzled-3, a new Drosophila Wnt receptor, acting as an attenuator of Wingless signaling in wingless hypomorphic mutants. *Development* **126**(20)**:** 4421-4430

Sato M, Umetsu D, Murakami S, Yasugi T, Tabata T (2006) DWnt4 regulates the dorsoventral specificity of retinal projections in the Drosophila melanogaster visual system. *Nat Neurosci* **9**(1)**:** 67-75

Schwarz-Romond T, Metcalfe C, Bienz M (2007) Dynamic recruitment of axin by Dishevelled protein assemblies. *J Cell Sci* **120**(Pt 14)**:** 2402-2412

Schweizer L, Varmus H (2003) Wnt/Wingless signaling through beta-catenin requires the function of both LRP/Arrow and frizzled classes of receptors. *BMC Cell Biol* **4:** 4

Semenov MV, Zhang X, He X (2008) DKK1 antagonizes Wnt signaling without promotion of LRP6 internalization and degradation. *J Biol Chem* **283**(31)**:** 21427-21432

Seto ES, Bellen HJ (2004) The ins and outs of Wingless signaling. *Trends Cell Biol* **14**(1)**:** 45-53

Seto ES, Bellen HJ (2006) Internalization is required for proper Wingless signaling in Drosophila melanogaster. *J Cell Biol* **173**(1)**:** 95-106

Seugnet L, Simpson P, Haenlin M (1997) Requirement for dynamin during Notch signaling in Drosophila neurogenesis. *Dev Biol* **192**(2)**:** 585-598

Sevrioukov EA, He JP, Moghrabi N, Sunio A, Kramer H (1999) A role for the deep orange and carnation eye color genes in lysosomal delivery in Drosophila. *Mol Cell* **4**(4)**:** 479-486

Sharma J, Mulherkar S, Mukherjee D, Jana NR (2012) Malin regulates Wnt signalling pathway through degradation of dishevelled 2. *J Biol Chem*

Sharma RP, Chopra VL (1976) Effect of the Wingless (wg1) mutation on wing and haltere development in Drosophila melanogaster. *Dev Biol* **48**(2)**:** 461-465

Sierra J, Yoshida T, Joazeiro CA, Jones KA (2006) The APC tumor suppressor counteracts beta-catenin activation and H3K4 methylation at Wnt target genes. *Genes Dev* **20**(5)**:** 586-600

Sigismund S, Argenzio E, Tosoni D, Cavallaro E, Polo S, Di Fiore PP (2008) Clathrin-mediumted internalization is essential for sustained EGFR signaling but dispensable for degradation. *Dev Cell* **15**(2)**:** 209-219

Sivasankaran R, Calleja M, Morata G, Basler K (2000) The Wingless target gene Dfz3 encodes a new member of the Drosophila Frizzled family. *Mech Dev* **91**(1-2)**:** 427-431

Slusarski DC, Yang-Snyder J, Busa WB, Moon RT (1997) Modulation of embryonic intracellular Ca2+ signaling by Wnt-5A. *Dev Biol* **182**(1)**:** 114-120

Sorensen EB, Conner SD (2010) gamma-secretase-dependent cleavage initiates notch signaling from the plasma membrane. *Traffic* **11**(9)**:** 1234-1245

Stambolic V, Ruel L, Woodgett JR (1996) Lithium inhibits glycogen synthase kinase-3 activity and mimics wingless signalling in intact cells. *Curr Biol* **6**(12)**:** 1664-1668

Strigini M, Cohen SM (1999) Formation of morphogen gradients in the Drosophila wing. *Semin Cell Dev Biol* **10**(3)**:** 335-344

Struhl G, Barbash DA, Lawrence PA (1997) Hedgehog organises the pattern and polarity of epidermal cells in the Drosophila abdomen. *Development* **124**(11)**:** 2143-2154

Strutt D (2003) Frizzled signalling and cell polarisation in Drosophila and vertebrates. *Development* **130**(19)**:** 4501-4513

Sun H, Chen QM (2008) Inhibitors of GSK-3 prevent corticosterone from inducing COX-1 expression in cardiomyocytes. *Cardiovasc Toxicol* **8**(2)**:** 93-100

Sverdlov M, Shajahan AN, Minshall RD (2007) Tyrosine phosphorylation-dependence of caveolae-mediumted endocytosis. *J Cell Mol Med* **11**(6)**:** 1239-1250

Szuts D, Freeman M, Bienz M (1997) Antagonism between EGFR and Wingless signalling in the larval cuticle of Drosophila. *Development* **124**(16)**:** 3209-3219

Taelman VF, Dobrowolski R, Plouhinec JL, Fuentealba LC, Vorwald PP, Gumper I, Sabatini DD, De Robertis EM (2010) Wnt signaling requires sequestration of glycogen synthase kinase 3 inside multivesicular endosomes. *Cell* **143**(7)**:** 1136-1148

Tagami S, Okochi M, Yanagida K, Ikuta A, Fukumori A, Matsumoto N, Ishizuka-Katsura Y, Nakayama T, Itoh N, Jiang J, Nishitomi K, Kamino K, Morihara T, Hashimoto R, Tanaka T, Kudo T, Chiba S, Takeda M (2008) Regulation of Notch signaling by dynamic changes in the precision of S3 cleavage of Notch-1. *Mol Cell Biol* **28**(1)**:** 165-176

Takacs CM, Baird JR, Hughes EG, Kent SS, Benchabane H, Paik R, Ahmed Y (2008) Dual positive and negative regulation of wingless signaling by adenomatous polyposis coli. *Science* **319**(5861)**:** 333-336

Takeichi M (1995) Morphogenetic roles of classic cadherins. *Curr Opin Cell Biol* **7**(5)**:** 619-627

Takemaru KI, Moon RT (2000) The transcriptional coactivator CBP interacts with beta-catenin to activate gene expression. *J Cell Biol* **149**(2)**:** 249-254

Tamai K, Zeng X, Liu C, Zhang X, Harada Y, Chang Z, He X (2004) A mechanism for Wnt coreceptor activation. *Mol Cell* **13**(1)**:** 149-156

Tokunaga F, Sakata S, Saeki Y, Satomi Y, Kirisako T, Kamei K, Nakagawa T, Kato M, Murata S, Yamaoka S, Yamamoto M, Akira S, Takao T, Tanaka K, Iwai K (2009) Involvement of linear polyubiquitylation of NEMO in NF-kappaB activation. *Nat Cell Biol* **11**(2)**:** 123-132

Tomlinson A, Strapps WR, Heemskerk J (1997) Linking Frizzled and Wnt signaling in Drosophila development. *Development* **124**(22)**:** 4515-4521

Tran H, Hamada F, Schwarz-Romond T, Bienz M (2008) Trabid, a new positive regulator of Wnt-induced transcription with preference for binding and cleaving K63-linked ubiquitin chains. *Genes Dev* **22**(4)**:** 528-542

Tsukazaki T, Chiang TA, Davison AF, Attisano L, Wrana JL (1998) SARA, a FYVE domain protein that recruits Smad2 to the TGFbeta receptor. *Cell* **95**(6)**:** 779-791

Vaccari T, Duchi S, Cortese K, Tacchetti C, Bilder D (2010) The vacuolar ATPase is required for physiological as well as pathological activation of the Notch receptor. *Development* **137**(11)**:** 1825-1832

Vaccari T, Lu H, Kanwar R, Fortini ME, Bilder D (2008) Endosomal entry regulates Notch receptor activation in Drosophila melanogaster. *J Cell Biol* **180**(4)**:** 755-762

Vaccari T, Rusten TE, Menut L, Nezis IP, Brech A, Stenmark H, Bilder D (2009) Comparative analysis of ESCRT-I, ESCRT-II and ESCRT-III function in Drosophila by efficient isolation of ESCRT mutants. *J Cell Sci* **122**(Pt 14)**:** 2413-2423

van de Wetering M, Oosterwegel M, Dooijes D, Clevers H (1991) Identification and cloning of TCF-1, a T lymphocyte-specific transcription factor containing a sequence-specific HMG box. *EMBO J* **10**(1)**:** 123-132

Varghese B, Barriere H, Carbone CJ, Banerjee A, Swaminathan G, Plotnikov A, Xu P, Peng J, Goffin V, Lukacs GL, Fuchs SY (2008) Polyubiquitination of prolactin receptor stimulates its internalization, postinternalization sorting, and degradation via the lysosomal pathway. *Mol Cell Biol* **28**(17)**:** 5275-5287

Verheyen EM, Mirkovic I, MacLean SJ, Langmann C, Andrews BC, MacKinnon C (2001) The tissue polarity gene nemo carries out multiple roles in patterning during Drosophila development. *Mech Dev* **101**(1-2)**:** 119-132

Vincent JP, O'Farrell PH (1992) The state of engrailed expression is not clonally transmitted during early Drosophila development. *Cell* **68**(5)**:** 923-931

Vinson CR, Adler PN (1987) Directional non-cell autonomy and the transmission of polarity information by the frizzled gene of Drosophila. *Nature* **329**(6139)**:** 549-551

Walters JW, Munoz C, Paaby AB, Dinardo S (2005) Serrate-Notch signaling defines the scope of the initial denticle field by modulating EGFR activation. *Dev Biol* **286**(2)**:** 415-426

Waltzer L, Bienz M (1998) Drosophila CBP represses the transcription factor TCF to antagonize Wingless signalling. *Nature* **395**(6701)**:** 521-525

Wan M, Tang Y, Tytler EM, Lu C, Jin B, Vickers SM, Yang L, Shi X, Cao X (2004) Smad4 protein stability is regulated by ubiquitin ligase SCF beta-TrCP1. *J Biol Chem* **279**(15)**:** 14484-14487

Wang B, Suzuki H, Kato M (2008) Roles of mono-ubiquitinated Smad4 in the formation of Smad transcriptional complexes. *Biochem Biophys Res Commun* **376**(2)**:** 288-292

Weake VM, Lee KK, Guelman S, Lin CH, Seidel C, Abmayr SM, Workman JL (2008) SAGA-mediumted H2B deubiquitination controls the development of neuronal connectivity in the Drosophila visual system. *EMBO J* **27**(2)**:** 394-405

Wehrli M, Dougan ST, Caldwell K, O'Keefe L, Schwartz S, Vaizel-Ohayon D, Schejter E, Tomlinson A, DiNardo S (2000) arrow encodes an LDL-receptor-related protein essential for Wingless signalling. *Nature* **407**(6803)**:** 527-530

Whittle JR (1990) Pattern formation in imaginal discs. *Semin Cell Biol* **1**(3)**:** 241-252

Wiechens N, Heinle K, Englmeier L, Schohl A, Fagotto F (2004) Nucleo-cytoplasmic shuttling of Axin, a negative regulator of the Wnt-beta-catenin Pathway. *J Biol Chem* **279**(7)**:** 5263-5267

Willert J, Epping M, Pollack JR, Brown PO, Nusse R (2002) A transcriptional response to Wnt protein in human embryonic carcinoma cells. *BMC Dev Biol* **2:** 8

Williams JA, Paddock SW, Carroll SB (1993) Pattern formation in a secondary field: a hierarchy of regulatory genes subdivides the developing Drosophila wing disc into discrete subregions. *Development* **117**(2)**:** 571-584

Winter CG, Wang B, Ballew A, Royou A, Karess R, Axelrod JD, Luo L (2001) Drosophila Rho-associated kinase (Drok) links Frizzled-mediumted planar cell polarity signaling to the actin cytoskeleton. *Cell* **105**(1)**:** 81-91

Wolf J, Palmby TR, Gavard J, Williams BO, Gutkind JS (2008) Multiple PPPS/TP motifs act in a combinatorial fashion to transduce Wnt signaling through LRP6. *FEBS Lett* **582**(2)**:** 255-261

Wu CH, Nusse R (2002) Ligand receptor interactions in the Wnt signaling pathway in Drosophila. *J Biol Chem* **277**(44)**:** 41762-41769

Wu G, Chen YG, Ozdamar B, Gyuricza CA, Chong PA, Wrana JL, Massague J, Shi Y (2000) Structural basis of Smad2 recognition by the Smad anchor for receptor activation. *Science* **287**(5450)**:** 92-97

Wu G, Huang H, Garcia Abreu J, He X (2009) Inhibition of GSK3 phosphorylation of beta-catenin via phosphorylated PPPSPXS motifs of Wnt coreceptor LRP6. *PLoS One* **4**(3)**:** e4926

Wu Z, Li Q, Fortini ME, Fischer JA (1999) Genetic analysis of the role of the drosophila fat facets gene in the ubiquitin pathway. *Developmental genetics* **25**(4)**:** 312-320

Wyatt D, Malik R, Vesecky AC, Marchese A (2011) Small ubiquitin-like modifier modification of arrestin-3 regulates receptor trafficking. *J Biol Chem* **286**(5)**:** 3884-3893

Xu L, Kang Y, Col S, Massague J (2002) Smad2 nucleocytoplasmic shuttling by nucleoporins CAN/Nup214 and Nup153 feeds TGFbeta signaling complexes in the cytoplasm and nucleus. *Mol Cell* **10**(2)**:** 271-282

Yamamoto H, Komekado H, Kikuchi A (2006) Caveolin is necessary for Wnt-3a-dependent internalization of LRP6 and accumulation of beta-catenin. *Dev Cell* **11**(2)**:** 213-223

Yumoto R, Nishikawa H, Okamoto M, Katayama H, Nagai J, Takano M (2006) Clathrin-mediumted endocytosis of FITC-albumin in alveolar type II epithelial cell line RLE-6TN. *Am J Physiol Lung Cell Mol Physiol* **290**(5)**:** L946-955

Zecca M, Basler K, Struhl G (1996) Direct and long-range action of a wingless morphogen gradient. *Cell* **87**(5)**:** 833-844

Zeng X, Huang H, Tamai K, Zhang X, Harada Y, Yokota C, Almeida K, Wang J, Doble B, Woodgett J, Wynshaw-Boris A, Hsieh JC, He X (2008) Initiation of Wnt signaling: control of Wnt coreceptor Lrp6 phosphorylation/activation via frizzled, dishevelled and axin functions. *Development* **135**(2)**:** 367-375

Zeng X, Tamai K, Doble B, Li S, Huang H, Habas R, Okamura H, Woodgett J, He X (2005) A dual-kinase mechanism for Wnt co-receptor phosphorylation and activation. *Nature* **438**(7069)**:** 873-877

Zhu H (2011) Spatiotemporally modulated Vestigial gradient by Wingless signaling adaptively regulates cell division for precise wing size control. *J Theor Biol* **268**(1)**:** 131-140